Scholar Commons
USF University of South Florida

University of South Florida
Scholar Commons

Graduate Theses and Dissertations

Graduate School

November 2019

Antarctic Deep Sea Coral and Tropical Fungal Endophyte: Novel Chemistry for Drug Discovery

Anne-Claire D. Limon
University of South Florida

Follow this and additional works at: https://scholarcommons.usf.edu/etd

 Part of the Chemistry Commons

Scholar Commons Citation

Limon, Anne-Claire D., "Antarctic Deep Sea Coral and Tropical Fungal Endophyte: Novel Chemistry for Drug Discovery" (2019). *Graduate Theses and Dissertations.*
https://scholarcommons.usf.edu/etd/8662

This Dissertation is brought to you for free and open access by the Graduate School at Scholar Commons. It has been accepted for inclusion in Graduate Theses and Dissertations by an authorized administrator of Scholar Commons. For more information, please contact scholarcommons@usf.edu.

المنارة للاستشارات

www.manaraa.com

Antarctic Deep Sea Coral and Tropical Fungal Endophyte:

Novel Chemistry for Drug Discovery

by

Anne-Claire D. Limon

A dissertation submitted in partial fulfillment
of the requirements for the degree of
Doctor of Philosophy in Chemistry
Department of Chemistry
College of Arts and Sciences
University of South Florida

Major Professor: Bill J. Baker, Ph.D.
Valerie J. Harwood, Ph.D.
James W. Leahy, Ph.D.
Edward Turos, Ph.D.

Date of Approval:
November 7, 2019

Keywords: Marine Natural Products, Alcyonacean, Penicillium, Epigenetic modifications, Metabolomics.

Copyright © 2019, Anne-Claire D. Limon

www.manaraa.com

DEDICATION

« Sa ki la pou'w dlo pa ka chayé'y. »

("No one escapes his destiny.")

– Creole proverb

To my parents, who always showed me where I come from, to make me who I am. My father, the man who instilled in me the taste for Science early on. I still remember that green board you built for us to do our homework; the smell of fresh chalk and these long hours teaching me the laws of physics and chemistry. Father, you may have left this world more than two decades ago, but mom perpetuated your vision and culture.

To my rock, my confident, my inspiration…

From afar, your tremendous courage and optimism have been carrying me all the way. You know more and better than anybody all it took to get here. You always walk by faith, not by sight and you agreed to this adventure since the beginning. This accomplishment is also yours. You may not be a trained scientist, but your undeniable taste of Nature provided the foundation to become who I am today. Mother, thank you for your everlasting love and support.

Owen, as we were just meeting, I received the news that I got accepted to the program. You embraced it and through mountains and valleys, you kept at it. In spite of the distance, you

www.manaraa.com

were a phone call away listening, supporting, and encouraging. You and I know what it took us to overcome. I will be selfish enough to keep it all for me and cherish it. Thank you for being who you are and lightening up the day for us. Now, let's travel the world!

David, we do share a lot: similar career path, taste for experimental sciences, cooking and baking, music and cinema. From homework assignments solving to leisure times on bicycle rides on the streets of Paris, you always had my back and advised me in the best ways. Thank you, David!

Dorothée, more than ever busy with your career and family, you still encourage me daily and push me to go beyond my limits. I do not forget the leap I took fifteen years ago and decided to "Come to America". You were instrumental in my decision by painting the picture of available opportunities I could and did encounter along the way. Thank you, Dorothée!

Jocelette, if my mother was one of my leg, you would be the other – the two of you together helping me stand. Everything you have done for me does not go unseen. If I did not in the past, I am acknowledging all your actions of support and guidance. Also, I take this opportunity to include Jean Rouch. As a young undergraduate, the both of you motivated me to eventually pursue my doctorate. Thank you always for keeping the mood happy.

Docey, we met as I was about to start graduate school, and you were on board from the get-go, and included me in your family. I appreciate everything you have done for us, Owen and me, and I cannot wait to catch up and spend more quality time together.

Lelette, Linette, Georgia, Yayi, Oum, and Richou, you are not forgotten. We have not talked much in the past five years, but I am fully aware and thankful for your presence and long-distance support.

To my love and support army…

www.manaraa.com

From way, way back, Titid, Caro, Myma, Walé, Vivi, Lu, Boom, and Thyeks. Your encouragement and support made my day. We may not talk often, but after all these years, our friendships are still standing strong and mean the world to me. Properce said it best: "Out of sight, near the heart".

My TSS crew and the associated ones I met along the way. Too many to cite you all, but just to name a few, in no particular order: JJLR, BB, Samar, Chels, Cami, Stef, Mark & Michella (M&M), Ashita, Doudou, Nikki, Livia, Carlito, Dani, Dara, Jaime, Alby, Erik, Virginie & Maymick, Eli & Adam, Brittany, Jarin. We meet randomly at any corner of the world and just pick up where we left off. It is always a pleasure to hear from each of you; you are my priceless international family. Thank you for all the long chat-conversations when I least expected it and was at my lowest point. Time zones and borders got nothing on us! Thank you for your support, stories, and laughs through this grad school exploration of mine.

The EVV crowd: Tara, Ebony, Lyndsee, Shanna, Erin, Cindi, Kathy, and Heidi, and USI! Thank you for welcoming me and being my home away from home.

The Fire & Ice crew: Clay, Clint, Kelly, George, Ted, Eric (x2), Steve, and Kristen, my ride-or-die woman on board, thank you for welcoming me in the Bay area. Without a doubt, you made me a better sailor, especially at low tide. Thank you all!

Thank you also to all my adversaries for giving me the strength, courage, and resilience to keep pushing even harder. Thank you everyone, near and far, for accompanying me on this journey.

www.manaraa.com

ACKNOWLEDGMENTS

This adventure would not have been possible without Dr. Bill Baker, who took a chance on me. I remember seven years ago, enjoying my coffee on a summer morning, and receiving your email suggesting that I apply for the program. A year and a half later, I was joining your lab. I navigated the meanders of research under your mentorship, but it was not without fears, doubts, tears, as well as growth, joy, and laughter. Thank you for believing in me, even when sometimes I did not. I am forever grateful for this opportunity.

My committee members, Dr. Valerie Harwood, Dr. James Leahy, and Dr. Edward Turos, thank you for your invaluable feedback and advice.

Dr. Laurent Calcul and Dr. Eduardo Caro-Diaz, thank you for your mentorship in research and professional development. You have been key listeners and advisors and I am looking forward to working together in the future. Dr. Edwin Rivera, thank you for your assistance and availability with all of my NMR experiments acquisitions. Dr. Lukasz Wojtas and Gaurav Verma, thank you for all your crystallographic contributions and the time devoted to help me out.

I would like to thank all the research collaborators who tested the compounds associated to the work presented in this thesis in their biological assays. Dr. Dennis Kyle and Dr. Ala Azhari who performed the *Leishmania donovani* parasite assay, Alison Roth and Dr. John Adams who developed the liver stage malaria assay, Dr. Xingmin Sun and his student Hiran Malinda performing the *Clostridium difficile* assay. The HeLa cancer cells assay done by Anthony Sanchez in Dr. Younghoon Kee's lab, and the Respiratory Syncitial Virus assay by Dr. Michael Teng and

www.manaraa.com

Kim-Chi Teng. For the organism identifications, I would like to thank Dr. Lindsey Shaw and Sarah Kennedy who took care of the endophytic species involved in this research, and Dr. Nerida Wilson who dealt with the Antarctic deep sea coral.

Thank you, Dr. Daniel Cruz-Ramirez de Arellano and Dr. Jeffrey Raker, for your teaching mentorship, encouragement, and suggestions. The long nights of grading were made much easier thanks to the funny stories we shared. Thank you, Oliva Pope, Analise Keating, and Jessica Pearson for showing me courage and resilience to keep going in life.

Also, I would like to thank the colorful Baker Lab bunch, my undergraduates, and the grad student friends who showed up no matter what: Nicole, Elena, Andrea, Linda, and Tim, the Periodically Right trivia team – Cole, Brian, Briana, Andrew, and "sometimes" Joshua - making "hump days" smoother, Christie and Béa for the relaxing evening conversations on the patio - Grazie mille! Overall, there was never a dull moment, but good memories to laugh about, and work was always accomplished in the end.

Ultimately, I would like to thank Dr. Marie-Ange Arsène, Dr. Lyn Udino, Dr. Paul Bourgeois, and Dr. Henry Joseph, whom provided me with the knowledge of chemistry, natural products and the academic support I needed. Everything started with you and led me to where I am today.

You all played an essential part in this achievement. Thank you.

www.manaraa.com

TABLE OF CONTENTS

www.manaraa.com

www.manaraa.com

www.manaraa.com

LIST OF TABLES

www.manaraa.com

LIST OF FIGURES

www.manaraa.com

www.manaraa.com

www.manaraa.com

www.manaraa.com

www.manaraa.com

www.manaraa.com

LIST OF SCHEMES

www.manaraa.com

LIST OF ABBREVIATIONS AND UNITS

ACC	Antarctic Circumpolar Current
ADME	absorption, distribution, metabolism, and excretion
APCI	atmospheric pressure chemical ionization
C18	octadecyl bonded silica
CC_{50}	cytotoxic concentration for half of the population
CD	circular dichroism
$CDCl_3$	deuterated chloroform
CL	cutaneous leishmaniasis
COSY	Correlation SpectroscopY
DCM	dichloromethane
DNMTi	DNA methyl transferase inhibitor
ECD	electronic circular dichroism
ED_{50}	median effective dose
EI	electron impact ionization
EtOAc	ethyl acetate
ESI	electron soft inonization
ESKAPE	acronym for group of bacteria: *Enterococcus faecium, Staphylococcus aureus, Klebsiella pneumoniae, Acinetobacter baumanii, Pseudomonas aeruginosa, Enterobacter.*
FAB	fast atom bombardment
GC	gas chromatography
GNPS	Global Natural Products Social Networking
HDACi	histone deacetylase inhibitor
Hex	hexanes
H_2O	water
HMBC	Heteronuclear Multiple Bond Correlation
HPLC	High Performance Liquid Chromatography
HRESIMS	High Resoloution Electron Soft Ionization Mass Spectrum
HSQC	Heteronuclear Single Quantum Correlation
IC_{50}	inhibitory concentration for half of the population
IR	infrared
LC	liquid chromatography
LD_{50}	lethal dose for half of the population
MASST	Mass Search Tool
m^3/s	cubed meter per second
MeOH	methanol
mg	milligram
mg/mL	milligram per milliliter
MHz	megahertz
MIC	minimum inhibitory concentration

www.manaraa.com

µM	micromole per Liter
mL	milliliter
ML	mucocutaneous leishmaniasis
mm	millimeter
mM	millimole per Liter
min	minute
MPLC	Medium Pressure Liquid Chromqtography
MS	mass spectrometry / mass spectrum
MS/MS	tandem mass spectrometry
MTT	3-(4,5-dimethylthiazol-2-yl)-2,5-diphenyltetrazolium
m/z	mass/charge ratio
nm	nanometer
nM	nanomole per Liter
NIST	National Institute of Standards and Technology
NOESY	Nuclear Overhauser Effect SpectroscopY
NP	normal phase
NMR	Nuclear Magnetic Resonance
OSMAC	One Strain Many Compounds
ppm	part per million
QQQ	triple quadrupole mass spectrometer
QToF	quadrupole time of flight mass spectrometer
ROESY	Rotating-frame Overhauser SpectroscopY
ROV	remotely operated vehicle
RP	reverse phase
SCUBA	self-contained underwater breathing apparatus
sp.	species
ToF	time of flight mass spectrometer
UV	ultraviolet
VL	visceral leishmaniasis
WHO	World Health Organization
^{1}H NMR	proton nuclear magnetic resonance
^{13}C NMR	carbon-13 nuclear magnetic resonance
°C	degree Celsius

www.manaraa.com

ABSTRACT

Considered the pulse controlling the biological interactions and contributing to the ecological survival of organisms, natural products have intrigued, challenged, and stimulated the scientific and non-scientific minds for millennia. Drug resistance and the lack of suitable potent drugs against neglected tropical disease further motivate the biological activity assessment of these secondary metabolites, when possible.

This thesis describes the chemical investigation of two marine organisms and the elucidation of eight novel structures.

The study of a deep sea Antarctic coral unveils six novel terpenoid structures from three different molecular classes: sesquiterpenoid alcyopterosins, a triterpene steroid, and three prostaglandins. While mass availability made it possible for the steroid and the prostaglandins to be tested for biological activity against the *Leishmania donovani* and the *Plasmodium falciparum* parasites, the potency of the novel alcyopterosin compounds could not be evaluated. However, a structure-activity relationship study comparing two of the known isolated alcyopterosin isolated along the process of investigation was feasible and contributed to the extension of the biological activity knowledge of these molecules.

The epigenetically modified culture of a tropical mangrove fungal endophyte yielded a potent antileishmanial novel sesterterpene. The originality and exclusivity of the molecular framework offered by this compound drove the research exploration to find conditions enhancing the compound production. The investigation methodology incorporated hyphenated

www.manaraa.com

liquid chromatography-mass spectrometry methods to evaluate the most favorable culture conditions and optimize the chemical isolation and purification of the compound of interest through dereplication methods. Despite some inconclusive results, serendipity on the research path led to the isolation of another novel sesterterpene.

Natural products research entails the alliance of various fields including organic, physical, and analytical chemistry with biology, ecology and medicine. This thesis illustrates these collaborations through the chemical investigation of marine organisms for the purpose of drug discovery.

www.manaraa.com

CHAPTER ONE:

INTRODUCTION ON NATURAL PRODUCTS AND DRUG DISCOVERY

Figure I.1. Natural products display from Atelier Bully in Paris (France).

Photo credit: David Limon (2019).

Natural Products are the pulse of Nature. They are the materialization of Nature's interacting forces. Thus, they have sparked interests for centuries and will remain as long as living organisms do. Whether therapeutic, fragrant, nutritive, or even mystic, their myriad of properties are all rooted in the knowledge of chemistry.[1,2] The intimate relationship of chemistry with medicine is probably one of the most meaningful and lucrative to date. It goes back to ancient times with records of natural products use for healing in Asian, African, and Mediterranean

www.manaraa.com

civilizations. These cultures have systematically turned to Nature's assets to facilitate living conditions. Nowadays, nature remains at the center of human life. More specifically, the use of natural organic substances to heal any pain felt in the human body has always been rooted in culture and continues to be explored through natural products drug discovery.[3,4]

I.1. Natural Products in History

Around 3000 BC, the Egyptian society recognized the profession of doctors, with the first one, Sekhet-enach healing the pharaoh's nostrils.[5] The actual symptoms and pain reliever treatments remain unknown, but the practices would use a variety of minerals and plants mixed in liquor or dough, documented in the Ebers Papyrus first known medical book (1500 BC).[6] Meanwhile in India, the Atharvaveda, a sacred text of Hinduism initiated the first medicine records.[7] It represents the foundation of Ayurveda, which deals with the potency of herbs and plants associated with theoretical conceptualizations to create therapies altering and prolonging life.[8] Composed of eight branches of medicine, additional knowledge of distillation, operative skills, cooking, horticulture, metallurgy, sugar manufacture, pharmacy is required.[9] All of these fields intertwined with chemistry principles, and centuries later, are still used in modern chemistry research. The combination of herbs in acupuncture and massage therapy, founded the Traditional Chinese Medicine. The Pen Tsao is the oldest record of Chinese pharmacopoeia that became known to the public around 1100 BC. The emperor Shen Nung is credited for writing it around the 3rd century BC.[3] Relying on Taoist physicians' views supporting empirical observations of disease and illness caused by the environment, traditional Chinese medicine started with the use of herbal medicines. As early as 1590 AD, approximately 1900 drugs were already recorded and 58% represented herbal medicines.[10] Traditional medicines from India (Ayurveda), China, Korea, Japan (Kampo), or Arabian origin (Unani) continue to live on as

www.manaraa.com

integrative part of modern healthcare practices in these regions.[11] Even though mysticism and rational analyses have been associated in medical practices, diagnosis, prognosis, physical examination and prescriptions were always tradition.[12]

The apogee of Greek medicine rationalized the theory of disease and the search for cures and attenuated the random incorporated mysticism in these customs. Hippocrates supported thorough observation of patient symptoms, believed in herbal remedies, but fully rejected the so-called magic component.[13,14] Thereafter their Greek conquest, Romans developed the valetudinaria,[15] the ancestors of nowadays hospitals, along with a public health system of aqueducts to bring clean waters to the cities. In spite of the Roman Empire split between East and West which created a schism affecting medical customs in the late 4th century, the following stages of the history of medicine combined knowledge of the human body and utilization of Nature's resources with biochemical knowledge to seek healthy balance. The 10th centuries saw the development hospitals in Italy and France, as well as in the Byzantine Empire and the Islamic world.[16] Not until the 16th century, was surgical knowledge expanded with illustrious figures such as Andreas Vesalius[17] who performed many dissections and Ambroise Paré who incorporated concoctions of egg whites, rose oil and turpentine to put on wounds.[18,19] Furthermore, the concept of infectious disease appeared with Girolamo Fracastoro's book called "On Contagion",[20] but the concept could not be tested until the development of a more scientific approach in the 17th century helped by the invention of the microscope in the early 1600s.[21]

Notwithstanding the limitations to identify the cause of diseases, exploiting natural products properties to heal infections was at the center of medicine. Doctors found a way to treat malaria, thanks to the French pharmacists Caventou and Pelletier.[21] In 1820, they isolated the alkaloid quinine from the bark of *Cinchona officinalis*.[23]

www.manaraa.com

Figure I.1.1. *Cinchona officinalis.*

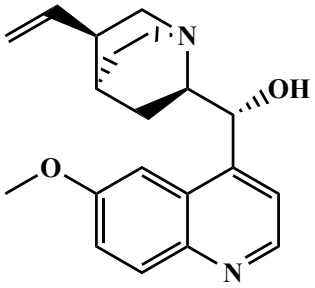

Quinine

Between 1857 and 1863, Louis Pasteur's work linked microorganisms to the cause of some diseases and found solutions against chicken cholera and rabies.[24,25] Ascorbic acid was not chemically isolated until 1930 by Albert Szent-Gyorgyi but has been in use since the 18th century. Sailors figured out how to feed on lime aboard ships to palliate vitamin C deficiency which could lead to scurvy.[26]

Figure I.1.2. Lime fruits on tree.

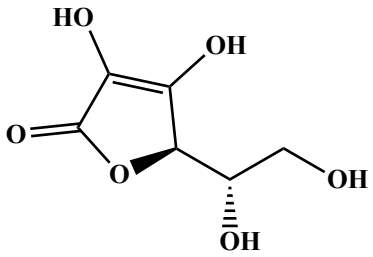

ascorbic acid

Robert Koch successfully isolated germs causing tuberculosis[27] and cholera in humans, and thereafter, Paul Ehrlich's work with synthetic dyes for the German chemical industry,[28] contributed to the screening for active drugs against syphilis, responsible for epidemics in Europe and the USA. All these biochemical developments marked the beginning of modern antimicrobial drug discovery and have led to the major antibacterial therapeutic discovery of the 20th century.

www.manaraa.com

I.2. Pharmacognosy & Drug Discovery

The understanding of the curative potential offered by Nature falls under the Greek derived term pharmacognosy, which means "knowledge of drugs".

The term emerged in the early 1800s in Austrian physician Johann A. Schmidt's manuscript on medical resources "Lehrbuch der Materia Medica".[3] Nowadays, these ancestral practices continue to be part of the popular medicine customs.

Figure I.2.1. Illustration from the National Pharmacy Order of France.

Due to economic reasons and long distances away from larger cities, rural communities continue to turn to traditional plant medicine and use ancestral knowledge of leaves, barks, and fruits properties to alleviate discomfort of the body and mind. An ethnopharmacological study conducted in Côte d'Ivoire, reported the use of 57 plant species in traditional routines to treat malaria infections.[29] South American Indians still chew coca leaves for diverse reasons: energy stimulant, dizziness reliever due to altitude.[30,31] Provided through citrus fruits, ascorbic acid was used to alleviate scurvy affections, and has since been recognized as an essential dietary supplement and is incorporated in daily health practices.[26] These habits and methods have been transmitted through generations and continue to be peregrinated even in the most isolated part of the world. In the French islands of the Caribbean, Guadeloupe and Martinique, the popular

www.manaraa.com

culture refers to leaves from the medicinal garden plants as *Mother's medicine*. Even if Nature is considered to be the mother of life, the alias definitely alludes to the female matriarch of a family valuing the medicinal knowledge learned from the previous generation including mothers and grandmothers in the family lineage. Some well-known and famous of these remedies find their ways in leaves infusions and decoctions as natural treatments for cutaneous, digestive and intestinal affections of all sorts, influenza, or diabetes.[32,33] Some memories of my life on the island involve the seasonal use of some unavoidable medicinal plants for preventive care such as: *Anacardium occidentale* to treat warts and horns, *Chenopodium ambrosioides* as an intestinal anthelmintic, *Cymbopogon citratus* used to relieve cold symptoms as well as digestive agents after heavy meals, and *Chrysophyllum caimito* for diabetes treatment.

a.  **b.**  **c.**  **d.** 

Figure I.2.2. *Anacardium occidentale* **(a.)**, *Chenopodium ambrosioides* **(b.)**, *Cymbopogon citratus* **(c.)**, and *Chrysophyllum caimito* **(d.)**. Photo credits: Henry Joseph.

Another maybe unorthodox but striking use is the rum maceration of *Heliotropium foertherianum* as a potent concoction used in these islands to alleviate the pain emerging from consumption of benthic fish carrying high ciguatoxin concentration.

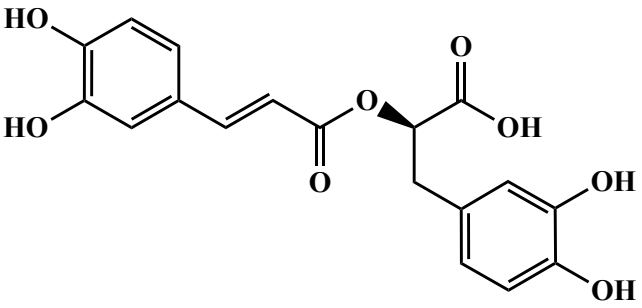

rosmarinic acid

www.manaraa.com

No marketed drug healing ciguatera food poisoning exists thus far, but scientific research has demonstrated the active principal, rosmarinic acid, to successfully flush the ciguatoxin out of the human body.[34] Acting as a competitive inhibitor, it slowly replaces the undesired toxin lodged in the sodium ion channels of the human nervous system cells and re-establishes a healthy physiological equilibrium.[35-36]

One major problem encountered with these popular practices remains the knowledge of the actual active principle responsible for therapeutic effect, and the dosage associated to it. Hence, finding ways to combine pharmacognosy with more conventional medicine could not only promote natural biochemical resources, it could also provide less aggressive health solutions preventing from drug resistance and more efficient options. Blending the knowledge of natural products, which has been around for centuries, with more modern medicine techniques and discoveries, became an essential part of the socio-economic agenda in many countries. American, European, Asian, even Caribbean medical products agencies have been created to evaluate and regulate, societies of pharmacognosy continue to explore ecosystems, discover new molecules, understand their modes of action, and share forthcoming remedies with first the scientific community, then the rest of the world.[37,38]

No panacea has been discovered yet and may not exist, but the idea of finding the cure in the surrounding environments remains a pillar of natural products drug discovery. These discoveries provide options and progress but still require scientific understanding, access to the patients in need, and contingently brings forward drug resistance. All of these are investigated by natural products research and represent the different facets of drug discovery.

Drugs generally fall under the umbrella of medicine. However, any substance with a physiological effect when ingested or otherwise introduced into the body, is considered a drug. Everything can be toxic to some level and, although not necessarily regarded as medicine, edible

www.manaraa.com

goods ought to be considered drugs. They help sustain life but can also become detrimental to human health if ingested in excessive amount or improperly. The presence of certain molecules, also referred to as active principles, are responsible for many physiological responses.[14,38-39] These molecules can be considered or turned into a drug, and what matters most is the tolerable quantity to maintain and preserve a healthy equilibrium. Tolerance, a very subjective notion, becomes inevitably part of the equation to avoid rupture of a healthy equilibrium. Precise quantitative dosage becomes the primordial concept to understand the effect of a drug and control its administration. Identification of a lead compound comprising knowledge of the active principle and its biological effect on targets, fall under the drug discovery stage.

Numbers describing the count of natural products referenced in the literature are increasing on daily basis, which proves the plethora of options offered by nature.[40–44] Even if the mathematics were to be askew, with the whole animal, plant, and microbial, from both land and sea, there is still a wide-open range of niches and opportunities to be explored daily and contribute to drug discovery.[45-46] Once discovered, a drug can then be tested *in vitro* and *in vivo* through animal studies and pre-clinical trials, to determine its biophysical ADME properties governing pharmacokinetics and pharmacodynamics of a compound. Further testing on human beings happens with clinical trials divided in three phases. Upon succeeding these phases, a drug may be approved by regulatory agencies. Currently, the drug approval pipeline may take about 15 years, and amongst 5,000 to 10,000 compounds offered, only one drug will make it to the market.[4,47–50]

Furthermore, studies have explained that more than genetic ruling evolution, there is a prevailing epigenetic phenomenon happening.[51–54] The genetic information evolves through meiosis happening during reproduction. However, as organisms go through their development, mitosis happens to maintain the pool of cells available. During mitosis the genetic information

www.manaraa.com

should be simply duplicated and transmitted to future cell generations. Nevertheless, epigenetic modifications naturally occur and create variations in the blueprints specific to an individual. The environmental conditions and stresses in which living organisms evolve affect the expression of the genetic information ruled by the activation of epigenetic factors. These epigenetic phenomena are responsible for the expression of particular gene factors leading to the production of original and exclusive secondary metabolites involved in survival mechanisms. The constant need for organisms to adapt and improve their living conditions translates into the biosynthesis of peculiar small molecules responsible for their ecological success, called secondary metabolites. The original molecular architectures created keep on expanding the chemical space of natural products and when the pharmaceutical industry has to face drug resistance issues, these compounds provide therapeutic alternatives. Indeed, whether used as is, or as inspiration, natural products constitute more than 50% of the marketed drugs of both marine and terrestrial origin.[40,41,43,55]

Despite the long timeline involved in the process of putting a drug on the market, and the rapid development of drug resistance, natural products research remains a pillar component of drug discovery. The exploration of unknown, understudied, or unappreciated ecosystems are available niches to tap into and increase the odds to find novel chemical options.

I.3. What are Natural Products?

The world of natural products chemistry is founded on interspecies communication and battles offering natural medicinal alternatives to be explored as remedies and exploited with explicit guidelines and instructions.[39,56–61] It encompasses many fields such as ecology, biosynthesis, chemical biology, chemical ecology, and drug discovery. Often, the future of natural products chemistry has been questioned and scientists have addressed the issue with chemical

www.manaraa.com

investigation of living organisms and statistical analyses. Studying ecosystems requires understanding of the trophic relationships between organisms ruled by chemical interactions.

Referred to as small molecule secondary metabolites, natural products are produced by living organisms to specifically contribute to their ecological success.[56,62] While primary metabolites are there to regulate basic day to day needs of an organism to exist, the secondary ones play a subtler role modulating reproduction, defense and survival mechanisms. They are post-translationally modified oligomers encompassing hormones, pheromones, and toxins.[63–65] More than being biochemical mediators, natural products are also proven to be great source of medicines. Throughout the years, pharmacognosy has evolved from terrestrial medicinal plants to microbial ecosystems and more recently marine organisms. Interesting niches for discovery encompass unknown, understudied, and unappreciated ecosystems.[60,66–69]

I.3.1. The Plant Kingdom

Approximately 370,000 different known plant species exist on the planet, and in 2016, the Royal Botanic Gardens, Kew estimated that 17,810 of them have a medicinal use.[70–72] According to the World Health Organization (WHO), globally 80% of people still rely on plant-base traditional medicines for primary health care.[43] A report showed that the uses of up to 80% of the 122 plant derived drugs were related to their original ethnopharmacological purpose.[73–75]

For centuries, alkaloid compounds have been isolated from various plant families and used for a broad range of pharmacological purposes. To name just a few, the aforementioned quinine (Rubiaceae) as antimalarial, morphine (Papaveraceae) as pain reliever, cocaine (Erythroxylacea) and nicotine (Solanaceae) as stimulants.

www.manaraa.com

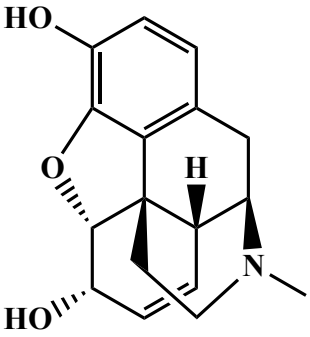

morphine

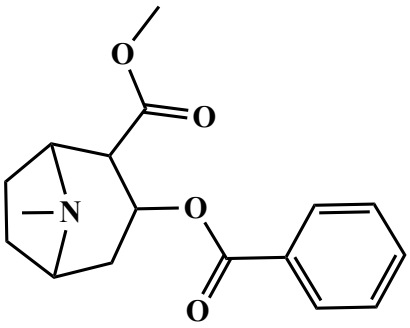

cocaine

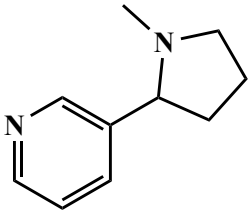

nicotine

Each of them displays nitrogen which place them in the molecular category of alkaloids. Due to the availability of the lone pair of electrons on the nitrogen, the alkalinity character is increased.

Since Antiquity, salicylic acid has been used to treat inflammation. Extracted from willow tree bark, it was not until 1829 that it was isolated in pure form.[76] However, it would cause stomach irritation. In 1853, French chemist Gerhardt synthetized its acylated version called acetyl salicylic acid.[77] Later on, looking for less irritating substitute of salicylic acid, German chemist Hoffmann found out that acetyl salicylic acid would solve the issue.[76,78,79] Acetyl salicylic acid commonly called and available as aspirin was turned into a drug.

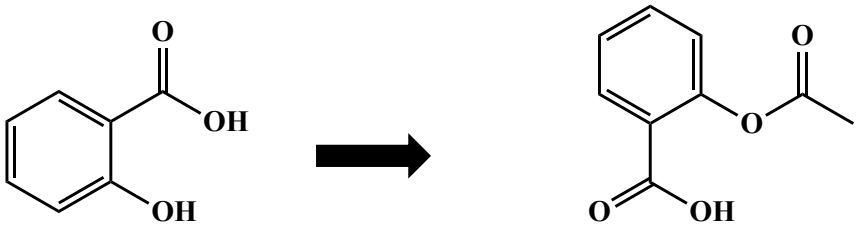

salicylic acid

acetyl salicylic acid

Despite the associated risks, aspirin saw a rebranding from a pain reliever to a heart health medicine and continues to generate sustainable large income for the pharmaceutical industry.[78-81]

www.manaraa.com

The paclitaxel alkaloid, most famous as an anticancer drug and originally isolated from Pacific yew tree bark of *Taxus brevifolia*, was put on the market as Taxol® in 1993.[11,75]

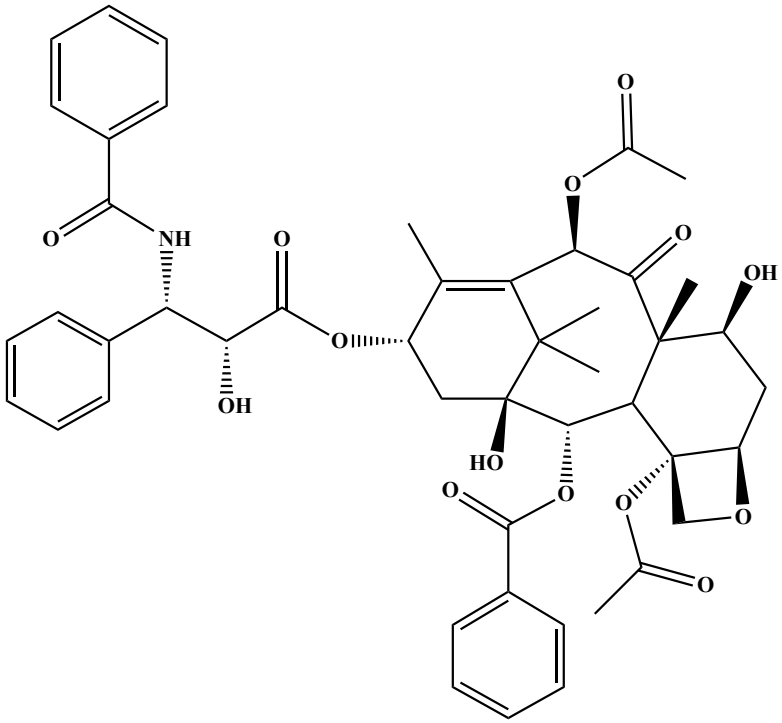

paclitaxel

The non-sustainable wood harvesting for isolation and time-consuming synthesis, called for improved alternative production. After the emergence of practical semisynthetic production routes in the early 1990's, a more recent process was industrialized by cultivating a specific *Taxus* cell-like in fermentation tanks. Despite the fact that paclitaxel has been also reported in many endophytic fungi living in yew trees, its independent production by the endophytes has yet to be confirmed.[82–84]

Metaphorically, macro-organisms can be described as petri dishes, as they enclose a multitude of microorganisms living in symbiosis. The biochemistry available in an organism is intrinsically connected to both the macro and micro world, interacting and contributing to

www.manaraa.com

chemical survival when optimized properly. Various examples have described microorganisms engineered to produce natural products.[85]

I.3.2. Microorganisms

Bacteria and fungi have also provided compounds with medicinal properties. Alexander Fleming's serendipitous discovery of penicillin created sort of an infatuation for the screening of microorganisms which led to the so-called "golden age of antibiotics".[86,87]

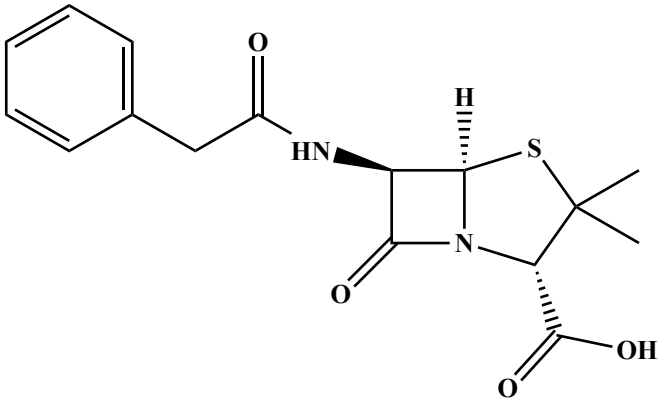

penicillin G

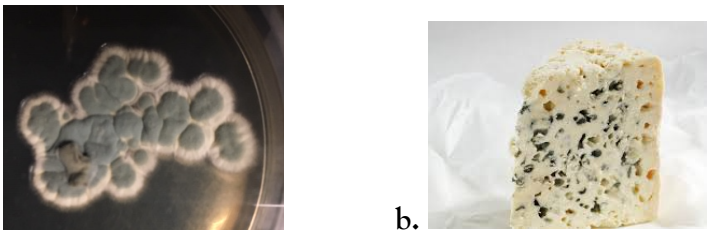

Figure I.3.2. *Penicillium guanacastense* growing on agar in a Petri dish. **(a.)** Penicillin producing fungus on Roquefort cheese **(b.)**. Photo credit: ACDL (2019).

Subsequently, an arsenal of antimicrobial agents was developed; with diverse molecular structures, most of them are used as antibacterial agents. However, microbial secondary metabolites have also served other purposes. [88-90] Lovastatin is a famous fungal secondary metabolite used clinically as statin medication to lower blood cholesterol levels.[49,91] Originally

www.manaraa.com

isolated from red yeast rice, the compound became a trademark by Merck and since has been created in various synthetic analogs.

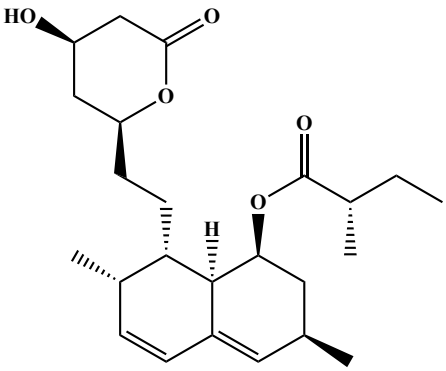

Lovastatin®

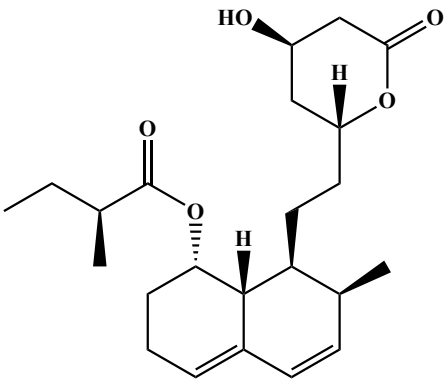

Mevastatin®

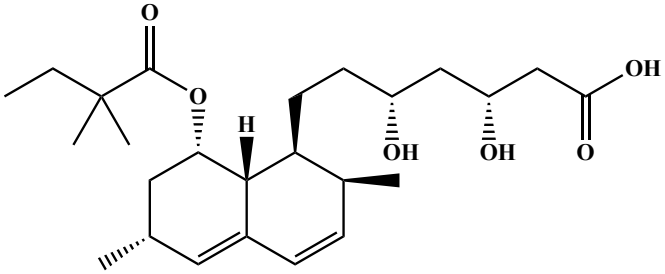

Tenivastatin®

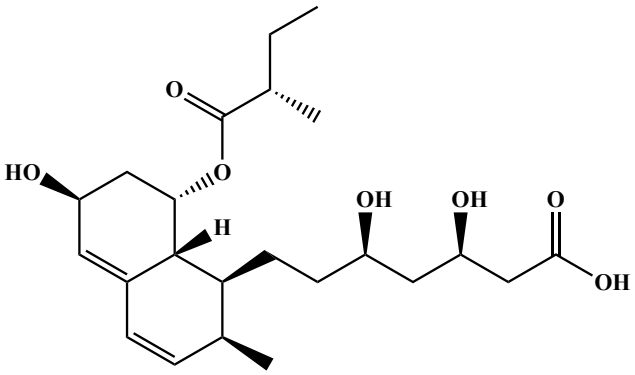

Pravastatin®

www.manaraa.com

The coexistence of macroscopic and microscopic systems, which can sometimes become a hindrance in the understanding of science, actually allows creation of more room for drug discovery. Looking at these endophytes, microorganisms present within larger organisms, became another angle of the natural products drug discovery agenda.[86] The large population of microbes encompasses prokaryotes and eukaryotes, which are responsible for secondary metabolites production representing close to 50,000 known compounds with versatile chemical structures.[92-94] However, when brought into laboratory conditions, these organisms tend to slow down their metabolism. Hence, scientists have recourse to epigenetic techniques affecting DNA transcription patterns responsible for secondary metabolites production.[58,95–97]

Coupled with the rise of antibiotics, drug resistance issues appeared and caused chemists to search for new drug candidates in new environments. Despite the 2% of biomass present in the water covering 70% of planet Earth, the marine ecosystems remain significant niches offering drug discovery opportunities.[98]

I.3.3. Marine Resources

Snorkeling (1960s) followed by the dawn of SCUBA (1970s) certainly helped improve the accessibility of marine resources and created this subdiscipline of natural products chemistry.[68,99,100] Submersibles (1980s) and remotely operated vehicles (ROVs) (1990s) provide daily advancements in the exploration of the marine environment, which has resulted in the isolation of over 30,000 compounds (Dictionary of Marine Natural Products) with unique bioactive structures.[4,43,101,102] Due to the vast environment to be surveyed and the difficulties to access it, equipment cost and performance, as well as drastic living conditions, are obstacles slowing down discovery progress. It is estimated that less than 5% of the deep ocean has been explored.[103,104] Nevertheless, algae, and soft marine invertebrates like corals, sponges, tunicates, nudibranchs, bryozoans, along with their associated microbial communities have generated a

www.manaraa.com

wealth of biologically potent chemicals (anti-inflammatory, antiviral, anticancer activities).[67,100,101,105,106] The following bioactive marine natural products created major drug discovery advances and reinforce their relevance. Some successful stories of approved therapeutics from marine natural products origin include: Prialt® in 2004 from isolated from the venom of the cone snail *Conus magus*, Halaven® in 2010 from the sponge *Halichodria okadai*, and Yondelis® in 2015 from a Caribbean tunicate *Ecteinascidia turbinate*. All are employed to battle discomforts created by cancer.[40,102,106,107]

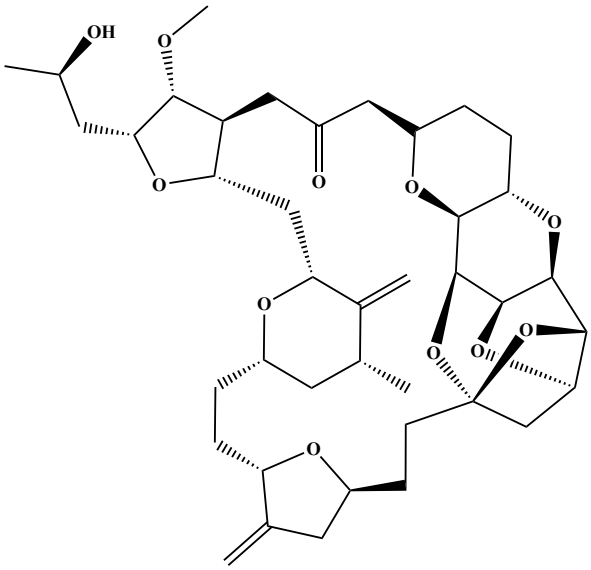

eribulin (Halaven®)

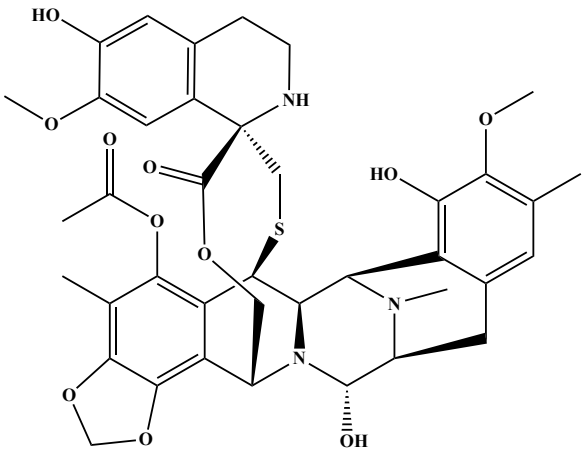

trabectedin (Yondelis®)

Most compounds turn out to be very toxic to human cells and like discussed previously, determination of required and safe dosage is key in the administration of a drug. Biological experiments are modelized to acquire specific parameters useful to evaluate a drug profile.

If organisms are able to deploy biochemical warfare to sustain their ecological survival battling stress and threat caused by predators, the chemical defenses they produce should and must be also potent against human pathogens, describes the founding rationale supporting

www.manaraa.com

natural products research. Finding targets and quantifying the necessary amount must be determined to assess potency of compounds.

I.4. Biological activity assessment

Biological assays evaluate the effect of a substance in a living organism qualitatively or quantitatively. In late 19th century, Paul Ehrlich who introduced the concept of standardization by reactions of living matter, is credited as the inventor of bioassays.[28,108] Since then, the practice of these studies has evolved into a full discipline of drug discovery. When performed quantitatively, these controlled experiments determined the potency of chemical compounds establishing future therapeutic dosage to be consumed. From these calculations arise different values. The mean concentration of a drug inhibiting 50% of a target activity (IC_{50}) and the mean effective dose of a drug necessary to produce a therapeutic effect in 50% of test sample (ED_{50}) describe the potency of drug. Also, the mean lethal dose of a drug required to kill 50% of the test sample (LD_{50}) defines the toxicity of a drug reflected in the so-called cytotoxicity (CC_{50}). In theory, the less toxic a drug is, the easier it can be prescribed, as the side effects will be low. However, very potent drugs like natural products often turn out to be very toxic for cells and require further thorough dosing determination. Hence, expressing the efficacy of a drug using the ratio of undesirable effects over desirable effects, translated as therapeutic index in medical jargon, gives better appreciation of a drug potency in term of safety. Compounds with high ratio will be favored as they will reflect to be safer, less toxic to use. Additional evaluations are necessary throughout the development of a drug. Pharmacodynamics pertain to the biophysical properties of drugs ruling its interactions with target receptors. Pharmacokinetics refer to the process of a drug in the body and include drug absorption, distribution, metabolism, and excretion, all summarized in the term ADME.[109]

www.manaraa.com

Alleviating the administration quantity and process is an additional concern. Essentially, avoiding burden and risk for the patient, the optimization of the amount consumed over time will define the safety and success of a drug. Ultimately, the ideal scenario demands having potent therapeutics with low toxicity for the targeted cells and optimal efficacy limiting the intakes to a minimum. Bioassays promote value of active principles and decide the fate of a medicine through clinical trials. Nature remains the source of unique diversity of chemical entities for pharmaceutical uses but concerns of re-isolation persist. Additionally, availability and access to the primary matter remain major obstacles to be faced.

I.5. Natural Products Chemistry

The performance of natural products chemistry translates into a sequence of actions often resulting in a tedious and time-consuming process. Whether from our own backyard, woods, or bodies of water, it starts with exploration of Nature which calls for adjustments to access the resources. The collection phase allows for preliminary observations telling the tales of chemical language and interactions happening. Back in the lab, extractions and separations are performed using a set of analytical chemistry techniques. Similar to a tea extraction or a coffee brew, the extraction process depends on the choice of solvent or mixture of solvents necessary to the targeted compounds polarity. Separation of the crude extracts obtained is typically more complex and requires more talent, patience, and skills to use more expensive instrumentation. After a partition stage, MPLC acts as prefractionation while HPLC helps purify the fractions.[72,110,111] Upon successful separation leading to the isolation of a pure compound, structure elucidation of the secondary metabolite can begin. Solving structures of unknown compounds entails many spectroscopic techniques such as IR, UV, NMR, MS, and when lucky to obtain a crystal, X-ray crystallography will also help. Structure elucidation is comparable to puzzle solving and demands

www.manaraa.com

perception of molecular signature pattern, deep database search and understanding of fundamental physico-chemical laws.[112]

Although the road leading to a novel pure compound can be tortuous, the elucidation process gives undeniable reward as Nature's never seen before exceptional microscopic creation can be witnessed. Furthermore, biological activity assessed by trained biologists provides value to the compounds isolated.

As part of everyday life, chemistry is considered the glue linking the multiple fields of Science, and natural products chemistry plays an undeniable role in it, by employing connections and collaborations to bring value to Nature's production. Due to all the undertakings involved with the classical approach natural products chemistry, the 21st century has seen the development of dereplication techniques through database searching to timely optimize the elucidation process. [63,112–115] The contributions of computational chemistry combined with mass spectroscopy techniques expand even more the interdisciplinary skills of natural products chemists.

In this thesis, the investigation of two marine organisms selected from two different marine ecosystems displaying opposite hostile conditions, were chemically investigated. Their biological relevance for drug discovery purpose was tested. First, a deep-sea coral was collected via trawling in the deep waters of Antarctica near the Northern Peninsula and the Falkland Islands. Whether tested against pathogens involved in nosocomial infectious or neglected tropical diseases, generally affecting populations from low income regions of the World, the isolated compounds offered a broad spectrum of bioactive chemistry. Then, a tropical mangrove fungal endophyte grown in epigenetically modified conditions was studied. A novel antileishmanial natural product was isolated. Additionally, a metabolomics study utilizing liquid chromatography

www.manaraa.com

and tandem mass spectroscopy method, was developed with the aim to optimize the production of a targeted isolated antileishmanial secondary metabolite.

References

(1) Leonti, M.; Verpoorte, R. Traditional mediterranean and european herbal medicines. *J. Ethnopharmacol.* **2017**, *199*, 161–167.

(2) Fortineau, A. D. Chemistry perfumes your daily life. *J. Chem. Ed.* **2004**, *81*, 45-50.

(3) Alamgir, A. N. M. Therapeutic use of medicinal plants and their extracts. Springer: Cham, **2017**, *71*. ISBN 978-3-319-63861-4

(4) Jiménez, C. Marine natural products in medicinal chemistry. *ACS Med. Chem. Lett.* **2018**, *9*, 959–961.

(5) Robert Thayer Sataloff. *Professional Voice*, Fourth.; Plural Publishing: San Diego, **2017**.

(6) Dias, D. A.; Urban, S.; Roessner, U. A historical overview of natural products in drug discovery. *Metabolites* **2012**, *2*, 303-336.

(7) Jaiswal, Y. S.; Williams, L. L. A glimpse of ayurveda – The forgotten history and principles of indian traditional medicine. *J. Tradit. Complement. Med.* **2017**, *7*, 50–53.

(8) Patwardhan, B.; Vaidya, A. D. B.; Chorghade, M. Ayurveda and natural products drug discovery. *Curr. Sci.* **2004**, *86*, 789–799.

(9) Mukherjee, P. K. Evaluation of Indian traditional medicine. *Ther. Innov. Regul. Sci.* **2001**, *35*, 623–632.

(10) Tang, C.; Ye, Y.; Feng, Y.; Quinn, R. J. TCM, Brain function and drug space. *Nat. Prod. Rep.* **2016**, *33*, 6–25.

(11) Yuan, H.; Ma, Q.; Ye, L.; Piao, G. The traditional medicine and modern medicine from

www.manaraa.com

natural products. *Molecules* **2016**, *21*, 559.

(12) Hajar, R.; Lewis, J. The air of history (Part II) medicine in the middle ages. **2019**, *13* (Part II), 158–162.

(13) Bulletin of the Institute. General Medicine. **2019**, *5*, 201–246.

(14) Zunic, L.; Skrbo, A.; Dobraca, A. Historical contribution of pharmaceutics to botany and pharmacognosy development. *Mater. Socio Medica* **2017**, *29*, 291.

(15) Byrne, E. H. West, M. Medicine in the roman army. *The Classical Association of the Middle West and South , Inc . (CAMWS)* Https://Www.Jstor.Org/Stable/3286964. **2019**, *5*, 267–272.

(16) Cilliers, L.; Culture, C. The evolution of the hospital from antiquity to the end of the middle ages. *Curationis*, **2002**, *25*, 60-66.

(17) Benini, Arnaldo & Bonar, S. K. Andreas Vesalius 1514-1564. *SPINE*. **1996**, *21*, 1388-1393.

(18) Drucker, C. B. Ambroise Paré and the birth of the gentle art of surgery. **2008**, *81*, 199–202.

(19) Hospital, D. R.; Oak, S. Premier chirurgien du roi: the life of Ambroise Pare (1510-1590). **1992**, *85* (May), 292–294.

(20) Hudson, M. M.; Morton, R. S. Fracastoro and syphilis : 500 years on. **1996**, *348*, 1495–1496.

(21) Bardell, D. The invention of the microscope. *Beta Biological Society*. Https://Www.Jstor.Org/Stable/4608700 The Invention of the Microscope. **2019**, *75*, 78–84.

(22) Achan, J.; Talisuna, A. O.; Erhart, A.; Yeka, A.; Tibenderana, J. K.; Baliraine, F. N.; Rosenthal, P. J.; D'Alessandro, U. Quinine, an old anti-malarial drug in a modern world: role in the treatment of malaria. *Malar. J.* **2011**, *10*, 144.

www.manaraa.com

(23) Seeman, J. I. The Woodward-Doering/Rabe-Kindler total synthesis of quinine: setting the record straight. *Angew. Chemie - Int. Ed.* **2007**, *46*, 1378–1413.

(24) Smith, K. A. Louis Pasteur, the father of immunology ? **2012**, *3* (April), 1–10.

(25) Berche, P. Louis Pasteur, from crystals of life to vaccination. **2012**, 1–6.

(26) Arrigoni, O.; Tullio, M. C. De. Ascorbic Acid : much more than just an antioxidant. **2002**, *1569*, 1–9.

(27) Koch, R. Tubercle bacillus, 1882. **1982**, 246–251.

(28) Beaven, M. A. Review our perception of the mast cell from paul ehrlich to now. **2009**, 11–25.

(29) Bi, F. H. T. Étude ethnopharmacologique de plantes antipaludiques utilisées en médecine traditionnelle chez les Abbey et Krobou d ' Agboville (Côte d ' Ivoire) Résumé. **2009**, *22*, 42–50.

(30) Weil, A. T. The therapeutic value of coca in contemporary medicine. *J. Ethnopharmacol.* **1981**, *3*, 367–376.

(31) Plowman, T. Efectos sobre las personas y las políticas en américa latina. *Acad. Manag. Annu. Meet. Proc.* **2006**, 1–11.

(32) Bougerol, C. Données de médecine populaire à la Guadeloupe. 163–183.

(33) Sylvestre, M.; Pichette, A.; Longtin, A.; Nagau, F.; Legault, J. Essential oil analysis and anticancer activity of leaf essential oil of croton flavens l. from Guadeloupe. *J. Ethnopharmacol.* **2006**, *103*, 99–102.

(34) Rossi, F.; Jullian, V.; Pawlowiez, R.; Kumar-Roin, S.; Haddad, M.; Darius, H. T.; Gaertner-Mazouni, N.; Chinain, M.; Laurent, D. Protective effect of *Heliotropium foertherianum* (boraginaceae) folk remedy and its active compound, rosmarinic acid, against a pacific ciguatoxin. *J. Ethnopharmacol.* **2012**, *143*, 33–40.

www.manaraa.com

(35) Krajčovičová, Z.; Meluš, V. Bioactivity and potential health benefits of rosmarinic acid. *Univ. Rev.* **2013**, *7*, 8–14.

(36) Amoah, S.; Sandjo, L.; Kratz, J.; Biavatti, M. Rosmarinic acid, pharmaceutical and clinical aspects. *Planta Med.* **2016**, *82* , 388–406.

(37) Badal, S.; Smith, K. N. Pharmacognosy learn more about pharmacognosy areas of science embraced by pharma- cognosy background to pharmacognosy. **2017**. ISBN 978-0-12-802104-0

(38) Balogun, F. O.; Ashafa, A. O. T.; Sabiu, S.; Ajao, A. A.; Perumal, C. P.; Kazeem, M. I.; Adedeji, A. A. Pharmacognosy: importance and drawbacks. *Pharmacogn. Med. Plants.* **2019**.

(39) Raguso, R.; Agrawal, A.; Douglas, A.; Jander, G.; Kessler, A.; Poveda, K.; Thaler, J. The raison d ' être of chemical ecology. *Ecology* **2015**, *96*, 617–630.

(40) Newman, D. J.; Cragg, G. M. Natural products as sources of new drugs over the last 25 years. *J. Nat. Prod.* **2007**, *70*, 461–477.

(41) Newman, D. J.; Cragg, G. M. natural products as sources of new drugs from 1981 to 2014. *J. Nat. Prod.* **2016**, *79*, 629–661.

(42) Gerwick, William H., Moore, B. H. Products drug discovery and chemical biology. *ACS Chem. Biol.* **2013**, *19*, 85–98.

(43) Cragg, G. M.; Newman, D. J. Medicinals for the millennia: the historical record. *Ann. N. Y. Acad. Sci.* **2001**, *953*, 3–25.

(44) Bade, R.; Chan, H. F.; Reynisson, J. Characteristics of known drug space. Natural products, their derivatives and synthetic drugs. *Eur. J. Med. Chem.* **2010**, *45*, 5646–5652.

(45) Pye, C. R.; Bertin, M. J.; Lokey, R. S.; Gerwick, W. H.; Linington, R. G. Retrospective analysis of natural products provides insights for future discovery trends. *Proc. Natl. Acad. Sci.* **2017**, *114*, 5601–5606.

www.manaraa.com

(46) Hawksworth, D. L. The magnitude of fungal diversity: the 1.5 million species estimate revisited. *Mycol. Res.* **2001**, *105*, 1422–1432.

(47) Khanna, I. Drug discovery in pharmaceutical industry: productivity challenges and trends. *Drug Discov. Today* **2012**, *17*, 1088–1102.

(48) David, B.; Wolfender, J.-L.; Dias, D. A. The pharmaceutical industry and natural products: historical status and new trends. *Phytochem. Rev.* **2015**, *14*, 299–315.

(49) Patridge, E.; Gareiss, P.; Kinch, M. S.; Hoyer, D. Natural products and their derivatives. *Drug Discov. Today.* **2016**, *21*, 204-207.

(50) Butler, M. S.; Robertson, A. A. B.; Cooper, M. A. Natural product and natural product derived drugs in clinical trials. *Nat. Prod. Rep.* **2014**, *31*, 1612–1661.

(51) Jones, P. A.; Takai, D. The role of DNA methylation in mammalian epigenetics. *Science.* **2001**, *293*, 1068–1070.

(52) Bird, A. DNA methylation patterns and epigenetic memory. *Genes Dev.* **2002**, *16*, 6–21.

(53) Wolfe, A. P.; Matzke, M. A. Epigenetics: regulation through repression. *Science.* **2001**, *286*, 481–486.

(54) Li, G.; Lou, H. X. Strategies to diversify natural products for drug discovery. *Medicinal Research Reviews*. John Wiley and Sons Inc. July 1, **2018**, 1255–1294.

(55) Cragg, G. M. Natural Products. A history of success and continuing promise for drug discovery and development. *Planta Medica*. **2014**, *80*, 43.

(56) Clardy, J. The chemistry of signal transduction. *Proc. Natl. Acad. Sci. U. S. A.* **1995**, *92*, 56–61.

(57) Amsler, C. D.; Mcclintock, J. B.; Baker, B. J. Chemical mediation of mutualistic interactions between macroalgae and mesograzers structure unique coastal communities along the western antarctic peninsula. *J. Phycol.* **2014**, *50*, 1–10.

www.manaraa.com

(58) Reen, F. J.; Romano, S.; Dobson, A. D. W.; O'Gara, F. The sound of silence: activating silent biosynthetic gene clusters in marine microorganisms. *Marine Drugs*. MDPI AG August 1, **2015**, 4754–4783.

(59) Dahms, H. U.; Dobretsov, S. Antifouling compounds from marine macroalgae. *Mar. Drugs* **2017**, *15*, 265.

(60) Salini, G. Pharmacological profile of mangrove endophytes - a review. *Int. J. Pharm. Pharm. Sci.* **2014**, *7*, 6–15.

(61) Newman, D. J.; Cragg, G. M. Marine natural products and related compounds in clinical and advanced preclinical trials. *J. Nat. Prod.* **2004**, *67*, 1216–1238.

(62) Williams, D. H.; Stone, M. J.; Hauck, P. R.; Rahman, S. K. Why are secondary metabolites (natural products) biosynthesized? *J. Nat. Prod.* **1989**, *52*, 1189–1208.

(63) Ziemert, N.; Alanjary, M.; Weber, T. The evolution of genome mining in microbes-a review. *Natural Product Reports*. **2016**, 988–1005.

(64) Bouslimani, A.; Sanchez, L. M.; Garg, N.; Dorrestein, P. C. Mass spectrometry of natural products: current, emerging and future technologies. *Nat. Prod. Rep.* **2014**, *31*, 718–729.

(65) Haliński, Ł.; Czerwicka, M.; Stepnowski, P. Współczesne metody ekstrakcji, izolacji i analizy metabolitów wtórnych roślin. *Żywność Nauk. Technol. Jakość* **2017**, *1*, 40–43.

(66) Invertebrates, M.; Blunt, J. W.; Copp, B. R.; Munro, M. H. G.; Northcote, T.; Hu, W.-P.; Munro, M. H. G.; Northcote, P. T.; Prinsep, M. R. Marine natural products. *Nat. Prod. Rep.* **2007**, *24*, 111–112.

(67) Blunt, J. W.; Carroll, A. R.; Copp, B. R.; Davis, R. A.; Keyzers, R. A.; Prinsep, M. R. Marine natural products. *Nat. Prod. Rep.* **2018**, *35*, 8–53.

(68) Pawlik, J. R.; Amsler, C. D.; Ritson-W, R.; McClintock, J. B.; Baker, B. J.; Paul, V. J. Marine chemical ecology: a science born of scuba. *Smithsonian Contributions to the Marine Sciences.*

www.manaraa.com

2013, *17*, 53-60.

(69) Liu, J.-T.; Lu, X.-L.; Liu, X.-Y.; Gao, Y.; Hu, B.; Jiao, B.-H.; Zheng, H. Bioactive natural products from the antarctic and arctic organisms. *Mini-Reviews Med. Chem.* **2013**, *13*, 617–626.

(70) Pennisi, E. Tending the global garden. *Science.* **2010**, *329* (5997), 1274–1277.

(71) Stearn, W. T. The self-taught botanists who saved the kew botanic garden. *Taxon* **1965**, *14*, 293–298.

(72) Bucar, F.; Wube, A.; Schmid, M. Natural product isolation-how to get from biological material to pure compounds. *Nat. Prod. Rep.* **2013**, *30*, 525–545.

(73) Farnsworth, N. R.; Akerele, O.; Bingel, A. S.; Soejarto, D. D.; Guo, Z. Medicinal plants in therapy. *Bull. World Health Organ.* **1985**, *63*, 965–981.

(74) Fabricant, D. S.; Farnsworth, N. R. The Value of Plants used in Traditional Medicine for drug discovery. **2001**, *109*, 69–75.

(75) McChesney, J. D.; Venkataraman, S. K.; Henri, J. T. Plant Natural Products: Back to the future or into extinction? *Phytochemistry* **2007**, *68*, 2015–2022.

(76) Connelly, D. A History of aspirin. *Clin. Pharm.* **2014**, *6*, 166–167.

(77) Lichterman, B. L. Aspirin: the story of a wonder drug. *BMJ.* **2004**, *329*, 1408–1411.

(78) Sneader, W. The discovery of aspirin: a reappraisal. *Br. Med. J.* **2000**, *321*, 1591–1594.

(79) Jones, A. W. Early drug discovery and the rise of pharmaceutical chemistry. *Drug Test. Anal.* **2011**, *3*, 337-344.

(81) Carleen, H. Take two aspirin and tweet me in the morning: how twitter, facebook, and other social media are reshaping health care. *Health Aff.* **2019**, *28*, 361.

(82) Engels, B.; Dahm, P.; Jennewein, S. Metabolic engineering of taxadiene biosynthesis in yeast as a first step towards taxol (paclitaxel) production. *Metab. Eng.* **2008**, *10*, 201–206.

www.manaraa.com

(83) Zhong, J. J. Plant cell culture for production of paclitaxel and other taxanes. *J. Biosci. Bioeng.* **2002**, *94*, 591–599.

(84) Howat, S.; Park, B.; Oh, I. S.; Jin, Y. W.; Lee, E. K.; Loake, G. J. Paclitaxel: biosynthesis, production and future prospects. *N. Biotechnol.* **2014**, *31*, 242–245.

(85) Beau, J.; Mahid, N.; Burda, W. N.; Harrington, L.; Shaw, L. N.; Mutka, T.; Kyle, D. E.; Barisic, B.; Van Olphen, A.; Baker, B. J. Epigenetic tailoring for the production of anti-infective cytosporones from the marine fungus *Leucostoma persoonii*. *Mar. Drugs* **2012**, *10*, 762–774

(86) Katz, L.; Baltz, R. H. Natural product discovery: past, present, and future. *J. Ind. Microbiol. Biotechnol.* **2016**, *43*, 155–176.

(87) Shen, B. A New golden age of natural products drug discovery. *Cell* **2015**, *163*, 1297–1300.

(88) Sharma, N.; Sharma, V.; Abrol, V.; Panghal, A.; Jaglan, S. An update on bioactive natural products from endophytic fungi of medicinal plants. In *Pharmaceuticals from Microbes: Impact on Drug Discovery. Environmental Chemistry for a Sustainable World. Springer International Publishing*: **2019**, 121–153.

(89) Gao, H.; Li, G.; Lou, H.-X. X. Structural diversity and biological activities of novel secondary metabolites from endophytes. *Molecules.* **2018**, *23*, 646.

(90) Lowe, D. Modifying natural products. *Science Translational Medicine*. **2019**.

(91) Patridge, E.; Gareiss, P.; Kinch, M. S.; Hoyer, D. An analysis of fda-approved drugs: natural products and their derivatives. *Drug Discov. Today.* **2016**, *21*, 204–207.

(92) Gouda, S.; Das, G.; Sen, S. K.; Shin, H.-S.; Patra, J. K. Endophytes: A treasure house of bioactive compounds of medicinal importance. *Front. Microbiol.* **2016**, *7*, 1538.

(93) Henkel, T.; Brunne, R. M.; Müller, H.; Reichel, F. Statistical investigation into the structural complementarity of natural products and synthetic compounds. *Angew. Chemie -*

www.manaraa.com

Int. Ed. **1999**, *38*, 643–647.

(94) Patridge, E.; Gareiss, P.; Kinch, M. S.; Hoyer, D. An analysis of fda-approved drugs: natural products and their derivatives. *Drug Discovery Today*. 2016, *21*, 204-207.

(95) Williams, R. B.; Henrikson, J. C.; Hoover, A. R.; Lee, A. E.; Cichewicz, R. H. Epigenetic remodeling of the fungal secondary metabolome. *Org. Biomol. Chem.* **2008**, *6*, 1895–1997.

(96) Henrikson, J. C.; Hoover, A. R.; Matthew Joyner, P. M.; Cichewicz, R. H. A chemical epigenetics approach for engineering the in situ biosynthesis of a cryptic natural product from *Aspergillus niger*. *Org. Biomol. Chem.* **2009**, *7*, 435–438.

(97) Demers, D. H.; Knestrick, M. A.; Fleeman, R.; Tawfik, R.; Azhari, A.; Souza, A.; Vesely, B.; Netherton, M.; Gupta, R.; Colon, B. L.; et al. Exploitation of mangrove endophytic fungi for infectious disease drug discovery. *Mar. Drugs* **2018**, *16*, 376.

(98) Dewi, A. S.; Tarman, K.; Uria, A. R. Marine natural products : prospects and impacts on the sustainable development in Indonesia. *Proceeding Indones. students' scientific Meet.* **2008**, *May*, 54–63.

(99) Tsao, F.; Morgan, L. E. Deep-sea corals corals that live on mountaintops. **2005**, *21*, 9-11.

(100) Malve, H. Exploring the ocean for new drug developments: marine pharmacology. J. Pharm. Bio. allied Sci. **2016**, *8*, 83-91.

(101) Montaser, R.; Luesch, H. Marine natural products: a new wave of drugs? *Future Med. Chem.* **2011**, *3*, 1475–1489

(102) Martins, A.; Vieira, H.; Gaspar, H.; Santos, S. Marketed marine natural products in the pharmaceutical and cosmeceutical industries: tips for success. *Marine Drugs*. February **2014**, pp 1066–1101.

(103) NOAA. How much of the ocean have we explored? Https://Oceanservice.Noaa.Gov/Facts/Exploration.Html,07/11/18.

www.manaraa.com

(104) Sen Nag, Oishimaya. "How much of the ocean have we explored?" WorldAtlas. **2018**. https://www.worldatlas.com/articles/how-much-of-the-ocean-is-still-unexplored.html

(105) Look, S. A.; Fenical, W.; Jacobs, R. S.; Clardy, J. The pseudopterosins: anti-inflammatory and analgesic natural products from the sea whip *Pseudopterogorgia elisabethae*. *Proc. Natl. Acad. Sci. U. S. A.* **1986**, *83*, 6238–6240.

(106) Molinski, T. F.; Dalisay, D. S.; Lievens, S. L.; Saludes, J. P. Drug development from marine natural products. *Nat. Rev. Drug Discov.* **2009**, *8*, 69–85.

(107) Newman, D. J. Developing natural product drugs: supply problems and how they have been overcome. *Pharmacol. Ther.* **2016**, *162*, 1–9.

(108) Beaven, M. A. Our perception of the mast cell from paul ehrlich to now. *Eur. J. Immunol.* **2009**, *39*, 11–25.

(109) Cannon, J. G. An introduction to medicinal chemistry By Graham L. Patrick, G. L. Oxford University Press, New York. 1995. ISBN 0-19-855872-4. *J. Med. Chem.* **1996**, *39*, 4131–4132.

(110) Bowman, J. M.; Braxton, M. S.; Churchill, M. A.; Hellie, J. D.; Starrett, S. J.; Causby, G. Y.; Ellis, D. J.; Ensley, S. D.; Maness, S. J.; Meyer, C. D.; et al. Extraction method for the isolation of terpenes from plant tissue and subsequent determination by gas chromatography. *Microchem. J.* **1997**, *56*, 10–18.

(111) Zhang, Q. W.; Lin, L. G.; Ye, W. C. Techniques for extraction and isolation of natural products: a comprehensive review. *Chinese Medicine (United Kingdom).* **2018**, *13*.

(112) McAlpine, J. B.; Chen, S.-N.; Kutateladze, A.; MacMillan, J. B.; Appendino, G.; Barison, A.; Beniddir, M. A.; Biavatti, M. W.; Bluml, S.; Boufridi, A.; et al. The value of universally available raw nmr data for transparency, reproducibility, and integrity in natural product research. *Nat. Prod. Rep.* **2019**, *36*, 35–107.

www.manaraa.com

(113) Grim, C. M.; Luu, G. T.; Sanchez, L. M. Staring into the void: demystifying microbial metabolomics. *FEMS Microbiol. Lett.* **2019**, *366*.

(114) Wolfender, J. L.; Marti, G.; Thomas, A.; Bertrand, S. Current approaches and challenges for the metabolite profiling of complex natural extracts. *Journal of Chromatography A*. Elsevier February 20, **2015**, 136–164.

(115) Hur, M.; Campbell, A. A.; Almeida-De-Macedo, M.; Li, L.; Ransom, N.; Jose, A.; Crispin, M.; Nikolau, B. J.; Wurtele, E. S. A global approach to analysis and interpretation of metabolic data for plant natural product discovery. *Nat. Prod. Rep.* **2013**, *30*, 565–583.

www.manaraa.com

CHAPTER TWO:

TARGETED DISEASES

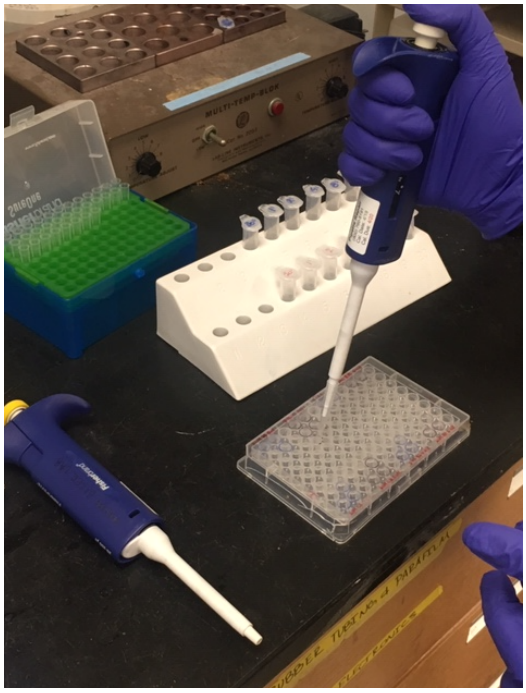

Figure II.1. Biological assays 96 well plate preparation. Photo credit: ACDL (2019).

The development of biological assay metrics and statistics requires biologists to test the molecules isolated by chemists, all assisted by engineered technology; this is another proof of the interdisciplinary characteristics of natural products drug discovery. In this thesis, the biological relevance of the isolated pure compounds was assessed against five targeted infectious diseases pathogens.

www.manaraa.com

II.1. Leishmaniasis

Found in over 90 countries spread over the tropics, subtropics, and Mediterranean zones, leishmaniasis is referred to as a parasitic neglected tropical disease.[1,2] With 25,000 to 65,000 estimated annual fatalities, it affects the poorest people on the planet.[1] Transferred to mammals through the bite of a female phlebotomine sand fly, the *Leishmania* sp. protozoan parasites invade macrophage cells and asexually multiply by simple division. Biological assays related to this thesis were conducted on the *Leishmania donovani* parasite. However, more than 20 species are pathogenic to human, including: *L. chagasi*, *L. mexicana*, *L. amazonensis*, *L. venezuelensis*, *L. tropica*, *L. major*, *L. viannia*, *L. braziliensis*, *L. guyanensis*, *L. panamensis*, and *L. peruviana*. They can generate three forms of the disease: cutaneous (CL), mucosal (ML), and the most serious form, visceral (VL), also known as Kala-Azar.[3-5] Leishmaniasis traces back to 1885 BC and is referred to as the "Nile Pimple" in Ebers Papyrus,[6] it became known successively as oriental sore around the 7th century BC, then Balkh sore, to leishmaniasis more recently. While the disease vector was described by Bonnani in 1691, detailed clinical explanations appeared only later on. In 1756, Alexander Russel provided the first description of cutaneous leishmaniasis, but Kala-Azar was not noticed until 1824 in Jessore in India.[7] At first confused with malaria, leishmaniasis does not actually respond to quinine treatment. The multiple species and subspecies of the Leishmania protozoa produce different degree of virulence and clinical effects, which require a tailored treatment for each patient. Clinical pattern, drug resistance, geography, parasite strain, immunologic status, and previous treatment are the various parameters to be taken in account. Parenteral and oral medications are the main currently available options, with high toxicity and expensive cost.[5,8] Pregnant women, children and patients with secondary or co-infections must face the scarcity of suitable treatment and often lose the battle against the infection.[9-11] All these obstacles continue to motivate the search for alternative therapeutic agents.

www.manaraa.com

In 1912, Gaspar Vianna introduced tartar emetic, chemically named antimony potassium tartrate, as treatment CL and ML in Brazil.

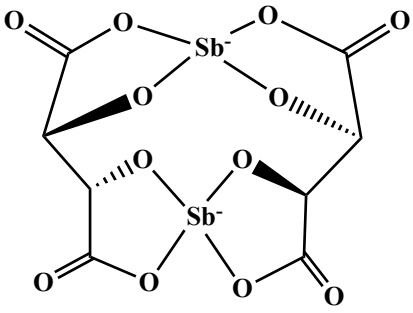

antimony potassium tartrate

Less than ten years later, Upendranath Brahmachari synthesized urea stibamine, a pentavalent antimony compound with chemotherapeutic properties against VL.[7]

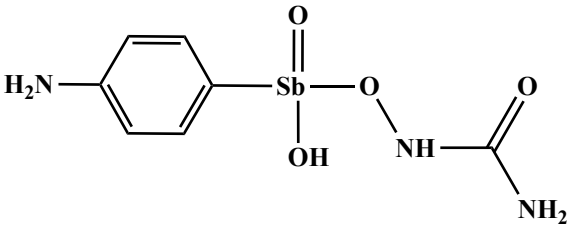

urea stibamine

These drug discovery advances allowed subsequent development of antiparasitic pentavalent antimonial agents in 1937 such as sodium stibogluconate (Pentostam®) in the United Kingdom and meglumine antimonate (Glucantime®) in France, but not FDA approved.[4,12–15]

www.manaraa.com

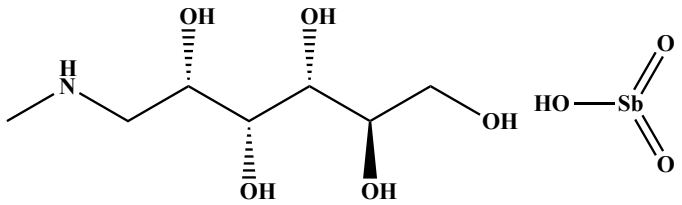

meglumine antimonate

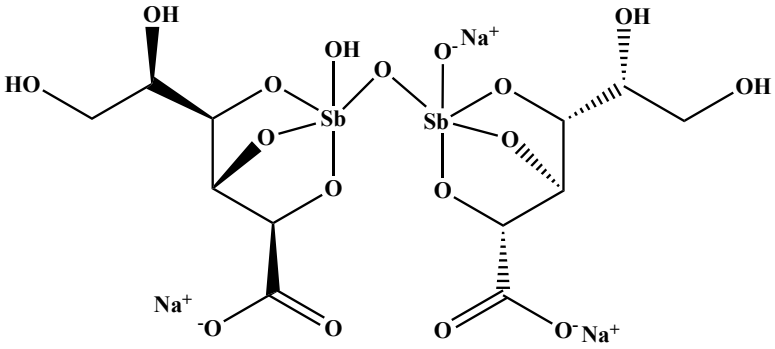

sodium stibogluconate

Intravenously administered, they are recommended in the treatment of any form of leishmaniasis. However, development of stibogluconate resistance prevents their use in certain geographical areas like India.[16,17]

In case of resistance to pentavalent antimonial agents in ML and VL, injections of amphotericin B is the effective alternative.[8,14,18]

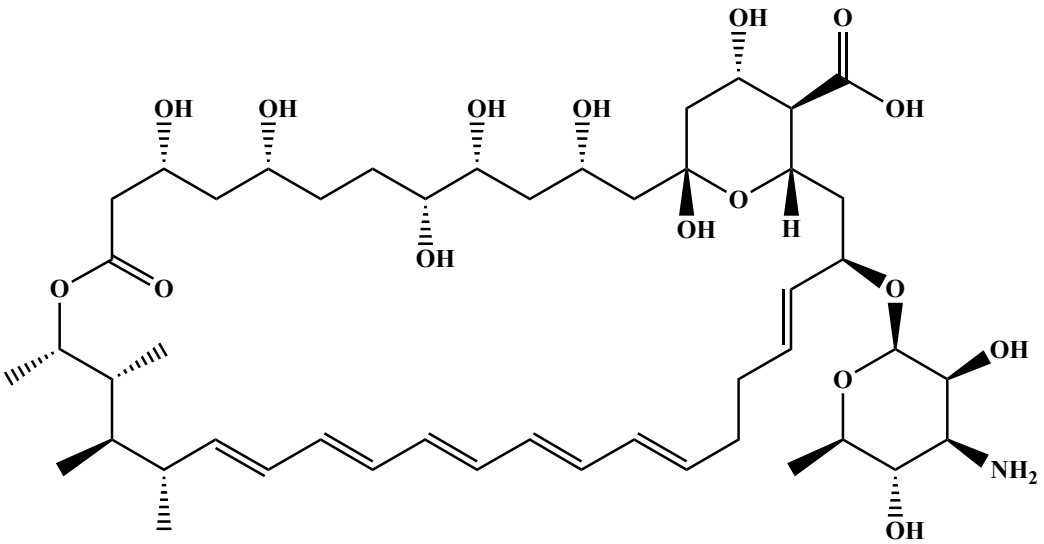

amphotericin B

www.manaraa.com

The associated toxic adverse effects motivated formulation improvement[19] and led to the development of lipidic complex, liposomal,[20] and colloidal dispersion forms[21] of amphotericin B in the 1990s.[4,4,11,22] The new lipidic formulations of the drug have proven more active and tolerated in the treatment of VL, but given mixed results with CL, and remain still expensive. One liposome can compete with 15 injections of conventional amphotericin B.[4,17,23] Also, studies have showed a single dose of liposomal amphotericin B to be 90% effective in curing with low adverse effects, making it the drug of choice in the Kala-Azar Programme of India.[24,25] Furthermore, combination of it with other antileishmanial drugs seems to provide a similar rate of efficacy with safer and cheaper treatment.

Orally administered and more affordable, miltefosine[4,13,14,26,27] was put on the market in 2002 and has shown 94% efficacy in curing compared to 97% amphotericin B, but it well tolerated by patients with VL.[28–31]

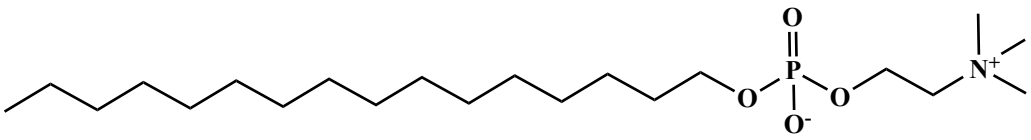

Miltefosine®

As a phosphocholine analogue, it interacts with membrane synthesis and signal production. However, longer treatment periods are required which can lead to gastrointestinal distress.

Used topically in cases of low spreading potential CL, paromomycin's antileishmanial activity was discovered since 1960, but it was not until recently in 2006, that it became part of the treatment against leishmaniasis.[7,12,14,29]

www.manaraa.com

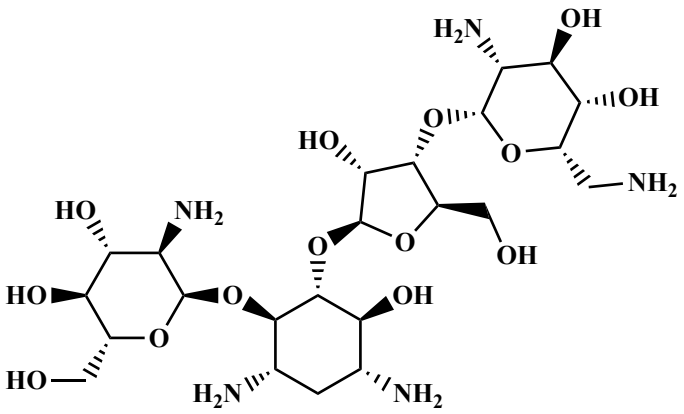

Paromomycin®

More invasive lesions would require more aggressive antimonial agents or even miltefosine alone. Combination with gentamicin or methyl benzethonium chloride have also proven successful.[33]

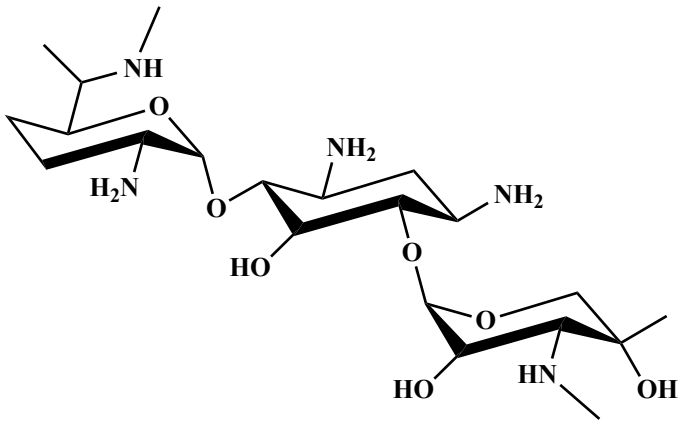

Gentamicin®

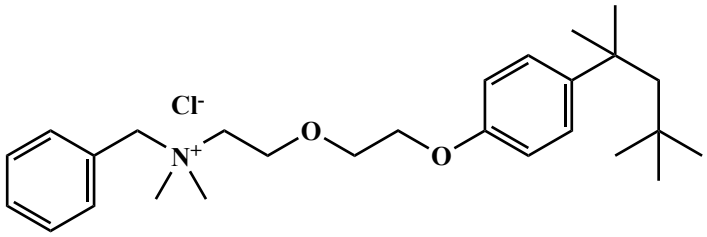

methyl benzethonium chloride

www.manaraa.com

Intramuscular pentamidine treatment has also prescribed in the treatment of VL where antimonial resistance prevails.[14,18,34,35]

However, persistent diabetes mellitus and disease recurrence may be the undesired side effects associated to its use.

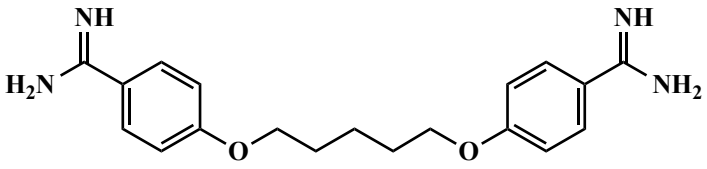

pentamidine

Isethionate and mesylate forms of Pentamidine antibiotic preparations exist under two chemical forms: isethionate (Pentam®) and the more effective mesylate (Lomidine®) and may be used in the treatment of CL and sometime an alternative in VL.[10,14,18,41,42]

The affordable therapeutic alternatives Ketoconazole,[13,34,36] itraconazole,[13,18] fluconazole,[37,38] and allopurinol,[18,34] are also used in canine treatment of the disease. Not as effective as pentavalent antimonial compounds, these drugs' efficacies are contingent upon parasitic strain, offering minimal adverse complementary effects while accelerating the healing phase.

www.manaraa.com

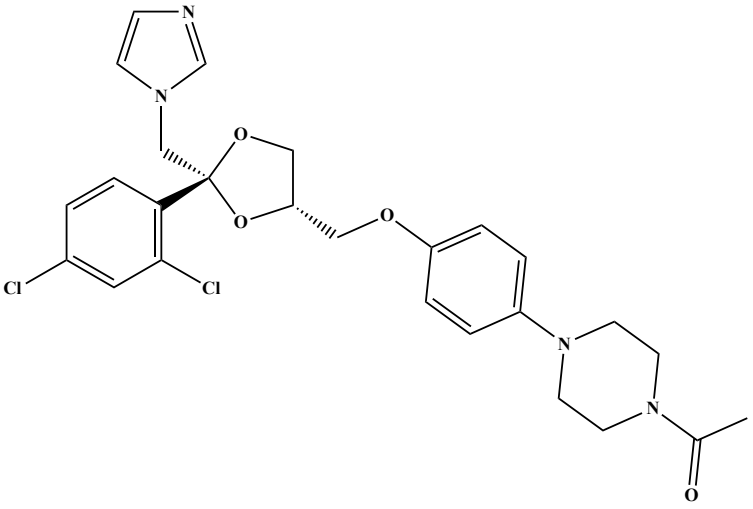

ketoconazole

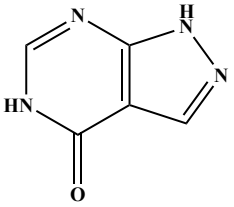

allopurinol

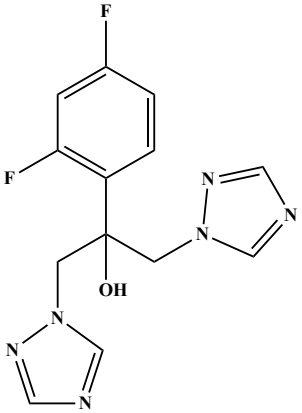

fluconazole

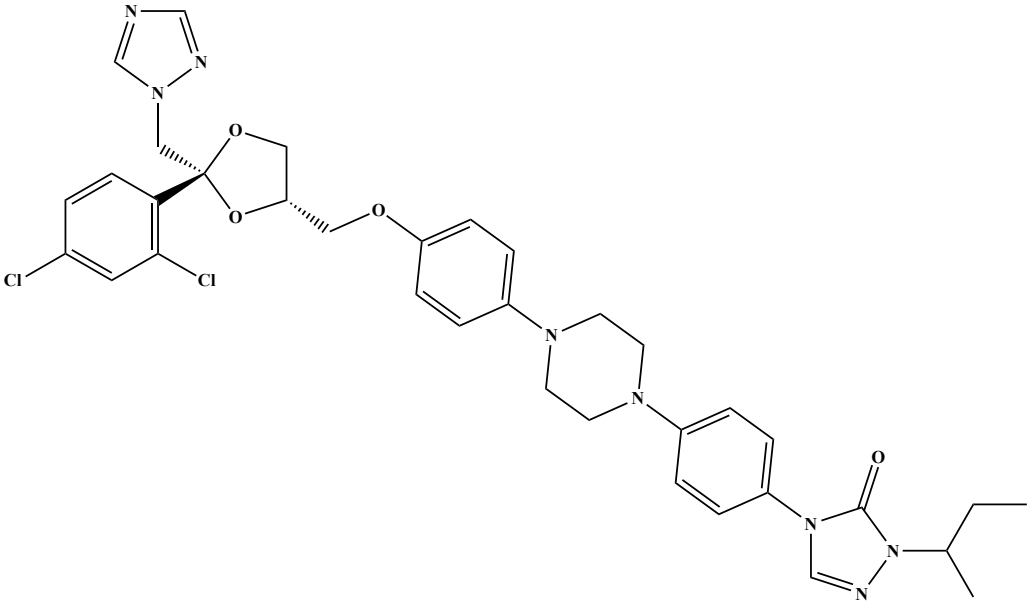

itraconazole

www.manaraa.com

Some successful cases have been recorded but again, parasite strain dependency seems to be the major factor affecting efficacy.

Looking at the current marketed antileishmanial drugs, nitrogen and antimony are important elements of these compounds exerting alkaline chemical properties. More recently, marine natural products drug discovery has pointed toward polycyclic terpenoids small molecules as potent compounds.[10] Research in our lab has confirmed this trend with the chemical investigations of various Antarctic invertebrates like sponges[43] and corals[44,45] which have provided a range of potent antileishmanial chemistry. Moreover, further described in this thesis, the tropical mangrove fungal endophyte *Penicillium guanacastense* has also contributed to additional potency against the *Leishmania donovani* parasite.

Also, synthetic analogs continue to be explored and have offered significant potency. Related to peptidic chemistry, the novel class of arylimidamide compounds inhibited at submicromolar levels the axenic *L. donovani* amastigote and the infected macrophage. Greater subnanomolar values were detected in the promastigote assay.[46]

On the drug discovery research side, compounds potencies are evaluated on the early stage of the parasite with an infected macrophage assay. Macrophages of the J774 cell line are seeded with the amastigote *Leishmania donovani* axenic pathogen and incubated for 24 hours. Then, various concentrations of natural product compounds are prepared by serial dilution of a starting at 10 µg/mL solution, and added to the assay plate, to be incubated at 37°C, 5% CO_2 for 72 hours. Afterward, a fixative dye process is used to stain the DNA of both the macrophage hosts and the amastigotes parasites within macrophage cytoplasm. Finally, imaging techniques will allow count of the number of infecting amastigotes per 500 macrophages to generate IC_{50} values. Cytotoxicity is calculated using the survival rate of J774.A1 macrophages in compounds solutions of different concentration.

www.manaraa.com

Even in the scenario of successful decimation of the responsible parasite, the development of therapeutics encompasses another angle. The secondary phenotypic affections such as scars and disfigurations arising from the three different types of leishmaniasis infections need to be addressed.[3,15] New current treatment approaches lean toward combination of drugs to accelerate healing or mediate secondary adverse effects. Since the protozoan is sensitive to temperature changes, cryotherapy and local heat therapy are additional practices. In spite of some successful clinical outcomes, whether the parasites are fully eradicated remains an essential question.

II.2. Other targets

II.2.1 Cancerous cells

Given to a collection of immune diseases of genetic origin, cancer refers to cells dividing non-stop and spreading into surrounding tissues. Normal human cells grow and divide to form new cells as needed. When old or damaged, cells die and are replaced by new ones. However, this orderly process is perturbed by the development of cancer, and defective cells survive instead, destroying immunity and healthy cell behavior. Whether malignant or benign, getting rid of the damaged cells with the less amount of pain has been catching scientists' attention for at least 250 years. It started with Percivall Pott in 1775,[47] linking the exposure to chimney soot to the incidence of squamous cell carcinoma of the scrotum, progress have defined key milestones. In 1895, Wilhelm Roentgen discovers X-rays which is a fundamental part of the process used for cancer diagnosis.[48] Anticancer drugs scientific research strategies started as early as in the 1940's, when hormonal therapy aimed at prostate cancer was born, followed by combination chemotherapy less than 20 years after.[49, 50] From the National Cancer Institute, Emil Freireich, and James Holland and colleagues were credited use of 6-mercaptopurine and methotrexate as remission inducer in leukemia.[51] Globally, big pharmaceutical companies make it a priority to

www.manaraa.com

find THE cure for cancer by investing as much as billions of dollars.[52, 53] Five of the fourteen oncologic treatment drugs approved by the FDA in 2019 are: Bavenico® against renal cell carcinoma, Keytruda® battling non-metastatic castration-resistant prostate cancer, as well as oesophageal, lung, or renal cell carcinoma, Cyramza® as agent against hepatocellular carcinoma, and Piqray® treating HR-positive, HER2-negative, PIK3CA-mutated advanced or metastatic breast cancer.[54]

Natural products potency is screened against various cell lines to find new and alternative targeted therapeutic options. Once a target found, drug improvements will still be required, but at least screening of these compounds opens the door to drug discovery progress. Using imaging detection via cell staining, a clonogenic assay records the number of surviving cells according to the concentration of compound added, to calculate IC_{50} values translating the potency via cytotoxicity of these natural products against cancerous cells.

II.2.2. *Clostridium difficile* Bacterial Infection

Shortened as C. *difficile*, *Clostridium difficile* is a bacterium living symbiotically in the colon, as part of the gut flora. It doesn't usually cause health issues, unless the microbial flora equilibrium gets disrupted.[55] Commonly associated with older adults, nosocomial disease environments, and excessive antibiotic treatment, it creates inflammation of the large intestine.[56] However, studies show increasing rates of infections among people traditionally not considered at high risk: younger, with no history of antibiotic and/or exposure to health care facilities. Some people carry the bacterium in their intestines but never become sick, though they may still spread the infection.[57] Although the antibacterial drugs vancomycin and fidaxomicin® are the two currently recommended treatments, fecal microbiota transplantation for patients remains the

www.manaraa.com

recommended guideline for patients with recurring infections failing to respond to antibiotic treatments.[58]

While Fidaxomicin® inhibits RNA synthesis Vancomycin alters bacterial cell wall construction leading to the deterioration and not-sustained proliferation of the bacteria.

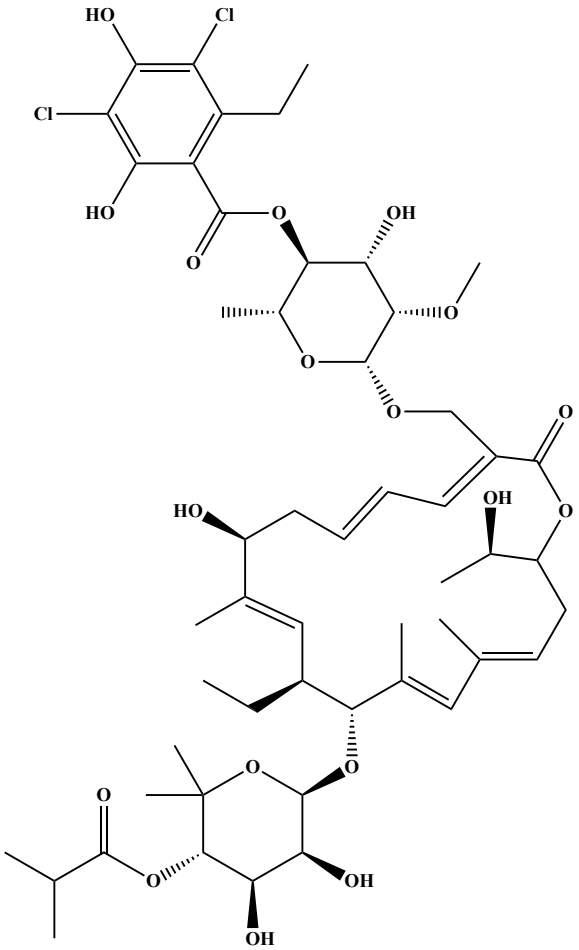

Fidamoxin®

www.manaraa.com

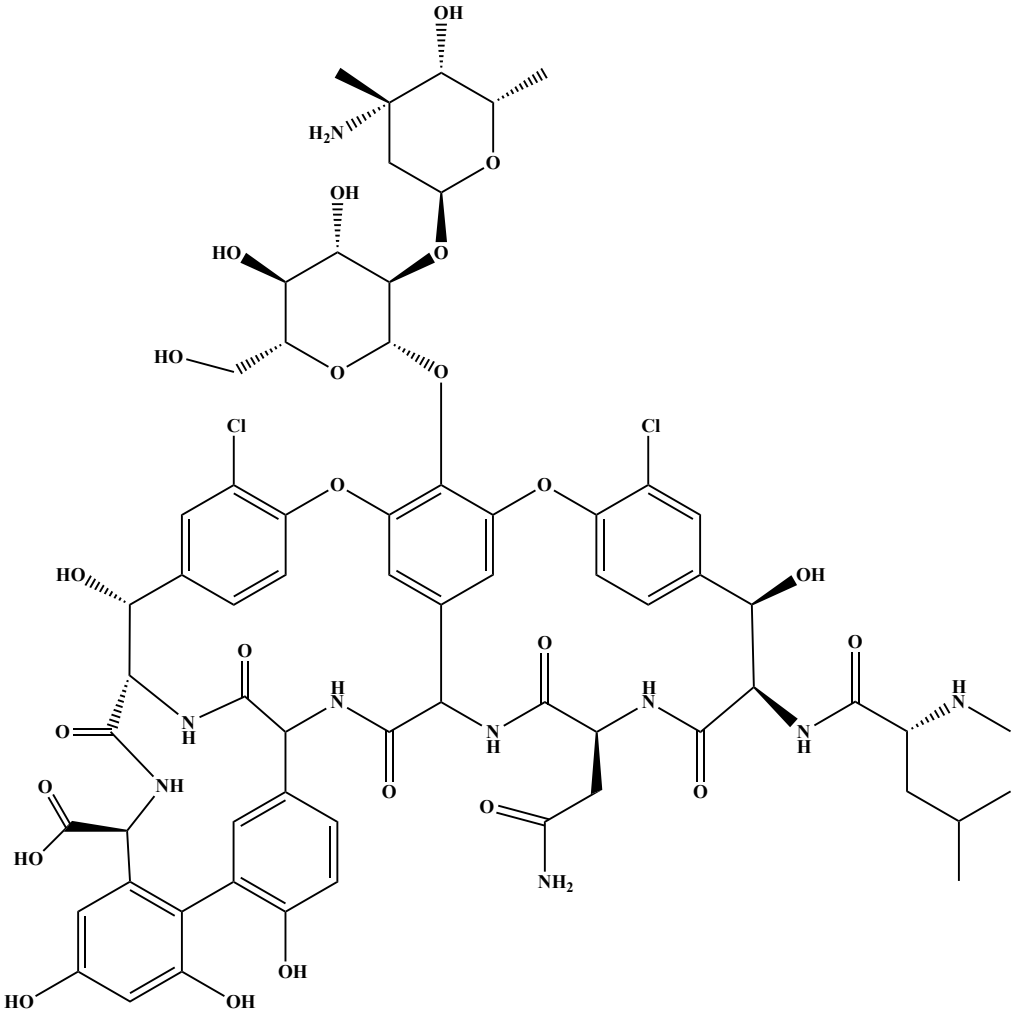

vancomycin

Using a colorimetric imaging assays, natural products are tested against the bacterial pathogen. The minimum inhibitory concentration of marine natural compounds was calculated against C. *diff.* bacterium to yield substantial potency. Additionally, the 3-(4,5-dimethylthiazol-2-yl)-2,5-diphenyltetrazolium bromide dye commonly called MTT, was used to stain cells and reveal the number of surviving ones to evaluate compounds cytotoxicity.

II.2.3. Respiratory Syncytial Virus

Responsible for bronchiolitis and pneumonia, respiratory syncytial viral (RSV) is a common respiratory virus usually causing mild, cold-like symptoms and can be serious for infants and older adults.[59,60] Current medication includes still not approved bronchodilators, but also,

www.manaraa.com

primarily indicated in hepatitis C and viral hemorrhagic fevers, the antiviral drug Ribavirin®, a synthetic guanosine nucleoside which interferes with viral mRNA synthesis.[61,62] Falling in the immunoprophylaxis category, the protein based therapeutic Palivizumab® may also be given.[63]

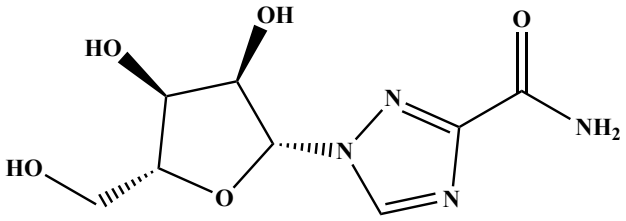

Ribavirin®

Testing of marine natural products potency against RSV were performed within the scope of this thesis. The percent inhibition of respiratory syncytial viral activity was calculated by the intensity of the luminescence given by the luciferase enzyme activity signaling the presence of the virus. The stronger the luminescence the more active the virus. The desired inhibition of this viral activity by the natural product compounds reflects their potency. Cytotoxicity was assessed with cell viability through an MTT assay.[64]

II.2.4. Malaria pathogen: *Plasmodium falciparum*

Different kind of parasitic neglected tropical disease, malaria is caused by *Plasmodium* parasites introduced to the body through the bite of female *Anopheles* mosquitoes, to infect red blood or liver cells. There are five parasites species responsible for human malaria: *P. falciparum and P.vivax*, the most threatening ones, *P. ovale*, *P. malariae*, and *P.knowlesi*, displaying smaller percentage.[65] Although generally curable if diagnosed properly, malaria is a life-threatening disease with symptoms ranging from absent or very mild to severe disease and even death. In 2017, about 219 million cases were recorded in 87 countries with a death rate of 435,000 cases.[66]

Available medicines are preventive and use chemoprophylaxis (chloroquine, sulfadoxine-pyrimethamine), which suppress the blood stage of the infection. In areas of the Sahel sub-region

www.manaraa.com

of Africa, seasonal chemoprevention is recommended, and combines amodiaquine and sulfadoxine-pyrimethamine to all children under 5 years of age over the course of one month.[67] To date, there is only one vaccine showing partial protection against malaria in young children.[68] Additionally, drug resistance is a recurring issue which requires drug discovery progress.[69]

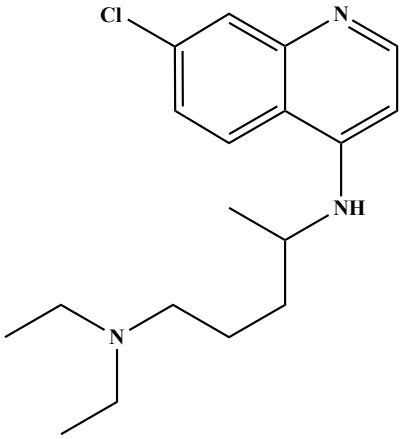

chloroquine

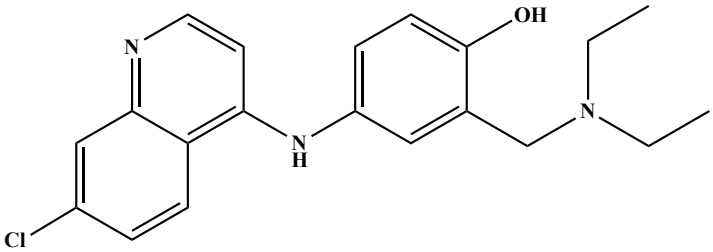

amodiaquine

In similar aforementioned colorimetric analyses, bioassay testing marine natural products against *Plasmodium falciparum* have revealed interesting and potent activities.

References

(1) Https://www.who.int/leishmaniasis/en/.

(2) Https://www.dndi.org/diseases-projects/leishmaniasis/.

(3) Murray, H. W.; Berman, J. D.; Davies, C. R.; Saravia, N. G. Advances in leishmaniasis. *Lancet* **2005**, *366*, 1561–1577.

(4) Copeland, N. K.; Aronson, N. E. Leishmaniasis: treatment updates and clinical practice guidelines review. *Curr. Opin. Infect. Dis.* **2015**, *28*, 426–437.

(5) Desjeux, P. Leishmaniasis: current situation and new perspectives. *Comp. Immunol.*

www.manaraa.com

Microbiol. Infect. Dis. **2004**, *27*, 305–318.

(6) Steverding, D. The history of leishmaniasis. *Parasites and Vectors* **2017**, *10* , 1–10.

(7) Www.Who.Int/Leishmaniasis/Disease/Leishmaniasis-Interactive-Timelines/En/.

(8) Cheuka, P. M.; Mayoka, G.; Mutai, P.; Chibale, K. The role of natural products in drug discovery and development against neglected tropical diseases. *Molecules* **2017**, *22*, 58 .

(9) Cota, G. F.; de Sousa, M. R.; Fereguetti, T. O.; Rabello, A. Efficacy of anti-leishmania therapy in visceral leishmaniasis among hiv infected patients: a systematic review with indirect comparison. *PLoS Negl. Trop. Dis.* **2013**, *7*, e 2195.

(10) Tchokouaha Yamthe, L. R.; Appiah-Opong, R.; Tsouh Fokou, P. V.; Tsabang, N.; Fekam Boyom, F.; Nyarko, A. K.; Wilson, M. D. Marine algae as source of novel antileishmanial drugs: a review. *Mar. Drugs* **2017**, *15*, 1–28.

(11) Pagliano, P.; Carannante, N.; Rossi, M.; Gramiccia, M.; Gradoni, L.; Faella, F. S.; Gaeta, G. B. Visceral leishmaniasis in pregnancy: a case series and a systematic review of the literature. *J. Antimicrob. Chemother.* **2005**, *55*, 229–233.

(12) Palumbo, E. Current treatment for cutaneous leishmaniasis: a review. *Am. J. Ther.* **2009**, *16*, 178–182.

(13) Arana, B.; Rizzo, N.; Diaz, A. Chemotherapy of cutaneous leishmaniasis: a review. *Med. Microbiol. Immunol.* **2001**, *190*, 93–95.

(14) Monzote, L. Current treatment of leishmaniasis: a review. *Open Antimicrob. Agents J.* **2009**, *1*, 9–19.

(15) Santos, D. O.; Coutinho, C. E. R.; Madeira, M. F.; Bottino, C. G.; Vieira, R. T.; Nascimento, S. B.; Bernardino, A.; Bourguignon, S. C.; Corte-Real, S.; Pinho, R. T.; et al. Leishmaniasis treatment - a challenge that remains: a review. *Parasitol. Res.* **2008**, *103*, 1–10.

www.manaraa.com

(16) Croft, S. L.; Sundar, S.; Fairlamb, A. H. Drug resistance in leishmaniasis. *Clin. Microbiol. Rev.* **2006**, *19*, 111–126.

(17) Sundar, S.; Agrawal, G.; Rai, M.; Makharia, M. K.; Murray, H. W. Treatment of Indian visceral leishmaniasis with single or daily infusions of low dose liposomal amphotericin b: randomised trial. *Br. Med. J.* **2001**, *323*, 419–422.

(18) Amato, V. S.; Tuon, F. F.; Siqueira, A. M.; Nicodemo, A. C.; Neto, V. A. Treatment of mucosal leishmaniasis in latin america: systematic review. *Am. J. Trop. Med. Hyg.* **2007**, *77*, 266–274.

(19) Hamill, R. J. Amphotericin B formulations: a comparative review of efficacy and toxicity. *Drugs* **2013**, *73*, 919–934.

(20) Macesic, N.; Stone, N. R. H.; Wingard, J. R. Liposomal amphotericin b. *Kucers Use Antibiot. A Clin. Rev. Antibacterial, Antifung. Antiparasit. Antivir. Drugs, Seventh Ed.* **2017**, *69*, 2612–2627.

(21) Leishmaniasis, V. Amphotericin B colloidal dispersion. **1998**, *56*, 365–383.

(22) Tchokouaha Yamthe, L. R.; Appiah-Opong, R.; Tsouh Fokou, P. V.; Tsabang, N.; Fekam Boyom, F.; Nyarko, A. K.; Wilson, M. D. Marine algae as source of novel antileishmanial drugs: a review. *Mar. Drugs* **2017**, *15*, 323.

(23) Sundar, S.; Sinha, P. K.; Rai, M.; Verma, D. K.; Nawin, K.; Alam, S.; Chakravarty, J.; Vaillant, M.; Verma, N.; Pandey, K.; et al. Comparison of short-course multidrug treatment with standard therapy for visceral leishmaniasis in india: an open-label, non-inferiority, randomised controlled trial. *Lancet* **2011**, *377*, 477–486.

(24) Https://Www.Who.Int/Leishmaniasis/Burden/Leishmaniasis_India/En/.

(25) Dhariwal, A.; Gupta, R.; Roy, N.; Raina, V. Operational guidelines on kala-azar (visceral leishmaniasis) elimination in India -2015. **2015**, No. October, 20.

www.manaraa.com

(26) Dorlo, T. P. C.; Balasegaram, M.; Beijnen, J. H.; de vries, P. J. Miltefosine: A review of its pharmacology and therapeutic efficacy in the treatment of leishmaniasis. *J. Antimicrob. Chemother.* **2012**, *67*, 2576–2597.

(27) Agrawal, V.; Singh, Z. Miltefosine: first oral drug for treatment of visceral leishmaniasis. *Med. J. Armed Forces India* **2006**, *62*, 66–67.

(28) Rubiano, L. C.; Miranda, M. C.; Muvdi Arenas, S.; Montero, L. M.; Rodríguez-Barraquer, I.; Garcerant, D.; Prager, M.; Osorio, L.; Rojas, M. X.; Pérez, M.; et al. Noninferiority of miltefosine versus meglumine antimoniate for cutaneous leishmaniasis in children. *J. Infect. Dis.* **2012**, *205*, 684–692.

(29) Sindermann, H.; Engel, K. R.; Fischer, C.; Bommer, W. Oral Miltefosine for leishmaniasis in immunocompromised patients: compassionate use in 39 patients with HIV infection. *Clin. Infect. Dis.* **2004**, *39*, 1520–1523.

(30) Sundar, S.; Jha, T. K.; Thakur, C. P.; Engel, J.; Sindermann, H.; Fischer, C.; Junge, K.; Bryceson, A.; Berman, J. Oral miltefosine for Indian visceral leishmaniasis. *N. Engl. J. Med.* **2002**, *347*, 1739–1746.

(31) Rahman, M.; Ahmed, B. N.; Faiz, M. A.; Chowdhury, M. Z. U.; Islam, Q. T.; Sayeedur, R.; Rahman, M. R.; Hossain, M.; Bangali, A. M.; Ahmad, Z.; et al. Phase IV trial of miltefosine in adults and children for treatment of visceral leishmaniasis (kala-azar) in Bangladesh. *Am. J. Trop. Med. Hyg.* **2011**, *85*, 66–69.

(32) Sundar, S.; Sinha, P. K.; Rai, M.; Verma, D. K.; Nawin, K.; Alam, S.; Chakravarty, J.; Vaillant, M.; Verma, N.; Pandey, K.; et al. Comparison of short-course multidrug treatment with standard therapy for visceral leishmaniasis in India: an open-label, non-inferiority, randomised controlled trial. *Lancet* **2011**, *377*, 477–486.

(33) Ben Salah, A.; Ben Messaoud, N.; Guedri, E.; Zaatour, A.; Ben Alaya, N.; Bettaieb, J.;

www.manaraa.com

Gharbi, A.; Hamida, N. B.; Boukthir, A.; Chlif, S.; et al. Topical paromomycin with or without gentamicin for cutaneous leishmaniasis. *N. Engl. J. Med.* **2013**, *368*, 524–532.

(34) Reveiz, L.; Maia-Elkhoury, A. N. S.; Nicholls, R. S.; Sierra Romero, G. A.; Yadon, Z. E. Interventions for American cutaneous and mucocutaneous leishmaniasis: a systematic review update. *PLoS One* **2013**, *8*, e61843.

(35) Tuon, F. F.; Amato, V. S.; Graf, M. E.; Siqueira, A. M.; Nicodemo, A. C.; Neto, V. A. Treatment of new world cutaneous leishmaniasis - a systematic review with a meta-analysis. *International Journal of Dermatology*. **2008**, 109–124.

(36) Ozgoztasi, O.; Baydar, I. A randomized clinical trial of topical paromomycin versus oral ketoconazole for treating cutaneous leishmaniasis in Turkey. *Int. J. Dermatol.* **1997**, *36*, 61–63.

(37) Vargas-Zepeda, J.; Gómez-Alcalá, A. V.; Vázquez-Morales, J. A.; Licea-Amaya, L.; De Jonckheere, J. F.; Lares-Villa, F. Successful treatment of naegleria fowleri meningoencephalitis by using intravenous amphotericin b, fluconazole and rifampicin. *Arch. Med. Res.* **2005**, *36*, 83–86.

(38) Alrajhi, A. A.; Ibrahim, E. A.; De Vol, E. B.; Khairat, M.; Faris, R. M.; Maguire, J. H. Fluconazole for the treatment of cutaneous leishmaniasis caused by leishmania major. *N. Engl. J. Med.* **2002**, *346*, 891–895.

(39) Romero, G. A. S.; Boelaert, M. Control of visceral leishmaniasis in Latin America - a systematic review. *PLoS Negl. Trop. Dis.* **2010**, *4*, e584.

(40) Slappendel, R. J. Prize-winning paper jubilee competition: canine leishmaniasis. *Vet. Q.* **1988**, *10*, 1–16.

(41) Noli, C.; Auxilia, S. T. Treatment of canine old world visceral leishmaniasis: a systematic review. *Veterinary Dermatology*. **2005**, 213–232.

www.manaraa.com

(42) Nacher, M.; Carme, B.; Sainte Marie, D.; Couppié, P.; Clyti, E.; Guibert, P.; Pradinaud, R. influence of clinical presentation on the efficacy of a short course of pentamidine in the treatment of cutaneous leishmaniasis in French Guiana. *Ann. Trop. Med. Parasitol.* **2001**, *95*, 331–336.

(43) Ma, W. S.; Mutka, T.; Vesley, B.; Amsler, M. O.; McClintock, J. B.; Amsler, C. D.; Perman, J. A.; Singh, M. P.; Maiese, W. M.; Zaworotko, M. J.; et al. Norselic acids a-e, highly oxidized anti-infective steroids that deter mesograzer predation, from the Antarctic sponge *Crella Sp. J. Nat. Prod.* **2009**, *72*, 1842–1846.

(44) von Salm, J. L.; Wilson, N. G.; Vesely, B. A.; Kyle, D. E.; Cuce, J.; Baker, B. J. Shagenes A and B, new tricyclic sesquiterpenes produced by an undescribed Antarctic octocoral. *Org. Lett.* **2014**, *16*, 2630–2633.

(45) Thomas, S. A. L. L.; von Salm, J. L.; Clark, S.; Ferlita, S.; Nemani, P.; Azhari, A.; Rice, C. A.; Wilson, N. G.; Kyle, D. E.; Baker, B. J. Keikipukalides, furanocembrane diterpenes from the antarctic deep sea octocoral *Plumarella delicatissima*. *J. Nat. Prod.* **2018**, *81*, 117–123.

(46) Wang, M. Z.; Zhu, X.; Srivastava, A.; Liu, Q.; Sweat, J. M.; Pandharkar, T.; Stephens, C. E.; Riccio, E.; Parman, T.; Munde, M.; et al. Novel arylimidamides for treatment of visceral leishmaniasis. *Antimicrob. Agents Chemother.* **2010**, *54*, 2507–2516.

(47) Brown, J. R.; Thornton, J. L. Percivall Pott (1714-1788) and chimney sweepers' cancer of the scrotum. *Br. J. Ind. Med.* **1957**, *14*, 68–70.

(48) Wilhelm Conrad Röntgen – Biographical. NobelPrize.Org. Nobel Media AB 2019. https://Www.Nobelprize.Org/Prizes/Physics/1901/Rontgen/Biographical/.

(49) Lefranc, F.; Tabanca, N.; Kiss, R. Assessing the anticancer effects associated with food products and/or nutraceuticals using in vitro and in vivo preclinical development-related

www.manaraa.com

pharmacological tests. *Semin. Cancer Biol.* **2017**, *46*, 14–32.

(50) Mould, D.R; Hutson, P. R. Critical considerations in anticancer drug development and dosing strategies: the past, present, and future. *J. Clin. Pharmacol.* **2017**, *57*, S116–S128.

(51) Frey, E.; Freireich, E. J.; Gehan, E.; Pinkel, D.; Holland, J. F.; Selawry, O.; Haurani, F.; Spurr, C. L.; Hayes, D. M.; James, G. W.; et al. Studies of sequential and combination antimetabolite therapy in acute leukemia: 6-mercaptopurine and methotrexate. *Blood* **1961**, *18*, 431–454.

(52) Research America. U.S. Investments in medical and health research and development 2013 - 2015. **2016**.

(53) Tay-Teo, K.; Ilbawi, A.; Hill, S. R. Comparison of sales income and research and development costs for FDA-approved cancer drugs sold by originator drug companies. *JAMA Netw. Open* **2019**, *2*,e186875.

(54) Https://Www.Centerwatch.Com/Drug-Information/Fda-Approved-Drugs/Therapeutic-Area/12/Oncology. **2019**.

(55) The progression of a C. *diff* infection. **2018**. https://www.cdc.gov/cdiff/pdf/Cdiff-progression-H.pdf

(56) Kelly, C. P.; Pothoulakis, C.; LaMont, J. T. Clostridium Difficile Colitis. *N. Engl. J. Med.* **1994**, *330*, 257-262.

(57) Hensgens, M. P. M.; Goorhuis, A.; Dekkers, O. M.; Kuijper, E. J. Time interval of increased risk for *Clostridium difficile* infection after exposure to antibiotics. *J. Antimicrob. Chemother.* **2012**, *67* (3), 742–748.

(58) Kelly, C. P.; LaMont, J.T. *Clostridium difficile* — more difficult than ever. *N. Engl. J. Med.* **2008**, *359*, 1932-1940.

(59) Respiratory syncytial virus in older adults : a hidden annual epidemic. *National Foundation*

www.manaraa.com

for Infectious Diseases. **2016**, 2-16.

(60) Hall, C. B. Respiratory syncytial virus and para influenza virus. **2001,** *344*, 1917-1928.

(61) Taber, L. H.; Knight, V.; Gilbert, B. E.; McClung, H. W.; Wilson, S. Z.; Norton, H. J.; Thurson, J. M.; Gordon, W. H.; Atmar, R. L.; Schlaudt, W. R. Ribavirin aerosol treatment of bronchiolitis associated with respiratory syncytial virus infection in infants. *Pediatrics* **1983**, *72*, 613–618.

(62) Domachowske, J. B.; Rosenberg, H. F. Respiratory syncytial virus infection: immune response, immunopathogenesis, and treatment. *Clin. Microbiol. Rev.* **1999**, *12*, 298–309.

(63) Boron, M. Palivizumab Prophylaxis of Respiratory syncytial virus disease in 2000-2001: results from the palivizumab outcomes registry. *Pediatric Pulmonology*. **2003**, 484–489.

(64) Fuentes, S.; Crim, R. L.; Beeler, J.; Teng, M. N.; Golding, H.; Khurana, S. Development of a simple, rapid, sensitive, high-throughput luciferase reporter based microneutralization test for measurement of virus neutralizing antibodies following respiratory syncytial virus vaccination and infection. *Vaccine* **2013**, *31*, 3987–3994.

(65) Miller, L. H.; DI, Baruch, D. I.; March, K.; Doumbo. O. K. The pathogenic basis of malaria. *Nature* **2002**, *415* (February), 673–679.

(66) Sachs, J.; Malaney, P. The economic and social burden of malaria. *Nature* **2002**, *415*, 680–685.

(67) Achan, J.; Talisuna, A. O.; Erhart, A.; Yeka, A.; Tibenderana, J. K.; Baliraine, F. N.; Rosenthal, P. J.; D'Alessandro, U. Quinine, an old anti-malarial drug in a modern world: role in the treatment of malaria. *Malar. J.* **2011**, *10*, 144.

(68) Foote, S. J.; Walter, T.; Office, P.; Hospital, R. M. Chemotherapy and drug resistance. *Br. J. Haematol.* **1994**, *87*, 83–89.

(69) Peter B. Bloland. Drug resistance in malaria. *World Heal. Organ.* **2001**, 1–24.

www.manaraa.com

CHAPTER THREE:

ANTARCTIC DEEP WATER OCTOCORAL CHEMISTRY

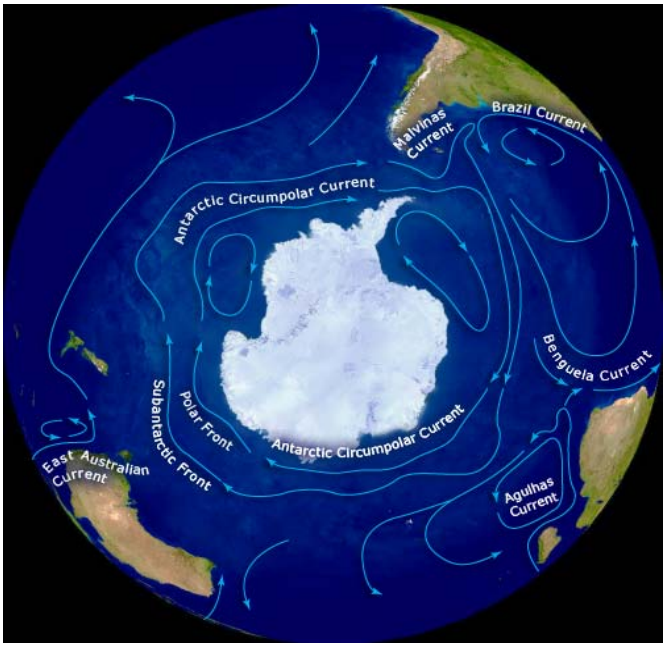

Figure III.1. Illustration of the Antarctic Circumpolar Current (ACC).[1]

III.1. The Antarctic marine ecosystem

Antarctica's singularity starts by being the fifth largest and Earth's southernmost continent. Nearly thirty million years ago, the separation of this land mass from Australia and South America resulted in the formation of the present Antarctic Circumpolar Current creating an environmental shield.[2,3] As a result, the sea waters stopped flowing into the tropics but rather isolated the polar territory. Averaging a flow of 10^6 m^3/s, it is considered mainly wind-driven, but flows to the seabed in most places. Powered by West-winds, the largest ocean current in the world

www.manaraa.com

developed a clockwise motion. Covered by ice, Antarctica offers the most extreme environmental conditions recorded on the planet, where peculiar ecosystems develop.

Though less diverse than the ones from the warm and tropical waters, high-latitude fauna and flora have fascinated ecologists who try to understand the relationship between adaptation and survival behaviors and evolutionary processes.[4,5] Due to accessibility and the extreme environmental conditions, the Antarctic ecosystems remain much more understudied than the tropical ones. Nonetheless, all of these encountered obstacles are in fact what drives and motivates the pursuit of Antarctic scientific research.[6–8] So far, the scientific research has been able to delve into chemical ecology of these ecosystems.[9,10] They have drafted some patterns and established others supporting phylogenic secondary metabolites productions and interactions. The segregation fosters unique species evolution between over 4100 benthic species described to date. Beyond the outstanding known megafauna, a versatile marine biodiversity of invertebrates encompasses sponges, corals, tunicates, and nudibranchs, mingling in cold water near algal species.[11] Often sessile, without physical defenses such as a shell or tough, spiny skin to protect themselves, these invertebrates must develop chemical protective mechanisms to survive and defend themselves against predators, creating interests and wonders for natural products chemists.[12] Numerous reports of natural products with ecological and medicinal values, for microorganisms, algae, sponges, cnidarians, bryozoans, ascidians, mollusks, and echinoderms have been published, and approximately 30,000 secondary metabolites from marine biodiversity have been identified within the past 40 years and less than 10% from the polar regions.[13]

III.2. Octocoral chemistry

Terpenes represent the most abundant natural products in the world and are widely involved in ecological cycles and medicinal properties.[14] Their volatile characteristic make them

www.manaraa.com

easy to detect, which is the main reason why they have been targeted and heavily studied. Moreover, they often provide biological activities worth exploring for drug discovery purposes. Well documented in the terrestrial environment, terpenes founded the chemistry of odor involved with food, fragrance and cosmetics industry.[15,16] In a similar way, they have guided marine natural products chemists in their studies. Priority has been given to organisms emanating robust scents manifesting the presence of terpenes responsible for the activation of ecological survival mechanisms such as reproductive, defensive, and allelopathic interactions. Terpenoids make up more than 60% of isolated marine natural products.[17]

The declination of terpenes is based on the number of isoprene units present in the molecule and defines the class of the molecules.[18] For example, algae tend to create more monoterpenes, while corals produce more sesqui-, di- and higher terpenes, which act as warfare deployed for space competition on a reef and species ecological survival. However, the success of one's battle becomes the defeat of another, as these compounds turn out to be detrimental to the scleratinian or hard corals responsible for building coral reefs.[12] Deeper understanding of these interactions by chemical ecology of marine natural products unveiled molecular structures revealed to be more than just toxins and venoms involved in the survival of species in ecosystems. These natural products have also revealed biological activities against human pathogens: antitumor (41%), antimicrobial (24%), anti-inflammatory (22%), antifoulant (10%), nervous system (2%), anti-HIV, antiulcer (1%). [19] From the animal realm, corals also offer relevant biological activities from the terpenoid compounds they produce. Corals are colonial marine invertebrates belonging to the phylum Cnidaria. They constitute the Anthozoa class, the largest one. A division in two subclasses is based on their skeletal firmness. The hard ones from the hexacorallia subclass are linked to the presence of an exoskeleton, opposed to the soft ones from the octocorallia subclass missing it. Due to the lack of physical defensive features, the secondary

www.manaraa.com

metabolites production is exacerbated in alcyonacean soft corals. Octocorals are the greatest contributors of cnidarian chemistry creating 80% of the biologically active compounds isolated.[20] Primarily exerting cytotoxicity against cancer cells,[21] cnidarian secondary metabolites have displayed a broader range of biological activities.[7,22–24] The antibacterial ainigmaptilone A was isolated from the coral *Ainigmaptilon antarcticus*.[7] The promising preclinical tests of the potent anti-inflammatory pseudopterosin A from *Pseudopterogorgia elisabethae*, did not prevail as the physical molecular properties hindered the ADME rules of drugability impeding its pharmaceutical success.[25] Interestingly though, peudopterosins found their way in the cosmetics marketplace as ingredient of the Resilience® Estée Lauder cosmetic skin care product instead.[19]

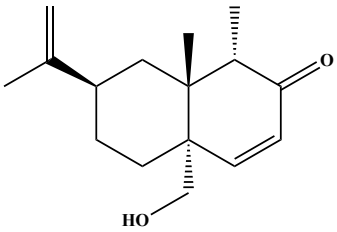

ainigmaptilone A

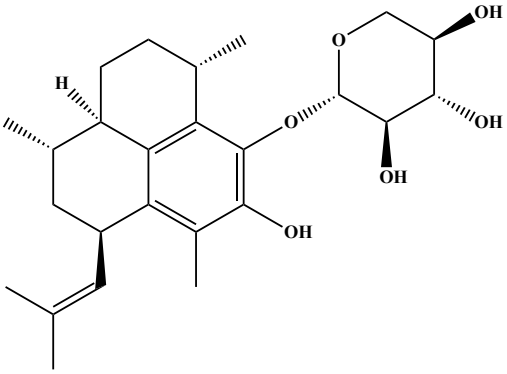

pseudopterosin A

Often compounds may be described but it is not until much later that biological activity assessments happen. Re-isolation and chemodiversity enlargement motivate biological activities studies, which can eventually lead to linking potency discovery with chemical features. This is exactly what happened for eleutherobin A and sarcodictyin A isolated from respective coral genera *Eleutherobia*[26] *and Sarcodictyon*[27] and their anticancer activities not recognized until years after their chemical isolation.

www.manaraa.com

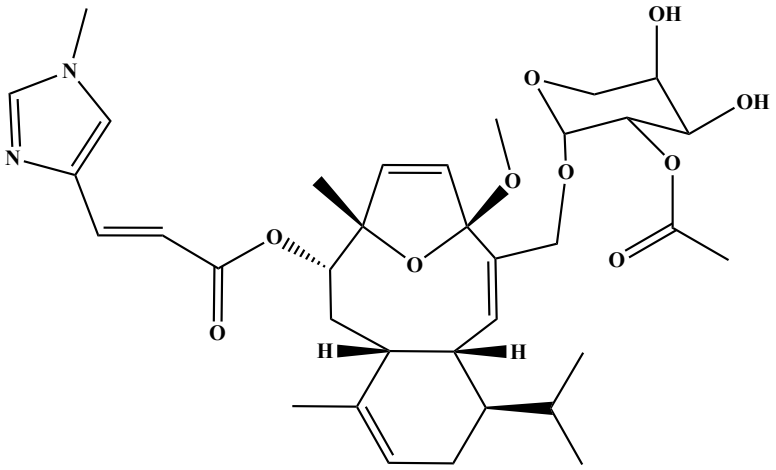

eleutherobin A

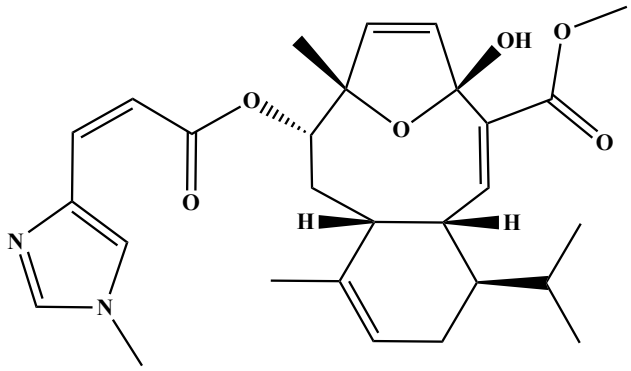

sarcodictyin

An analogous scenario is described in this thesis regarding the alcyopterosin class of molecules. In 2013, during a trip near the South Georgia islands, an octocoral was collected via trawling. The chemical investigation of an undescribed Antarctic deep sea octocoral has led to the isolation of novel compounds. After prior lyophilization of the organism, two extraction protocols varying in solvent polarity were performed and led to the isolation of three types of molecules: the alcyopterosins more polar than a steroid and three prostaglandins.

www.manaraa.com

Figure III.2. Undescribed deep sea Antarctic octocoral.

III.3. Alcyopterosin sesquiterpenoids

Alcyopterosin molecules are related to illudalane compounds. Originally found in fungi and ferns from terrestrial ecosystems, illudalanes are also encountered in alcyonacean corals from deep sea waters and called alcyopterosins.[21,28–31] The minimal number of 15 carbon atoms constituting the molecular backbone, places them in the sesquiterpenoid class of molecules. The molecular shape is derived from a central indene bicyclic framework, and decorating substituents can be found in positions 3, 6, 7, 10, and 11.

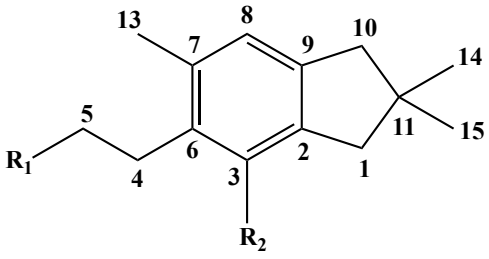

Figure III.3.1. Molecular scaffold of alcyopterosin compounds.

The chemical diversity of isolated alcyopterosin compounds rests mainly on the terminal substitution appearing on the aliphatic chain placed in position 6, where chlorination, acetylation, or more striking nitration can be found. Indeed, despite the large presence of nitrate

www.manaraa.com

in oceans, the incorporation of nitrate in marine secondary metabolites remains exceptional and encountered in alcyopterosin only. Previous chemical investigations of *Alcyonium grandis* and *Alcyonium paesleri* established a suite of alcyopterosin compounds, and provided substantial supporting information aiding the elucidation of novel compounds Alcyopterosin T and U.

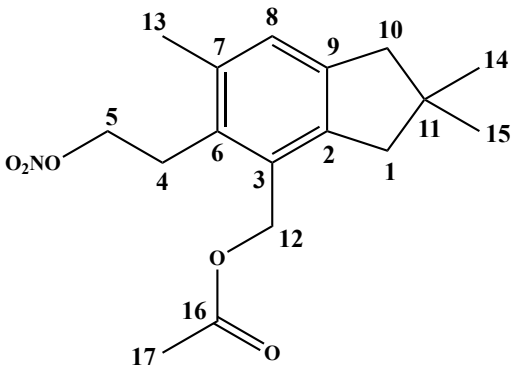

alcyopterosin T (1)

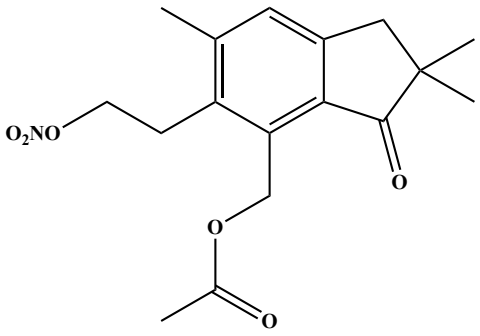

alcyopterosin U (2)

III.3.1. Isolation and structure elucidation

After lyophilization of the undescribed deep sea coral, a methylene chloride: methanol (1:1) extraction was performed over three days. The dry extract was reconstituted in ethyl acetate and subjected to a partition against water. The ethyl acetate layer was dried out and adsorbed onto silica gel for preliminary normal phase separation using Medium Pressure Liquid Chromatography (MPLC), through a gradient of 0% to 100% of ethyl acetate in hexanes. The following signature proton NMR signals essentially revealed the presence of alcyopterosin compounds: three methyl groups signals between 1.00 ppm and 2.5 ppm, and a single aromatic proton found between 7.00 and 8.00 ppm. These signature signals led the way to choose the MPLC fractions of interest D, E, F, G, H, and L which were prioritized for purification.

www.manaraa.com

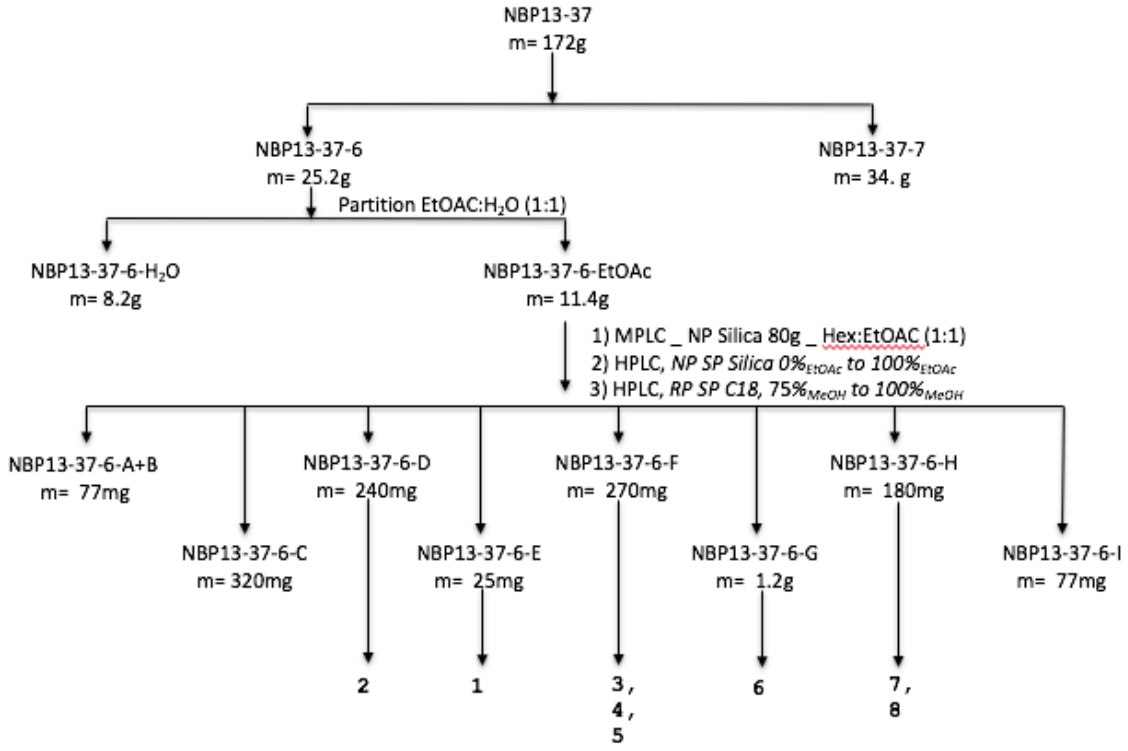

Scheme III.3.1.1. Fractionation Scheme of Antarctic deep sea octocoral extracted in DCM:MeOH (1:1).

Subsequent stages of normal phase and reverse phase High Performance Liquid Chromatography (HPLC) facilitated the purification of alcyopterosin compounds. Previous publications confirmed the isolation of six known compounds, and two novel ones. Semipreparative normal phase HPLC of fraction F led to the known alcyopterosins: C (**3**), G (**4**), and 4,12-Bis(acetyl)alcyopterosin O (**5**). Fractions G yielded alcyopterosin E (**6**), while fraction H provided the synthetically known(*S*)-3-(hydroxymethyl)-4,7,7-trimethyl-3,6,7,8-tetrahydro-1*H*-indeno[4,5-*c*]-furan-1-one (**7**) along with alcyopterosin L (**8**). The two novel compounds originated from MPLC fraction E. Although alcyopterosins T (0.5 mg) emerged as a pure compound, alcyopterosin U required further purification. Reverse phase HPLC using acetonitrile in H_2O provided alcyopterosin U as well as pure compounds 12-Bis(acetyl)alcyopterosin O (1.6 mg), alcyopterosins C (2.0 mg), E (7.5 mg), G (0.6 mg), L (1.4 mg), and U (0.3 mg). A final round of

www.manaraa.com

reverse phase HPLC using CH_3OH/H_2O with an analytical Synergi 5-micron column provided pure alcyopterosin U (0.5 mg).

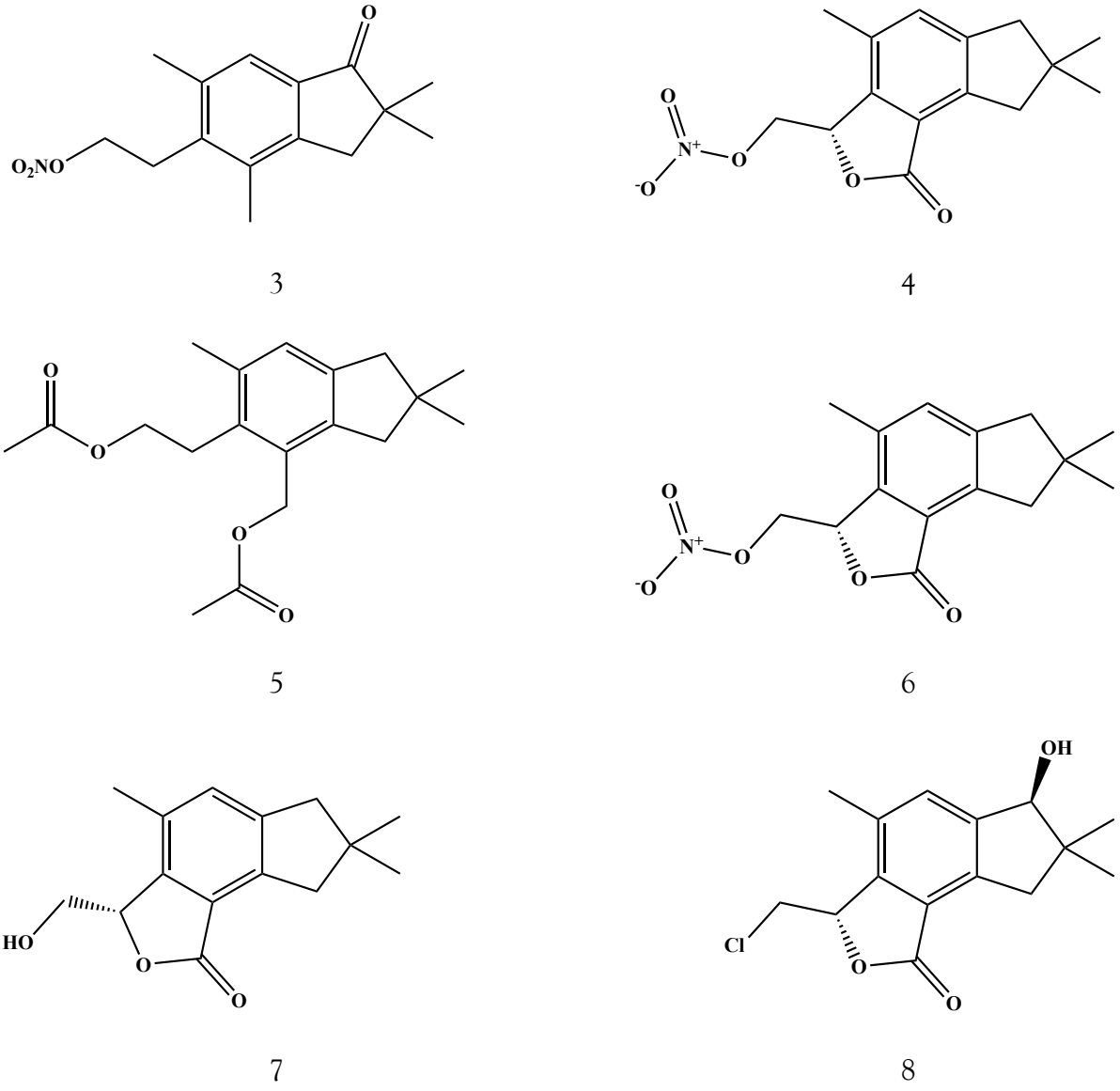

Figure III.3.1.1. Isolated known alcyopterosin compounds.

The proton NMR spectrum of alcyopterosin T (**1**) displayed nine signals: two coupled triplets and seven other singlets, but the lack of sufficient material prevented the acquisition of ^{13}C NMR spectrum.

www.manaraa.com

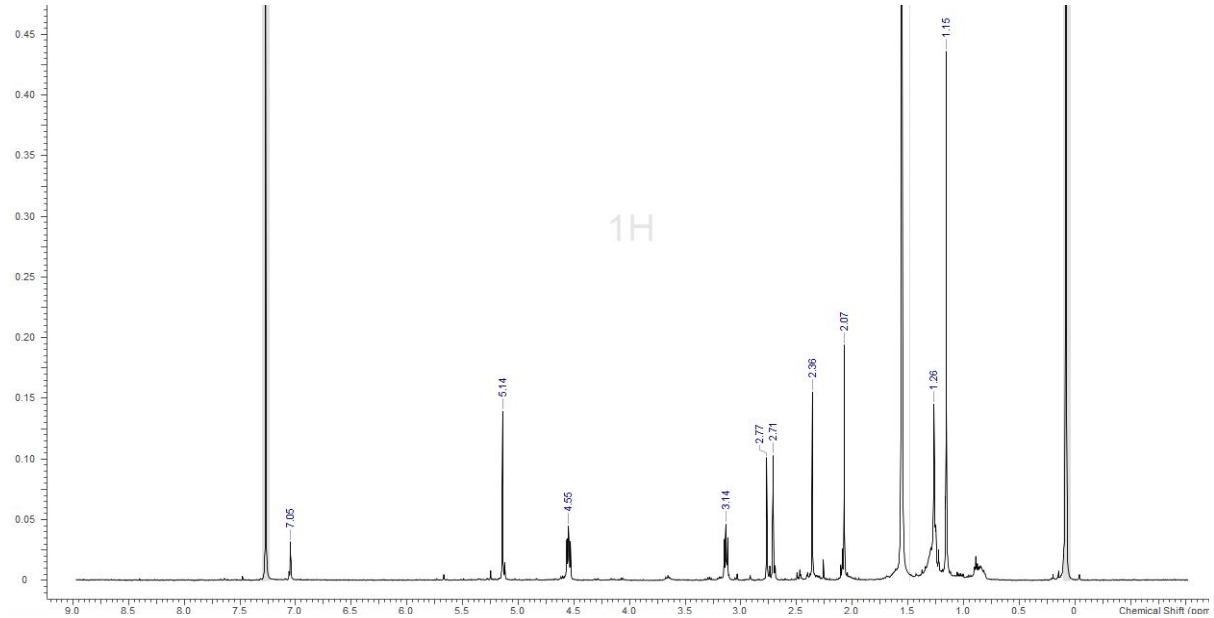

Figure III.3.1.2. ^{1}H NMR spectrum for alcyopterosin T in $CDCl_3$ (500 MHz).

However, the two-dimensional HSQC experiment, revealing direct connection of the hydrogen atoms bonds with the carbon atoms bearing them, provided the correlation of eight proton signals to carbons part of the alcyopterosin compound core structure.

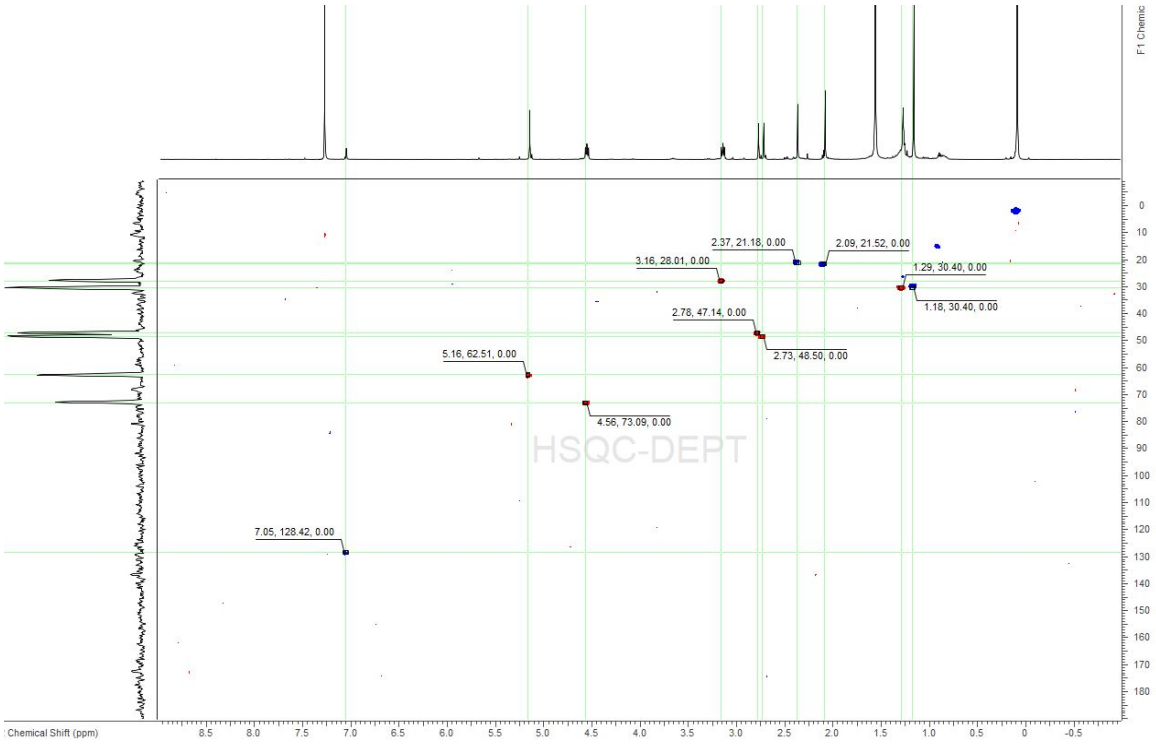

Figure III.3.1.3. HSQC NMR correlations for alcyopterosin T in $CDCl_3$ (500 MHz).

www.manaraa.com

The detected High Resolution Electron Soft Ionization Mass Spectrum (HRESIMS) $[M + Na]^+$: m/z 344.1460, calcd. for $C_{17}H_{23}NO_5Na$, m/z 344.1468, unveiled the proposed molecular formula $C_{17}H_{23}NO_5$ for the compound and indicated the presence of a nitrogen atom.

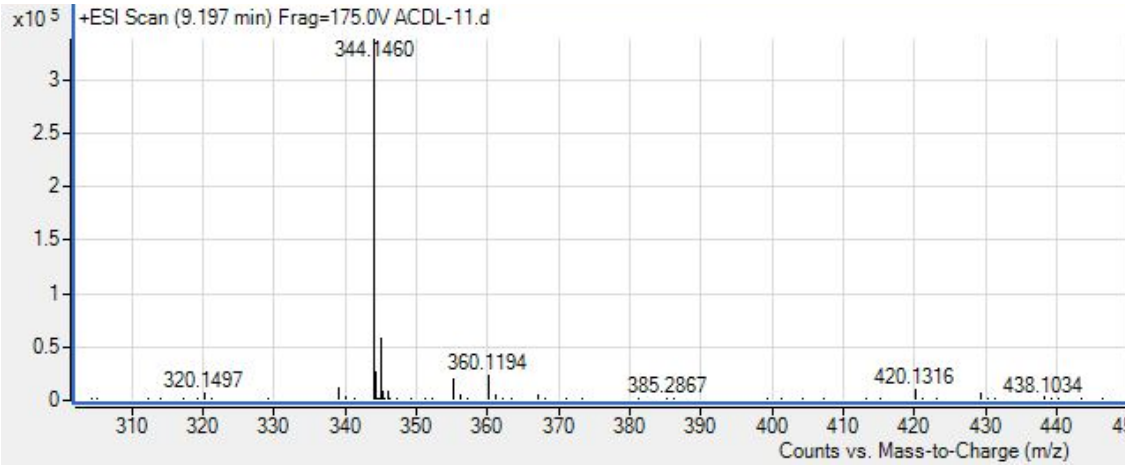

Figure III.3.1.4. MS for alcyopterosin T.

Seven degrees of unsaturation were determined with five of them related to the indane ring framework, one from the nitrate ester function on C-5 (δ_C 73.0) and the last one from the acetate moiety on C-3 (δ_C 128.4). The chemical shifts recorded supported the dereplication of alcyopterosin scaffold pattern. A carbonyl stretch found on the IR spectrum (1720 cm^{-1}) corroborated the presence of a ketone carbonyl. The proton singlet at 7.05 ppm was the only aromatic signal seen, correlated to the olefinic carbon C-16 (δ_C 171.2) on HSQC 2D NMR spectrum, but did not depict any COSY homonuclear correlation. However, three-bond HMBC correlations appeared between C-10 (δ_C 48.5) and C-13 (δ_C 20.9) (**Figure III.3.1.5.**). A second proton singlet found at 2.36 ppm related to methyl C-13 was observed on the HSQC 2D spectrum. The HMBC experiment displayed three unique heteronuclear three-bond correlations with olefinic carbons C-8 (δ_C 128.8), C-7 (δ_C 131.6) and C-6 (δ_C 143.4).

www.manaraa.com

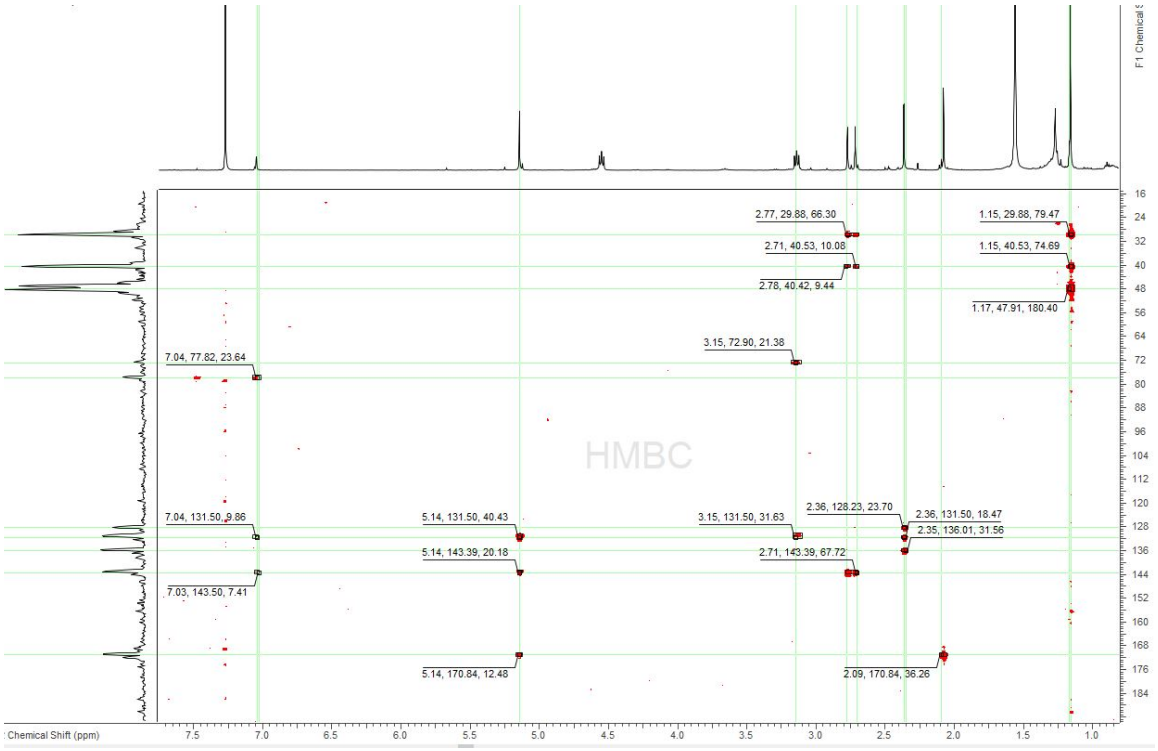

Figure III.3.1.5. HMBC NMR spectrum for alcyopterosin T in $CDCl_3$ (500 MHz).

From the HSQC results, the proton singlet at 2.70 ppm related to C-10 (δ_C 48.5), established additional three-bond correlations with the geminal dimethyl motif created by C-14 (δ_C 30.5) and C-15 (δ_C 30.5). According to two-dimensional HSQC spectrum, the proton singlet at 2.71 ppm correlated to C-10 while the proton singlet at 2.77 ppm correlated to C-1. Both proton signal signals integrated for two hydrogens. On one hand, despite the absence of heteronuclear correlations between the quaternary aromatic carbons C-2 and C-3, the methylene protons on C-1 showed HMBC correlations with C-11, C-14, C-15, and the aromatic C-9. On the other hand, seen on the HMBC spectrum, the methylene on C-10 displays identical correlations with an additional one with the aromatic C-8 (δ_C 128.8). The striking proton signal at 1.15ppm, integrating for 6 hydrogen atoms, was confirmed to be linked to both C-14 and C-15 via HSQC. The heteronuclear HMBC correlations with C-1 (δ_C 47.3), C-10 and between themselves, C-14

www.manaraa.com

and C-15, supported the existence of the peculiar geminal dimethyl motif on quaternary carbon C-11 (δ_C 40.6).

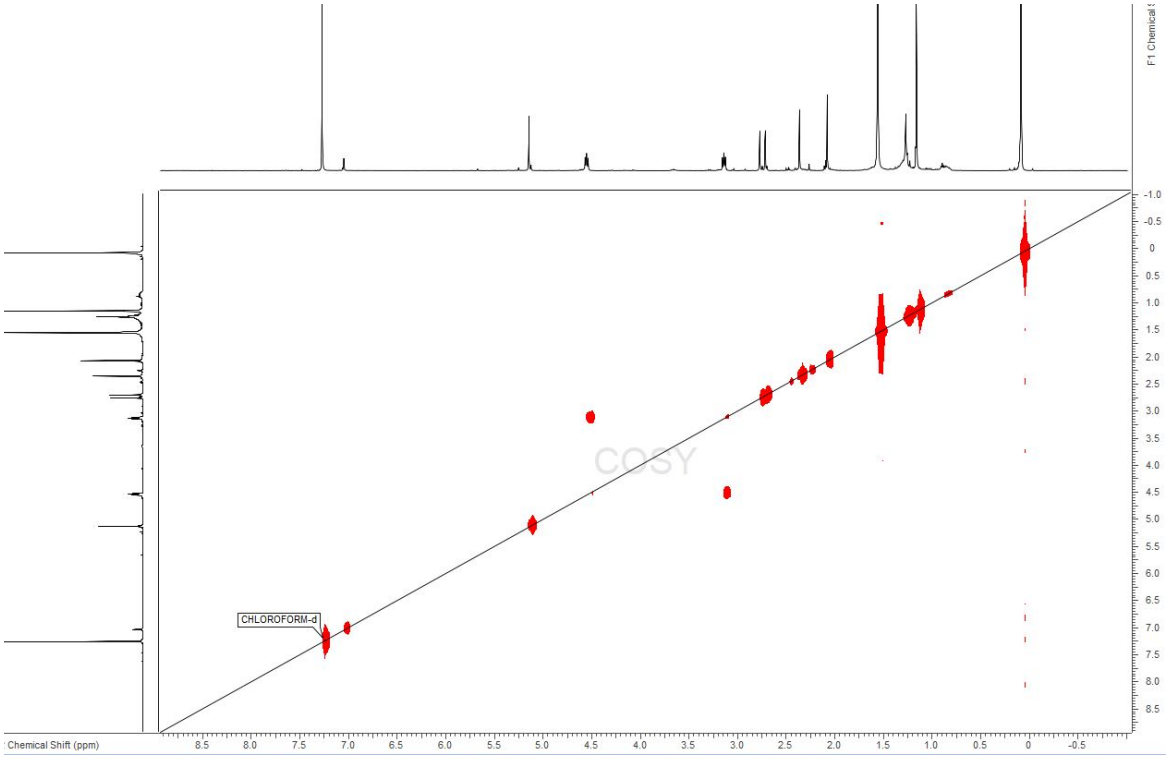

Figure III.3.1.6. COSY NMR spectrum for alcyopterosin T in $CDCl_3$ (500 MHz).

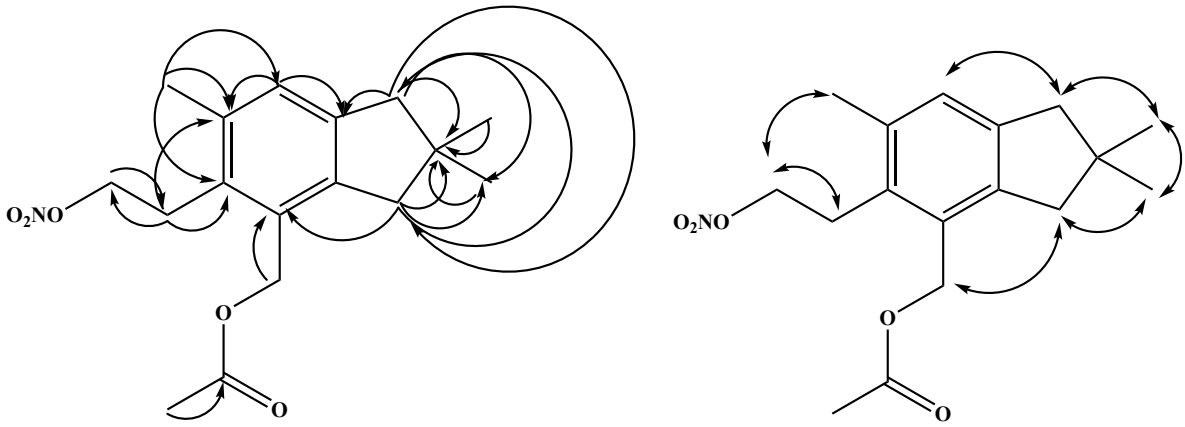

Figure III.3.1.7. Key HMBC (⌒) and ROESY (⌒) correlations establishing the planar structure of alcyopterosin T (**1**).

www.manaraa.com

Furthermore, six degrees of unsaturation remained to be assigned. The proton singlet at 2.07 ppm, integrating for 3 protons is characteristic of an acetate bound methyl and was assigned to C-17 (δ_C 21.8) from HSQC analysis. The HMBC spectrum displayed a unique correlation existing with carbonyl C-16 (δ_C 171.2) confirming this methyl to belong to the acetate moiety. The HSQC revealed the last proton singlet seen at 5.14 ppm to be assigned to C-12 (δ_C 62.9). The two protons integration seen on the proton NMR spectrum confirmed the methylene nature of it. Moreover, bonding the acetate moiety at C-12 is confirmed by HMBC correlation seen between the methylene on C-12 and the carbonyl function on C-16 (δ_C 171.2).

The observed deshielding effect experienced by this methylene can be explained by the proximity with the oxygen atom part of the acetate moiety carbonyl function. This effect is even more intensified through the olefinic correlations with C-2 (δ_C 143.4), C-3 (δ_C 128.4) and C-6 (δ_C 135.9) aromatic carbons seen on HMBC. Finally, the triplets observed at δ_H 3.14 ppm and δ_H 4.55 ppm reflect the coupled methine groups respectively associated to C-4 (δ_C 27.9) and C-5 (δ_C 73.0) on the HSQC spectrum. Their shared coupling constants J = 7.9 Hz and the clear COSY correlations between this two methylene groups supports their locations on adjacent carbon atoms. The HMBC analysis corroborated heteronuclear correlation between protons on C-4 and C-6, while the more deshielded C-5 methylene only displayed correlation to C-4. The proton and carbon shift values of C-5 within the vicinity of a nitrate ester moiety have been described in previous literature. The presence of oxygen atoms from the nitrate ester generate a deshielding effect experienced by protons on C-5, supported by the carbon signal at 73.0 ppm for C-5 seen on HSQC. Above all, the nitrogen presence was reflected through HRESIMS (m/z 344.1484 $[M+Na]^+$) leading to the odd mass value m/z 321.1586.

The five olefinic carbon correlations seen with the HMBC experiment and the aromatic proton shift value of δ_H 7.64 ppm supported the presence of a phenyl ring. The other three

www.manaraa.com

unsaturations were assigned to the acetate moiety, the nitrate ester and the five-membered ring part of the indene skeleton.

Table III.3.1. ^{13}C and ^{1}H NMR Data for Alcyopterosin T-U (**1-2**).

Compounds	**1**		**2**	
Position	δC^a, type	δH^b, mult. (J in Hz)	δC^a type	δH^b, mult. (J in Hz)
1	47.3, CH_2	2.77, s	210.4, C	
2	143.4, C		134.2, C	
3	128.4, C		131.9, C	
4	27.9, CH_2	3.14, t (7.9)	28.4, CH_2	3.28, t (7.6)
5	73.0, CH_2	4.55, t (7.9)	72.0, CH_2	4.60, t (7.6)
6	135.9, C		137.4, C	
7	131.6, C		141.0, C	
8	128.8, CH	7.05, s	126.5, CH	7.64, s
9	143.4, C		150.4, C	
10	48.5, CH_2	2.71, s	41.3, CH_2	3.03, s
11	40.6, C		45.6, C	
12	62.9, CH_2	5.14, s	61.7, CH_2	5.25, s
13	20.9, CH_3	2.36, s	21.2, CH_3	2.47, s
14	30.5, CH_3	1.15, s	24.8, CH_3	1.25, s
15	30.5, CH_3	1.15, s	24.8, CH_3	1.25, s
16	171.2, C		170.4, C	
17	21.8, CH_3	2.07, s	21.2, CH_3	2.10, s

[a] ^{13}C shift and multiplicity determined by HSQC and HMBC correlations, recorded in $CDCl_3$ at 500 MHz, reported in ppm. [b] ^{1}H shift and multiplicity recorded in $CDCl_3$ at 500 MHz, reported in ppm.

The elucidation of alcyopterosin U (**2**) was confirmed by one- and two-dimensional NMR results. The HRESIMS $[M + H]^+$: m/z 336.1451, calcd. for $C_{17}H_{21}NO_6H$, m/z 336.1442, revealed the odd exact mass value m/z 335.1369 for the compound which reflected the presence of a

www.manaraa.com

nitrogen atom. Moreover, the presence of an additional oxygen was depicted in the molecular formula $C_{17}H_{21}NO_6$.

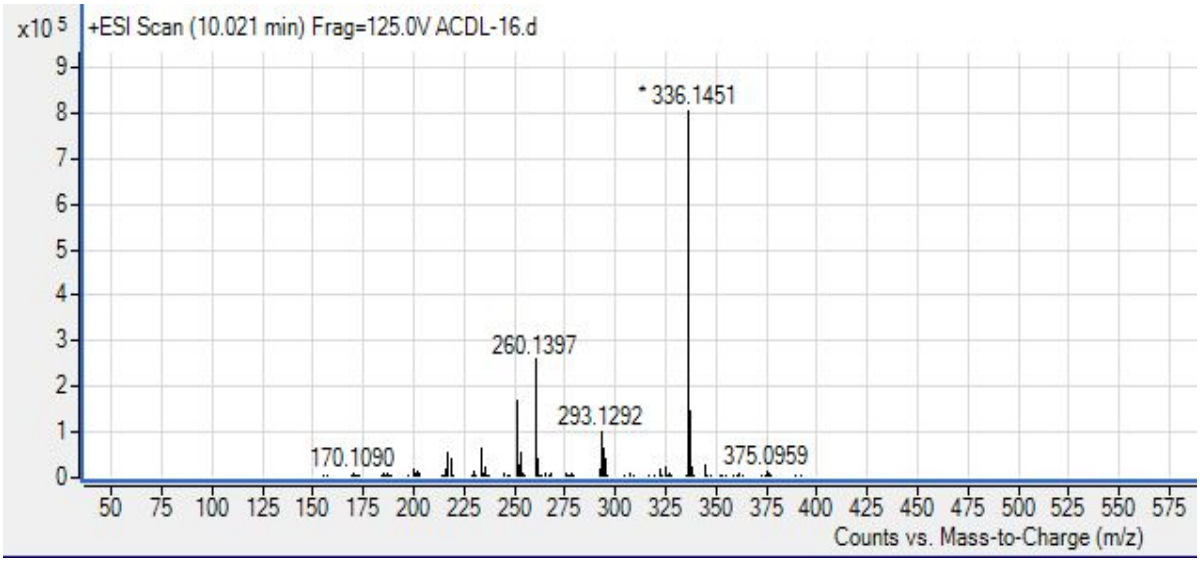

Figure III.3.1.8. MS for alcyopterosin U.

Five of the seven degrees of hydrogen deficiency were attributed to the indene ring, one to the nitrate ester moiety on C-5 (δ_C 72.0) and the last one to a ketone on C-1 (δ_C 210.4). Similar ranges of chemical shifts recorded for protons on C-4 (δ_C 28.4), C-5, C-12 (δ_C 61.7) and C-13 (δ_C 21.2) projected the conserved phenyl ring portion substitutions seen in alcyopterosin T. Also, carbons C-2 (δ_C 134.2), C-3 (δ_C 131.9), and C-6 (δ_C 137.4) supported the classic quaternary aromatic carbons arrangement found in the alcyopterosin compounds class.

www.manaraa.com

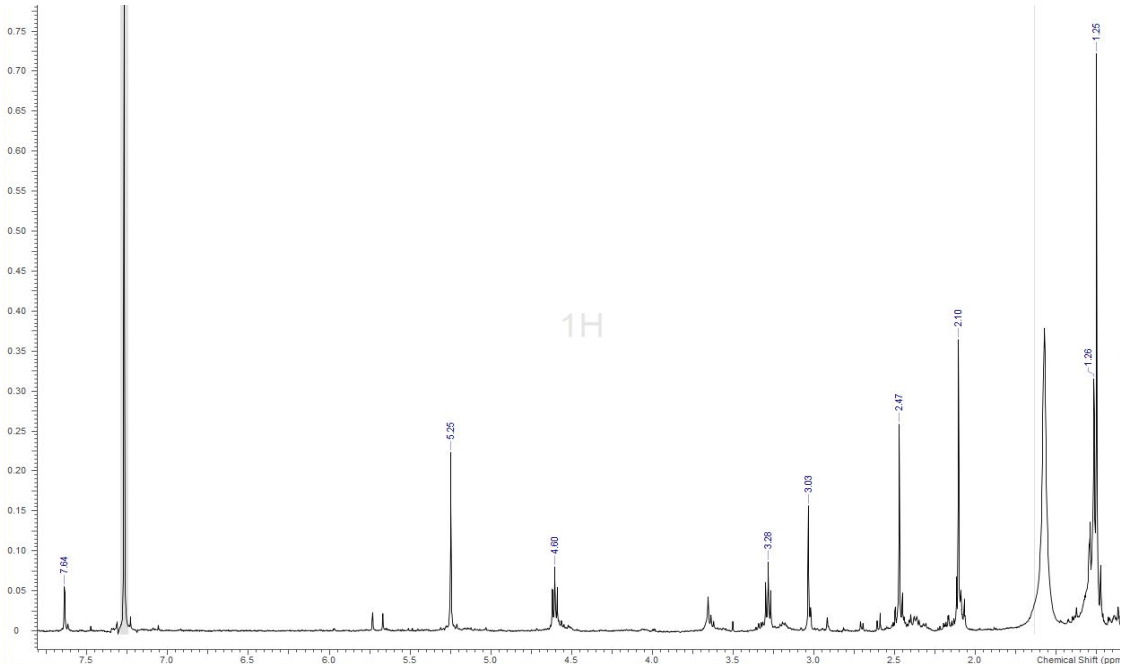

Figure III.3.1.9. ^{1}H NMR spectrum for alcyopterosin U in $CDCl_3$ (500 MHz).

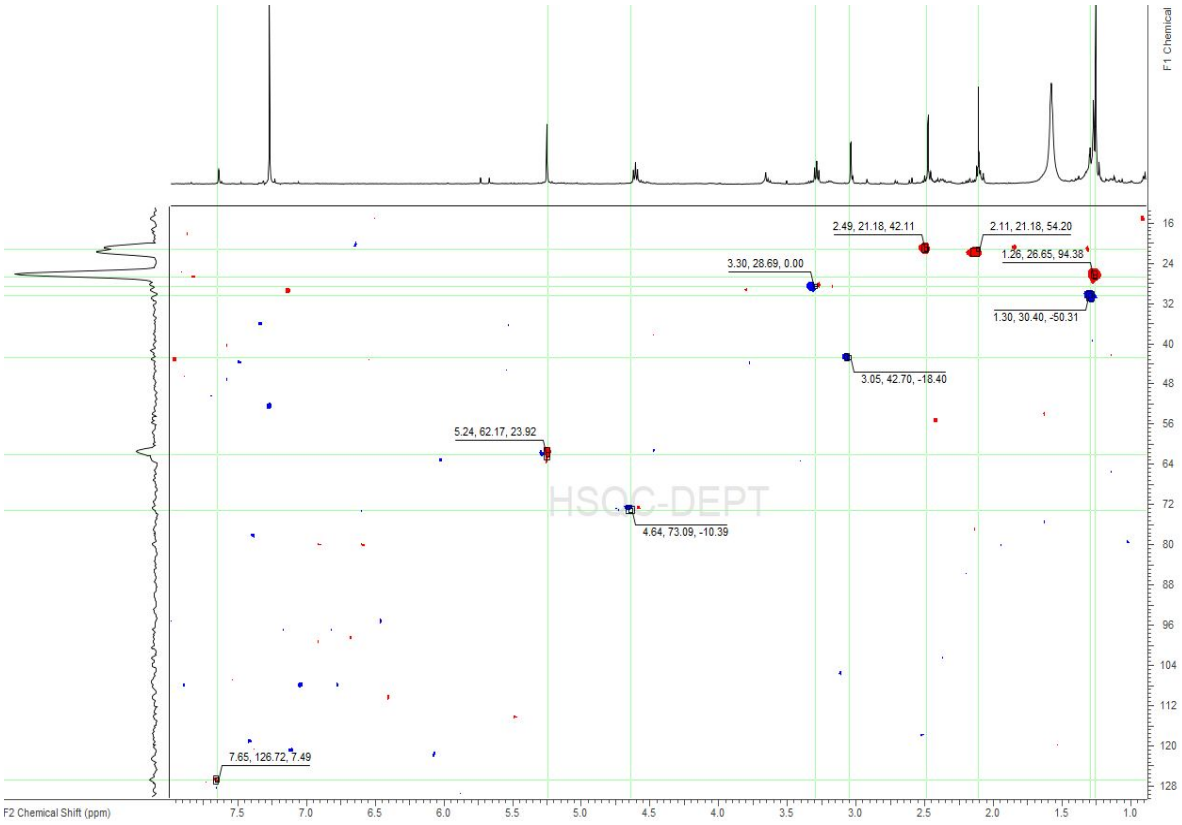

Figure III.3.1.10. HSQC spectrum for alcyopterosin U in $CDCl_3$ (500 MHz).

www.manaraa.com

Two-bond correlations between the aromatic proton singlet at 7.64 ppm on C-8 (δ_C 126.5) were clearly established with carbons C-7 (δ_C 141.0), C-9 (δ_C 150.4), and C-13 and reinforced the classic architecture found in northwest portion of the molecule. However, the higher carbon chemical shift value recorded for C-9, C-11 (δ_C 45.6), C-14 (δ_C 24.8), C-15 (δ_C 24.8), and the proton chemical shift values for protons on C-10 (δ_C 41.3), hinted at the presence of a deshielding functional group.

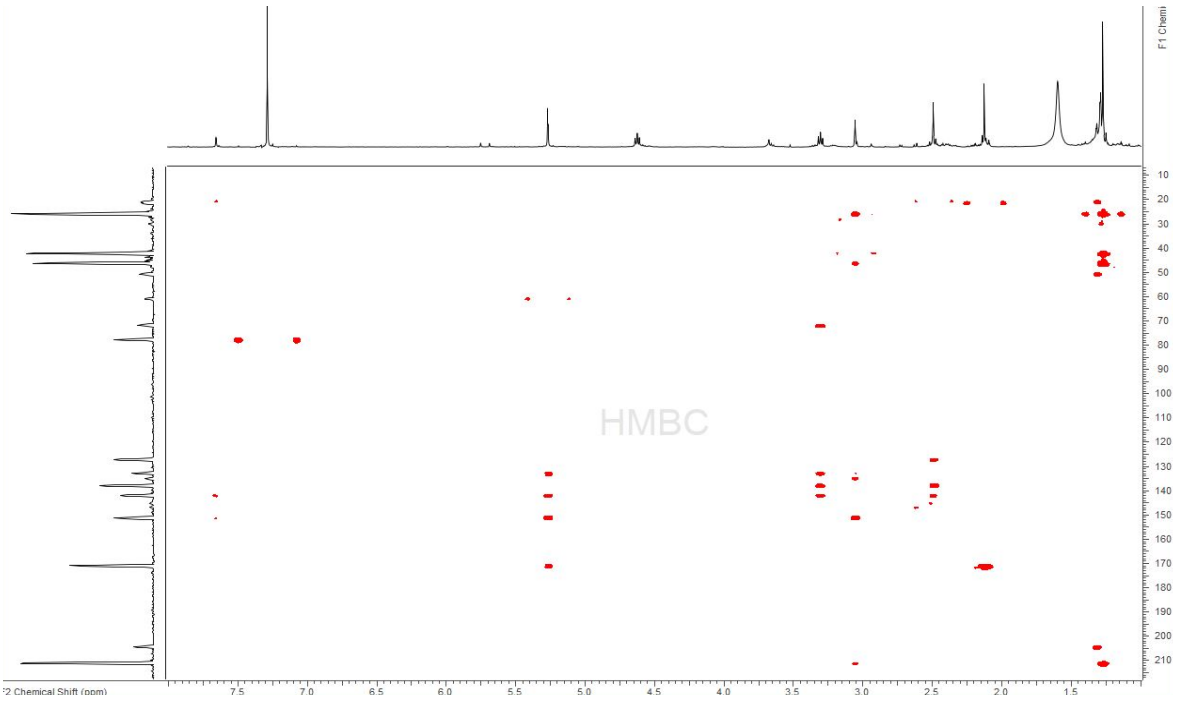

Figure III.3.1.11. HMBC spectrum for alcyopterosin U in $CDCl_3$ (500 MHz).

Moreover, the loss of HSQC and HMBC heteronuclear correlations related to C-1 clarified and supported the presence of a carbonyl function listed at δ_C 210.4 ppm. The novelty of alcyoterosin U resides in the appearance of a ketone functional group at C-1, also confirmed by IR spectrum value (1700 cm^{-1}) and increasing the chemical shifts values of the protons located in beta position on C-10, C-14, and C-15, and confirming the loss of two protons in comparison to alcyopterosin T.

www.manaraa.com

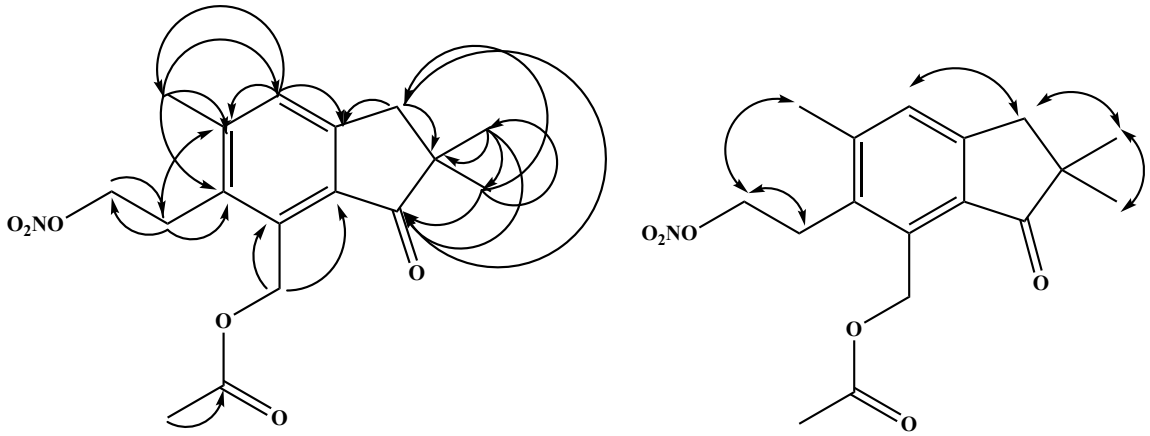

Figure III.3.1.12. Key HMBC (⌒) and ROESY (⌒) correlations establishing the planar structure of alcyopterosin U (**2**).

Previously isolated alcyopterosin C (**5**) shows HMBC correlation of the proton on C-8 with the ketone located on C-10.[29] The disappearance of this HMBC correlation in the case of alcyopterosin U corroborates and reinforces positioning the ketone on C-1 instead. As seen in alcyopterosin T, a characteristic acetate bound methyl was found as the proton singlet at δ_H 2.10. The HSQC experimentation assigned it to C-17 (δ_C 21.2) and confirmed the unique single correlation existing on HMBC analysis with carbonyl C-16 (δ_C 170.4) also recorded on IR spectra at 1750 cm^{-1}.

When Palermo et al. first isolated alcyopterosin E, they also performed its hydrolysis in 70% aqueous methanol over 3 days, which brought forward the hydroxylated version of the nitrate ester compound. Literature records of compound **7** describes it as the hydrolysis degradation product of alcyopterosin E (**6**),[29] but not as a natural product.

www.manaraa.com

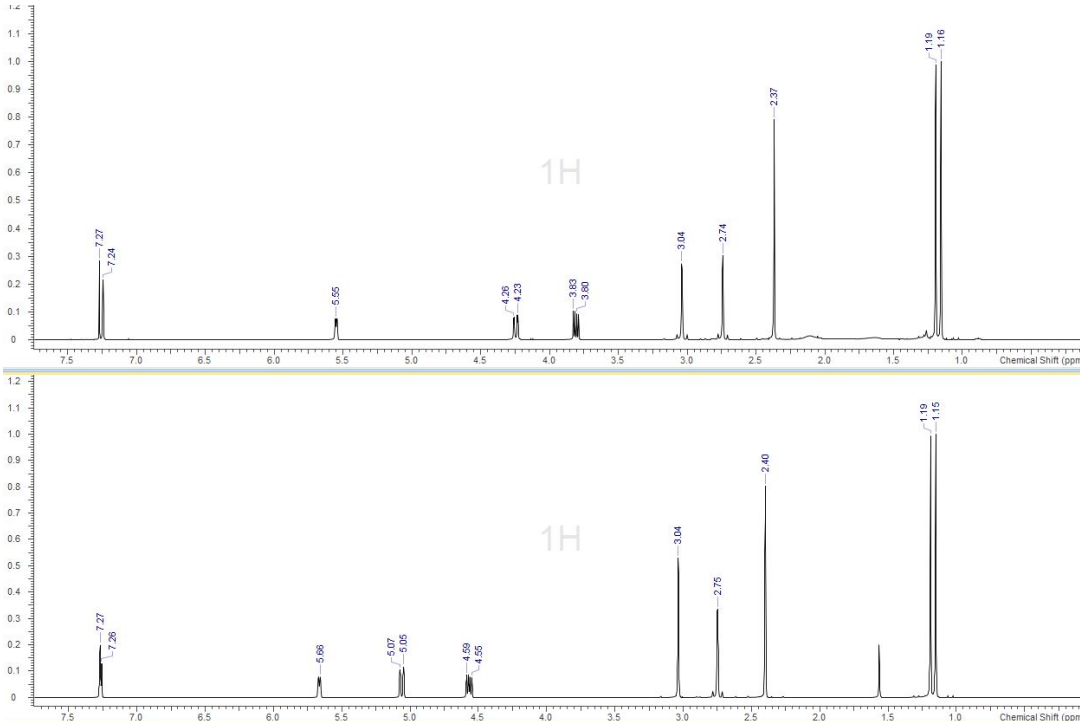

Figure III.3.1.13. ^{1}H NMR spectrum for (*S*)-3-(hydroxymethyl)-4,7,7-trimethyl-3,6,7,8-tetrahydro-1*H*-indeno[4,5-*c*]furan-1-one (**7**)(top) and alcyopterosin E (bottom) in $CDCl_3$ (500 MHz).

Proton and carbon chemical shifts of the isolated natural product match exactly the values found in the case of the hydroxylated degradation product.[29] The protons on C-5 (δ_C 63.3) appearing as doublet of doublet at 4.25 and 3.81 ppm. The geminal nature of these protons is supported by a coupling constant of J = 12.6 Hz expressing a trans configuration. Additionally, the signal at δ_H 3.81 ppm couples with the proton on C-4 with a coupling constant J = 6.0 Hz, suggesting a relative cis arrangement of the vicinal protons. The HRESIMS $[M + H]^+$: m/z 247.1379, calcd. for $C_{15}H_{18}O_3H$, m/z 247. 1329, revealed the even exact mass value m/z 246.1256 leading to the molecular formula $C_{15}H_{18}O_3$. (see Appendix A **Figure A.III.4.**) Due to their high degree of resemblance and the only difference residing in the C-5 substitution, compounds (**6**) and (**7**) were chosen to be tested in four biological assays and assess potency of the nitrate ester versus the hydroxyl moiety.

www.manaraa.com

III.3.2. Biological activities

The amount of isolated novel compounds was not sufficient to provide tangible biological activity results. However, the known nitrated alcyopterosin E and its hydroxylated version were fortunately found in much more substantial quantities which allowed further biological testing work. This study provides a comparative study of the influence of chemical substitution on biological activity. Alcyopterosin E and revealed potency against the following pathogens: *Leishmania donovani*, HeLa cancer cells, *Clostridium difficile*, and Respiratory Syncitial Virus.

A clonogenic assay evaluating the survival rate of HeLa cancer cells was conducted by Anthony Sanchez of the Kee lab and showed a minimum inhibitory concentration of 3.4 nM for alcyopterosin E (**6**) greater than the one of 81 nM for compound **7**. From the Kyle lab, assays against the *Leishmania donovani* parasite performed by Ala Azhari revealed alcyopterosin E to be more potent (IC_{50} 3.1 µM) than its hydroxylated version of it (IC_{50} 7.0 µM). However, against the J774.A1 macrophages strain, compound **4** (CC_{50} 62 µM) was more cytotoxic than compound **7** (CC_{50} 0.11 mM) laying in the low millimolar range. From the Sun lab, Hiran Malinda tested the two known alcyopterosin compounds against *Clostridium difficile*. Compound **7** (MIC > 6.9 µM) was more potent than compound **6** (IC_{50} > 8.1 µM) in killing 100% of the bacterium cells, but less cytotoxic against human tissue. Cytotoxicity values were acquired against HepG2 and HEK293T cell lines affording respective survival rates of 95% and 90% for compound **7** (CC_{50} 0.26 mM), while compound **6** (CC_{50} 0.22mM) provided a 5% decrease for both types of cell lines. Finally, a respiratory syncytial virus (rA2Rluc) assay, performed by Kim-Chi Teng of the Teng lab, demonstrated once more compound **7** (CC_{50} 0.03 mM) to be less cytotoxic than alcyopterosin E (CC_{50} 0.01 mM).

www.manaraa.com

Table III.3.2.1 Biological activity of sesquiterpenoids **6** and **7**.

Compounds	Cancer	*Leishmania donovani*		*Clostridium difficile*		Respiratory Syncitial Virus
	HeLa cells	J774.A1 IC_{50}	Cytotoxicity	MIC	CC_{50}	CC_{50}
6	3.4 nM	62 µM	3.1 µM	8.1 µM	0.22 mM	0.01 mM
7	81 nM	0.11 mM	7.0 µM	6.9 µM	0.26 mM	0.03 mM

Despite the stronger cytotoxic effects seen with compound **6**, the exerted versatility of activity begs for the exploration of other nitrated alcyopterosin compounds to confirm the structure-activity relationship related to the presence of the nitrate ester moiety at C-5. The presence of the γ- lactone may also be implicated, and combination of both functional groups may turn out to be crucial.

Previous biological studies[29] reported mild cytotoxicity of alcyopterosin E (**6**) toward Hep-2 human larynx carcinoma cell line Hep-2 (IC_{50} 13.5 µM). However, a synthetic approach ought to be outlined to palliate the mass limitations. Total synthesis routes have already been outlined for alcyopterosin A, C, E, I, L, M, and N, with still room for optimization.

Novel potency of already known alcyopterosin compounds encourages the development of synthetic methods to study the potency of the novel isolated structures alcyoterosins T and U, and the exploration of more structure activity relationships. Above all, the collaborative work of biology, synthetic and computational chemistry to offer more experimentation with analogs is desired and necessary to assess a full structure-activity relationship offered by these molecules and benefit the drug discovery field.

III.4. Triacetyl steroid

A less polar extraction process using dichloromethane was performed and led to the isolation of a novel steroid. When thinking about steroids, one's mind will most likely drift toward the infamous reputation of these metabolites in sports and the medical use of these.

www.manaraa.com

However, naturally produced by living organisms, steroids regulate the physiology. The biosynthesis of steroids starts with the cyclization of squalene, a triterpene, in sterols further modified in steroid. The steroid core structure is based on seventeen carbons arranged in three six-membered fused rings (A, B, C) and a five-membered ring (D). Previous studies have reported cytotoxic, anti-inflammatory, antimicrobial, even antileukemic activities from soft coral steroids.[32,33] Here, a novel antileishmanial tri-acetyl terpenoid lipid, from an undescribed octocoral, is elucidated and broadens the scope of steroids biological relevance.

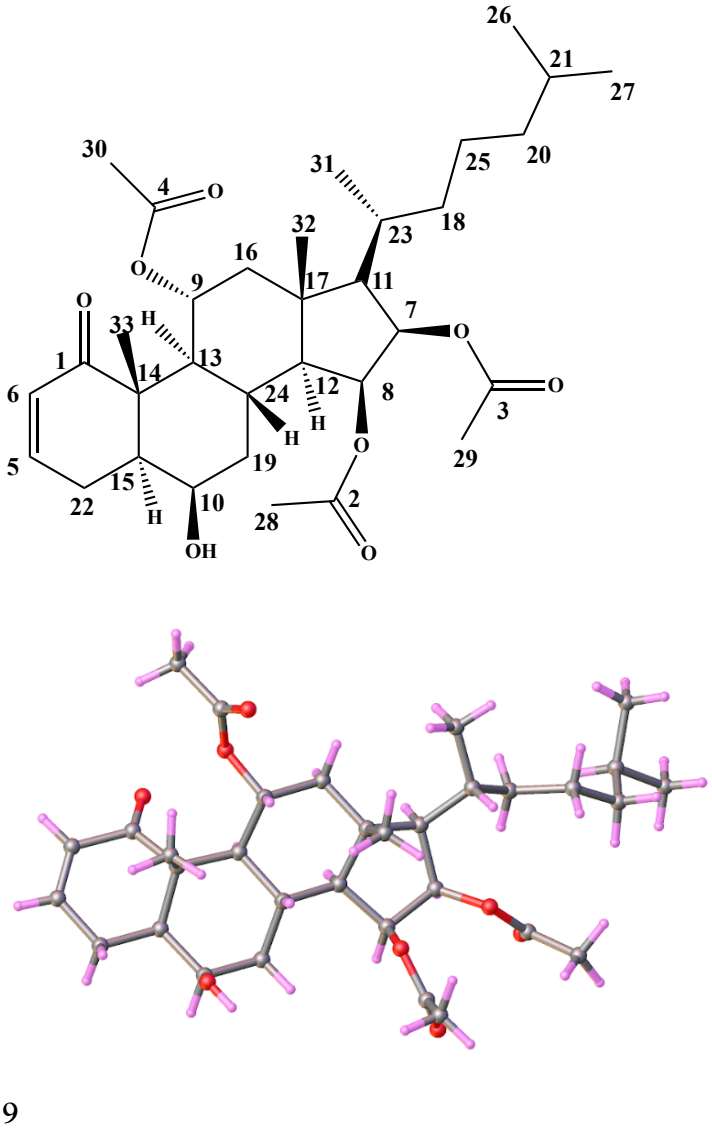

9

Figure III.4.1. Planar molecular and crystal structures of triacetyl steroid (**9**).

www.manaraa.com

III.4.1. Isolation and structure elucidation

Two batches of coral samples lyophilized, then extracted through three solvent cycles of a Soxhlet extraction with methylene chloride. Each dry extract was reconstituted in ethyl acetate and subjected to a partition against water. The ethyl acetate layer was converted into a silica gel for normal phase MPLC separation over a 0% to 100% gradient of ethyl acetate in hexanes.

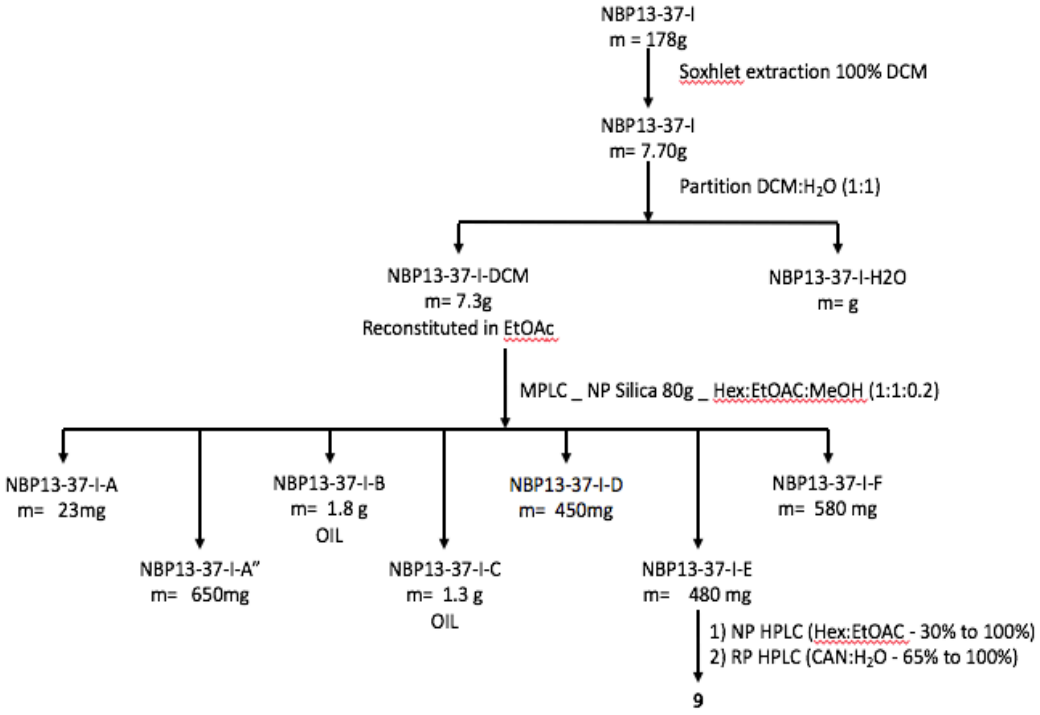

Scheme III.4.1.1. Fractionation Scheme of Antarctic deep sea octocoral sample I extracted in 100% DCM with Soxhlet apparatus.

The extract from the first batch yielded six fractions A through F were generated. Further purification of fraction E via a round of normal phase HPLC with a hexane:ethyl acetate (1:1) gradient, followed by another round of reverse phase HPLC using a water:acetonitrile (70% to 100%) gradient, led to the pure highly acetylated steroid compound described below.

www.manaraa.com

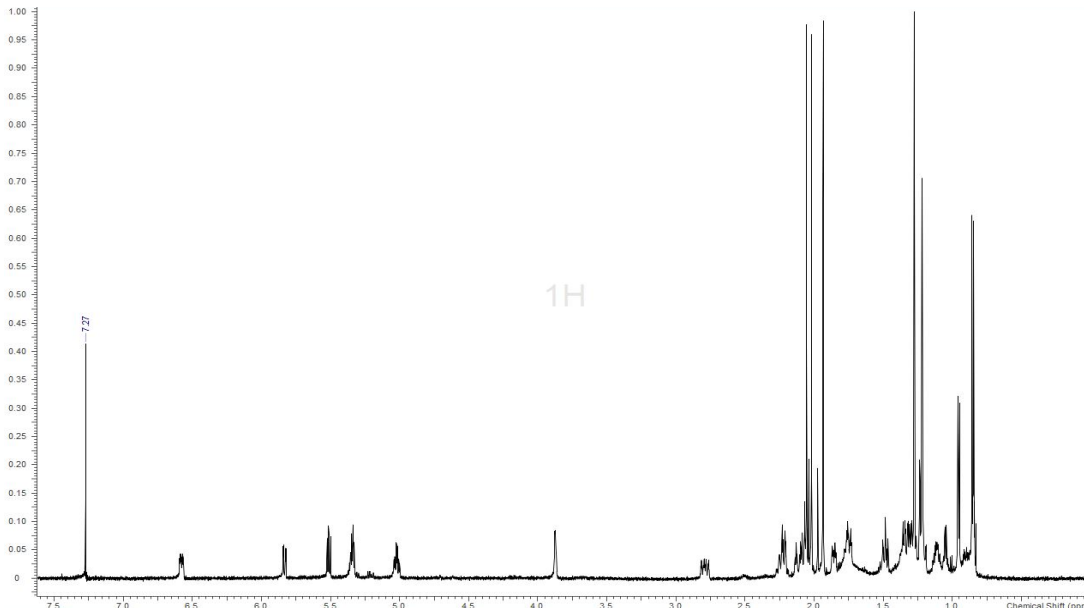

Figure III.4.1.1. ^{1}H NMR spectrum of triacetyl steroid **9** in $CDCl_3$ (500 MHz).

Despite the larger HRESIMS value [M - acetate]$^{+}$: m/z 515.3384 calcd. for $C_{31}H_{47}O_6^{\bullet}$ m/z 515.3367 detected, the molecular ion [M + H]$^{+}$: m/z 575.3550 calcd. for $C_{33}H_{50}0_8H$, m/z 575.3578, was also simultaneously seen and led to the chemical formula $C_{33}H_{50}0_8$ indicative of 9 degrees of unsaturation.

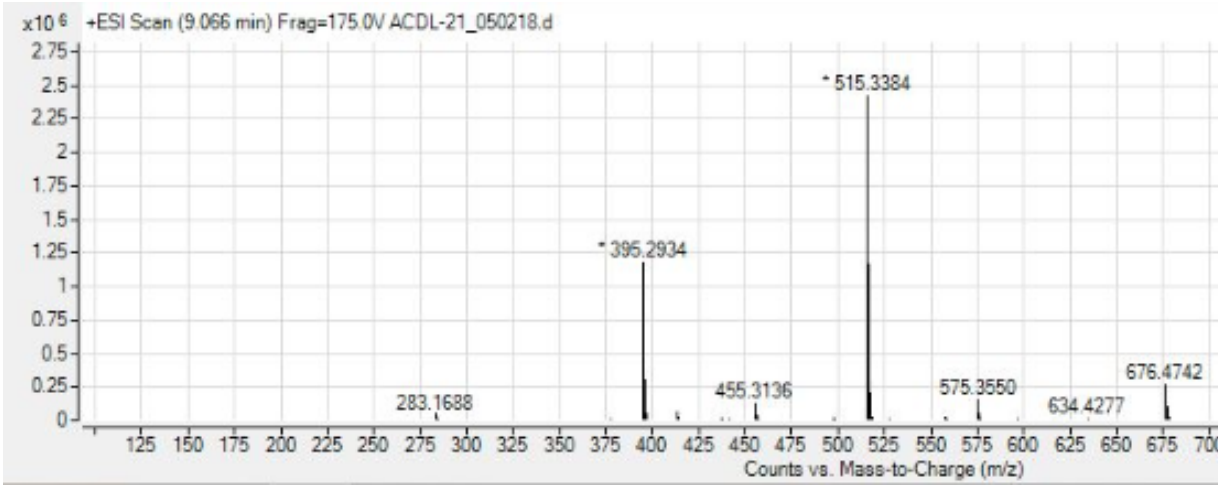

Figure III.4.1.2. MS of triacetyl steroid **9**.

www.manaraa.com

Table III.4.1. ^{13}C and ^{1}H NMR Data for triacetyl steroid **9**.

Position	δC[a]	δH[b], integration	HMBC
1	204.0		
2	170.4		
3	169.9		
4	169.4		
5	142.5	6.58, 1H	1, 15
6	128.4	5.81, 1H	14, 22
7	73.0	5.50, 1H	4, 8, 17
8	70.5	5.38, 1H	3, 7, 11, 17
9	70.5	5.01, 1H	14, 12, 24
10	69.7	3.87, 1H	14, 24
11	59.9	1.35, 1H	17, 20, 21
12	56.6	1.30, 1H	1, 13
13	47.9	2.06, 1H	1, 9, 12, 14, 25, 28
14	47.8	IV	
15	46.8	1.86, 1H	13, 28
16	46.6	2.19 and 1.49, 2H	9, 17, 29, 32
17	43.8	IV	
18	39.2	1.10, 2H	11
19	36.9	1.75, 2H	10, 14
20	35.6	0.91, 2H	18, 25, 26, 27
21	30.0	1.78, 1H	20, 25,10, 14
22	28.5	2.80 and 2.12, 2H	5, 6, 10, 14, 15, 19
23	28.0	1.50, 1H	8, 17
24	25.0	2.22, 1H	9, 12, 14
25	24.4	1.36 and 1.11, 2H	23, 26, 27
26	22.7	0.86, 3H	18, 23, 27
27	22.4	0.86, 3H	18, 23, 26
28	21.5	1.94, 3H ACETATE	2, 11, 19
29	20.7	2.05, 3H ACETATE	3, 8, 28
30	20.5	2.00, 3H ACETATE	4
31	18.2	0.95, 3H	11, 20, 21,
32	15.9	1.23, 3H	11, 12, 17,
33	13.2	1.28, 3H	1, 14

[a] ^{13}C shift recorded in $CDCl_3$ at 125 MHz, reported in ppm. [b] ^{1}H NMR spectrum shift and integration recorded in $CDCl_3$ at 500 MHz, reported in ppm.

Of the 33 signals seen on the carbon NMR spectrum, six appear in the above 100 ppm regions: C-1 associated to a ketone (δ_C 204.0), three quaternary carbons, C-2, C-3, and C-4

www.manaraa.com

respectively involved in acetylate moieties (δ_C 170.4, 169.9, and 169.4), and two other primary carbon signals (δ_C 142.5 and 128.4) describing C-5 and C-6 olefinic.

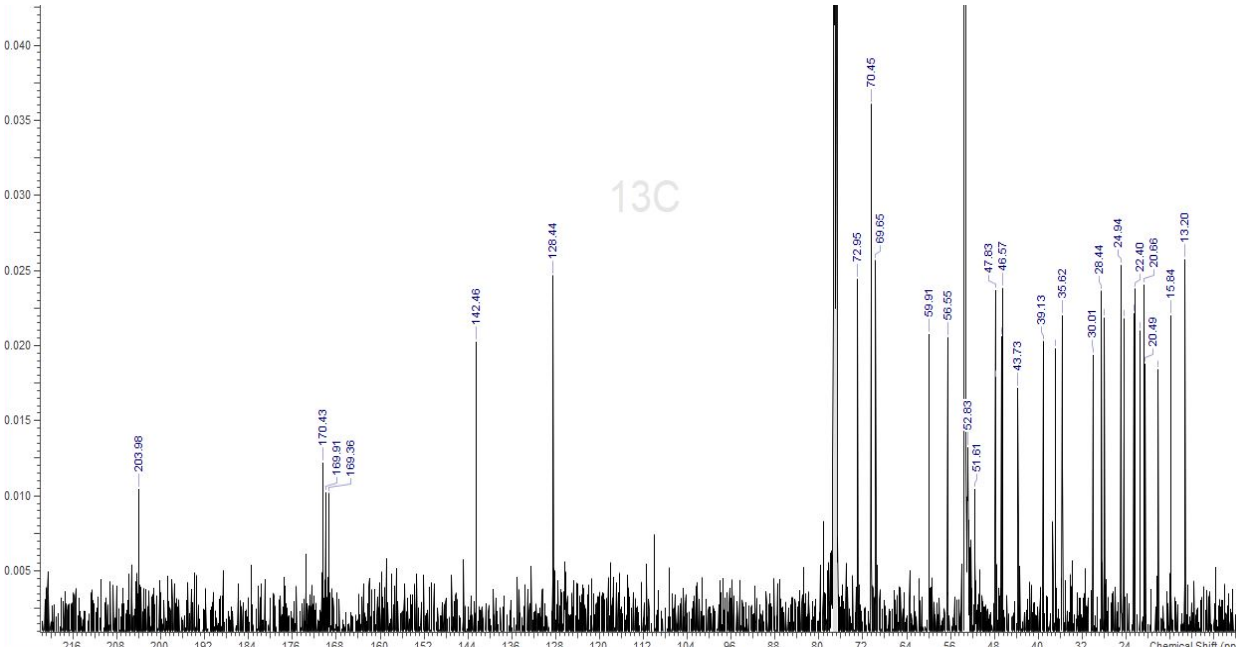

Figure III.4.1.3. ^{13}C NMR spectrum of triacetyl steroid **9** in $CDCl_3$ (125 MHz).

Proton and 2D HSQC NMR settled the relationship of these two protons (δ_H 6.58 and 5.81) associated with this olefinic carbons, respectively C-5 and C-6, while COSY correlations established their mutual adjacency. Additionally, HMBC correlations supported the three-bond connectivity of the proton on C-5 with the ketone on C-1 and the primary carbon C-15 (δ_C 46.8), and the one on C-6 connected to quaternary C-14 (δ_C 43.8) and secondary C-22 (δ_C 28.5). These relationships describe the conjugated feature of this olefinic functional group with the ketone on C-1. Further HMBC spectrum analysis of the methylene protons on C-22 provided two and three-bond correlations of these with C-5, C-6, C-14 and C-15, and an extra correlation with primary carbon C-10 (δ_C 69.7).

www.manaraa.com

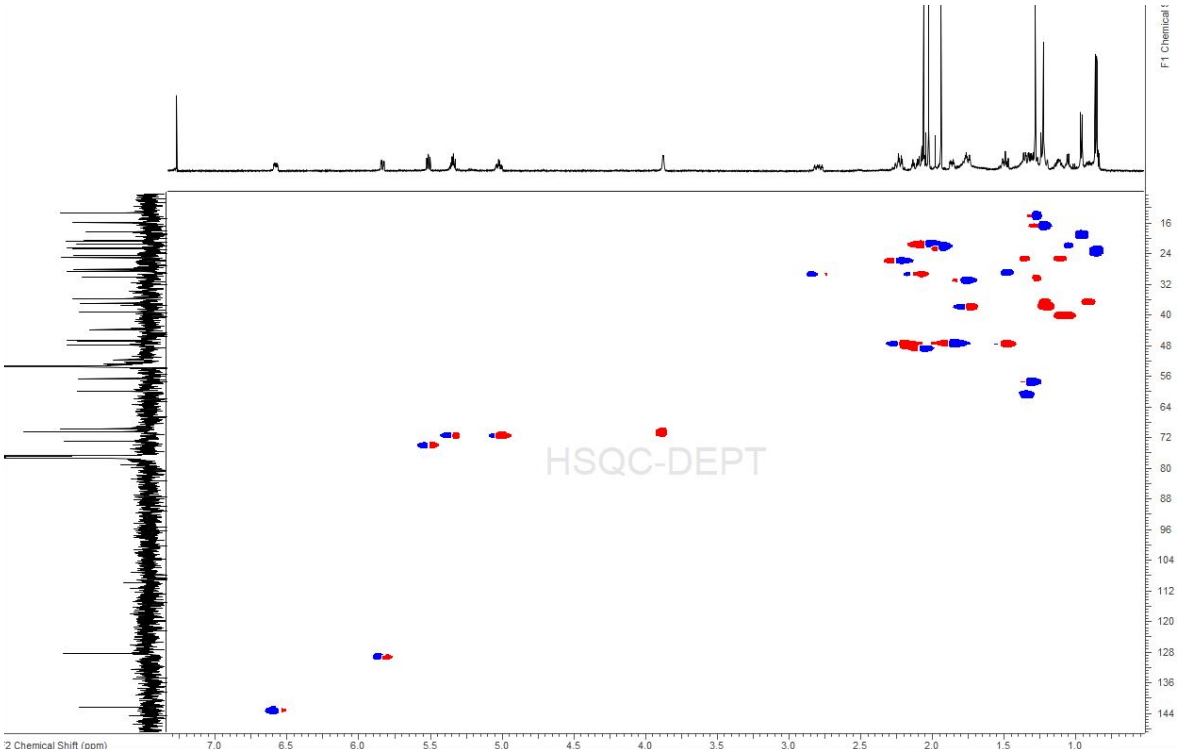

Figure III.4.1.4. HSQC NMR spectrum of triacetyl steroid **9** in $CDCl_3$ (500 MHz).

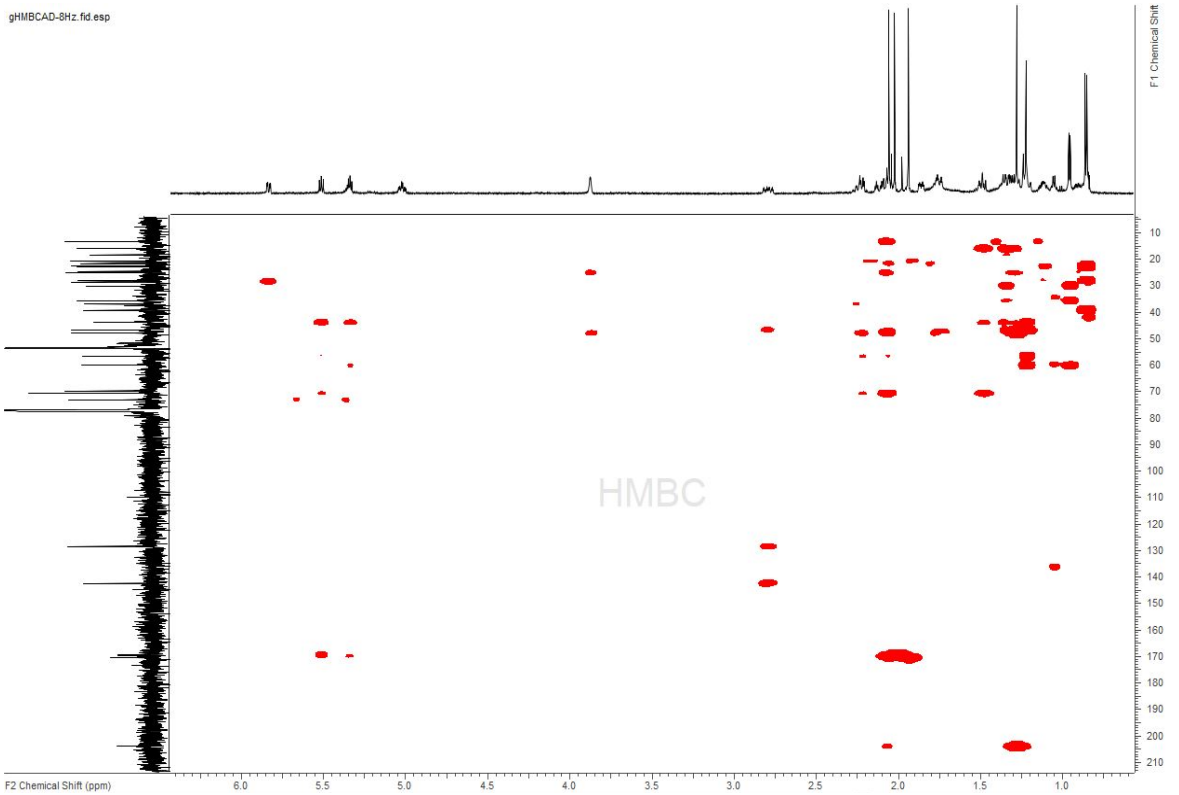

Figure III.4.1.5. HMBC NMR spectrum of triacetyl steroid **9** in $CDCl_3$ (500 MHz).

www.manaraa.com

The methine proton (δ_H 1.86) associated with C-15 illustrates a three-bond correlation with C-13 (δ_C 47.9) with COSY correlations with methylene protons on C-22, while the C-10 methine proton (δ_H 3.87) shows COSY correlations with C-19 (δ_C 36.9) methylene protons (δ_H 1.75). Furthermore, the chemical shift of C-10 hints binding with a heteroatom, oxygen in this case, and a hydrogen (δ_H 3.87) confirmed by HSQC. The C-10 methine proton, further displayed three-bond correlations with quaternary C-14 and C-24 (δ_C 25.0) bearing a single proton (δ_H 2.22) displayed a methine on HSQC. The methine proton on C-24 also showed two-bond HMBC correlation with C-12 (δ_C 56.6) and three-bond correlations with C-9 (δ_C 70.5) and C-14. Compared to C-12, the carbon shifts of C-9 indicated the presence of another heteroatom oxygen connectivity, confirmed by the deshielded chemical shift (δ_H 5.01) related to the associated proton. Additionally, a COSY correlation is seen with the adjacent C-9 methylene protons (δ_H 2.19 and 1.49) on C-16 (δ_C 46.6).

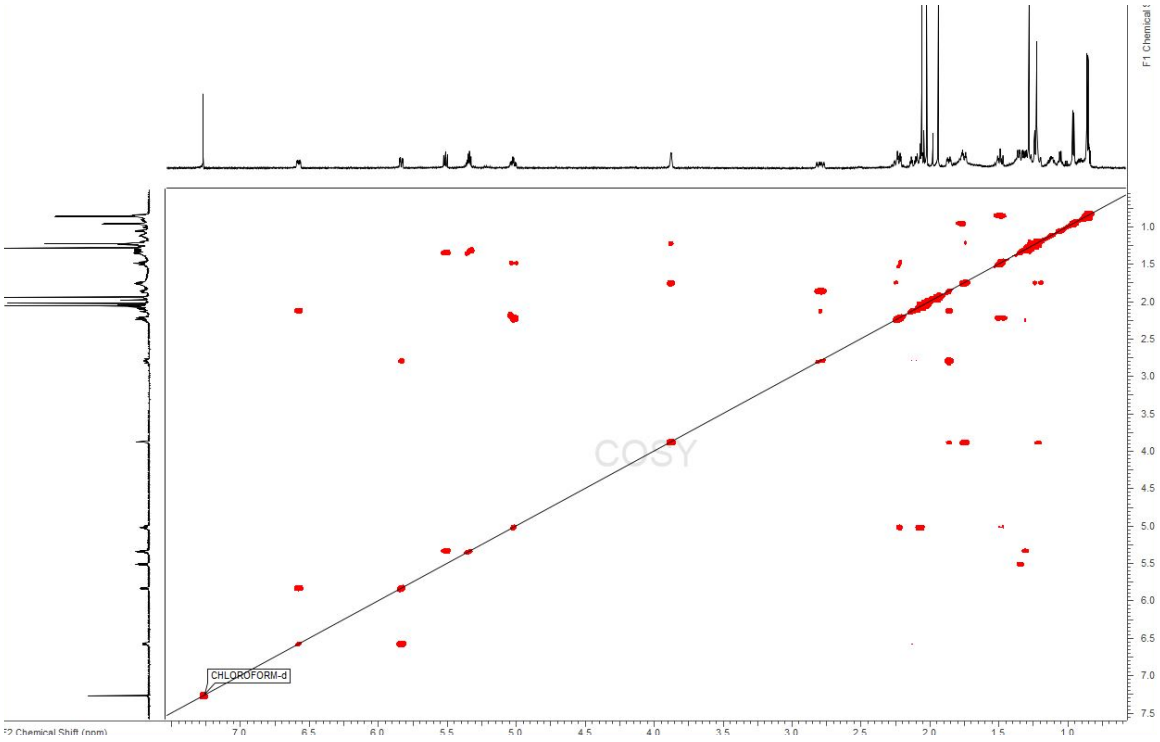

Figure III.4.1.6. COSY NMR spectrum of triacetyl steroid **9** in $CDCl_3$ (500 MHz).

www.manaraa.com

Two-bond HMBC correlations of C-16 protons with quaternary carbon C-17 (δ_C 43.8), along with three-bond correlations with C-9 and C-32 (δ_C 15.9). Concomitantly, a methine on C-13 (δ_C 47.9) described HMBC correlations two-bond correlations with C-9 and C-14, and three-bond correlations with C-1 and C-12, providing the full atom connectivity describing the intrinsic A-B-C juxtaposed rings, known in steroids. Finally, protons on C-33 (δ_C 13.2) methyl group display two and three-bond correlations with C-14 and C-1 respectively, while C-30 (δ_C 20.5) and its associated methyl protons (δ_H 2.00), describe typical shifts pertaining to an acetate moiety, which are confirmed by the two-bond HMBC correlation seen with C-4. A conjugated ketone (C-1, C-5, C-6), an alcohol (C-10), two methyl groups (C-32 and C-33), and an acetate moiety on C-9 are the various features customizing this steroidal pattern and creating molecular originality. The five membered D ring completing the steroidal ring pattern is put together from C-12 displaying proton COSY correlation of its methine (δ_H 1.30) with another methine proton (δ_H 5.38) on C-8 (δ_C 70.5). The high proton and carbon shifts associated with the methine on C-8 transcribe the connectivity with an oxygen heteroatom. The auxiliary HMBC two-bond correlation between methyl protons (δ_H 1.94) on C-28 (δ_C 21.5) and C-2 are reflective of an acetate moiety. The COSY spectrum also elucidates the adjacent position of another methine (δ_H 5.50) on C-7 (δ_C 73.0) with the one on C-8. These similar high chemical shifts can explain the presence of a third acetyl moiety on C-7, confirmed by the HMBC correlation of methyl protons (δ_H 2.05) related to C-29 (δ_C 20.7) correlate to the acetate carbonyl C-3. Lastly, two and three-bond HMBC correlations involving C-7, C-8, C-11 (δ_C 59.9), C-12, C-17, and C-32, allow closure of the five membered D ring of the steroid framework. Three-bond HMBC correlations exist between the methine on C-7, C-12 and C-17, while the one on C-8 shows relationships with C-11 and C-17. Moreover, the C-32 methyl displays the two-bond correlation with C-17 and three-bond one with C-11. COSY correlation of the C-11 methine (δ_H 1.35) with methines on C-7 and C-23 (δ_C 28.0) supports ring

www.manaraa.com

closure and extension to the aliphatic chain final emblematic steroidal feature. The region between 0.00 ppm and 1.50 ppm describes the proton chemical shifts related to the aliphatic chain. COSY and HMBC correlations confirm the atomic connectivity.

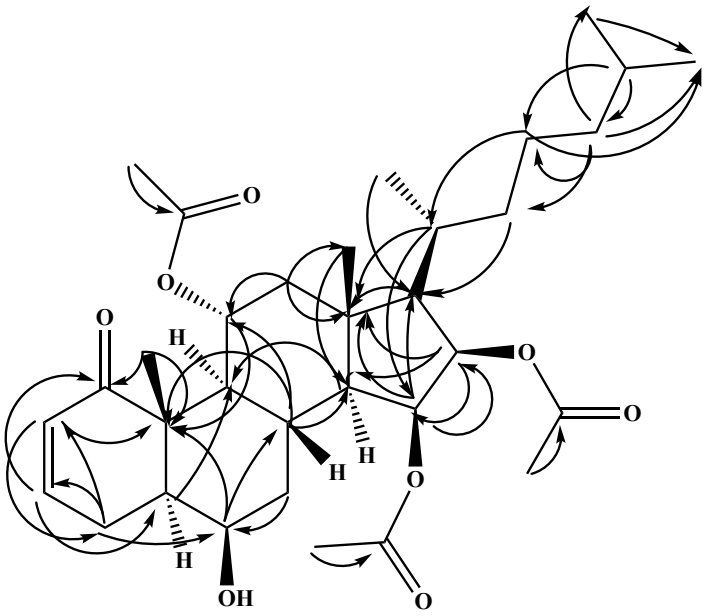

Figure III.4.1.7. Key HMBC (⁀) correlations establishing the planar structure of compound **9**.

While the C-11 methine confirms its adjacent position to the one on C-23, the methylene protons on C-18 (δ_C 39.2) display a unique three-bond HMBC relationship with C-11, and provide COSY correlations with C-23 methine (δ_H 1.50) and methylene protons (δ_H 1.11 and 1.36) on C-25 (δ_C 24.4). The C-25 protons confirm the COSY correlation with C-18 proton and another one with the methylene protons (δ_H 0.91) on C-20 (δ_C 35.6). Finally, the HMBC spectrum supports a three-bond correlation of the methine proton (δ_H 1.78) on C-21 (δ_C 30.0) with C-25, and a two-bond one with C-20, C-26 (δ_C 22.7) and C-27 (δ_C 22.4). Both methyl protons of C-26 and C-27 display three-bond HMBC correlation with C-20 as well as mutual ones between each other. Above all, crystallization of the compound in ethyl acetate, and thanks to the work done by Dr. Lukasz

www.manaraa.com

Wojtas and his student Gaurav Verma, the crystal structure confirmed the atoms connectivity elucidated via NMR analysis with additional stereochemistry features.

III.4.2. Biological activity

Sarah Kennedy from the Shaw lab tested the triacetyl steroid against a group of bacterial pathogens *Enterococcus faecium, Staphylococcus aureus, Klebsiella pneumoniae, Acinetobacter baumanii, Pseudomonas aeruginosa,* and *Enterobacter* involved in severe nosocomial infections and summarized under the acronym *ESKAPE*, but no activity was recorded. However, when tested against the *Leishmania donovani* parasite by Ala Azhari from the Kyle lab, the triacetyl steroid revealed potent at IC_{50} 1.5 µM. Insufficient amount of compound prevented cytotoxicity assessment.

III.5. Prostaglandins

In the 1930's, Ulf von Euler was the first to stumble upon prostaglandins. He discovered that they were present in the seminal fluid and vesicle of most animals including man and named them after the prostate gland where they were thought to be secreted from. Twenty years later, Sune K. Bergström made outstanding discoveries regarding chemistry and biochemistry of these molecules. With his graduate student Bengt I. Samuelsson, he described the conversion of arachidonic acid, an unsaturated fatty acid, in prostaglandins. In early the 1960's, complementary biological experiments performed by John R. Vane unveiled the almost ubiquitous characteristic of prostaglandins as they are actually produced by many tissues and organs and not just the prostate. The collaborative work of these three gentlemen led to the Nobel Prize in Medecine in 1982. Prostaglandins are lipid compounds with hormone-like effects in animals. They can stimulate a reaction in one tissue and inhibit it in another. Receptors to which the molecules bind govern the fate of the enzymatic cascade triggered. This multi-role asset of prostaglandins

www.manaraa.com

makes them useful in many treatments. They demonstrate powerful anti-inflammatory and vasodilating properties implicated in reproduction, hemostasis, digestive, and respiratory regulation functions. Two biosynthetic pathways cyclooxygenase (COX) and lipoxygenase (LOX) operate the oxidation of polyunsaturated acids and govern the molecular structure outcome. Prostaglandins are made of 20 carbon atoms, including a five membered ring. The degrees of oxidation in the ring, side chain, and the fatty acid chain reflect structure-activity specificity and allow categorization of the analogs in different classes.

The earliest report of prostaglandins in marine invertebrates dates back from 1969; Weinheimer and Spraggins isolated the 15-epi-prostaglandin A and its acetate methyl ester from a gorgonian-type coral *Plexaura homomalla*. Subsequent intense study of gorgonians contributed to more accumulated prostaglandin chemical discovery and motivated pharmaceutical studies. The study of this deep-water Antarctic coral led to three undescribed prostaglandin A structures.

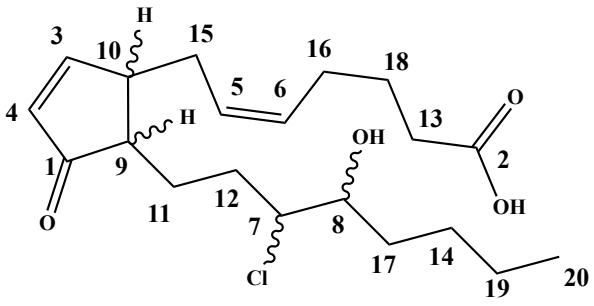

10

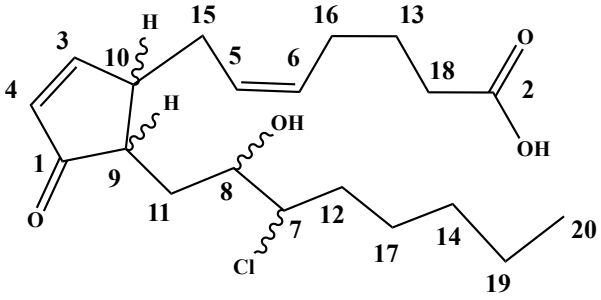

11

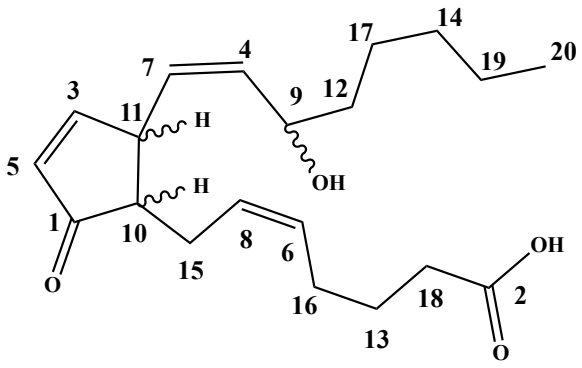

12

www.manaraa.com

III.5.1. Isolation and structure elucidation

The Soxhlet crude extract from the second batch of lyophilized undescribed octocoral was also investigated. The chromatographic purification process provided three novel prostaglandins compounds.

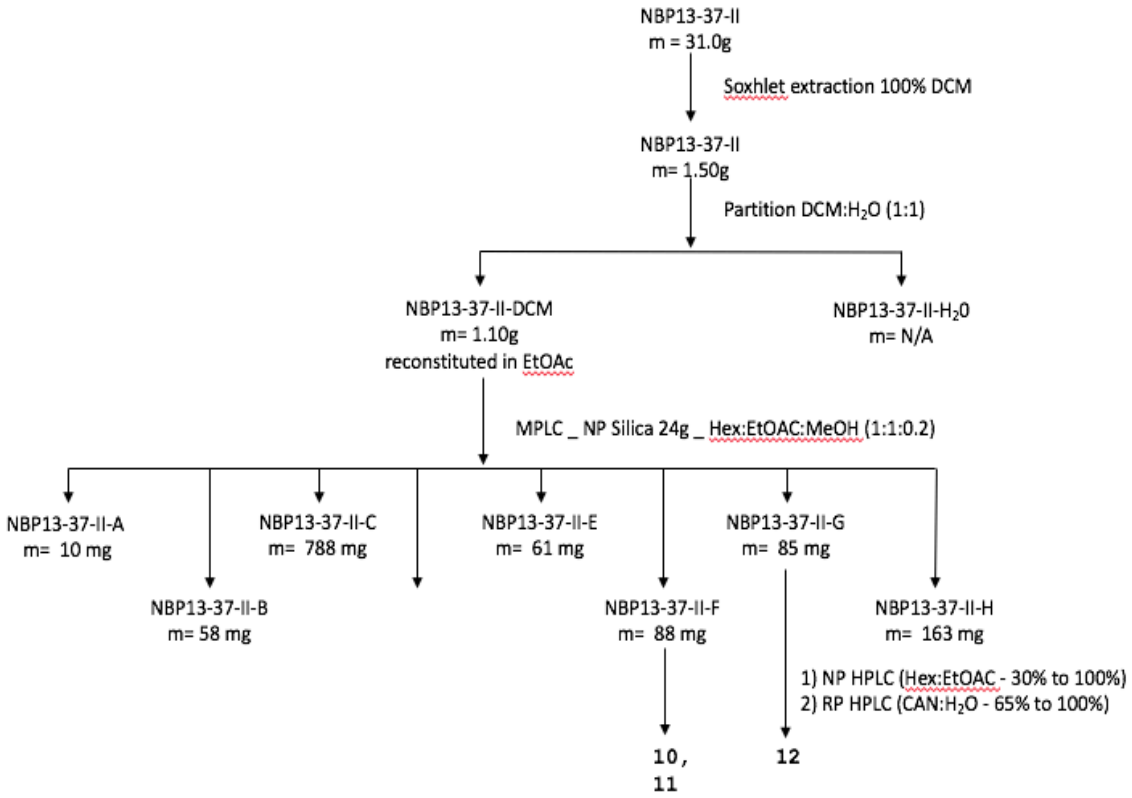

Scheme III.5.1.1. Fractionation Scheme of Antarctic deep sea octocoral sample II extracted in 100% DCM with Soxhlet apparatus.

MPLC fractions A through H were generated. Fractions F and G were carried over normal phase HPLC using an hexane:ethyl acetate (1:1) gradient over 30 min. Three novel prostaglandins arose: compounds **10** and **11** from fraction F, while compound **12** was isolated from fraction G. Despite the very similar mass value detected for both compounds **10** ($[M + Na]^+$: m/z 393.1798 calcd. for $C_{20}H_{31}ClO_4Na$, m/z 393.1803) and **11** ($[M + Na]^+$: m/z 393.1804 calcd. for $C_{20}H_{31}ClO_4Na$, m/z 393.1803), the NMR spectra displayed distinctive signals supporting their novel status. Both mass

www.manaraa.com

spectra displayed a 1:3 ratio pattern of the parent peak, hinting at the presence of a chlorine atom, which led to the chemical formula $C_{20}H_{31}ClO_4$ predicting a hydrogen deficiency of 5 unsaturations.

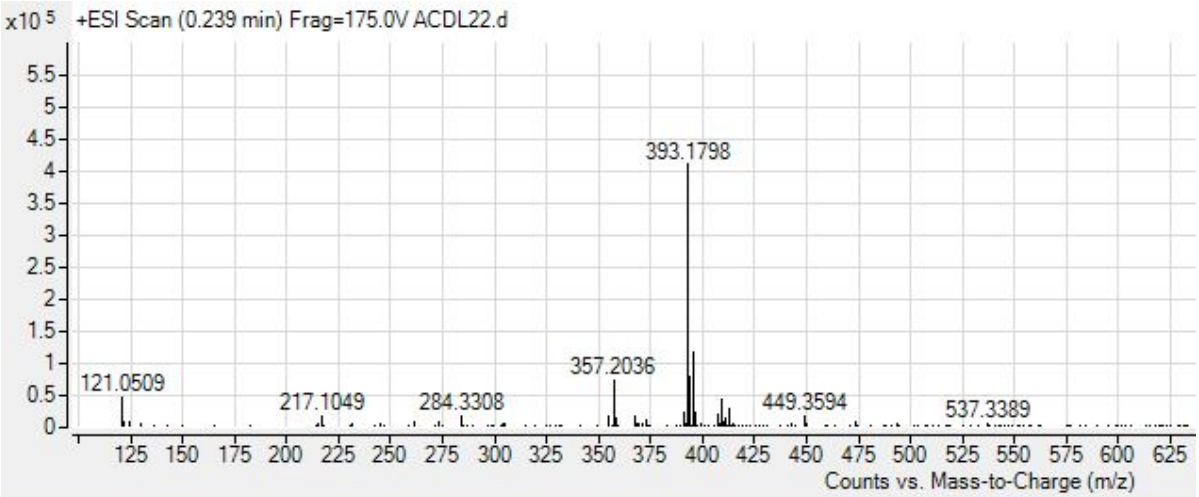

Figure III.5.1.1. MS of prostaglandin **10**.

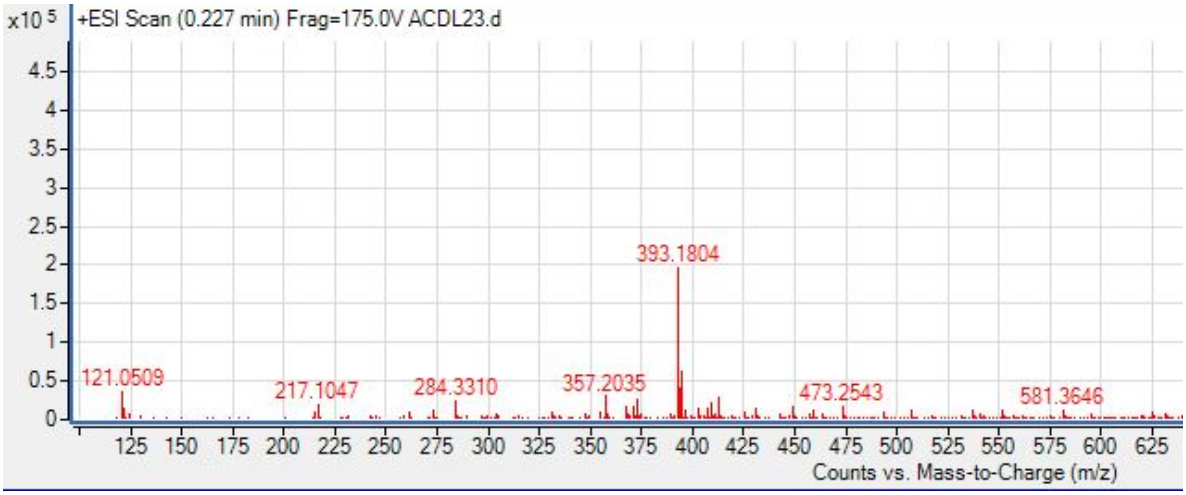

Figure III.5.1.2. MS of prostaglandin **11**.

www.manaraa.com

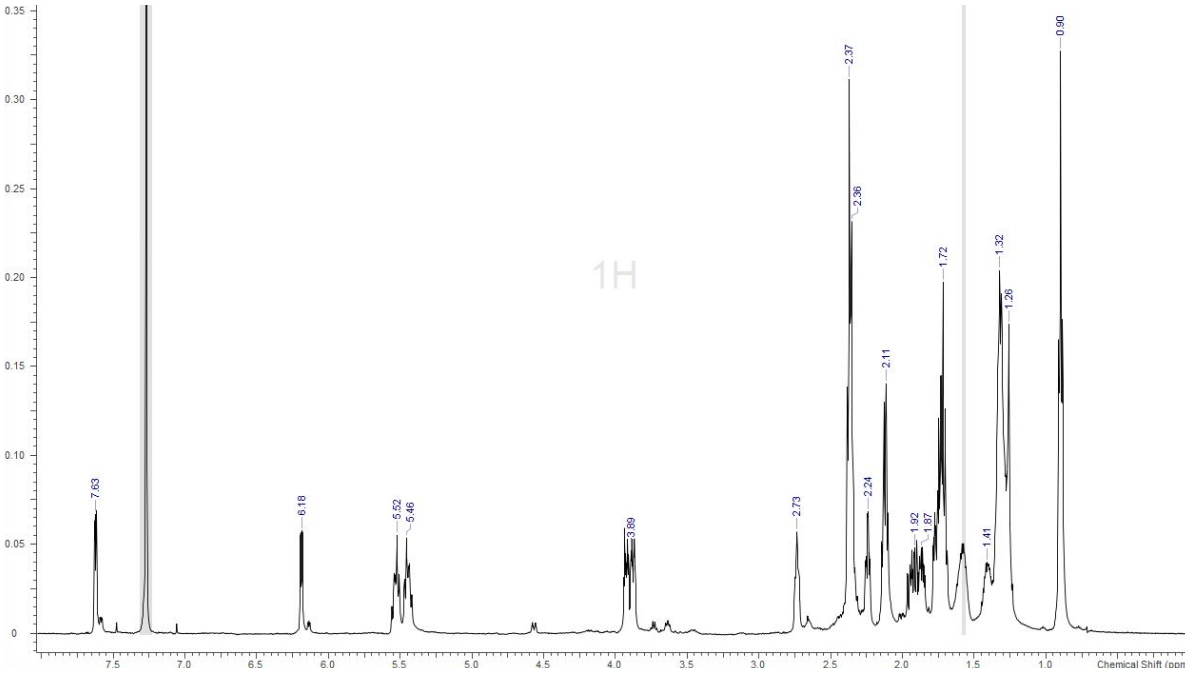

Figure III.5.1.3. ^{1}H NMR spectrum of prostaglandin **10** in $CDCl_3$(500 MHz).

Regarding **10**, the proton signals at δ_H 7.63 and δ_H 6.20 respectively connected to C-3 (δ_C 167.2) and C-4 (δ_C 133.0) suggest the presence of a conjugated π electrons system, while the proton signals at δ_H 5.54 and δ_H 5.46, respectively located on C-5 (δ_C 131.7) and C-6 (δ_C 126.4), belong to an isolated olefinic system. Two additional unsaturations are explained by the carbon shifts belonging to two quaternary carbon atoms C-1 (δ_C 213.0) and C-2 (δ_C 178.6) and revealing the presence of carbonyl functions. With only sp^3 hybridized carbon left, the last unsaturation to be accounted for probably refers to a ring structure being present. Moreover, the chemical shifts δ_H 2.25 and δ_H 2.74 belonging to protons respectively located on C-9 (δ_C 49.4) and C-10 (δ_C 48.8), are typical of ring junction positioned protons. The HMBC spectrum describing the correlations between protons and surrounding carbons within a two to three-bond distance of each other, revealed strong correlations of the proton on C-9 with C-1, C-11 and while a weaker one with C-10.

www.manaraa.com

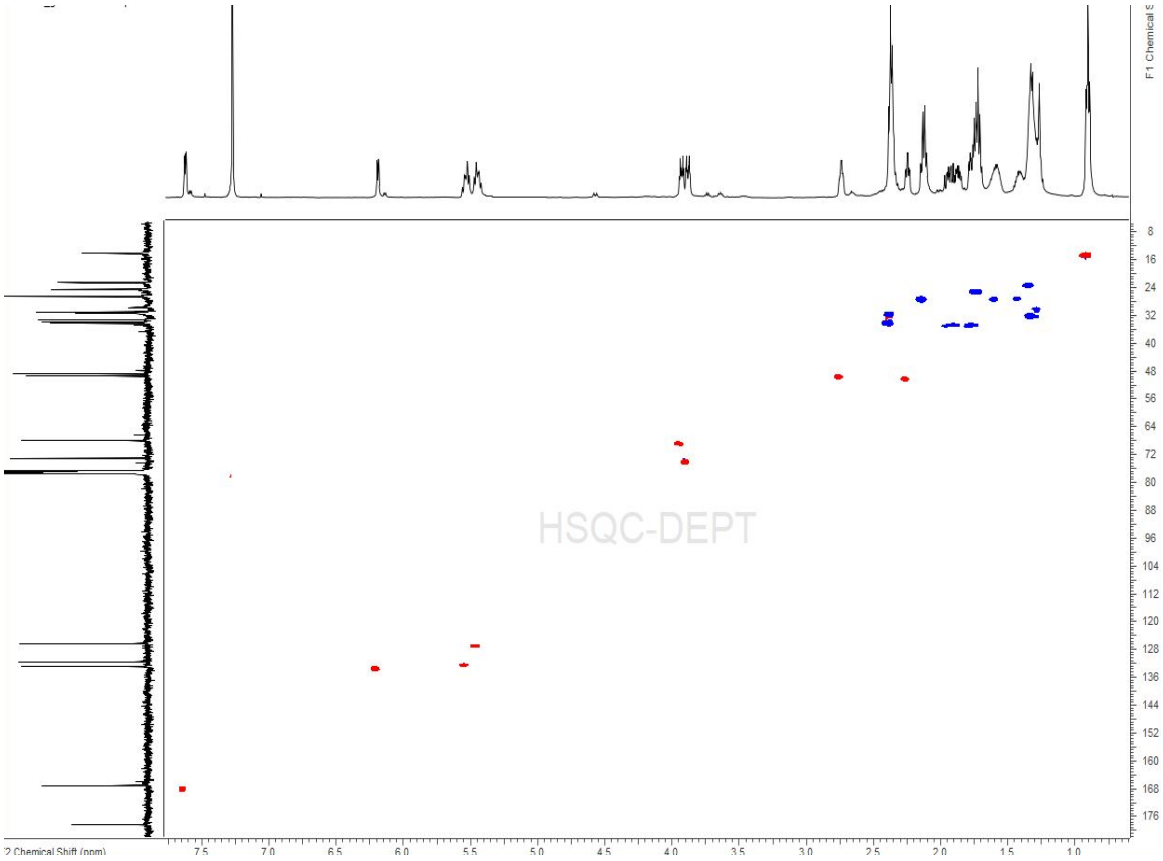

Figure III.5.1.4. HSQC NMR spectrum of prostaglandin **10** in $CDCl_3$ (500 MHz).

Observing the proton on C-10, the correlation with C-9 was not seen. However, it correlated strongly with C-3 and C-15 (δ_C 30.9). The COSY correlations describing proton-proton interactions on adjacent carbons confirmed the adjacent position of the proton on C-9 with the ones on C-10 and C-11 (δ_C 34.2), while the one on C-10 is neighboring the ones on C-3 and C-15.

Finally, the strong HMBC correlations of the protons located on C-4 and C-3 determined the orientation of the conjugated olefinic system. The proton on C-4 correlates with C-1, C-3, and C-9 while the one on C-3 correlates with C-1, C-4, and C-10. The conjugated π electrons system exists between C-1, C-3, and C-4, and is part of a five membered ring system. COSY and HMBC analysis established the connectivity between C-9 and C-11. Additionally, according to COSY correlations, the protons on C-11 interact with the ones on C-12 (δ_C 33.8). The HMBC

www.manaraa.com

readings for the methylene C-11 show correlations with C-9 and C-7 (δ_C 73.1). The HSQC spectrum displayed C-7 correlated to the proton shift at δ_H 3.88 and C-8 (δ_C 67.9) associated with the proton shift at at δ_H 3.93, both typical of carbon atoms bonded to heteroatoms. Furthermore, the HMBC helped settle the relative position of C-7 and C-8 on the lower aliphatic chain of the molecule. A strong correlation of C-7 with C-12 and a low one with C-17 (δ_C 26.4), indicated the presence of a carbon between C-7 and C-17.

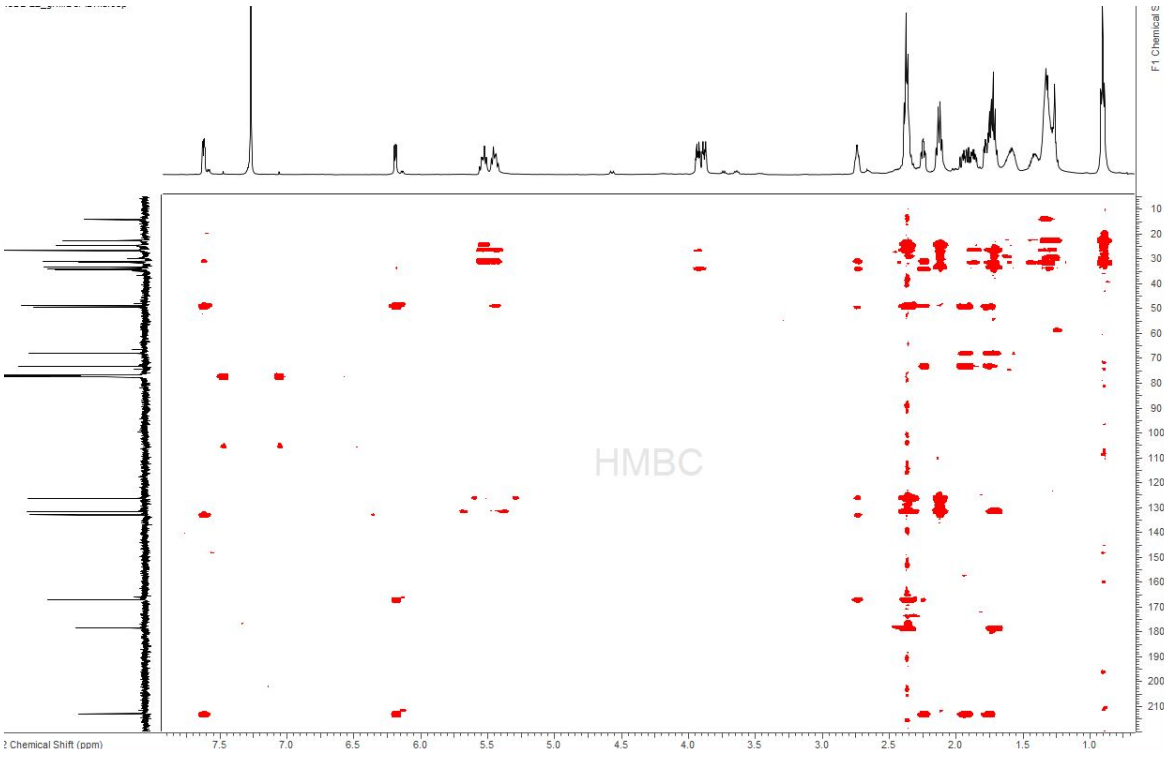

Figure III.5.1.5. HMBC NMR spectrum of prostaglandin **10** in $CDCl_3$ (500 MHz).

The COSY correlation reflected communication of the proton on C-7 with those on C-8 and C-12, confirming C-7 being placed between C-12 and C-8. The protons on C-12 correlate to the ones on C-11 and C-7, while the proton on C-8 only does so with the proton on C-7. The COSY correlations for protons on C-17 do not support a tangible explanation of adjacent protons, but the HMBC confirmed two-bond correlations with C-8 and C-14 (δ_C 31.3). Moreover, HMBC

www.manaraa.com

interpretation for C-14 supported two unique correlations with the methylene on C-19 (δ_C 22.5) and methyl on C-20 (δ_C 14.0), which completed the description of the southern aliphatic chain sequence as C-9, C-11, C-12, C-7, C-8, C-17, C-14 followed by C-19 and C-20.

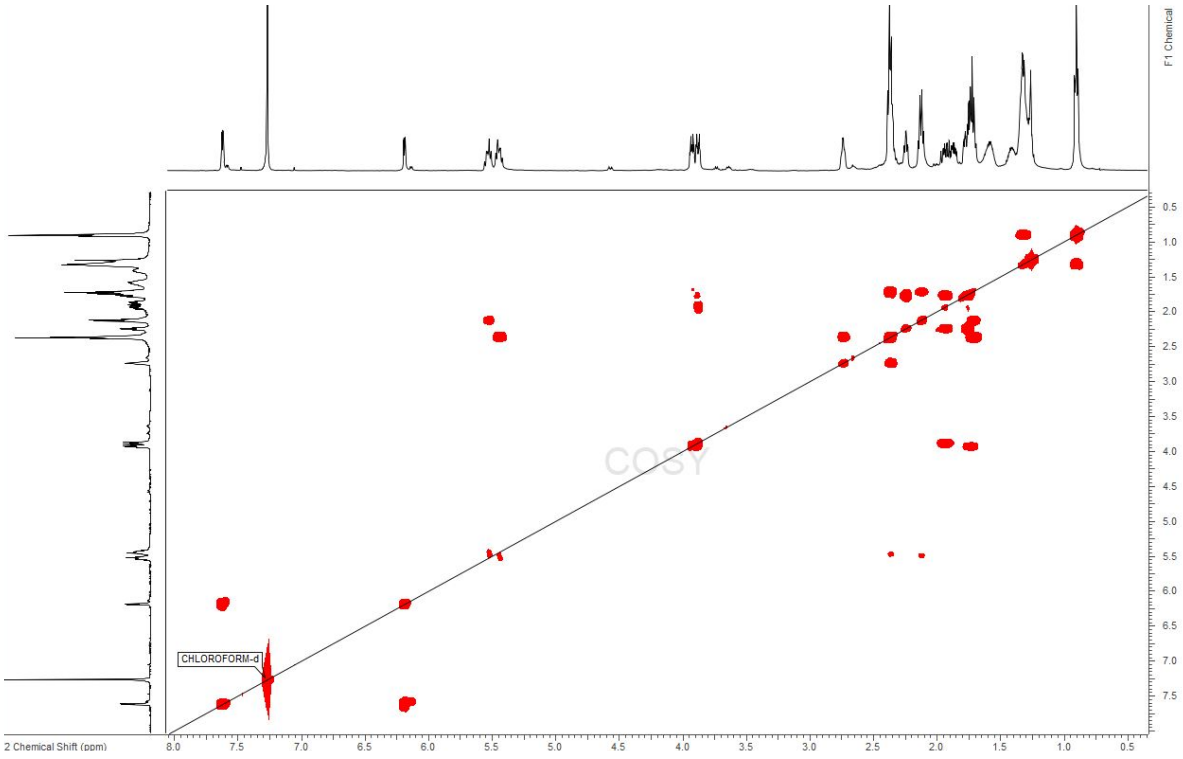

Figure III.5.1.6. COSY NMR spectrum of prostaglandin **10** in $CDCl_3$ (500 MHz).

The northern aliphatic chain contains an olefinic system between C-5 and C-6, confirmed by HSQC spectrum, which corroborated the adjacent position of the protons on C-5 and C-6 seen on the COSY spectrum. Additionally, these C-5 and C-6 adjacent protons established two-bond HMBC correlations with the methylene ones on C-15 (δ_C 26.5) and C-16 respectively. Looking at the C-16 methylene protons, the COSY spectrum interpretation revealed correlation with the immediate methylene proton on C-18 in the vicinity. Additionally, a three-bond HMBC correlation of protons of C-6 with C-13 (δ_C 33.1) was seen as well as a two-bond HMBC correlation of C-18 methylene with C-13, which helped elongate the chain. The clear unique

www.manaraa.com

HMBC correlation between the protons on C-13 and C-2 (δ_C 178.6) concluded the order C-10, C-15, C-6, C-5, C-16, C-18, C-13, and C-2 for the northern chain sequence.

Due to stronger electronegativity, the oxygen atom exerts a stronger deshielding effect than the chlorine, turning the chemical shift of the carbon bearing it higher than the one bearing the chlorine atom. After putting together both southern and northern aliphatic chain sequences, C-9 and C-10 are the respective ring connectors. Attribution of the halogen to C-7 and the alcohol function to C-8 displaying a higher chemical shift was performed with literature comparisons. Additionally, the Rotating-frame Overhauser Spectroscopy (ROESY) correlation between the protons at the ring junctions (C-9 and C-10) provided the relative orientation of the protons at the ring junction to each other. (Appendix A **Figure A.III.15a.** and **15.b.**) The C-9 proton at δ_H 2.25 ppm clearly displayed ROESY correlations with the C-15 ones at δ_H 2.36, but no correlation was witnessed with the adjacent proton on C-10. Reciprocally, C-10 proton at δ_H 2.74 provided homonuclear correlation with the ones at δ_H 1.77 on C-11, but none with the adjacent proton on C-9. This configuration suggests that the protons at the ring junctions C-9 and C-10 do not reside on the same face of the plane of the ring structure, but rather in opposite spaces created by the ring structure, which establishes a distance longer than 5 Å between protons and prevents ROESY correlations.

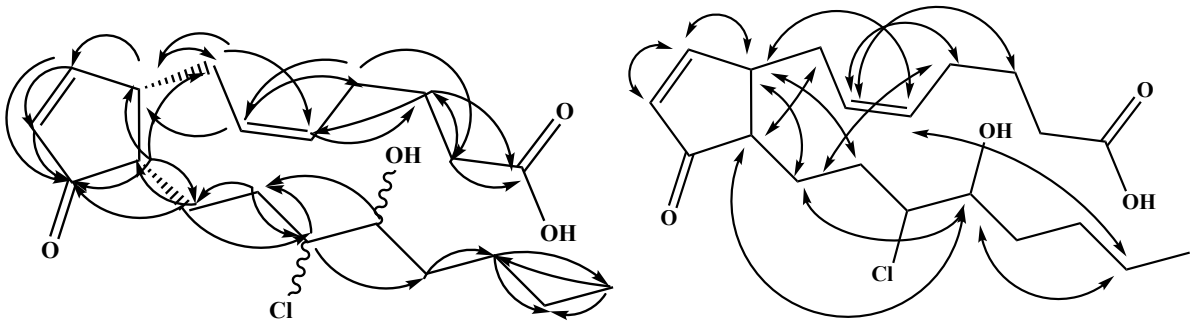

Figure III.5.1.7. Key HMBC ( ) and ROESY ( ) correlations establishing the planar structure of compound **10**.

www.manaraa.com

With the same molecular mass and the same molecular formula as compound **10**, the constitutional isomer **11** showed the same NMR patterns with variation in chemical shifts values proving its individuality.

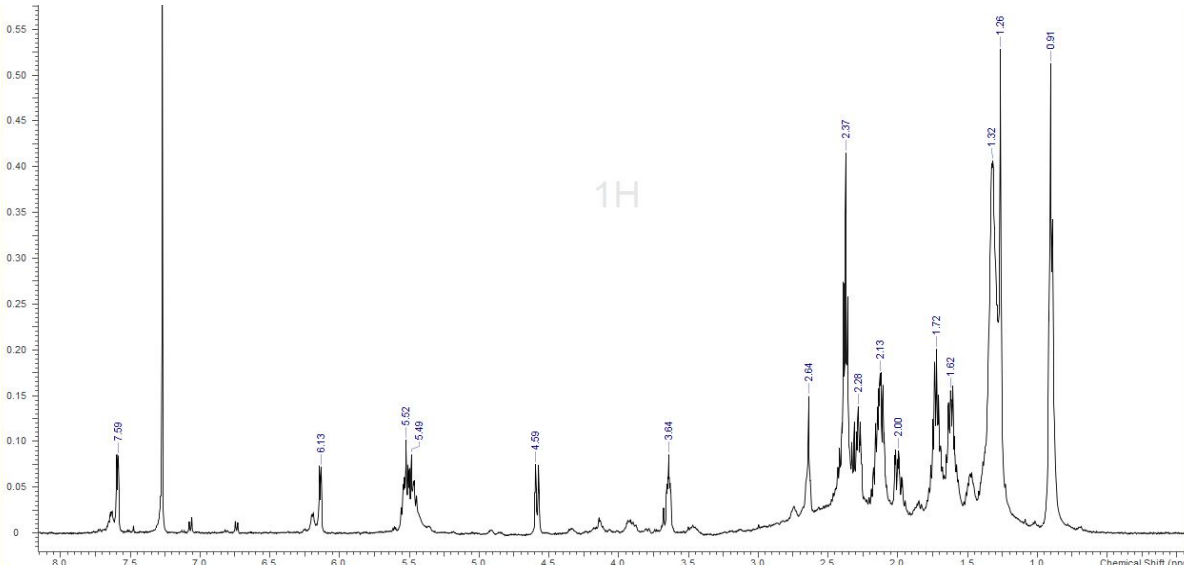

Figure III.5.1.8. ^{1}H NMR spectrum of prostaglandin **11** in $CDCl_3$ (500 MHz).

Except for an inversion in position for C-13 (δ_C 32.9) and C-18 (δ_C 24.5), the structure of the northern aliphatic chain remains the same.

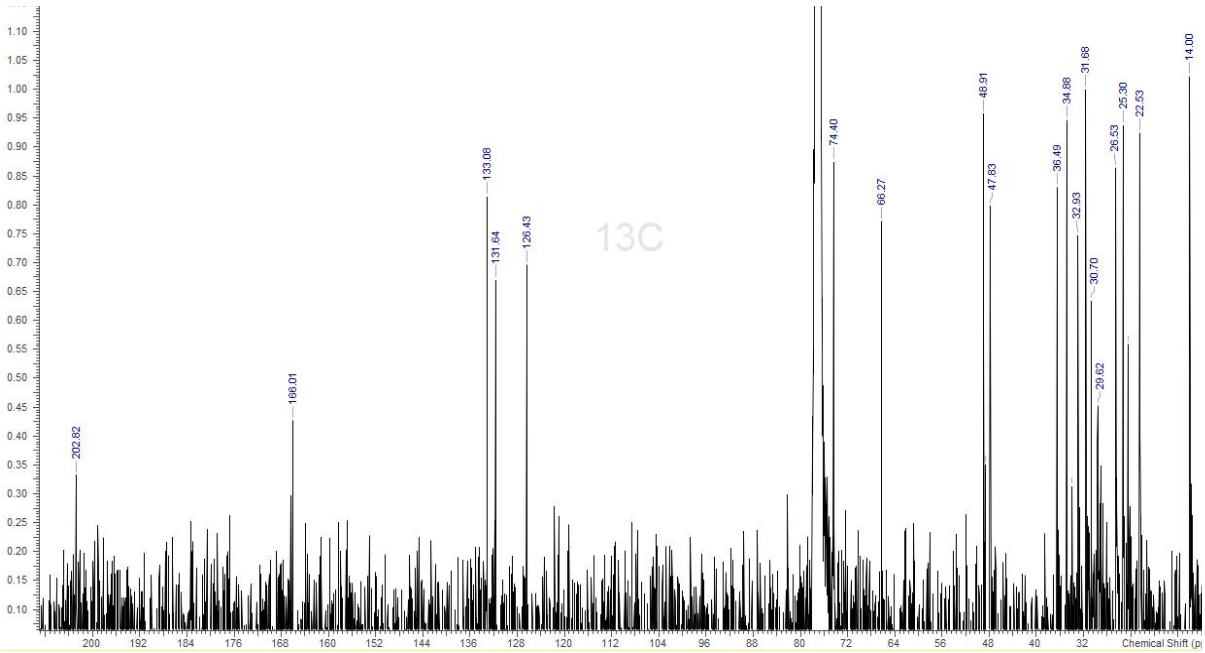

Figure III.5.1.9. ^{13}C NMR spectrum of prostaglandin **11** in $CDCl_3$ (125 MHz).

www.manaraa.com

However, divergences in the HMBC interpretations result in a modified southern aliphatic chain. The protons on C-11 (δ_C 36.5) lost correlation to C-12 (δ_C 34.9) but gained a strong one with C-8 (δ_C 66.3). The proton on C-8 strongly correlated to C-9 (δ_C 49.0) and C-7 (δ_C 74.4). The chemical shifts pattern for C-7 and C-8 were conserved, guiding the assignment chlorine assignment to C-7 and the hydroxyl group to C-8. Moreover, COSY correlations showing for C-7 proton vicinal interactions with protons on C-8 and C-12, while the proton on C-8 interacts with the ones on C-11 and C-7. Further COSY correlations study revealed C-12 to interact with C-7 and C-17 (δ_C 25.3) while C-17 does so with C-12 and C-14 (δ_C 31.7). The same connectivity patterns seen with **10** are described between C-14, C-19 (δ_C 74.4), and C-20 (δ_C 74.4), and confirm the southern aliphatic chain sequence of compound **11** being: C-11, C-8, C-7, C-12, C-17, C-14, C-19, and C-20 instead.

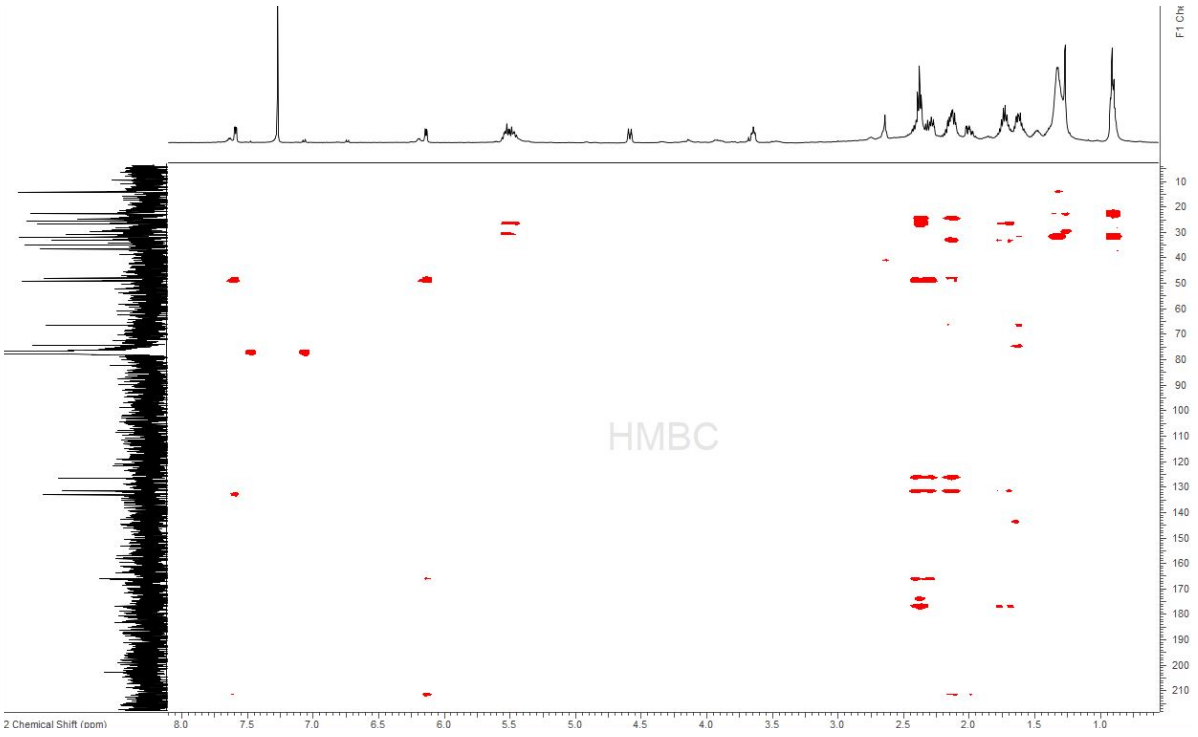

Figure III.5.1.10. HMBC NMR spectrum of prostaglandin **11** in $CDCl_3$ (500 MHz).

www.manaraa.com

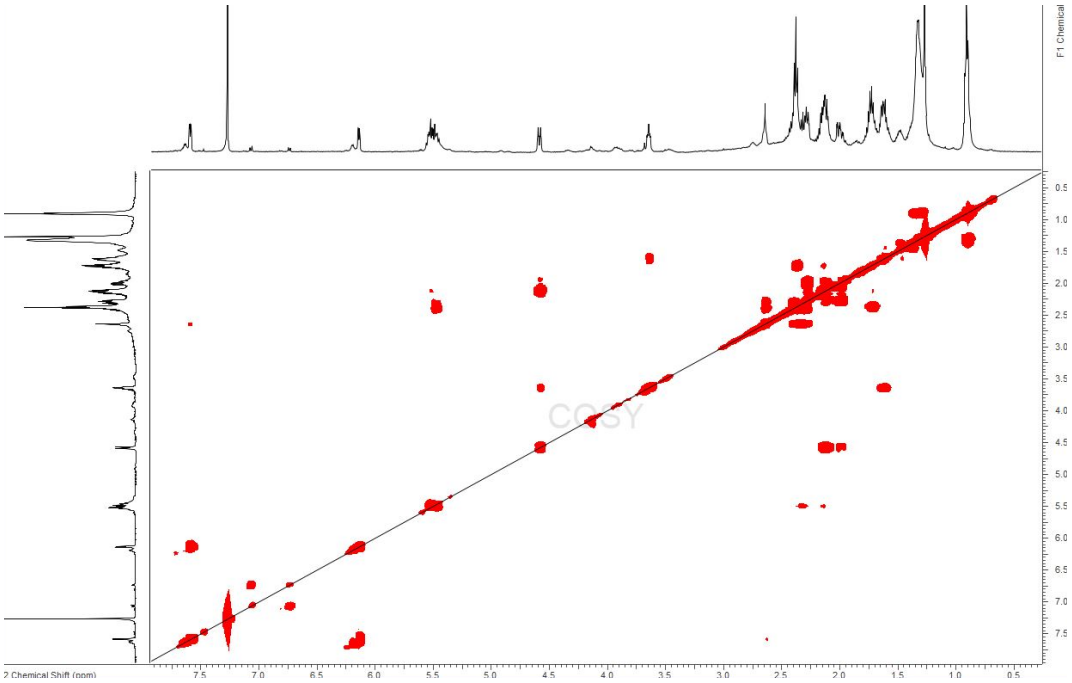

Figure III.5.1.11. HMBC NMR spectrum of prostaglandin **11** in $CDCl_3$ (500 MHz).

Observing the ROESY patterns displayed for **11** (Appendix A **Figure A.III.16a.** and **16.b.**), the spectrum shows distinct correlations between the ring junction protons on C-9 at δ_H 2.65 and C-10 at δ_H 2.29, but none with the protons on C-15 and C-11 respectively, which suggests that both protons may be cis from each other and are away from the methylene on C-11 and C-15, found on the opposite side of the plane created by the ring structure.

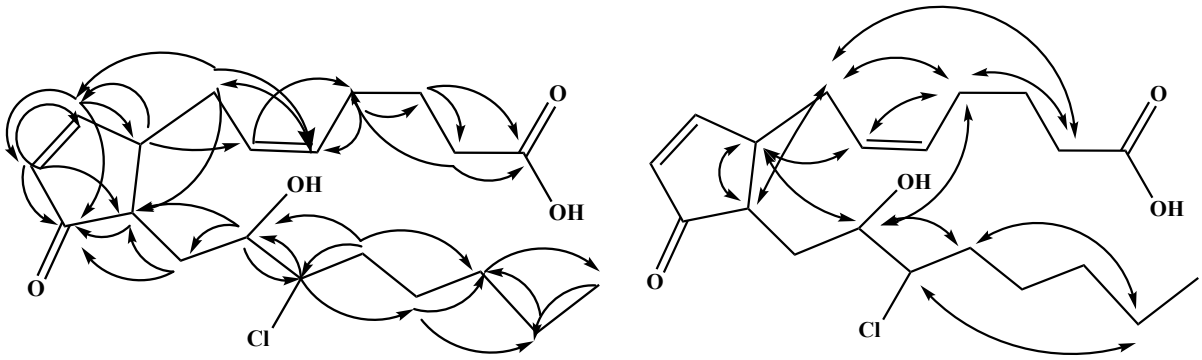

Figure III.5.1.12. Key HMBC ( ) and ROESY ( )correlations establishing the planar structure of compound **11**.

www.manaraa.com

Lastly, compound **12** ([M + Na]$^+$: m/z 357.2038 calcd. for $C_{20}H_{30}O_4Na$, m/z 357.2036) lost the 1:3 ratio pattern, classic for chloride atom being present. The chemical formula $C_{20}H_{30}O_4$ predicted a hydrogen deficiency of six degrees of unsaturation. The loss of a chloride atom resulted in the creation of a third olefinic system seen with the appearance of two new carbon shifts for C-4 (δ_C 134.5) and C-7 (δ_C 130.3), and the disappearance of proton signal between 3.50 ppm and 4.00 ppm.

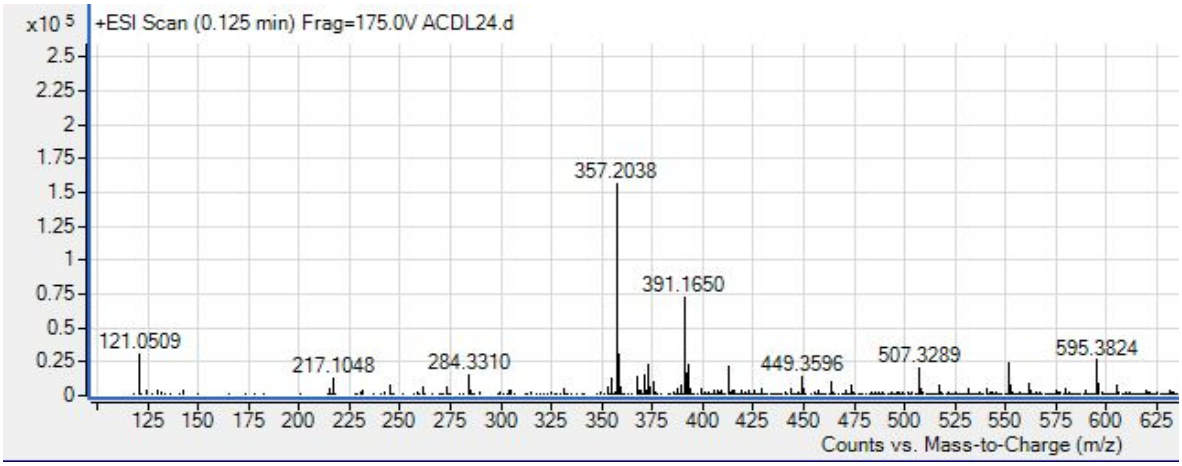

Figure III.5.1.13. MS of prostaglandin **12.**

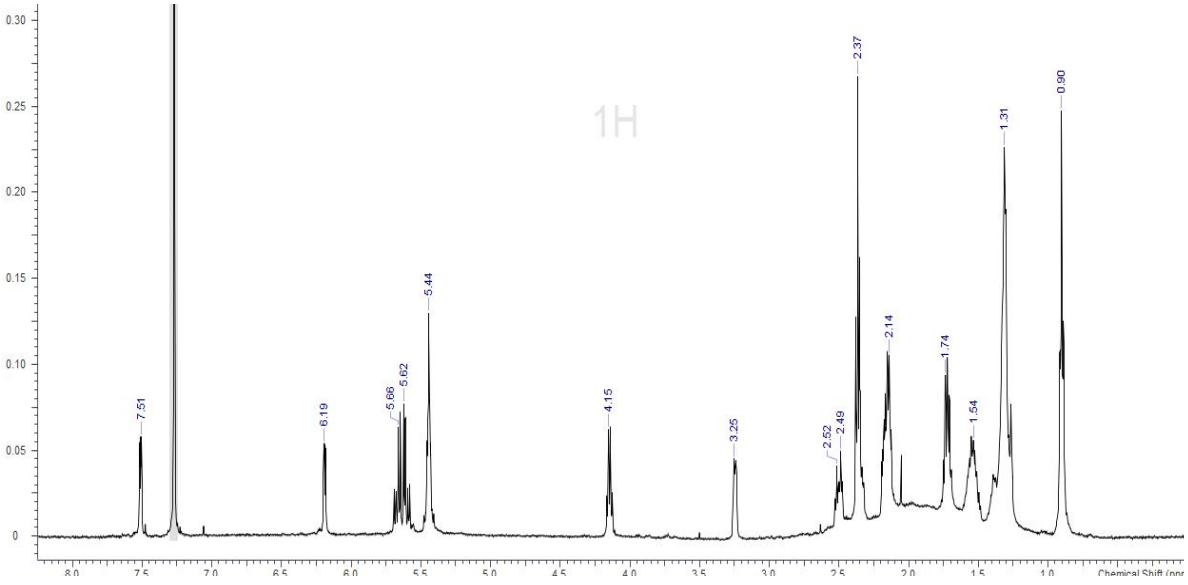

Figure III.5.1.14. ^{1}H NMR spectrum of prostaglandin **12** in $CDCl_3$ (500 MHz).

www.manaraa.com

Again, COSY and HMBC interpretations led to conservation of the northern aliphatic chain scaffold seen in the previously elucidated compounds **10** and **11**. However, variations occurred on the southern aliphatic chain resulting in C-7 being adjacent to C-4 and C-11 (δ_C 49.4) through COSY correlation pattern. Additionally, HMBC correlation confirmed two-bond correlation with C-11 and a three-bond correlation with C-9 (δ_C 72.5). The proton on hydroxyl bearing carbon C-9 exhibits two-bond correlations with C-4 and C-12 (δ_C 37.2), and three-bond kind with C-7 and C-17 (δ_C 25.1).

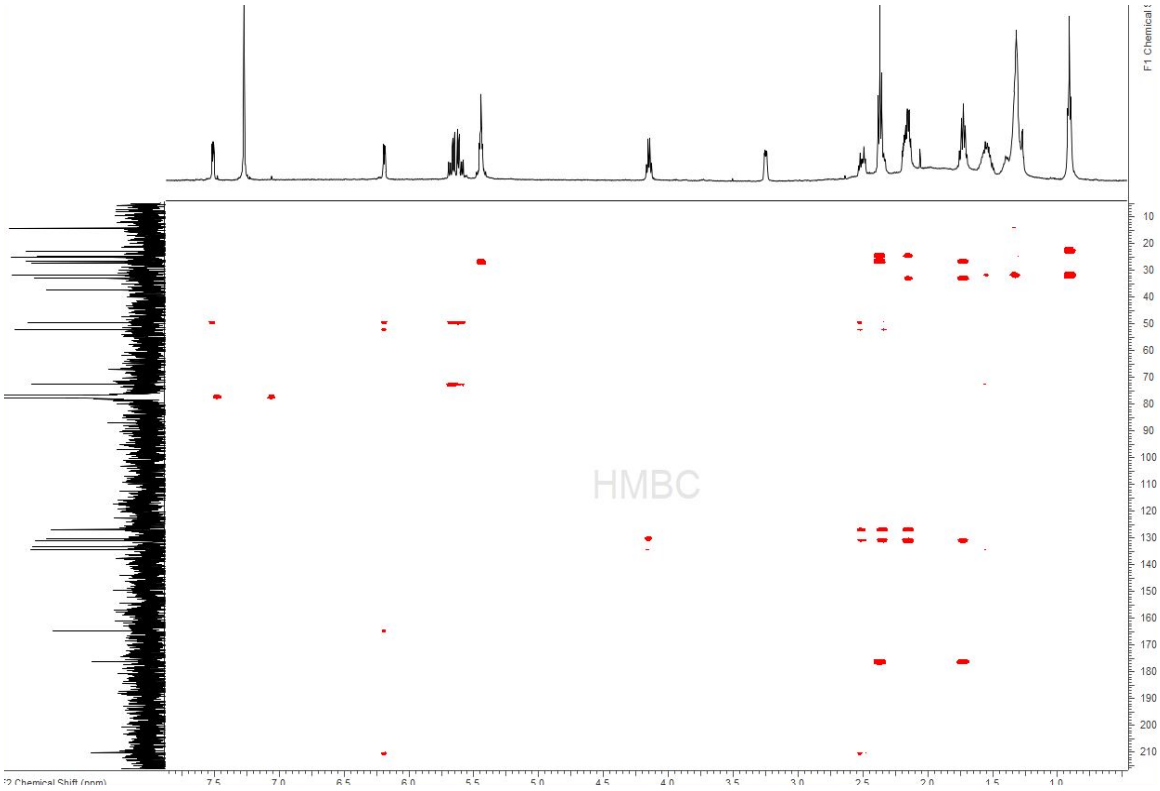

Figure III.5.1.15. HMBC NMR spectrum of prostaglandin **12** in $CDCl_3$ at 500 MHz.

COSY analyses confirmed the adjacent position of the proton on C-9 with C-4 and C-12, the C-12 methylene protons placed between C-9 and C-17 (δ_C 25.1), and the protons on C-17 surrounded by the protons on C-12 and C-14 (δ_C 31.7). The previously encountered pattern between C-14, C-19, and C-20 remained and confirmed the southern aliphatic chain sequence

www.manaraa.com

to be C-11, C-7, C-4, C-9, C-12, C-17, C-14, C-19, and C-20. Values of *J* coupling between olefinic protons on the side chains provided the alkenes configurations to be in a Z, as all olefinic protons displayed *J* coupling values within a 6 Hz range.

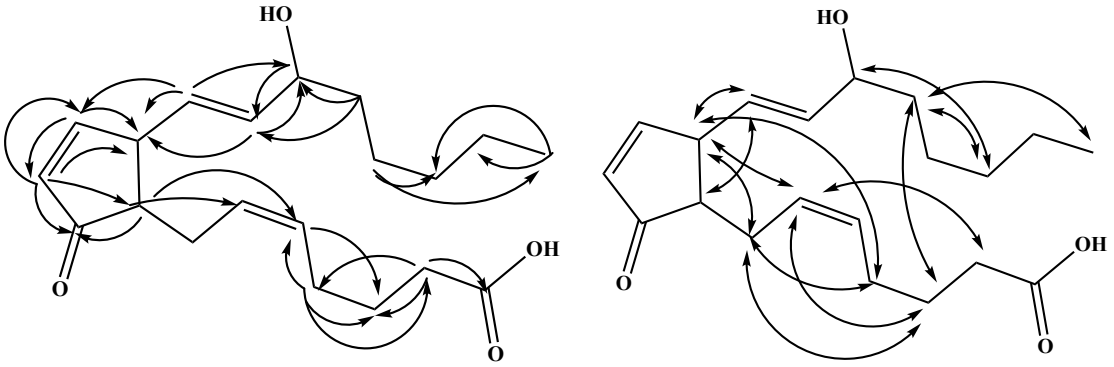

Figure III.5.1.16. Key HMBC (⌒) and ROESY (⌒)correlations establishing the planar structure of compound **12**.

Finally, the ROESY correlations offered by **12** (Appendix A **Figure A.III.18a.** and **18.b.**), displayed a trans configuration of the ring junction protons (δ_H 2.18 and 3;26), similar to the one seen with compound **10,** involving C-10 and C-11 respectively. No correlation between the two methine protons at the ring junction was detected. In fact, the C-10 proton correlated with the one on C-7, while the one on C-11 correlated to the methylene ones on C-15.

ROESY correlations helped provide the cis and trans relative configurations of the methine protons located at the ring junction for each compound **10**, **11**, and **12**. However, the chiral centers appearing on C-7 and C-8 in the case of **10** and **11**, and C-9 for **12**, require different techniques to assess configurations.

www.manaraa.com

Table III.5.1. ^{13}C and ^{1}H NMR Data for prostaglandins **(10, 11, 12)**.

Compounds	**10**		**11**		**12**	
Position	δC[a]	δH[b], int. (J in Hz)	δC[a]	δH[b], int. (J in Hz)	δC[a]	δH[b], int. (J in Hz)
1	213.0		210.0		210.3	
2	178.6		176.1		176.3	
3	167.2	7.63, 1H (5.70, 2.12)	165.9	7.59, 1H (5.72, 2.10)	164.8	7.54, 1H (5.66, 2.31)
4	133.0	6.20, 1H (5.68, 1.72)	133.1	6.14, 1H (5.66, 1.51)	134.5	5.63, 1H (7.21, 6.03)
5	133.7	5.54, 1H	131.6	5.52, 1H	133.0	6.18, 1H (5.66, 2.04)
6	126.4	5.46, 1H	126.4	5.46, 1H	131.0	5.46, 1H
7	73.1	3.88, 1H	74.4	3.66, 1H	130.0	5.67, 1H (7.21, 6.03)
8	67.9	3.93, 1H	66.3	4.61, 1H	127.5	5.45, 1H
9	49.4	2.25, 1H	49.0	2.65, 1H	72.5	4.15, 1H
10	48.8	2.74, 1H	47.8	2.29, 1H	52.1	2.18, 2H
11	34.2	1.77, 2H	36.5	2.12, 2H	49.4	3.26, 2H
12	33.8	1.94, 2H	34.9	1.64, 2H	37.2	1.54, 2H
13	33.1	2.38, 2H	32.9	2.38, 2H	32.8	2.37, 2H
14	31.3	1.31, 2H	31.7	1.32, 2H	31.7	1.31, 2H
15	30.9	2.36, 2H	30.7	2.42, 2H	27.0	2.52, 2.38, 2H
16	26.5	2.12, 2H	26.5	2.16, 2H	26.4	2.15, 2H
17	26.4	1.58, 2H	25.3	1.50, 2H	25.1	1.31, 2H
18	24.4	1.72, 2H	24.5	1.74, 2H	24.5	1.72, 2H
19	22.5	1.32, 2H	22.5	1.34, 2H	22.5	1.34, 2H
20	14.0	0.90, 3H	14.0	0.91, 3H	14.0	0.91, 2H

[a] ^{13}C shift recorded in $CDCl_3$ at 125 MHz, reported in ppm. [b] ^{1}H NMR spectrum shift and integration recorded in $CDCl_3$ at 500 MHz, reported in ppm.

III.5.2. Stereochemistry assessments

Beyond the similarity in atomic composition of these compounds, the stereochemistry dealing with the orientation of the chloride and hydroxyl groups in space, must be determined.

The absence of symmetry in a molecule creates chirality, which determines and defines the so-called face of a molecule.[34] Stereochemistry appears at different locations of the prostaglandin compounds. Not only do the two carbons joining the side chains to the ring also

www.manaraa.com

introduced relative stereochemistry, which ROESY NMR helped assess, chiral carbon centers also exist on one of the aliphatic side chains. Natural Products research may recourse to synthetic chemistry to create intramolecular modifications, which will inevitably affect the molecular architecture and symmetry, hence the NMR spectrum of a compound. One experiment commonly used to assign the stereochemistry of a hydroxyl-bearing carbon is called Mosher's method. The esterification of a chiral alcohol with each chiral α-methoxy-α-trifluoromethylphenylacetyl chloride - *(R)*-MTPCl and *(S)*-MTPCl - generates two diastereomeric esters with specific NMR shifts. The aromatic ring is responsible for a deshielding effect on the part of the molecule it is facing. As the effect attenuates with distance, the protons alpha to the esterified carbon are the most influenced and will see their chemical shifts increase when facing the aromatic ring. Hence, the esterified chiral acyl chlorides will produce opposite effects on the proton chemical shifts depending on the direction of the aromatic ring. Comparing the shifts of each diastereomer proton NMR spectrum, a variation of chemical shifts can be calculated to express the deshielding effect.

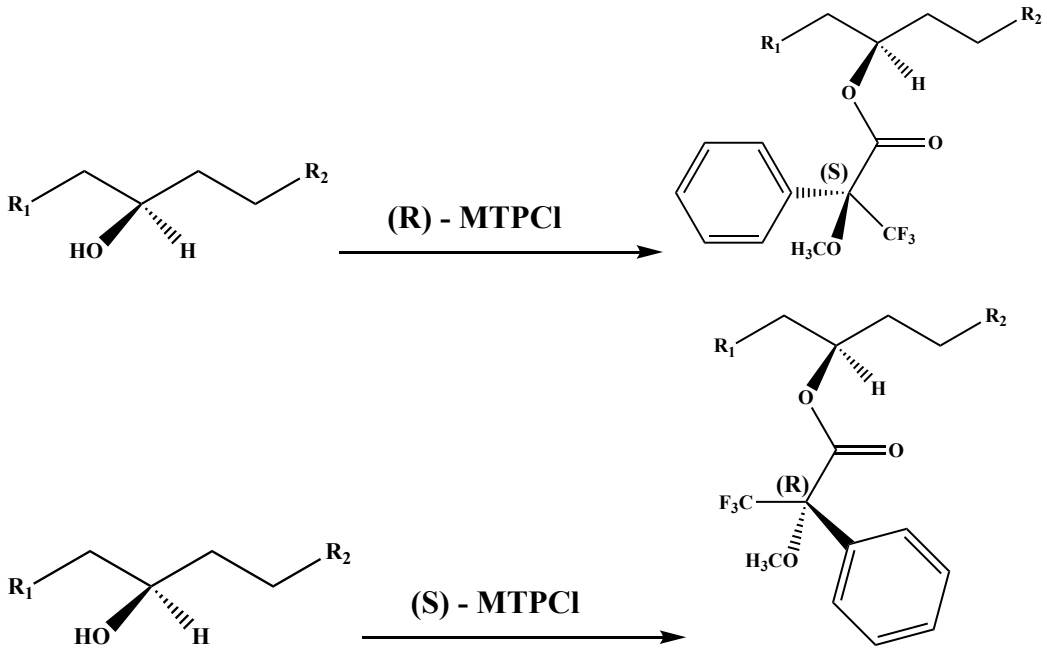

Figure III.5.2.1. Mosher's reaction scheme.

www.manaraa.com

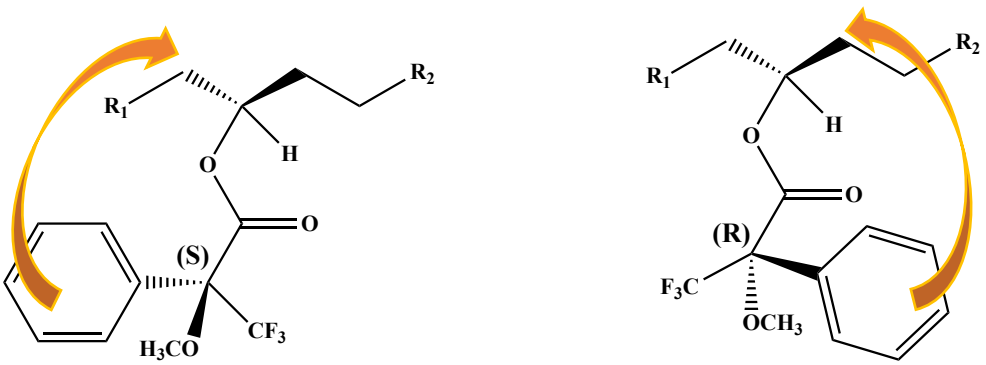

Figure III.5.2.2. Representation of deshielding effect.

Due to the limited amount of available natural products material, the experiment was attempted directly in a 3mm NMR tube using 0.2 mg of compound. Unfortunately, the quality of results did not allow assertive confirmation of stereochemistry.

Another route is being considered using circular dichroism. Chiral molecules have the ability to interact with light differently according to the orientation of the substituents involved in the chirality. With the advantage of not having to sacrifice mass, the electronic circular dichroism calculations method may provide trends, which will be then used to compare the experimental absorbance measurements and determine the stereochemistry of the remote chiral centers associated with compound **10**, **11**, and **12**.

III.5.3. Biological activity

Ala Azhari from the Kyle lab tested all three compounds against the *Leishmania donovani* parasite. However, all returned inactive. A malaria bioassay performed by the Adams lab by Alison Roth was also conducted and displayed potency for **10**. It inhibited 100% of the *Plasmodium falciparum* parasite growth, while **11** and **12** remained inactive. Looking at structure-activity relationship, as much similar as they can be in atomic composition, the stereochemistry, orientation of the atoms in space, is crucial for activity translation.

www.manaraa.com

Since 1969, a total of seven marine natural products or marine natural products derived drug candidates have been approved by the Food and Drug Administration (FDA) for public use with more of them entering the clinical trials pipeline.[38,39]

Although marine invertebrates have been a significant source of natural products, with Cnidaria phyla being the most prolific, microorganisms living in symbiosis appear to be the true manufacturer of most marine natural products. Due to their soft body characteristics, most sessile marine invertebrates are subject to potential parasite predation. These microorganisms are responsible for the production of secondary metabolites further utilized by the invertebrates for defense mechanisms and ecological survival.

III.6. Experimental

III.6.1. General Procedures

Normal phase Medium Pressure Liquid Chromatography (MPLC) separations were conducted using a Teledyne CombiFlash Rf200i fitted with UV and ELS detection with a RediSepRf 24g or 80g silica column. For HPLC separation, all solvents were obtained from Fisher Scientific and were HPLC grade (>99% purity) unless otherwise stated. All HPLC analysis were performed on a Shimadzu LC20-AT system equipped with either an evaporative light scattering detector (ELSD) ELSD II and/or SPD-M20A UV-Vis detector. For normal phase separation, analytical [Phenomenex Luna Silica, 250 x 4.6 mm, 5 µm], semi-preparative [Phenomenex Luna Silica, 250 x 10 mm, 5 µm], or preparative [Phenomenex Luna Silica, 250 x 21.2 mm, 5 µm] were used, while reverse phase separation employed analytical [YMC packed C-18, A-304-10, S-10, 120 Å ODS], or semi-preparative [Phenomenex Luna C-18, 250 x 10 mm, 5 µm] columns. All NMR spectra were acquired in $CDCl_3$ with residual solvent referenced as an internal standard (7.26 ppm). All ^{1}H NMR spectra were recorded on a Varian 500 MHz Direct Drive instrument and ^{13}C

www.manaraa.com

NMR spectra were recorded at 125 MHz. Analytical LC/MS was performed on a Phenomenex Kinetex C18 column (50 x 2.1 mm, 2.6 μm) on an Agilent 6230 LC/TOF-MS with electrospray ionization detection. Optical rotations were measured on a Rudolph Research Analytical AUTOPOL IV digital polarimeter.

III.6.2. Spectral Data

Alcyopterosin T (1): colorless oil; UV (CH_2Cl_2) λ_{max} (log ε) (1.52) 225 nm ; (1.45) 245 nm; (1.24) 340 nm; IR ν_{max}: 3000; 2900; 2850; 1720; 1600 cm^{-1}; ^1H and ^{13}C NMR data see **Table III.3.1.**; HRESIMS $[M + Na]^+$: m/z 344.1460 (calcd. for $C_{17}H_{23}NO_5Na$, m/z 344.1468).

Alcyoptersosin U (2): colorless oil; UV (CH_2Cl_2) λ_{max} (log ε) 225 (1.76); 230 (1.59); 250 (1.55); 264 (1.54); 305 (1.52); 330 (1.47); 365 (1.44) nm; IR ν_{max}: 3000; 2900; 2850; 1750; 1700; 1600 cm^{-1}; ^1H and ^{13}C NMR data see **Table III.3.1.**; HRESIMS M + H]$^+$: m/z 336.1451 (calcd. for $C_{17}H_{21}NO_6H$, m/z 336.1442).

Triacetyl steroid (9) translucent solid; $[\alpha]^{24.6}_{365}$ -10.0° (c = 5x10^{-3} g/mL, ACN); UV (ACN) λ_{max} (log ε) 215 (2.60); 235 (2.68) nm; IR υ (thin film): 1250; 1690; 1700; 1750; 2850; 2900; 2950 cm^{-1}; ^1H and ^{13}C NMR data see **Table III.4.1.**; HRESIMS $[M + H]^+$: m/z 575.3550 (calcd. for $C_{33}H_{50}0_8H$, m/z 575.3578).

Prostaglandin (10) colorless oil; ; $[\alpha]^{21.7}_D$ +18.09° (c = 4x10^{-3} g/mL, CH_3Cl), UV (CH_2Cl_2) λ_{max} (log ε) 215 (2.61); 235 (2.68) nm; IR ν_{max}: 2950; 2900; 2850; 1700 cm^{-1}; ^1H and ^{13}C NMR data see **Table III.5.1.**; HRESIMS $[M + Na]^+$: m/z 393.1798 (calcd. for $C_{20}H_{31}ClO_4Na$, m/z 393.1803).

Prostaglandin (11) colorless oil; $[\alpha]^{22.1}_D$ -10.05° (c = 4x10^{-3} g/mL, CH_3Cl), UV (CH_2Cl_2) λ_{max} (log ε) 215 (2.60); 235 (2.68) nm; IR ν_{max}: 2950; 2900; 2850; 1700 cm^{-1}; ^1H and ^{13}C NMR data see **Table III.5.1.**; HRESIMS m/z $[M + Na]^+$: m/z 393.1804 (calcd. for $C_{20}H_{31}ClO_4Na$, m/z 393.1803).

www.manaraa.com

Prostaglandin (12) colorless oil; $[\alpha]^{24.6}_{365}$ +5.20° (c = 4x10^{-3} g/mL, CH_3Cl), UV (ACN) λ_{max} (log ε) 230 (3.35); 235 (2.68) nm; IR ν_{max}: 2950; 2900; 2850; 1700 cm^{-1}; ^{1}H and ^{13}C NMR data see **Table III.5.1.**; HRESIMS m/z [M + Na]$^+$: m/z 357.2038 (calcd. for $C_{20}H_{30}O_4Na$, m/z 357.2036).

III.6.3. X-ray Crystallography

The crystal structure analysis was performed by Gaurav Verma and Lukasz Wojtas. Crystals of 9 were obtained from $CHCl_3$. The X-ray diffraction data were measured on Bruker D8 Venture PHOTON II CPAD diffractometer equipped with a Cu Kα INCOATEC ImuS micro-focus source (λ = 1.54178 Å). Indexing was performed using APEX3[40] (Difference Vectors method). Data integration and reduction were performed using SaintPlus.[41] Absorption correction was performed by multi-scan method implemented in SADABS.[42] Space group was determined using XPREP implemented in APEX3.[40] Structure was solved using SHELXT[43] and refined using SHELXL-2018[44] (full-matrix least-squares on F2) through OLEX2 interface program.[45] Crystal data and refinement conditions are shown in Appendix A **Table A.III.1**.

III.6.4. *Leishmania donovani* and J774A.1-Cells Cytotoxicity Assay

The leishmania screen was conducted by Ala Azhari in the Kyle lab. The cytotoxicity was assessed testing compounds **1** and **2** against J774.A1 macrophages using the CellTiter 96 AQueous one-solution cell proliferation assay (Promega, Madison, WI). In a 96 well drug plate (Costar, Assay Plate, 96 well with low Evaporation Lid, Flat Bottom, None-Treated, #3370) compounds were diluted in a series of 6 two-fold dilutions in media to produce a concentration range from 500µg/ml to 15.625µg/ml. From each well 10 µL were transferred to another 96 well plate (Costar, Assay Plate, 96 well with low Evaporation Lid, Flat Bottom, Tissue culture Treated, # 3628) and 90µL of macrophages in media in a 50,000 cell per well concentration was added to produce a final concentration range from 50 µg/ml to 1.562 µg/ml. The plates were then incubated at 37 °C, 5% CO_2 for 72 hrs. Then, 20 µL of 3-(4,5-dimethylthiazol-2-yl)-5(3-

www.manaraa.com

carboxymethoxyphenyl)-2-(4-sulphophenyl)-2H-tetrazolium (MTS: Promega, Madison, WI) solution was added to each well and incubated for an additional 4 hours. A Spectra Max M2^{e} (molecular Devices, Sunnyvale, Ca) was used to measure optical density (OD) at 490nm. Non-linear regression via Trifox software was used to determine IC_{50} values. Additionally, potency against infected macrophage cells was conducted. In a 384 well assay plate (CellCarrier-384 Black, Optically Clear Bottom, Tissue Culture Treated, Sterile, 6007550), 2000 J774 cells are seeded and incubated for at least an hour to allow adherence. The plate is then washed with pre-warmed media to get rid of the unadhered cells. *L. donovani* axenic amastigotes are then added to the plate at a ratio of 10:1 and incubated at 37 $^{\circ}$C, 5% CO_2 for 24 hours. The excess extracellular amastigotes are then washed away using pre-warmed media. Compounds are prepared in a 384-drug plate (Thermo Scientific™ Nunc™ 384-Well Clear Polystyrene Plates with Non /treated Surfaces, #242757) with a starting concentration of 10 μg/ml and serially diluted at 1:2. Drugs are then added to the assay plate and incubated at 37 $^{\circ}$C, 5% Co_2 for 72 hours. After that, drugs are removed from the plate and adhered cells are fixed with 2% paraformaldehyde (Alfa Aesar™ Paraformaldehyde, 16% w/v aq. soln., methanol free, #30525-89-4) and incubated for 15 minutes at room temperature. Fixative is then removed, and cells are stained with 5 μM Draq5 (Thermo Scientific DRAQ5 FLUORESCENT PROBE, DNA stain, #62251) and incubated for 5 minutes at room temperature. Stain is then removed, and fresh media is added to the plate. A Perkin Elmer Operetta (High content imager) is then used to capture images for each well and find macrophage and amastigotes nuclei within macrophage cytoplasm using Harmoney software that counts the number of amastigotes per 500 macrophages in each well and generate IC_{50} values.

www.manaraa.com

III.6.5. HeLa Cancer Cells Cytotoxicity Assay

Anthony Sanchez of the Kee lab performed the clonogenic survival assay. HeLa cells were seeded into 96 well plates at a concentration of 100 cells/ml in Dulbecco's Modified Eagle's Medium (DMEM) supplemented with 10% Bovine serum. Drugs were added to the medium 24hours after seeding at the indicated concentrations, the cells were allowed to grow for 14 days. The cells were fixed with a 10%methanol, 10% Acetic acid solution (in water) for 15minutes at room temperature and stained with 1% crystal violet (in methanol) for 5minutes, excess dye was removed with water and the plates were allowed to dry at RT overnight. Cells were de-stained with Sorenson's buffer (.1M sodium citrate, 50% ethanol). The colorimetric intensity of each solution was quantified using Gen5 software on a Synergy 2 (BioTek, Winooksi, VT) plate reader (OD at 595 nm). Error bars are representative of 3 independent experiments.

III.6.6. Respiratory Syncytial Virus (rA2Rluc) Cytotoxicity Assay

Kim-Chi Teng from the Teng lab performed the cytotoxicity experiments. The respiratory syncytial virus (rA2Rluc) assay was performed using a luciferase inhibition assy. A549 cells were seeded at 1.6 x 10^4 cells in 100 µl of 5% FBS/1X Penicillin-Streptomycin/F12 medium per well in 96-well µClear® black plates with clear bottom (Greiner 655090). Cells were infected with rA2-Rluc [1] (400 PFU/well in total volume of 50 µl/well) and allowed to adsorb for 1 h. Two-fold dilutions of test samples were serially diluted in triplicate. After the adsorption period, 50 µl of the diluted extracts were added to the infected cells and incubated at 37°C, 5% CO_2 for 24 h. Cells were then lysed using 1x *Renilla* lysis buffer (Promega). Luciferase activity was measured with the Renilla Luciferase reagent (Promega) on a BioTek Synergy Mx microplate reader using Gen5 version 2.00.18 software. Percent RSV inhibition was calculated by normalizing the luminescence for test samples to that of DMSO-treated controls and multiplying by 100.[15] An additional MTT proliferation assay was conducted to evaluate cell viability. Duplicate 96-well

www.manaraa.com

plates of A549 cells were set up in parallel with the RSV-Luciferase Inhibition Assay. After the 24 hours incubation period, cells were processed for MTT Proliferation Assay (Provost & Wallert Research) according to the manufacturer's protocol. 2% DMSO and 2 μM PDK1 inhibitor (CalBioChem) were used as positive and negative controls, respectively, for cell viability.

III.6.7. *Clostridium difficile* Bacterium Potency and Cytotoxicity Assay

Screening against the *Clostridium difficile* bacterium was done by Hiran Malinda from the Sun lab. The antimicrobial activities of compounds **1** and **2** against *C. difficile* UK6 were tested using media and methods recommended by the Clinical and Laboratory Standards Institute for susceptibility testing of anaerobes.[16] Compounds at 5mg/ml were added to 96 well microplates containing UK6 culture at a density of 0.5 McFarland (100μL per well) in BHIS (Brain Heart Infusion Salt Broth) Medium to make final concentrations of extracts ranging from 128 μg/mL to 0.5 μg/mL at a twofold dilution. Then these plates were incubated at 37.8 °C for 24 hours. The MICs were determined as the lowest concentration that completely inhibited bacterial growth in the wells. Vancomycin was included as a positive control. MTT (3-(4,5-dimethylthiazol-2-yl)-2,5-diphenyltetrazolium bromide Sigma–Aldrich, St. Louis, MO, USA) was used for a cell viability assy to evaluate the cytotoxicity of these compounds on human HepG2 and HEK293T cell lines. HEK293T is a specific cell line originally derived from human embryonic kidney cells grown in tissue culture. HepG2 is an immortalized cell line consisting of human liver carcinoma cells. Both cells were maintained in Dulbecco's modified Eagle's medium (DMEM) with 4.5 gL-1 glucose, 1- glutamine, and sodium pyruvate (Corning; Manassas, VA, USA) containing 10% FBS (Thermo Scientific) and 1% penicillin/streptomycin at 37.8 °C in 5% CO_2. 10^4 cells per well were plated in 96 well plates and incubated overnight. Then the cells were treated with the compounds at concentrations ranging from 64 mg/mL to 0.0125 mg/mL or 1% DMSO (as a control reagent) for 24 hours at 37.8 °C. After careful removal of media from each well without

www.manaraa.com

disturbing cells, 100 µl of DMSO was added to each well, and incubated for 15 min at 37.8 °C. Absorbance at 540 nm was read in a Synergy HTX multi-mode reader (Bio Tek Instruments, Inc., Winooski VT, USA). Data were analyzed using Graph pad PRISM 6 (GraphPad Software, Inc., La Jolla, CA, USA). The 50% cytotoxic concentration (CC_{50}) was reported as the extract concentration that decreased cell viability by 50% relative to the untreated control.

III.6.8. Liver-stage *Plasmodium falciparum* Assay

Alison Roth in the Adams lab conducted the screening experiment. Primary human hepatocytes (PHHs) were plated at 18,000 per well in 40 µL of fresh media on day 0 and were incubated overnight at 37°C, 5% CO_2. Of the original PHHs plated, roughly 10,000 adhere to the plate. *P. falciparum* sporozoites were added to each well on day 3 post seed of hepatocytes and allowed to incubate for 24 h at 37 °C, 5% CO_2. On days 0, 1, 2, and 3 post sporozoite infection, media was replaced with 40 µL of fresh media, with simultaneous drug administration of compounds **10**, **11**, and **12** as well as the primaquine control, at a 40 nL volume of a 5 mg/mL drug using a pin tool (V & P Scientific). The pin tool performs a 1000-fold dilution, thus making the final drug concentration 5 µg/mL. The drug-treated media administered on day 3 was removed on day 4 and replaced with fresh media with no further drug administration. On day 6, the media was removed, and the PHHs were chemically fixed using 4% paraformaldehyde, then immunofluorescent staining was performed for quantification and analysis of parasite infection as previously described.[39] This mode is termed "prophylactic", where it is measuring the drugs ability to block sporozoite invasion and subsequent liver-stage parasite development.

References

(1) Stevens, C.; Chiswell, S. Ocean Currents and tides - currents, te ara - the encyclopedia of

www.manaraa.com

New Zealand, Http://Www.TeAra.Govt.Nz/En/Map/5915/Circumpolar-Currents (Accessed 14 October 2019).

(2) Park, Y.-H.; Park, T.; Kim, T.-W.; Lee, S.-H.; Hong, C.-S.; Lee, J.-H.; Rio, M.-H.; Pujol, M.-I.; Ballarotta, M.; Durand, I.; et al. Observations of the antarctic circumpolar current over the Udintsev fracture zone, the narrowest choke point in the Southern Ocean. *J. Geophys. Res.: Oceans.* **2019,** *124*, 4511-4528.

(3) Livermore, R.; Eagles, G.; Morris, P.; Maldonado, A. Shackleton fracture zone: no barrier to early circumpolar ocean circulation. *Geology* **2004**, *32*, 797–800.

(4) Clarke, A.; Crame, J. A. Evolutionary dynamics at high latitudes: speciation and extinction in polar marine faunas. *Philos. Trans. R. Soc. B Biol. Sci.* **2010**, *365*, 3655–3666.

(5) Liu, J.-T.; Lu, X.-L.; Liu, X.-Y.; Gao, Y.; Hu, B.; Jiao, B.-H.; Zheng, H. Bioactive natural products from the Antarctic and Arctic organisms. *Mini-Reviews Med. Chem.* **2013**, *13*, 617–626.

(6) McClintock, J. B.; Amsler, C. D.; Baker, B. J. Overview of the chemical ecology of benthic marine invertebrates along the Western Antarctic peninsula. *Integr. Comp. Biol.* **2010**, *50*, 967–980.

(7) Lebar, M. D.; Heimbegner, J. L.; Baker, B. J. Cold-water marine natural products. *Nat. Prod. Rep.* **2007**, *24*, 774.

(8) Avila, C. Biological and chemical diversity in Antarctica: from new species to new natural products. *Biodiversity* **2016**, *17*, 5–11.

(9) Núñez-Pons, L.; Avila, C. Natural products mediating ecological interactions in Antarctic benthic communities: a mini-review of the known molecules. *Nat. Prod. Rep.* **2015**, *32*, 1114–1130.

(10) Avila, C.; Taboada, S.; Núñez-Pons, L. Antarctic marine chemical ecology: what is next?

www.manaraa.com

Mar. Ecol. **2008**, *29*, 1–71.

(11) Gibson, R. N. , Atkinson, R. J. A. Oceanography and marine biology, an annual review. Vol. 41. **2003**. ISBN 9780415254632.

(12) Coll, J. C. The chemistry and chemical ecology of octocorals (Coelenterata, Anthozoa, Octocorallia). *Chem. Rev.* **1992**, *92*, 613–631.

(13) Carroll, A. R.; Copp, B. R.; Davis, R. A.; Keyzers, R. A.; Prinsep, M. R. Marine natural products. *Nat. Prod. Rep.* **2019**, *36*, 122–173.

(14) Gershenzon, J.; Dudareva, N. The function of terpene natural products in the natural world. *Nat. Chem. Biol.* **2007**, *3*, 408–414.

(15) von Rudloff, E. Volatile leaf oil analysis in chemosystematic studies of North American conifers. *Biochem. Syst. Ecol.* **1975**, *2*, 131–167.

(16) Muzika, R.-M.; Campbell, C. L.; Hanover, J. W.; Smith, A. L. Comparison of techniques for extracting volatile compounds from conifer needles. **1990**, *16*, 2713–2722.

(17) Hu, G.-P. P.; Yuan, J.; Sun, L.; She, Z.-G. G.; Wu, J.-H. H.; Lan, X.-J. J.; Zhu, X.; Lin, Y.-C. C.; Chen, S.-P. P. Statistical research on marine natural products based on data obtained between 1985 and 2008. *Mar. Drugs* **2011**, *9*, 514–525.

(18) Gross, H.; König, G. M. Terpenoids from marine organisms: unique structures and their pharmacological potential. *Phytochemistry Reviews*. **2006**, 115–141.

(19) Martins, A.; Vieira, H.; Gaspar, H.; Santos, S. Marketed marine natural products in the pharmaceutical and cosmeceutical industries: tips for success. *Marine Drugs*. **2014**, 1066–1101.

(20) Rocha, J.; Peixe, L.; Gomes, N. C. M.; Calado, R. Cnidarians as a source of new marine bioactive compounds - an overview of the last decade and future steps for bioprospecting. *Marine Drugs*. **2011**, 1860–1886.

www.manaraa.com

(21) Carbone, M.; Núñez-Pons, L.; Castelluccio, F.; Avila, C.; Gavagnin, M. Illudalane sesquiterpenoids of the alcyopterosin series from the Antarctic marine soft coral *Alcyonium Grandis*. *J. Nat. Prod.* **2009**, *72*, 1357–1360.

(22) Soldatou, S.; Baker, B. J. Cold-water marine natural products, 2006 to 2016. *Nat. Prod. Rep.* **2017**, *34*, 585–626.

(23) Cragg, G. M.; Newman, D. J. Medicinals for the millennia: the historical record. *Ann. N. Y. Acad. Sci.* **2001**, *953*, 3–25.

(24) Huang, C. Y.; Su, J. H.; Liaw, C. C.; Sung, P. J.; Chiang, P. L.; Hwang, T. L.; Dai, C. F.; Sheu, J. H. Bioactive steroids with methyl ester group in the side chain from a reef soft coral *Sinularia brassica* cultured in a tank. *Mar. Drugs* **2017**, *15*, 1–11.

(25) Look, S. A.; Fenical, W.; Jacobs, R. S.; Clardy, J. The pseudopterosins: anti-inflammatory and analgesic natural products from the sea whip *Pseudopterogorgia elisabethae*. *Proc. Natl. Acad. Sci. U. S. A.* **1986**, *83*, 6238–6240.

(26) Hooper, G. J.; Davies-Coleman, M. T.; Schleyer, M. New diterpenes from the South African soft coral *Eleutherobia aurea*. *J. Nat. Prod.* **1997**, *60*, 889–893.

(27) Ketzinel, S.; Rudi, A.; Schleyer, M.; Benayahu, Y.; Kashman, Y. Sarcodictyin A and two novel diterpenoid glycosides, eleuthosides a and b, from the soft coral *Eleutherobia aurea*. *J. Nat. Prod.* **1996**, *59*, 873–875.

(28) Suzuki, S.; Murayama, T.; Shiono, Y. Illudalane sesquiterpenoids, echinolactones a and b, from a mycelial culture of *Echinodontium japonicum*. *Phytochemistry* **2005**, *66*, 2329–2333.

(29) Palermo, J. A.; Rodriguez Brasco, M. F.; Spagnuolo, C.; Seldes, A. M. Illudalane sesquiterpenoids from the soft coral *Alcyonium Paessleri* : the first natural nitrate esters. *J. Org. Chem.* **2000**, *65*, 4482–4486.

(30) Nord, C.; Menkis, A.; Broberg, A. Cytotoxic Illudalane sesquiterpenes from the wood-

www.manaraa.com

decay fungus *Granulobasidium vellereum* (Ellis & Cragin) *jülich*. *Molecules* **2014**, *19*, 14195–14203.

(31) Kokubun, T.; Scott-Brown, A.; Kite, G. C.; Simmonds, M. S. J. Protoilludane, Illudane, illudalane, and norilludane sesquiterpenoids from *Granulobasidium vellereum*. *J. Nat. Prod.* **2016**, *79*, 1698–1701.

(32) Wang, S. K.; Puu, S. Y.; Duh, C. Y. New Steroids from the soft coral *Nephthea chabrolii*. *Mar. Drugs* **2013**, *11*, 571–581.

(33) Williams, D. E. Novel secondary metabolites from selected cold water marine invertebrates. Thesis. **1987**, 1983.

(34) Gerwick, W. H. The face of a molecule. *J. Nat. Prod.* **2017**, *80*, 2583–2588.

(35) Neuhaus, G. F.; Adpressa, D. A.; Bruhn, T.; Loesgen, S. Polyketides from marine-derived *Aspergillus porosus* : challenges and opportunities for determining absolute configuration. *J. Nat. Prod.* **2019**, *82*, 2780-2789.

(36) Xu, W. F.; Mao, N.; Xue, X. J.; Qi, Y. X.; Wei, M. Y.; Wang, C. Y.; Shao, C. L. Structures and absolute configurations of diketopiperazine alkaloids chrysopiperazines a-c from the gorgonian-derived *Penicillium chrysogenum* fungus. *Mar. Drugs* **2019**, *17*, 1–9.

(37) Kwit, M.; Gawronski, J.; Boyd, D. R.; Sharma, N. D.; Kaik, M. Circular dichroism, optical rotation and absolute configuration of 2-cyclohexenone-cis-diol type phenol metabolites: redefining the role of substituents and 2-cyclohexenone conformation in electronic circular dichroism spectra. *Org. Biomol. Chem.* **2010**, *8*, 5635–5645.

(38) Jiménez, C. Marine natural products in medicinal chemistry. *ACS Med. Chem. Lett.* **2018**, *9*, 959–961.

(39) Newman, D. J.; Cragg, G. M. Natural products as sources of new drugs from 1981 to 2014. *J. Nat. Prod.* **2016**, *79*, 629–661.

www.manaraa.com

(40) Bruker (2019). *APEX3* Bruker AXS Inc., Madison, Wisconsin, USA.

(41) Bruker (2019) SAINT V8.35A. Data Reduction Software.

(42) Sheldrick, G. M. (1996). *SADABS. Program for Empirical Absorption Correction.* University of Gottingen, Germany.

(43) XT, G.M. Sheldrick, Acta Cryst. (2015). A71, 3-8

(44) XL, Sheldrick, G. M. (2008). Acta Cryst. A64, 112-122.

(45) Dolomanov, O.V.; Bourhis, L.J.; Gildea, R.J.; Howard, J.A.K.; Puschmann, H., OLEX2: A complete structure solution, refinement and analysis program (2009). J. Appl. Cryst., 42, 339-341.

www.manaraa.com

CHAPTER FOUR:

CHEMISTRY OF AN EPIGENETICALLY MODIFIED

FUNGAL ENDOPHYTE FROM TROPICAL MANGROVE

Figure IV.1. Boating through the tropical mangrove habitat. Photo credit: ACDL (2015).

Since the "golden age" era of microbial chemistry drug discovery, the role and value of microorganisms keeps extending.[1-3] Split in three domains Archaea, Prokarya,[4] and Eukarya,[5] microorganisms can be found anywhere, and are essential to life.[6] Most microorganisms are free living, but sometimes, as endophytes, they can engage in symbiotic relationship and use the

www.manaraa.com

primary resources of their hosts.[7] The microbial population surpasses the human one. However, mainly due to challenges when growing cultures in laboratory conditions, it is estimated that only 1% have been studied.[8] An individual endophyte is capable of synthesizing up to 50 secondary metabolites.[2] Of the near couple hundred thousand of known natural products, about half are from microbes. The early 2000s saw the discovery of 129 marine bioactive microbial compounds, and the marine environment, still greatly understudied, provides opportunities to expand the microbial chemodiversity.[1,2,9-11] In natural conditions, the environmental stress is responsible for triggering the activation of biosynthetic pathways producing a variety secondary metabolites deeply involved in adaptative, reproductive, and defensive mechanisms.[9,12-14] The resulting small molecules produced by symbiotic microbes serve as biochemical warfare used for both their own and their host's ecological survival.

IV.1. Tropical mangrove marine ecosystem

Focusing only the eukaryotic endophytes, it is considered that there are between four and six species of fungal endophytes living within each vascular plant available on land. [15] This represents a potential of 10^6 fungal species, with only about 120,000 species studied and known so far.[15] The substantial wealth of available natural products in plants becomes even more important with harsh environmental pressure exhibited in extreme ecological conditions.

Growing at the interface between land and sea in tropical and sub-tropical latitudes, mangroves are a forest of plants. They develop where fresh water from rivers meet salted sea water. Tropical mangrove ecosystems represent the second largest source of biodiversity after coral reefs.[16] Divided in three classes, red, black and white mangrove forests ought to develop physiological adaptations in high salinity brackish water, extreme tides, strong winds, high temperatures and muddy anaerobic soils conditions.[17,18] The unique ecological environments of mangroves host rich communities of species. Studies of the submerged roots, trunks, and

www.manaraa.com

branches are habitat for microbial populations including bacteria, fungi, macroalgae and invertebrates, while the aerial parts welcome higher order organisms such as crabs, insects, reptiles, amphibians, birds and mammals.[12] The additional harsh environmental conditions of temperature, salinity, anoxia, and light exposure associated with the biological stress of coexisting species make mangrove ideal ecosystems to stimulate diverse secondary metabolites production for ecological survival.[19-22] However, they are also easily disturbed by human activities turning them into waste dumps. However, an alternative to destruction may be the investigation of mangrove endophytes valuing their chemical diversity asset.[17,18] Collection of these organisms for drug discovery purposes allows storage of biological material that may be regrown in unlimited amount in laboratory conditions.

IV.2. Fungal Endophyte Chemistry

Endophytic microbial communities from mangrove are known to produce diverse bioactive compounds distributed between terpenes, peptides, polyphenol, polyketides, and quinoline derivatives.[23,24] Although mostly antibacterial and antifungal, the exhibited antimicrobial chemistry has also shown antiparasitic properties. High metabolite production rate and chemical diversity offered by microorganisms from understudied niches are worth investigating.[25,26] Unfortunately, microbes tend to slow their metabolism when exposed to laboratory conditions, as the lack of ecological and biological stresses impedes the need for survival. Not being as challenged as in their natural environment, cultured fungal endophytes shut down their biosynthesis of secondary metabolites. Reactivation of the silent pathways for secondary metabolites production can be induced and is made possible with the use of epigenetic modifiers.[27-30]

www.manaraa.com

Understanding of epigenetic transformations explains that, rather than the conservation of DNA information, the expression of DNA information, ruled by epigenetic regulations, is responsible for the existence of an individual. The genome is the blueprint doing the work to provide the essential elements maintaining life; however, epigenetic markers tells the genome what to do. In the case of twins, they possess the exact same genetic code, but epigenetic regulations are responsible for specific traits in each twin's biology. Similarly, it is like the same painting being done using two different sets of colors. They look alike but the color variation makes them unique. The expression of particular sequences of DNA can happen if exposed for enzymes to access, and epigenetic factors are directly affecting this process by loosening or tightening the DNA strands.

In our laboratory, two kinds of epigenetic modifiers are used: a Histone Deacetylase inhibitors (HDACi) and a DNA Methyl Tranferase inhibitor s(DNMTi).[19,21,31] Sodium butyrate is used as an HDACi to target the compacting stage of the DNA on the histone. The DNA strands are coiled onto the histones in a resting state and are relaxed and exposed when the translation process happens. The acetylation moieties on lysine residues of the histones signals the location of desired transcription sites when needed. Acetylase enzymes hydrolyze the acetyl residue at defined location where the transcription process must ensue. This yields space for the topoisomerase enzymes to cut the DNA strands accordingly and for the polymerase enzymes to start the transcription job. Inhibiting the regular deacetylase processes, influences where the DNA will remain uncoiled on the histone. Using HDACi, gives the chance to generally down-regulated DNA sites (coiled onto histones) to be chosen and get transcribed.

Methylation of the DNA is an epigenetic regulation happening on the 5' position of the cytosine bases. When present the methylation induces silencing of genes and prevents transcription regulation from happening.[32,34] Inhibiting this signaling by incorporating 5-

www.manaraa.com

azacytidine in the environment is used as the DNMTi process. The introduced 5-azacytidine competes and replaces cytidine in the DNA building process during growth and development of an organism. Generally, the regularly methylated cytidine nucleotides act as a stop sign silencing the transcription of specific DNA sequences. Inhibiting this process using a cytidine deprived of methyl in position 5', acts as a switch turning on the recognition of a specific DNA sequence to be regulated through transcriptional process. When the DNA nucleotide is not methylated, it does appear visible to regulating enzymes and becomes of interests making its up-regulation possible.[35] The generally less or under regulated sequences affected by DNMTi mechanisms, can now be seen and transcribed.

Further biological studies may pin-point the exact sequences and processes involved. However, even in the unknown of understanding, natural products chemists can exploit and value the chemistry being produced during these biological pathways.[3,28]

IV.3. Screening Campaign and Library of crude extracts

In 2012, a screening campaign in the laboratory, operated by my predecessors, focused on endophytes from Floridian and Mexican mangroves. Leaves, stems, and bark from the mangrove forest were collected. Isolation of pure single strains fungal endophytes was performed leading to the creation of a library of 536 fungal isolates. Taking advantage of epigenetic modifications, three growth conditions on rice cultures were created for each organism: HDACi, DNMTi, and no epigenetic modifier as control. Subsequent extraction of each culture with 100% ethyl acetate generated 1608 crude extracts entered in a high-throughput screening against various pathogens: *Naegleria fowleri*, *Leishmania donovani*, *Mycobacterium tuberculosis*, and a bacterial group of pathogens *Enterococcus faecium, Staphylococcus aureus, Klebsiella pneumoniae, Acinetobacter baumanii, Pseudomonas aeruginosa,* and *Enterobacter* involved in severe nosocomial infections and summarized under the acronym *ESKAPE*. Statistics showed that 254 (16%) of the crude extracts

www.manaraa.com

came back active in one or more assay. More than 60% of these lead extracts were selective to a single pathogenic target. A population of 162 fungal endophytes was responsible for these lead extracts. Fungi from all three culture conditions provided active extracts, but specifically, 44% of the fungi produced active extracts resulting from HDACi or DNMTi conditioned cultures.[19] All these evidences proved the potential of mangrove fungal endophytes as source of bioactive chemistry. Ranking of the most potent 40 extracts against each tested pathogen was done using the Cubic scale.

Screening of the crude extracts provided biological activities data, but the chemistry responsible for these still needed to be explored and determined. Upon my arrival in the lab, I took on the chemical investigation of the *Leishmania donovani* assay most potent extract, resulting from a DNMTi modified culture of *Penicillium guanacastense*, originally isolated from a senescent piece of wood from the Mexican mangrove of Tapachula collected by Dr. Mario Rodriguez, of the Instituto Politécnico Nacional, Centro de Biotechnología Genómica in Reynosa, Tamaulipas, Mexico. The endophyte identification was performed via Polymerase Chain Reaction (PCR) analysis by Sarah Kennedy in the Shaw lab. I proceeded to scaling up the culture conditions to facilitate enough crude extract material to perform separations, purifications, and characterization of the secondary metabolites responsible for the biological activities recorded during the screening campaign stage.

www.manaraa.com

Figure IV.3.1 *Penicillium guanacastense* on a Petri dish. Photo credit: ACDL (2019).

IV.4. Isolation and structure elucidation of an antileishmanial sesterterpene

The fungal endophyte from the Tapachula mangrove was retrieved from the library and regrown on Sabouraud dextrose (SD) agar plate. Twenty pieces (1 mm x 1 mm) of fungus were introduced into 100 mL of a 2.4 $x10^{-2}$ mg/mL solution of 5-azacytidine SD broth to allow epigenetic exposure. The resulting solution was added to 300 g of brown rice autoclaved in 500 mL of deionized water. The culture was left at room temperature on a shelf in the lab for 21 days to allow growth of the organism. A three-day extraction with ethyl acetate created a crude extract (m = 5.1 g). First a defatting step, consisting in a partition of the reconstituted sample in 70% aqueous methanol against hexanes, was performed. After drying out the methanol present in the aqueous part, a second partition of the sample in water against ethyl acetate was executed. This two-step process yielded three refined extracts. Separation of the hexane extract through MPLC yielded fractions A through H.

www.manaraa.com

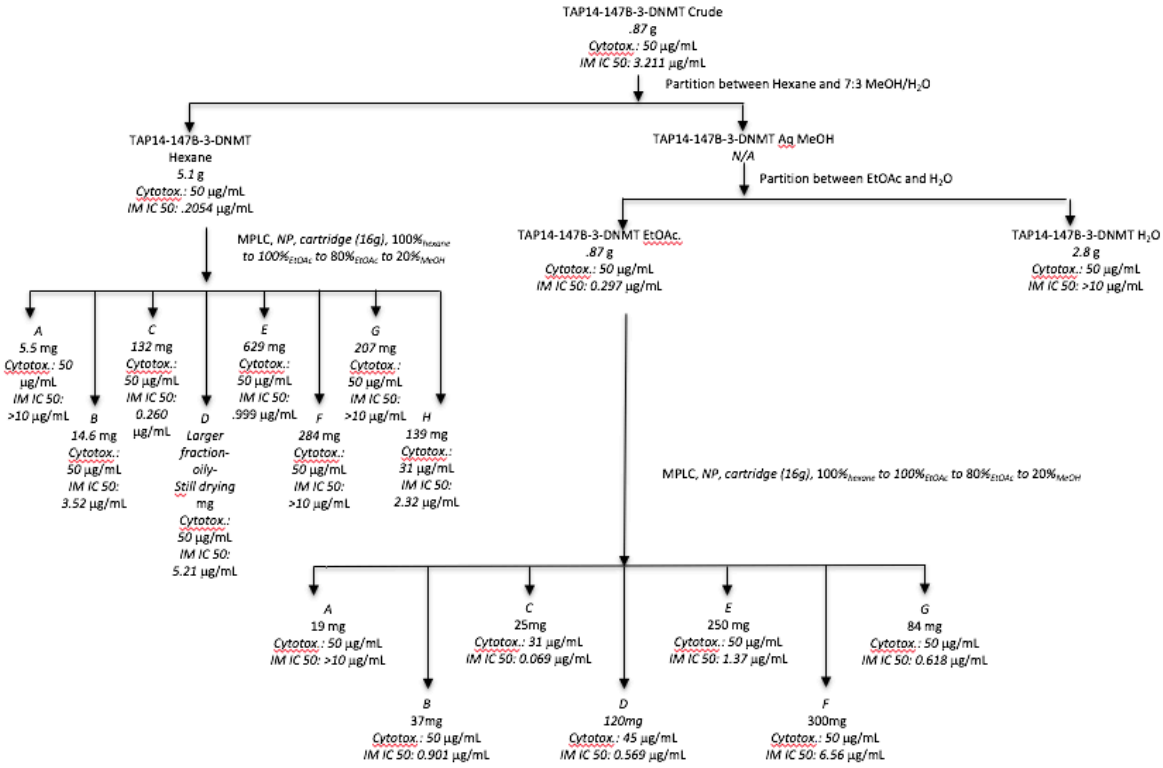

Scheme IV.4.1. Fractionation Scheme of crude extract obtained from a DNMT modified culture of *Penicillium guanacastense* grown on rice medium.

NMR studies revealed fractions E (88 mg), F (300 mg), and G (200 mg) to be interesting ones. The display of signals between 3.50 ppm and 6.00 ppm in the proton NMR spectrum, motivated further investigations. Subsequent rounds of normal phase and reverse phase HPLC led to three sestertepenes: a novel compound, tapachulanone A (**13**), was isolated alongside the two known atlantinones A and B. The crystal structure of tapachulanone A (**13**), determined by Dr. Lukasz Wojtas supported the NMR structure elucidation.

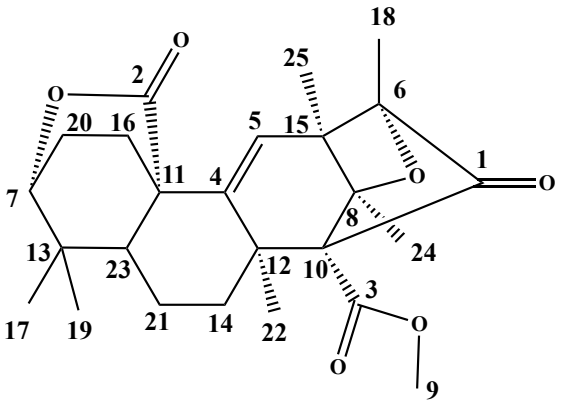

www.manaraa.com

13

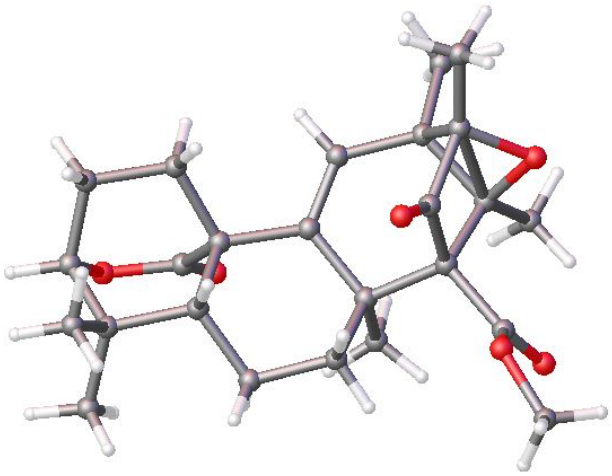

Figure IV.4.1. Molecular and crystal structures of tapachulanone A (**13**).

The HRESIMS value $[M + H]^+$: m/z 429.2276, calcd. for $C_{25}H_{32}O_6H$, m/z 429.2272, provided the molecular formula $C_{25}H_{32}O_6$ for **13**, which indicated the presence of 10 degrees of unsaturation. (*See Appendix* **Figure B.IV.2.**) The carbon spectrum reveals the presence of 11 quaternary carbons, 7 tertiary, 4 secondary, and 3 primary ones. Of the five carbons above 100 ppm, four are quaternary ones: a ketone related to C-1 (δ_C 199.5), two ester-like carbonyl carbons C-2 (δ_C 176.2) and C-3 (δ_C 169.0), and an olefinic carbon C-4 (δ_C 134.0). The fifth one C-5 (δ_C 125.4) appears on HSQC to be connected to a single proton (δ_H 5.15).

www.manaraa.com

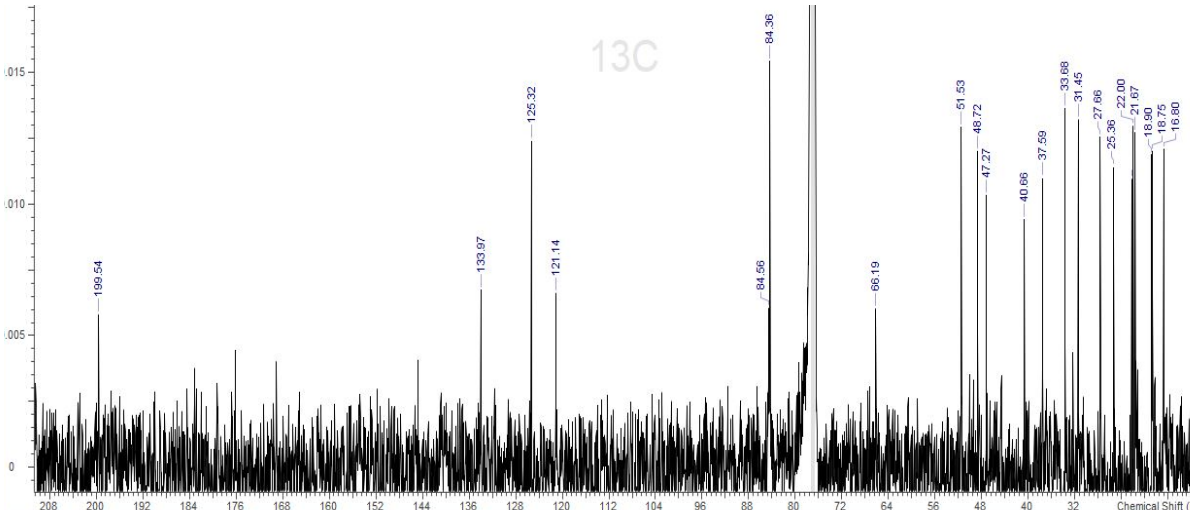

Figure IV.4.2. ^{13}C NMR spectrum for tapachulanone A **(13)** in $CDCl_3$ (125 MHz).

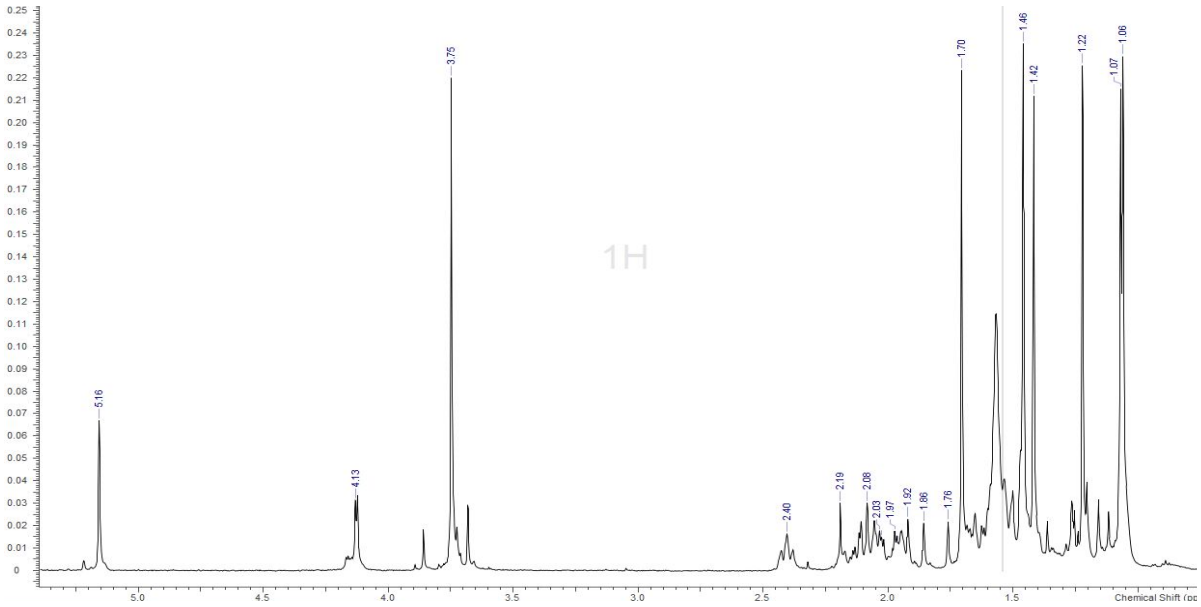

Figure IV.4.3. ^{1}H NMR spectrum for tapachulanone A **(13)** in $CDCl_3$(500 MHz).

The chemical shifts associated with quaternary C-4 and tertiary C-5 are characteristic of an olefinic system. A single strong three-bond HMBC correlation exists between this olefinic methine and quaternary carbon C-11 (δ_C 47.3). Beside the C-5 methine proton, the methylene protons (δ_H 1.64 ppm and 2.13) on C-16 (δ_C 47.3) are the only ones establishing a two-bond HMBC correlations with C-11.

www.manaraa.com

Table IV.4.1. ^{13}C and ^{1}H NMR Data for novel tapachulanone A (**13**)

Position	δC[a] type	δH[b], int.(J in Hz)
1	199.5	
2	176.1	
3	169.0	
4	134.0	
5	125.4	5.16, 1H
6	84.6	
7	84.4	4.13, 1H
8	66.2	
9	51.5	3.75, 3H
10	48.7	
11	47.3	
12	40.7	
13	37.6	
14	33.7	1.50 and 2.42, 2H
15	32.4	
16	31.5	1.64 and 2.13, 2H
17	27.7	1.08, 3H
18	25.4	1.46, 3H
19	22.3	1.07, 3H
20	22.0	1.98 and 2.07, 2H
21	21.7	1.50 and 1.69, 2H
22	18.9	1.22, 3H
23	18.8	1.94, 1H
24	16.8	1.70, 3H
25	12.3	1.42, 3H

[a] ^{13}C shift recorded in $CDCl_3$ at 125 MHz, reported in ppm. [b] ^{1}H NMR spectrum shift and integration recorded in $CDCl_3$ at 500 MHz, reported in ppm.

www.manaraa.com

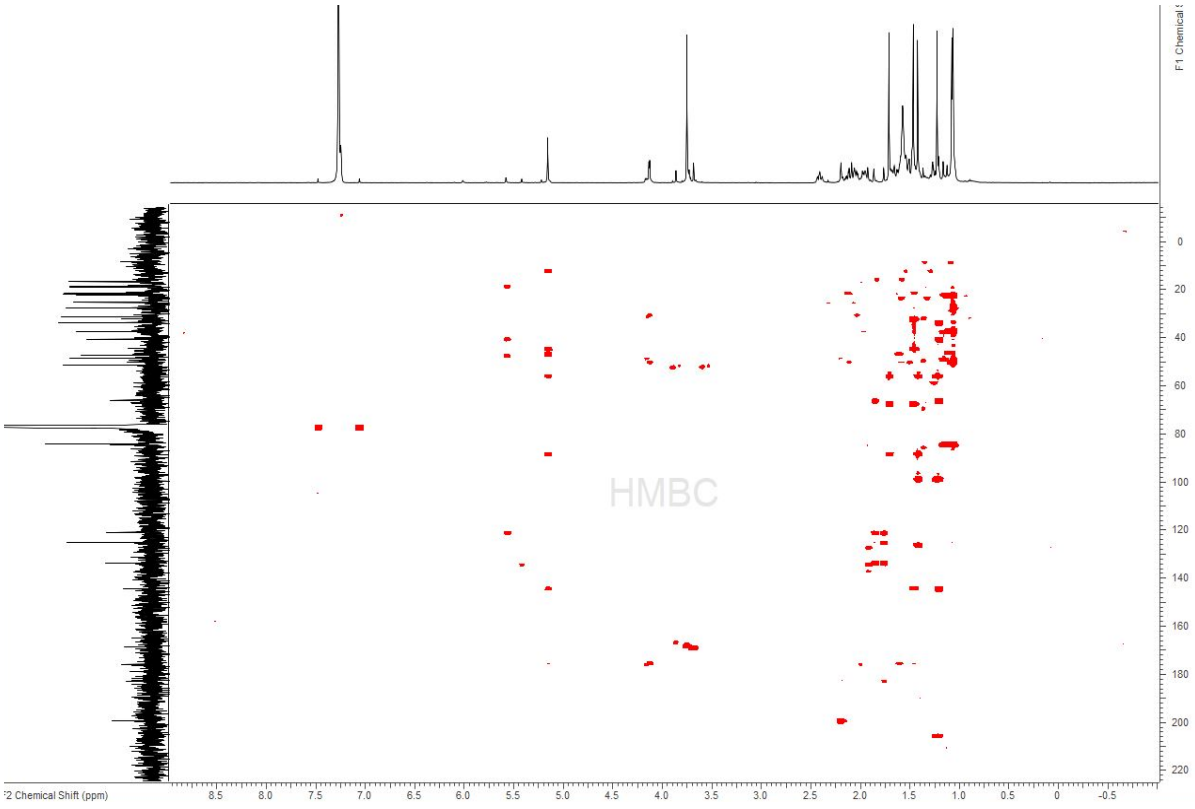

Figure IV.4.4. HMBC NMR spectrum for tapachulanone A **(13)** in $CDCl_3$ (500 MHz).

An additional two-bond correlation is seen with C-20 (δ_C 22.0) and a longer three-bond range one exists with C-2. The three different kinds of protons correlating seen with C-2, suggest a cyclic lactone configuration of C-2 rather than a linear ester shape, which would have led to correlation with only one kind of protons. Indeed, methylene protons on C-16 and C-20, and methine on C-7 (δ_C 84.4) all exhibit long range HMBC correlation with C-2.

Compared to C-2, C-3 offers only one HMBC correlation with protons of C-9 (δ_C 51.5); the proton chemical shift (δ_H 3.75) signature of a methoxy group, confirms the ester character of C-3. A spin system involving C-7, C-13 (δ_C 37.6), C-17 (δ_C 27.7) and C-19 (δ_C 22.3) is seen through mutual C-17 and C-19 correlation, as well as for both, additional ones with C-7, C-13, and C-20. The methine (δ_H 1.94) linked to C-23 (δ_C 18.8) offers a two-bond HMBC correlation with quaternary C-11 and a three-bond range with C-7, which allows closure of a six-membered ring.

www.manaraa.com

Furthermore, the higher chemical shift of 84.4 ppm of C-7 suggests connectivity to an oxygen atom from the lactone moiety, while the lower 47.3 ppm shift for C-11 supports connectivity with quaternary C-2 involved in the lactone ring. Methylene protons (δ_H 1.50 and 2.42) on C-14 (δ_C 33.7) establish three-bond HMBC correlation with C-10 (δ_C 48.7) as well as a COSY correlation with the methylene protons (δ_H 1.50 and 1.69) found on C-21 (δ_C 21.7). The quaternary C-10 offers long range correlation with the C-21 methylene protons, and shorter ones with methyl protons (δ_H 1.22) on C-22 (δ_C 18.9). The C-22 methyl communicating with two quaternary C-8, C-10, and C-12 (δ_c 40.7) allows the description of a spin system connecting three successive quaternary carbons. The increasing values of chemical shifts for C-12, C-10, and C-8 hint the presence of heteroatom creating a deshielding effect. Carbon C-8 connected to a methyl group (δ_H 1.70) on C-24 (δ_c 16.8) confirms the presence of a neighboring oxygen atom involved in an ether moiety between C-6 and C-8. Carbon C-6 being in alpha position of both a ketone and an ether exhibits higher chemical shift than C-8 in alpha position of an ether while in beta position of ketone on C-1 and ester on C-3. Contrary to C-8, C-10 is found α to the C-1 ketone and the C-3 ester, but β to the ether on C-8. C-10 and C-11 experience similar chemical environments giving them a similar range of shifts. The methyl protons (δ_H 1.46) associated with C-18 (δ_c 25.4) display three bond correlation with C-25 (δ_c 12.3) and occupy a highly oxygenated environment β to the C-1 and C-6, deshielding the protons more than the ones from the other methyl groups. Finally, C-25 bearing methyl (δ_H 1.42) correlated with C-5 and C-6.

The crystal structure of tapachulanone A (**13**) and the literature from the known atlantinone compounds facilitated the NMR structure elucidation.[27,36]

The original screening results provided potency of the DNMTi crude extracts of *Penicilium guanacastense* in the *Leishmania donovani* assay. Testing of the refined crude extracts from the scaled-up conditions confirmed that the biological activity was retained. Both ethyl acetate and

www.manaraa.com

hexane extracts exhibited potency against the parasite with respective IC_{50} values of 0.30 µg/mL and 0.21 µg/mL, which guided the subsequent purification stages. Specific investigation of the ethyl acetate refined crude extract was favored over the hexane one as additional NMR and MS spectra dereplication supported potentials for chemical novelty. Indeed, upon purification, compound **13** revealed novel and retain potency at IC_{50} 1.42 µM and mild cytotoxicity CC_{50} > 0.12 mM in the *Leishmania donovani* assay performed by Ala Azhari of the Kyle lab.

Epigenetic modifications have come in handy to expand the chemical space of fungal bioactive chemistry in the field of drug discovery. Microorganisms can be seen as microscopic productive factories, allowing on demand quantity of crude material to facilitate natural products chemists' investigations. However, Nature is an unlimited force to be reckoned with, continuously making snub at natural products chemists. Rather than control and monotony, unpredictability and originality seem to be the essential motto of biodiversity. This experimental success motivated the search for experiment reproducibility to acquire more biochemical material. Scaled up cultures in the same conditions were repeated but did not provide probing results to produce substantial amount of the compound of interest (**13**). A new approach was required for better understanding and optimization. Despite the constant challenge of finding more, natural products chemists keep optimizing ways to improve isolation efficiency and yield. Not only would larger quantities bring satisfaction and reward, the increase of yield would allow more biological tests to broaden the scope of activity for a compound.

With these goals in mind, the isolation of the antileishmanial novel sesterterpene from epigenetically modified cultures motivated further experimentation described in the next chapter. Ever improving technology and methods help develop a different approach to isolate novel chemistry.

www.manaraa.com

IV.5. Experimental

IV.5.1. General Procedures

Normal phase Medium Pressure Liquid Chromatography (MPLC) separations were conducted using a Teledyne CombiFlash Rf200i fitted with UV and ELS detection with a RediSepRf 40g silica column. For HPLC separation, all solvents were obtained from Fisher Scientific and were HPLC grade (>99% purity) unless otherwise stated. All HPLC analysis were performed on a Shimadzu LC20-AT system equipped with either an evaporative light scattering detector (ELSD) ELSD II and/or a SPD-M20A UV-Vis detector. For normal phase separation, analytical [Phenomenex Luna Silica, 250 x 4.6 mm, 5 µm], semi-preparative [Phenomenex Luna Silica, 250 x 10 mm, 5 µm], or preparative [Phenomenex Luna Silica, 250 x 21.2 mm, 5 µm] were used, while reverse phase separation employed analytical [YMC packed C-18, A-304-10, S-10, 120 Å ODS], or semi-preparative [Phenomenex Luna C-18, 250 x 10 mm, 5 µm] columns. All NMR spectra were acquired in $CDCl_3$ with residual solvent referenced as an internal standard (7.26 ppm). All ^{1}H NMR spectra were recorded on a Varian 500 MHz Direct Drive instrument and ^{13}C NMR spectra were recorded at 125 MHz. Analytical LC/MS was performed on a Phenomenex Kinetex C18 column (50 x 2.1 mm, 2.6 µm) on an Agilent 6230 LC/TOF-MS with electrospray ionization detection. Optical rotations were measured on a Rudolph Research Analytical AUTOPOL IV digital polarimeter.

IV.5.2. Scaled up culture preparation

The *Penicillium guanacastense* fungal strain was plated on Sabouraud Dextrose Agar (SDA) plate and culture for 3 days. A DNMT-modified Sabouraud Dextrose Broth (SDB) solution was prepared at 0.025 mg/mL, in two 50 mL falcon tubes. The fungal grown on a Petri dish was diced in 2 mm x 2 mm pieces. Ten pieces of fungus were added to each 50 mL Falcon tubes and shaken for 2 minutes.

www.manaraa.com

Unicorn bags containing 300 g of brown rice and 500 mL of deionized water were autoclaved according to the liquid 15/121 menu selection of the autoclave. Upon sterilization, each rice bag was partly open in the biohood and inoculated with two 50 mL of DNMT-modified SDB, each containing 10 pieces of fungus. The bag was re-sealed and placed at room temperature on a laboratory shelf for culture growth for 21-day period of time. An exhaustive ethyl acetate extraction allowed the fungal culture to seat overnight and filtered to obtain a crude extract. The procedure was repeated two subsequent times. The crude extracts obtained from each filtration was dried down and reconstitutes using a 70% aqueous methanol solution. A partition with hexanes was then applied. Both parts were dried down. The dried material from the aqueous part was reconstituted in water and partitioned using ethyl acetate. Upon solvent evaporation, the ethyl acetate extract was separated on normal phase MPLC using a Teledyne CombiFlash fitted with UV and ELS detection. RediSep silica columns were used according to the mass of crude extracts to be separated. The choice of the column size was determined to allow half of the capacity of the column to be used for optimal separation and peak resolution purposes.

IV.5.3. Spectral data (13)

Tapachulanone A (13): translucent solid; $[\alpha]^{24.6}_{365}$ +4.80° (*c* = 0.6, CH_2Cl_2); UV (ACN) λ_{max} (log ε) (2.59) 220; (2.50) 240 nm; IR υ (thin film): 2920, 2850, 1700 cm^{-1}; ^1H and ^{13}C NMR data see **Table IV.4.1.**; HRESIMS $[M + H]^+$: m/z 429.2276, calcd. for $C_{25}H_{32}O_6H$, m/z 429.2272.

IV.5.4. X-ray Crystallography

The crystallographic analysis was done by Dr. Lukasz Wojtas. The crystal of **13** was obtained from slow evaporation of $CHCl_3$ at room temperature. The X-ray diffraction data were measured on Bruker D8 Venture PHOTON 100 CMOS diffractometer equipped with a Cu Kα INCOATEC ImuS micro-focus source (λ = 1.54178 Å). Indexing was performed using APEX3 (Difference Vectors method). Data integration and reduction were performed using SaintPlus.

www.manaraa.com

Absorption correction was performed by multi-scan method implemented in SADABS. Space group were determined using XPREP implemented in APEX3. Structure was solved using SHELXT and refined using SHELXL-2018 (full-matrix least-squares on F2) through OLEX2 interface program. All molecules are conformationally strained: corresponding hydrogen atoms were refined with restraints and with Uiso = 1.2 Ceq (1.5 for -CH_3 group). All other hydrogen atoms were placed in geometrically calculated positions and were included in refinement process using riding model with isotropic thermal parameters. Absolute configuration for all compounds was established based on Flack parameter value and verified additionally with Bijvoet-Pair Analysis and Bayesian Statistics Methods. P2 = 1 for all cases and is the probability that the current model is correct assuming two possibilities: one out of two enantiomers present. Crystal data and refinement conditions are shown in **Table B.IV.2**. in *Appendix B*.

IV.5.5. *Leishmania donovani* and J774A.1-Cells Cytotoxicity Assay

The leishmania screen was conducted by Ala Azhari in the Kyle lab. The cytotoxicity was assessed testing compound **13** against J774.A1 macrophages using the CellTiter 96 AQueous one-solution cell proliferation assay (Promega, Madison, WI). In a 96 well drug plate (Costar, Assay Plate, 96 well with low Evaporation Lid, Flat Bottom, None-Treated, #3370) compounds were diluted in a series of 6 two-fold dilutions in media to produce a concentration range from 500µg/ml to 15.625µg/ml. From each well 10 µL were transferred to another 96 well plate (Costar, Assay Plate, 96 well with low Evaporation Lid, Flat Bottom, Tissue culture Treated, # 3628) and 90µL of macrophages in media in a 50,000 cell per well concentration was added to produce a final concentration range from 50 µg/ml to 1.562 µg/ml. The plates were then incubated at 37 ˚C, 5% CO_2 for 72 hrs.

Then, 20 µL of 3-(4,5-dimethylthiazol-2-yl)-5(3-carboxymethoxyphenyl)-2-(4-sulphophenyl)-2H-tetrazolium (MTS: Promega, Madison, WI) solution was added to each well and incubated for an

www.manaraa.com

additional 4 hours. A Spectra Max M2^{e} (molecular Devices, Sunnyvale, Ca) was used to measure optical density (OD) at 490nm. Non-linear regression via Trifox software was used to determine IC_{50} values. Additionally, potency against infected macrophage cells was conducted. In a 384 well assay plate (CellCarrier-384 Black, Optically Clear Bottom, Tissue Culture Treated, Sterile, 6007550), 2000 J774 cells are seeded and incubated for at least an hour to allow adherence. The plate is then washed with pre-warmed media to get rid of the unadhered cells. *L. donovani* axenic amastigotes are then added to the plate at a ratio of 10:1 and incubated at 37 °C, 5% CO_2 for 24 hours. The excess extracellular amastigotes are then washed away using pre-warmed media. Compounds are prepared in a 384-drug plate (Thermo Scientific™ Nunc™ 384-Well Clear Polystyrene Plates with Non /treated Surfaces, #242757) with a starting concentration of 10 µg/ml and serially diluted at 1:2. Drugs are then added to the assay plate and incubated at 37 °C, 5% Co_2 for 72 hours. After that, drugs are removed from the plate and adhered cells are fixed with 2% paraformaldehyde (Alfa Aesar™ Paraformaldehyde, 16% w/v aq. soln., methanol free, #30525-89-4) and incubated for 15 minutes at room temperature. Fixative is then removed, and cells are stained with 5 µM Draq5 (Thermo Scientific DRAQ5 FLUORESCENT PROBE, DNA stain, #62251) and incubated for 5 minutes at room temperature. Stain is then removed, and fresh media is added to the plate. A Perkin Elmer Operetta (High content imager) is then used to capture images for each well and find macrophage and amastigotes nuclei within macrophage cytoplasm using Harmoney software that counts the number of amastigotes per 500 macrophages in each well and generate IC_{50} values.

References

(1) Cragg, G. M.; Newman, D. J. Medicinals for the millennia: the historical record. *Ann. N.*

www.manaraa.com

Y. Acad. Sci. **2001**, *953*, 3–25.

(2) Demain, A. L. Importance of microbial natural products and the need to revitalize their discovery. *J. Ind. Microbiol. Biotechnol.* **2014**, *41*, 185–201.

(3) Ziemert, N.; Alanjary, M.; Weber, T. The evolution of genome mining in microbes-a review. *Natural Product Reports*. Royal Society of Chemistry August 1, 2016, pp 988–1005.

(4) IWilliam B. Whitman*†, David C. Coleman‡, and W. J. W. Prokaryotes: The unseen majority. *Proc. Natl. Acad. Sci.* **1998**, *95*, 6578–6583.

(5) Taylor, J. W.; Turner, E.; Townsend, J. P.; Dettman, J. R.; Jacobson, D. Eukaryotic microbes, species recognition and the geographic limits of species: examples from the kingdom fungi. *Philos. Trans. R. Soc. B Biol. Sci.* **2006**, *361*, 1947–1963.

(6) Sapp, J.; Fox, G. E. The singular quest for a universal tree of life. *Microbiol. Mol. Biol. Rev.* **2013**, *77*, 541–550.

(7) Wilson, D. Endophyte: The evolution of a term, and clarification of its use and definition. *Oikos* **1995**, *73*, 274–276.

(8) Demain, A. L. Importance of microbial natural products and the need to revitalize their discovery. *J. Ind. Microbiol. Biotechnol.* **2014**, *41*, 185–201.

(9) Carroll, A. R.; Copp, B. R.; Davis, R. A.; Keyzers, R. A.; Prinsep, M. R. Marine natural products. *Nat. Prod. Rep.* **2019**, *36*, 122–173.

(10) Cheuka, P. M.; Mayoka, G.; Mutai, P.; Chibale, K. The role of natural products in drug discovery and development against neglected tropical diseases. *Molecules*. MDPI AG January 1, 2017.

(11) Newman, D. J.; Cragg, G. M. Natural products as sources of new drugs from 1981 to 2014. *J. Nat. Prod.* **2016**, *79*, 629–661.

(12) Gouda, S.; Das, G.; Sen, S. K.; Shin, H.-S.; Patra, J. K. Endophytes: a treasure house of

www.manaraa.com

bioactive compounds of medicinal importance. *Front. Microbiol.* **2016**, 7.

(13) Williams, D. H.; Stone, M. J.; Hauck, P. R.; Rahman, S. K. Why are secondary metabolites (natural products) biosynthesized? *J. Nat. Prod.* **1989**, *52*, 1189–1208.

(14) Clardy, J. The chemistry of signal transduction. *Proc. Natl. Acad. Sci. U. S. A.* **1995**, *92*, 56–61.

(15) Hawksworth, D. L. The magnitude of fungal diversity: the 1.5 million species estimate revisited. *Mycol. Res.* **2001**, *105*, 1422–1432.

(16) Mumby, P. J.; Edwards, A. J.; Arias-González, J. E.; Lindeman, K. C.; Blackwell, P. G.; Gall, A.; Gorczynska, M. I.; Harborne, A. R.; Pescod, C. L.; Renken, H.; et al. Mangroves enhance the biomass of coral reef fish communities in the caribbean. *Nature* **2004**, *427*, 533–536.

(17) Valiela, I.; Bowen, J. L.; York, J. K. Mangrove Forests: One of the World's Threatened Major Tropical Environments. *Bioscience.* **2001**, *51*, 807–815.

(18) Kathiresan, K.; Bingham B. L. Biology of mangroves and mangrove ecosystems. **2001**, Vol. 40.

(19) Demers, D. H.; Knestrick, M. A.; Fleeman, R.; Tawfik, R.; Azhari, A.; Souza, A.; Vesely, B.; Netherton, M.; Gupta, R.; Colon, B. L. Exploitation of mangrove endophytic fungi for infectious disease drug discovery. *Mar. Drugs* **2018**, *16*, 376.

(20) Demers, D. H. Chemical investigations of fungal natural products for drug discovery. *Grad. Theses Diss.* **2017**, No. July.

(21) Knestrick, M. A. From Florida to Antarctica: dereplication strategies and chemical investigations of marine organisms. **2018**, No. April.

(22) Romano, S.; Jackson, S. A.; Patry, S.; Dobson, A. D. W. Extending the one strain many compounds (osmac) principle to marine microorganisms. *Mar. Drugs* **2018**, *16*, 244.

www.manaraa.com

(23) Sharma, N.; Sharma, V.; Abrol, V.; Panghal, A.; Jaglan, S. An update on bioactive natural products from endophytic fungi of medicinal plants. in pharmaceuticals from microbes: impact on drug discovery; Arora, D., Sharma, C., Jaglan, S., Lichtfouse, E., Eds.; *Environmental Chemistry for a Sustainable World; Springer International Publishing: Cham*. **2019**, 121–153.

(24) Salini, G. Pharmacological profile of mangrove endophytes - a review. *Int. J. Pharm. Pharm. Sci.* **2014**, *7*, 6–15.

(25) Strobel, G. The emergence of endophytic microbes and their biological promise. *J. Fungi.* **2018**, *4*, 57.

(26) Vasundhara, M.; Kumar, A.; Reddy, M. S. Molecular approaches to screen bioactive compounds from endophytic fungi. *Frontiers in Microbiology*. **2016**.

(27) Wang, X.; Sena Filho, J. G.; Hoover, A. R.; King, J. B.; Ellis, T. K.; Powell, D. R.; Cichewicz, R. H. Chemical epigenetics alters the secondary metabolite composition of guttate excreted by an Atlantic-forest-soil-derived *Penicillium citreonigrum*. *J. Nat. Prod.* **2010**, *73*, 942–948.

(28) Cichewicz, R. H. Epigenome Manipulation as a pathway to new natural product scaffolds and their congeners. *Nat. Prod. Rep.* **2010**, *27*, 11–22.

(29) Henrikson, J. C.; Hoover, A. R.; Joyner, P. M.; Cichewicz, R. H. A Chemical Epigenetics approach for engineering the in situ biosynthesis of a cryptic natural product from *Aspergillus niger*. *Org. Biomol. Chem.* **2009**, *7*, 435–438.

(30) Wolfe, A. P.; Matzke, M. A. Epigenetics: Regulation through repression. *Science.* **1999,** *286*, 481-486.

(31) Beau, J.; Mahid, N.; Burda, W. N.; Harrington, L.; Shaw, L. N.; Mutka, T.; Kyle, D. E.; Barisic, B.; Van Olphen, A.; Baker, B. J. Epigenetic tailoring for the production of anti-

www.manaraa.com

infective cytosporones from the marine fungus *Leucostoma persoonii*. *Mar. Drugs* **2012**, *10*, 762–774.

(32) Bird, A. DNA methylation patterns and epigenetic memory. *Genes Dev.* **2002**, *16*, 6–21.

(33) Jeon, J.; Choi, J.; Lee, G.-W.; Park, S.-Y.; Huh, A.; Dean, R. A.; Lee, Y.-H. Genome-Wide Profiling of DNA methylation provides insights into epigenetic regulation of fungal development in a plant pathogenic fungus, *Magnaporthe oryzae*. *Sci. Rep.* **2015**, *5*.

(34) Jones, P. A.; Takai, D. The role of DNA methylation in mammalian epigenetics. *Science.* **2001**, *293*, 1068–1070.

(35) C. Henrikson, J.; R. Hoover, A.; Matthew Joyner, P.; H. Cichewicz, R. A chemical epigenetics approach for engineering the in situ biosynthesis of a cryptic natural product from *Aspergillus niger*. *Org. Biomol. Chem.* **2009**, 7, 435–438.

(36) Dalsgaard, P. W.; Petersen, B. O.; Duus, J.; Zidorn, C.; Frisvad, J. C.; Christophersen, C.; Larsen, T. O. Atlantinone A, a meroterpenoid produced by *Penicillium ribeum* and several cheese associated *Penicillium* species. *Metabolites* **2012**, *2*, 214–220.

www.manaraa.com

CHAPTER FIVE:

OPTIMIZATION OF SECONDARY METABOLITES PRODUCTION USING A TARGETED LIQUID CHROMATOGRAPHY TANDEM MASS SPECTROMETRY APPROACH

a. 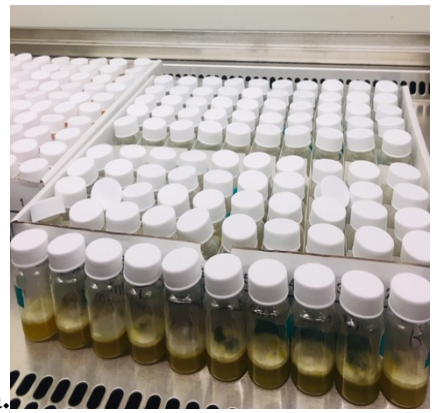 b. 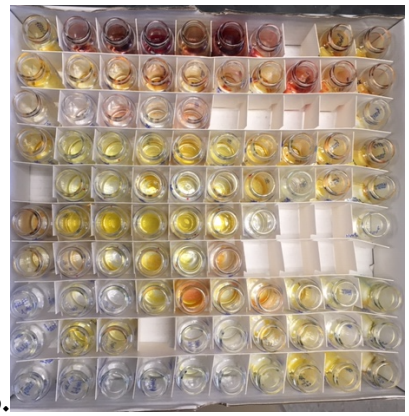

Figure V.1. Small scale fungal endophytic cultures. **(a)** Fractions generated from one crude extract separation. **(b)**.

Whether it is through the collection stage or at the isolation and purification one, mass remains the major concern in natural products research. A substantial amount of material will always facilitate further acquisition of analytical data used to elucidate structures. However, Nature not always complying with the production of sufficient amount for scientists, has motivated human technological progress to develop more analytical tools such as mass spectroscopy.

www.manaraa.com

The characterization of chemical structures is fundamental to the identification of chemical structures, discovery of novel ones and may complement the comprehension of biological process. With the various methodologies it has to offer, the field of mass spectrometry has proven essential to the field of drug discovery. It has evolved from compound elementary mass characterization for structure elucidation to high-throughput methods allowing further data mining and metabolomics study comparisons, which alleviates the constant fear of re-isolating known compounds.[1,2] The instruments can generate plethora of spectra in few hours and require the use of computational tools as manual interpretation becomes impractical.[3] Whether to access the whole scope of metabolites present in a sample or to find specific ones, mass spectrometry is suited for untargeted or targeted metabolomics studies.[2,4,5] Hyphenated analytical chemistry methods facilitate sample analysis with fast, efficient, and accurate search for compound identification.

Tactics increasing production of biomass in laboratory conditions and creating opportunities for novel discoveries are constantly being developed and improved.[6-9] For example, the development cycle of microorganisms can be controlled through variations of environmental growth conditions to optimize biosynthetic pathways to provide more resources. The analysis of these culture conditions via hyphenated techniques using mass spectrometry helps narrow down the best adequate conditions.

V.1. Relevance of hyphenated techniques in natural products drug discovery

The combination of classical analytical techniques such as IR, UV, MS and NMR spectroscopy provide information for molecular structure elucidation. Sometimes, further stereochemistry is required, and providing sufficient amount of material with luck of crystallization, X-ray crystallography analysis can be performed to solve this problem. However,

www.manaraa.com

many a time, synthetic routes must be sought to palliate the problem of available mass but is not always straightforward and feasible.[10] The tedious, challenging and time consuming classical approach of natural products research motivated the development of hyphenated spectrometric methods to deliver more efficient separation and facilitate compound isolation, identification, and biosynthetic understanding. Out of all the physical characteristics defining a compound, the mass remains the most unique and tangible one, and technological progress has made it possible for scientist to accurately observe the mass of compounds and identify it. Prior ionization of the compound, ruled by analytes polarity, is required for mass analysis. Hyphenated methods combine chromatography and mass spectroscopy. Upon successfully separating compounds using gas chromatography (GC) for volatile compounds and liquid chromatography (LC) for non-volatile ones, mass spectroscopy (MS) is applied to identify each constituent of a sample.[10,11]

Mainly used to rinse the needle injecting the sample, solvents may also be used for samples solubilization prior to injection. The minute amounts of material handled with MS techniques makes the overall usage of dissolving solvent very minimal. Thus, GC-MS is considered a solventless technique as it uses a heat gradient for separation and column elution of compounds. Additional development of techniques such as thermal desorption also referred to as headspace help in reducing solvent usage.[12,13] Once injected, the sample will move through a capillary column according to its affinity for the stationary phase and the temperature rise. The less polar gaseous samples can be introduced through electron impact ionization (EI) fragmentation or the softer chemical ionization (APCI) method.

LC-MS is best suited for polar constituents and as natural product extracts represent complex mixtures constituted of hydrophilic and lipophilic molecules. Experimental conditions involving solvent compositions, stationary phases, buffers and different ionization source need to be determined and optimized. Generally, a C18 (nonpolar) analytical column associated with

www.manaraa.com

a gradient of polar solvents (water, acetonitrile) allows the separation of the variety of compounds present in a sample. In the early 80's to early 90's, Fast Atom Bombardment (FAB)[14] allowed ionization of liquid non-volatile samples but has been phased out since by Electrospray Ionization (ESI),[15] currently, the most popular technique.

Subsequent separation, elution, and ionization, the analytes enter a mass analyzer.[16,17] Nowadays, the most used ones encompass:

- the Time-of-flight (ToF) based on the time taken by a compound to reach the detector after being accelerated in an electric field.
- the Quadrupole (Q) using oscillating electric fields to affect the paths of ions passing through a radio frequency quadrupole and acting as a mass-selective filter. Resolution and sensitivity may be enhanced when an additional magnetic field is applied.
- the Ion Trap (IT) very similar to the quadrupole mass analyzer in principle. The main difference resides in trapping the ions before ejecting them sequentially.

The goal being to determine the mass of the unknown compound to figure out a potential molecular formula to further assemble the atoms, whether used in LC-MS (ESI) or GC-MS (APCI), soft ionization is a natural products chemist best friend. It uses lower ionization energy which prevents further fragmentation of the molecule. Molecular ions are formed and detected without the burden of additional fragments that may arise from higher energy ionization being seen.

As frustrating as a classic approach can be, the suspense of not knowing where a chemical investigation is heading has a charm that is being sacrificed when using hyphenated techniques. The rapid turnover of these instruments led to the accumulation of massive metadata

www.manaraa.com

information. Turned into databases, they are useful for data mining and dereplication method to reveal early identity features, and ultimately save time through the isolation process.

In this thesis, LC-MS metabolomics has been set to target the production of the specific compound tapachulanone A from chapter 4. The use of two databases monitored the presence and unknown status of the compounds, while providing supplemental information about potential other unknown compounds.

V.2. *One Strain Many Compounds* method

The One Strain Many Compounds (OSMAC) approach simulates multiple environmental conditions on one individual strain to observe their influence on biosynthetic profiles and secondary metabolites production.[18-21]

In this manner, the production of the specific novel compound tapachulanone A, which displayed a novel tricyclic fused system and 1.4 μM antileishmanial activity, was targeted. Different environmental variations were applied to the fungal endophytic cultures to evaluate the presence of the targeted compound. A total of 526 cultures were generated on a miniature scale; temperature, light exposure, medium of culture, acidity, salinity, and culturing time were the variable parameters. The different environmental conditions created in each autoclaved medium condition were summarized as:

M – T – X – Y – Z – E

M= medium (A, B, C, D, or R), T= Temperature (23 or 30), X= Light conditions (L or D), Y= pH (6.2 or 8.4) or salinity (3.4 or 6.8), Z = amount of fungus inoculated (2, 4 or 8), E= extraction stage (E1 or E2).

www.manaraa.com

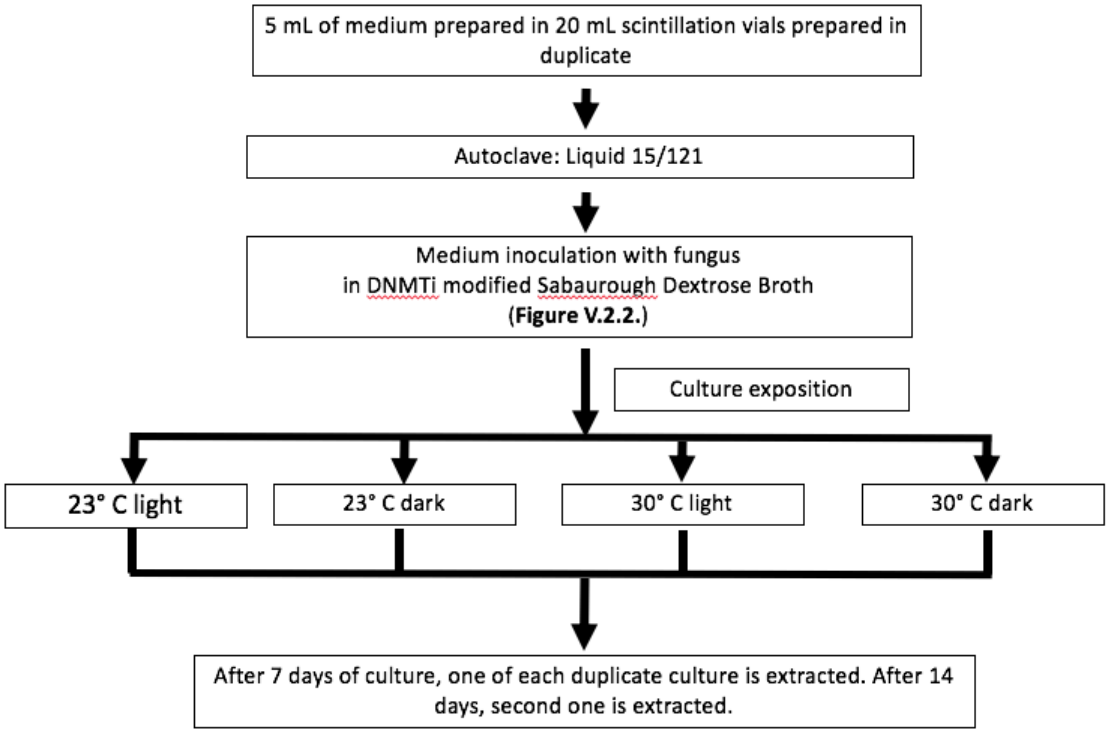

Scheme V.2.1. Scheme for one OSMAC small-scale culture.

In order to assess the influence of the medium on the production of compound of interest, five different media were tested. Rice being the original culture medium used when tapachulalone A (**13**) was isolated, was obviously one of the media studied. Four other media available in the lab were tested: actino agar glycerol (A), potato dextrose with agar (B), Sabouraud dextrose broth with agar, (C), malt broth with agar (D). Preparation of these media in different pH and salinity aqueous solutions provided additional variations. However, actual pH of the culture was not determined. The fungus TAP14-147B-3 was regrown on Sabouraud Dextrose Agar (SDA) plates and cut in small 2mm x 2mm squares upon fungal growth on 50% of the agar surface. Two, four, or eight squares were placed in 1mL DNMTi Sabouraud dextrose broth (0.024 mg/mL) to allow exposure to the epigenetic modifier. Each medium prepared in a 20 mL scintillation vial was then inoculated with one specific Eppendorf tube biomaterial to accommodate all possible options of the matrix similar to the description shown in **Table C.V.1.**

www.manaraa.com

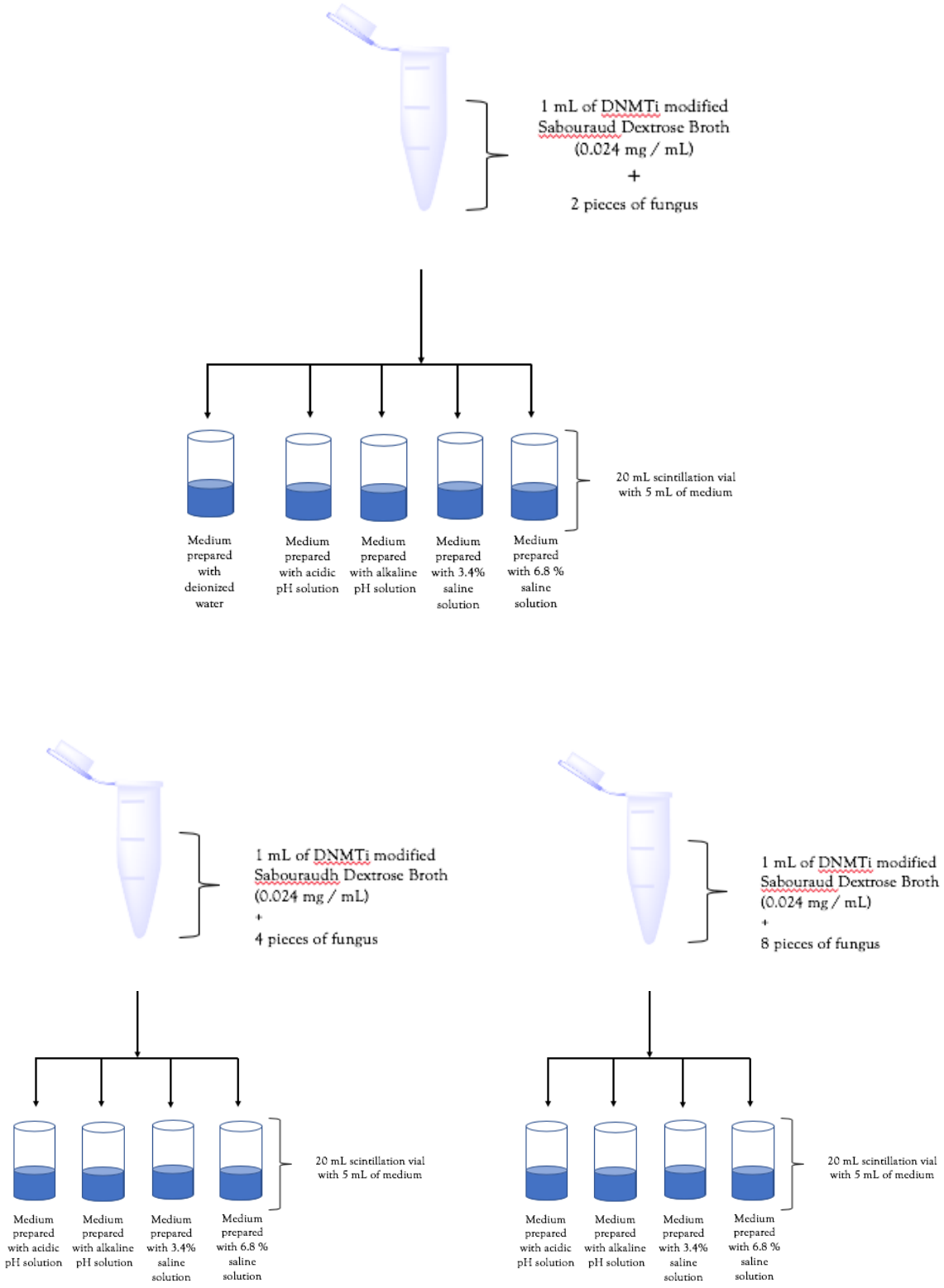

Figure V.2.1. Sequence for small-scale culture preparation for one medium, one period of culturing time, and one set of light and temperature conditions.

www.manaraa.com

The schemes presented on **Figure V.2.2.** describe the culture inoculation for one kind of medium exposed to one set of temperature and light condition. This sequence was duplicated to accommodate the time of extraction parameter. Overall, the whole procedure was reproduced for each medium in specific temperature and light conditions.

At the time of extraction (E1 or E2), 5mL of ethyl acetate was added to each small culture. The decanted crude extracts were dried down, filtered and reconstituted in LC-MS grade acetonitrile. Aliquots of 1mg/mL concentration were screened for the presence of Tapachulanone A **(13)** using liquid chromatography – tandem mass spectroscopy coupled with a quadrupole time of flight detector (LC-MS/MS-QToF) instrumentation. Samples ran on a C18 Kinetex column using a 2% to 100% of acetonitrile in water gradient over 12 minutes. The analysis of each extracts used signal intensity values at the specific retention time of tapachulanone A to assess presence of the compound of interest and culture environment trends.

V.3. Databases resources

Each generated OSMAC extract was ran on Agilent LC-MS QToF instrument. A tandem mass spectroscopy (MS/MS) was performed to facilitate subsequent dereplication. The technique consists in a two rounds of molecular ionization: the first one detects the molecular ion for each compound present in a mixture, while the second one allows further fragmentation of each compound to generate a spectral fingerprint.[22,23] Many molecules share the same mass value; however, their unique atomic arrangement will govern their fragmentation pattern and provide specific signature fragments. The first round reveals presence of compounds in the mixture and the specific retention time displayed with the method performed, while the second round reveals the signature for each compound pertaining to their identity. Ultimately, the signature from each molecule can be compared within a set of data and dereplicated for the reference signature of

www.manaraa.com

tapachulanone A (**13**). Two mass spectrometry databases were exploited to find the most efficient process producing the compound of interest.

V.3.1. Mass Hunter Software Program

Each crude's LC-MS data was initially treated with the Mass Hunter software. As samples were run, the Agilent qualitative analysis software was used to analyze their composition at the specific retention time of Tapachulanone A (**13**). Furthermore, each chromatogram was extracted for the molecular formula of the targeted compound, using the "Find compounds by formula" menu option and plugging in the chemical formula of **13** to confirm its presence. Comparison of retention time and the MS/MS signature provided the most fitted culture conditions to potentially produce Tapachulanone A (**13**) in substantial yield.

An additional screening of the extracts for known compounds was performed using compounds libraries provided PCDL-Metlin-PCDL, PCDL-Mycotoxins-PCDL, and Antimarin. On top of identified known molecules present, the novel status of **13** and other compounds could also be assessed. Another software was then used for more dereplication with public database information and metabolomic study.

V.3.2. Global Natural Products Networking (GNPS)

Sometimes, mass and retention time may be detected but with very low abundance of the compound of interest. Comparing the MS/MS fragmentation fingerprint obtained to a reference one, increases confidence of the presence of the compound.

The MS/MS files obtained through LC-MS/MS performed on QToF were surveyed using the GNPS public platform. A multi-step sequence uploading the data to the platform requires prior conversion of the Mass Hunter LC-MS/MS data to a *mzXML* format. The conversion folder is free and provided on the platform.[24] Obviously, the more files to be converted the longer the process. The 526 files handled in this experiment were converted in less than two hours. The

www.manaraa.com

quantity of converted files often requires the use of a cross platform FTP application uploading the mass spectra information via the help of a server. Once the data uploaded, metabolomics analyses may ensue using the various features offered by the GNPS platform.

A molecular network assessing the variability and resemblance of secondary metabolites produced in each culture can be created. Each MS/MS spectrum is defined by a spectrum vector based on mass and peak intensity values, and a cosine value is generated ($0 < \text{cosine value} < 1$). During the dereplication process, the vectors are compared and matched according to a cosine similarity.[254] A cosine value closer to 1, expresses converging results, hence a more accurate prediction. The threshold used for this cosine values determines the extent of molecular similarity between samples tested. For the purpose of this experiment, a 0.7 cosine value was set. The higher the threshold, the narrower connection created between molecules, and the less amount of edges will appear. The smaller threshold, the larger the tolerance for molecular connection, hence less accurate results. Additionally, a parameter requesting 6 matching peaks between unknown and known reference samples narrowed down the population of similar sample to increase accuracy. It is like classifying objects based on their features. The larger the number of features, the larger the selected population of objects. However, limiting the number of features, hence increasing the threshold value, creates greater selection to form a rather elitist group of objects.[25,26]

Not only can molecular networking from MS/MS data offer a broader view of relationships within a community of molecules, dereplication can also be performed using the available National Institute of Standards and Technology (NIST), Natural Products Atlas (NPA), and GNPS library databases for comparisons.

LC-MS/MS monitoring of the crude extracts, partition layers, and MPLC fractions guided the chemical investigation. Chromatograms were extracted for the tapachulanone A **(13)** molecular formula $C_{25}H_{32}O_6$. Moreover, perfect matching of the MS/MS fingerprint

www.manaraa.com

fragmentation patterns of the various cultures with the one of tapachulanone A (**13**) was sought and required to increase confidence about the presence of the compound of interest. Furthermore, the Mass Search Tool (MASST) provided on the GNPS platform was performed to compare the MS/MS fingerprint profile of ACDL-34 with other profiles from database.

V.4. Results and discussion

The database search with both software programs, corroborated the novelty of tapachulanone A (**13**). The Mass Hunter dereplication finding compounds using tandem mass spectroscopy databases return with no hit at the specific retention time of the compound. Furthermore, the MASST feature offered by GNPS led to the same conclusion that it is a novel compound, later used as a filter to dereplicate and screen the cultures in GNPS.

V.4.1. OSMAC cultures

When extracting the chromatograms in Mass Hunter, out of the 526 cultures, 392 cultures responded to the detection of tapachulanone A (**13**). However, further studies of the retention time, revealed on 59 cultures potentially containing the compound with 29 of them displaying an abundance, represented by the peak intensity, greater than $2x10^4$. The scheme below highlights the greatest amount of compound produced according to environmental conditions. The peak intensity reflecting the compound abundance was recorded and provided the following scheme.

www.manaraa.com

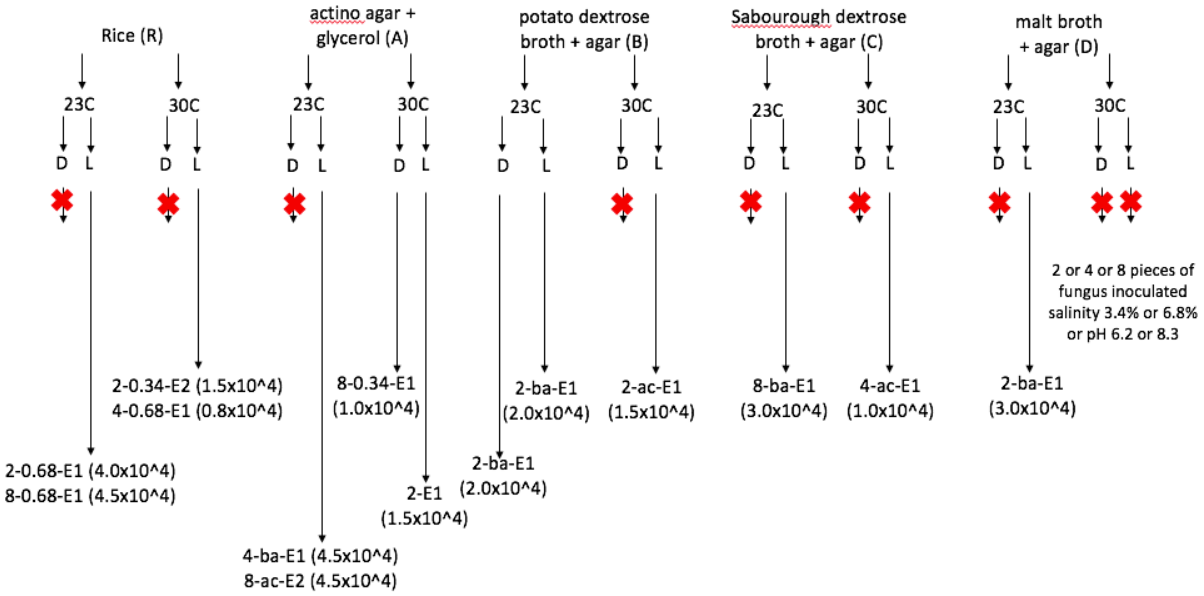

Scheme V.4.1.1. Compound abundance for tapachulanone A **(13)**, according to signal intensity recorded and reported in parenthesis, for the various culture conditions explored in the OSMAC experiment.

As the original compound arose from a neutral rice culture, further scaled up experimentations focused on the rice conditions. However, the alkaline malt broth and agar medium conditions hosting the fungal culture at room temperature with light for a week provided similar yield of the compound of interest with a molecular ion intensity of 3.0 x 10^4. From the Mass Hunter software program studies, the OSMAC experiment revealed that 6.8% salinity rice culture provided the largest abundance of tapachulanone A **(13)** with a recorded intensity (4.5 x 10^4). Two parallel culture experiments were conducted: one with neutral rice recreating the original conditions of discovery and the other with high salinity rice. However, the growth of a *Streptomyces* sp. was seen in some cultures was also detected during the OSMAC studies. Further species analysis by Sarah Kennedy in the Shaw lab, identified it as *Streptomyces azureus*. Hence, not knowing how its presence would affect the production of tapachulanone A **(13)** motivated the additional study of a co-culture in regular condition. Three kinds of scaled up cultures were

www.manaraa.com

created: pure fungal strain on high saline rice, pure fungal strain on neutral rice, and co-culture on neutral rice, and evaluated through LC-MS/MS method analysis. Upon 21 days of culture, an exhaustive extraction with ethyl actetate was performed. A defatting step was inserted using a partition of the dry crude extracts reconstituted in a 70% aqueous methanol solution against hexane. A second partition using a ethyl acetate:water (1:1) solvent system was performed on the dry aqueous fraction. Aliquots of crude, hexane and ethyl acetate fractions were studied with a LC-MS/MS QToF instrumentation. An unfortunate column damage required the samples generated with the neutral rice conditions to be run on a different column. To evaluate retention time and mass accuracy, a standard of tapachulanone A **(13)** (0.2 mg/mL) was always run prior to data acquisition. Despite overtime compound degradation giving rise to contaminants seen on the chromatogram, tapachulanone A **(13)** was still present, which made the detection of its molecular ion possible and serve as a standard.

V.4.2. Rice cultures in regular conditions

The extracts of the pure fungal strain culture in regular conditions was unfortunately unsuccessful. Both Mass Hunter and GNPS did not detect the presence of the compound of interest tapachulanone A **(13)**. Each of the three days of extraction generated a crude extract which was kept separate and screened by LC-MS/MS. A solution of tapachulanone A **(13)** (0.2 mg/mL) in acetonitrile was run as standard to compare retention time and presence of the compound of interest. Compound dereplication for the mass of tapachulanone A **(13)** happened in the case of day 1 and 2 crude extracts. **(Figure V.4.2.1.** and **Figure V.4.2.2.)** Comparison of retention time, molecular ion, and MS/MS fragmentation pattern between the crude extract (black) with a standard sample of tapachulanone A **(13)** (pink) did not provide any match. The retention time differs by a minute, and the molecular ion recorded provides a molecular ion different by at least 10 amu. Finally, even while performed in the same experimental condition,

www.manaraa.com

the fragmentation pattern recorded for the crude extract provided a M+K value not reciprocated with the tapachulanone A **(13)** standard solution, showing instead a M+Na value.

Figure V.4.2.1. MS/MS spectra for day 1 crude extract (black) prepared from pure strain neutral culture and standard solution of tapachulanone A **(13)** (pink).

In a similar fashion, the crude extracts from the second and third days of extraction were analyzed. While the second day crude extract **(Figure V.4.2.2.)** provided a hit, the extract from the third day did not. However, the MS/MS signature of the hit compound did not replicate with the one from the standard. Moreover, the retention time of the hit compound does not match the standard. The presence of tapachulanone A **(13)** may have been detected but buried in the baseline and the investigation of the neutral rice culture was not worth pursuing.

www.manaraa.com

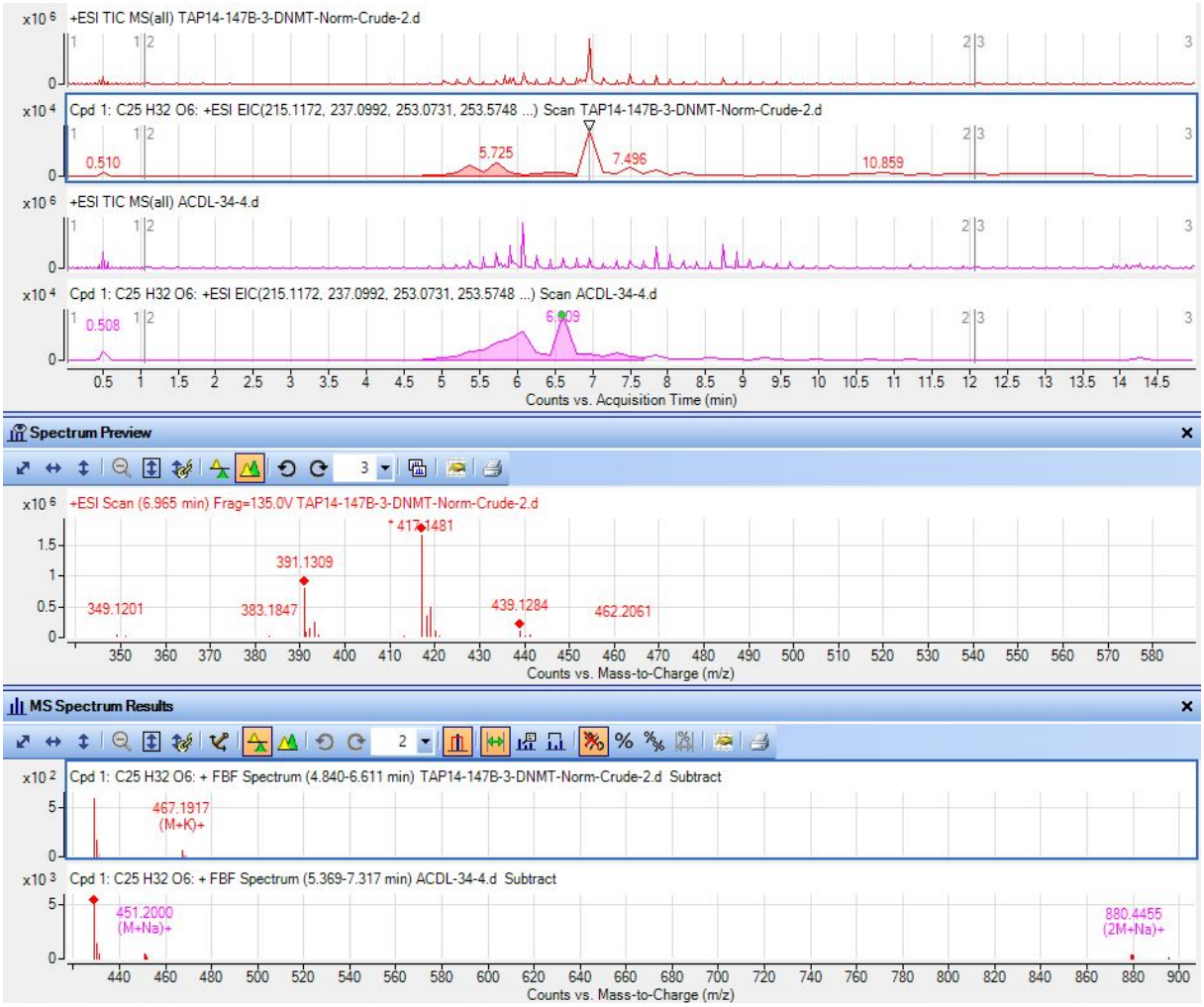

Figure V.4.2.2. MS/MS spectra for day 2 crude extract (red) prepared from pure strain neutral culture and standard solution of tapachulanone A **(13)** (pink).

The same approach was used to study the three crude extracts generated from the neutral co-culture conditions. The third day extract **(Figure V.4.2.3.)** is the only one providing a hit when dereplicated for the mass $[M+H]^+$ 429.2273. However, when analyzed, the extracted chromatogram revealed a different compound mass. The mass of Tapachulanone A **(13)** may be detected but remains buried in the spectrum baseline. The compound abundance is not significant to provide a matching fragmentation pattern.

www.manaraa.com

Figure V.4.2.3. MS/MS spectra for day 3 crude extract (black) prepared from co-culture and standard solution of tapachulanone A **(13)** (pink).

But, once again, retention time and MS/MS signature did not match the standard results. The GNPS software confirmed the trend observed. When dereplicating for the precursor ion of tapachulanone A, the only samples providing match are the standard solutions themselves. Although the hexane fraction obtained from crude liquid partition is found right below, the difference in mass accuracy does not support the possibility to find tapachulanone A in that fraction. Also, even if two different columns were used throughout the experiments, the retention times from the studied extract and the standard do not match either.

www.manaraa.com

ClusterIdx	Spec Family	AnnotatetoGNPS	AddtoChallenge	NumSpectra	NumFiles	PrecursorMZ	PrecursorInt	RTMean	AllGroups
						429 ~			
Cluster - 742		AnnotatetoGNPS	AddtoChallenge	2	1	429.22700	140034.00000	398.519	ACDL-34-4,SAMPLE
Cluster - 743	View Network	AnnotatetoGNPS	AddtoChallenge	9	2	429.22900	10563800.00000	575.7807777777778	ACDL-34,ACDL-34-4,SAMPLE
Cluster - 744	View Network	AnnotatetoGNPS	AddtoChallenge	15	1	429.22900	15984300.00000	596.5036	ACDL-34,SAMPLE
Cluster - 746	View Network	AnnotatetoGNPS	AddtoChallenge	4	2	429.33600	879778.00000	627.155	TAP14-Co-DNMT-hex3,SAMPLE,TAP14-Co-DNMT-hex1
Cluster - 747	View Network	AnnotatetoGNPS	AddtoChallenge	9	5	432.20400	1781470.00000	638.1745555555556	TAP14-Co-DNMT-hex3,SAMPLE,TAP14-Co-DNMT-crude2,TAP14-Co-DNMT-hex1,TAP14-Co-DNMT-hex2,TAP14-Co-DNMT-etoac1
Cluster - 749		AnnotatetoGNPS	AddtoChallenge	3	2	429.37300	97044.10000	789.486	SAMPLE,TAP14-Co-DNMT-crude2,TAP14-Co-DNMT-hex2
Cluster - 751		AnnotatetoGNPS	AddtoChallenge	2	2	430.32800	26895.10000	887.71	TAP14-Co-DNMT-hex3,SAMPLE,TAP14-Co-DNMT-crude3
Cluster - 752		AnnotatetoGNPS	AddtoChallenge	4	3	430.66700	41411.50000	891.1202499999999	TAP14-Co-DNMT-hex3,SAMPLE,TAP14-Co-DNMT-hex2,TAP14-Co-DNMT-crude3
Cluster - 753		AnnotatetoGNPS	AddtoChallenge	12	5	431.24300	2515020.00000	494.4891666666667	TAP14-Co-DNMT-etoac3,SAMPLE,TAP14-Co-DNMT-crude1,TAP14-Co-DNMT-etoac2,TAP14-Co-DNMT-crude3,TAP14-Co-DNMT-etoac1

Figure V.4.2.4. GNPS metabolomics MS/MS clusters with IDs for a precursor ion (m/z 429 amu) in the range of tapachulanone A (**13**).

V.4.3. Rice culture in saline condition

The attempt to yield tapachulanone A (**13**) in high saline conditions also failed. Again, the main detected compound with similar mass does not match the standard retention time and MS/MS signature parameters. The GNPS analysis corroborated all of these results and provided a list of all the known and unknown compounds detected in each tested sample. Sorting through all the choices by filtering the results for the molecular ion mass of tapachulanone A (**13**). Simultaneously, mass dereplication and presence of the compound happens and is reported in the chart below.

www.manaraa.com

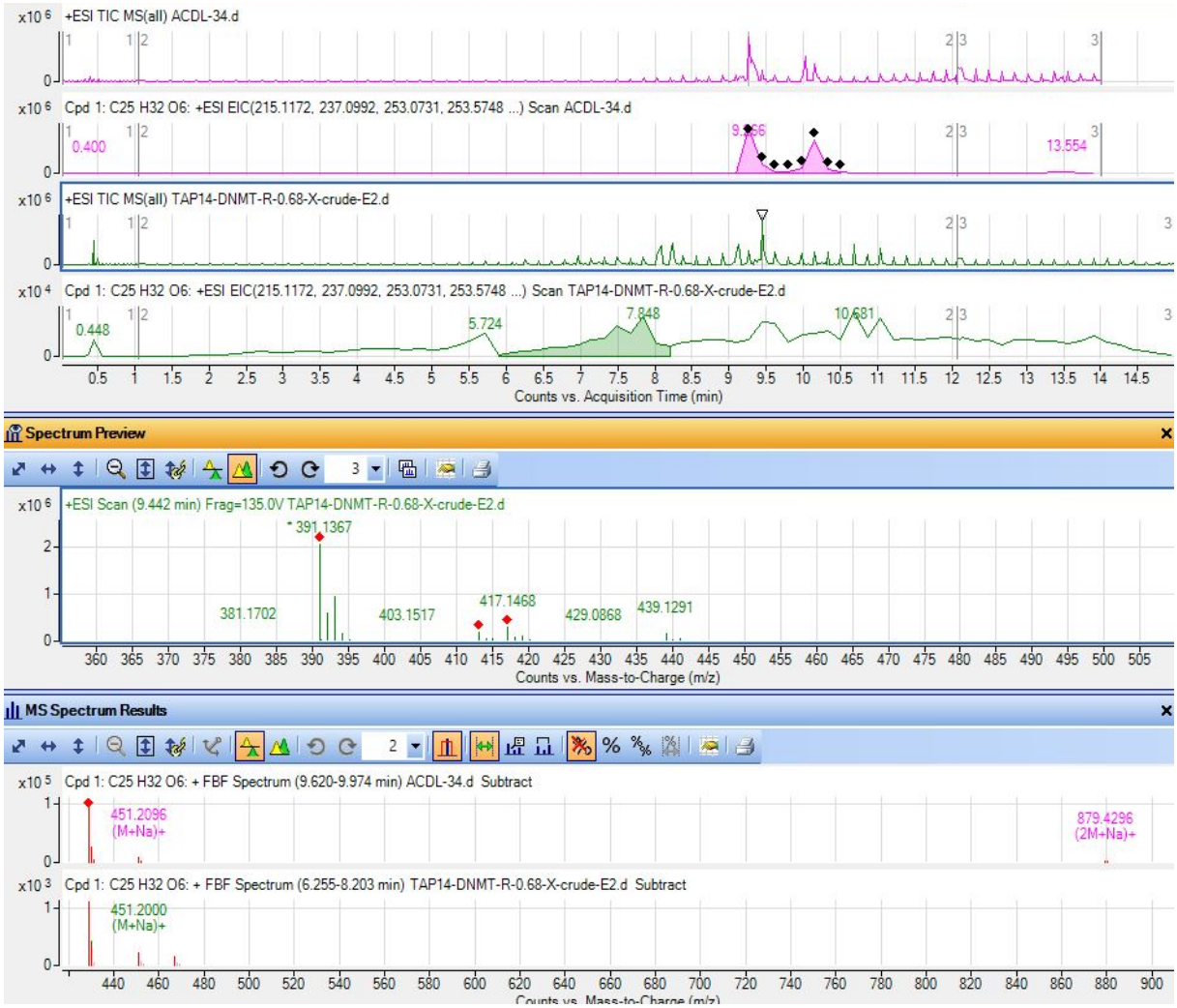

Figure V.4.3.1. MS/MS crude extract (red) prepared from saline culture and standard solution of tapachulanone A (**13**) (pink).

ClusterIdx	Spec Family	AnnotatetoGNPS	AddtoChallenge	NumSpectra	NumFiles	PrecursorMZ	PrecursorInt	RTMean	AllGroups
						429			
Cluster - 982	View Network	AnnotatetoGNPS	AddtoChallenge	15	1	429.22900	15984300.00000	596.5036	SAMPLE,ACDL-34
Cluster - 983	View Network	AnnotatetoGNPS	AddtoChallenge	8	1	429.22900	10499600.00000	597.75	SAMPLE,ACDL-34
Cluster - 986		AnnotatetoGNPS	AddtoChallenge	2	1	431.24400	148311.00000	454.6055	SAMPLE,TAP14-DNMT-R-0.68-X-Hex
Cluster - 988		AnnotatetoGNPS	AddtoChallenge	12	6	431.28000	1509970.00000	506.88991666666664	TAP14-DNMT-R-X-crude,TAP14-DNMT-R-0.68-X-crude-E1,TAP14-DNMT-R-0.68-X-crude-E2,SAMPLE,TAP14-DNMT-R-0.68-X-Hex,TAP14-DNMT-R-0.68-X-EtOAc

Figure V.4.3.2. GNPS metabolomics MS/MS clusters with IDs for saline culture and a precursor ion (m/z 429).

www.manaraa.com

Once again, the dereplication results worked for the standard sample itself. Additionally, various known compounds not affiliated to tapachulanone A **(13)** were found through Mass Hunter dereplication. The GNPS analysis corroborated all of these results and offered additional hits. Amongst the known compounds, isochromophilones VI **(14)** and IX **(15)** were found in fraction K, while the related compound (R)-5-chloro-3-((S,1E,3E)-3,5-dimethylhepta-1,3-dien-1-yl)-7-methyl-6,8-dioxo-7,8-dihydro-6H-isochromen-7-yl acetate **(16)** was found spread between fractions B, C, and D.

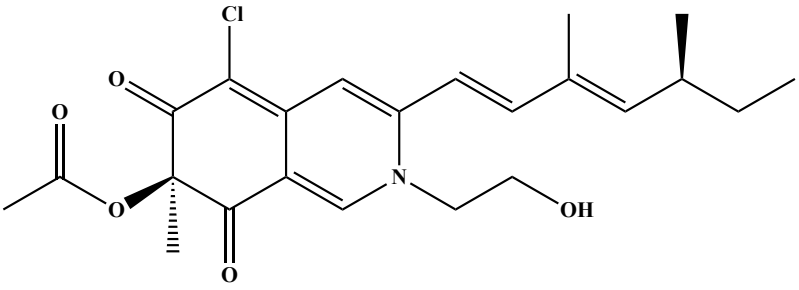

14

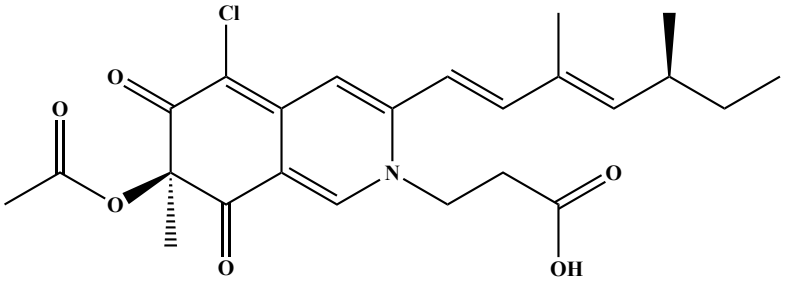

15

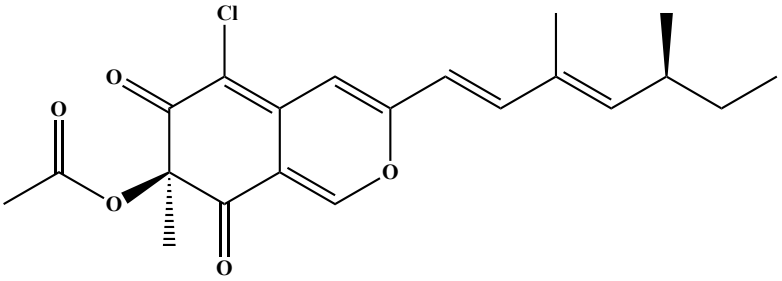

16

www.manaraa.com

Despite the disappointment experienced through this experiment, proton NMR screening of fractions D through H displayed some similar chemical shifts to the ones of the targeted tapachulanone A (**13**). However, the lack of the characteristic ^{1}H NMR olefinic signal at δ_H 5.15 ppm was enough to conclude the absence of tapachulanone A (**13**). Through dereplication compound **17** from the ethyl acetate fraction and present in substantial amount came back unknown and motivated further investigation and purification. A normal phase MPLC separation of the ethyl acetate extract (m = 5.3 g) provided fractions A through R.

Further LC-MS analysis revealed fractions E and G containing the potential novel compound. Normal phase HPLC using an hexanes:ethyl acetate(1:1) solvent system, and subsequent rounds of reverse HPLC with a methanol:water system 65% to 100% over 25 minutes yielded pure fractions of tapachulanone B (**17**) from fractions D, E and G, providing a total mass of 8 mg.

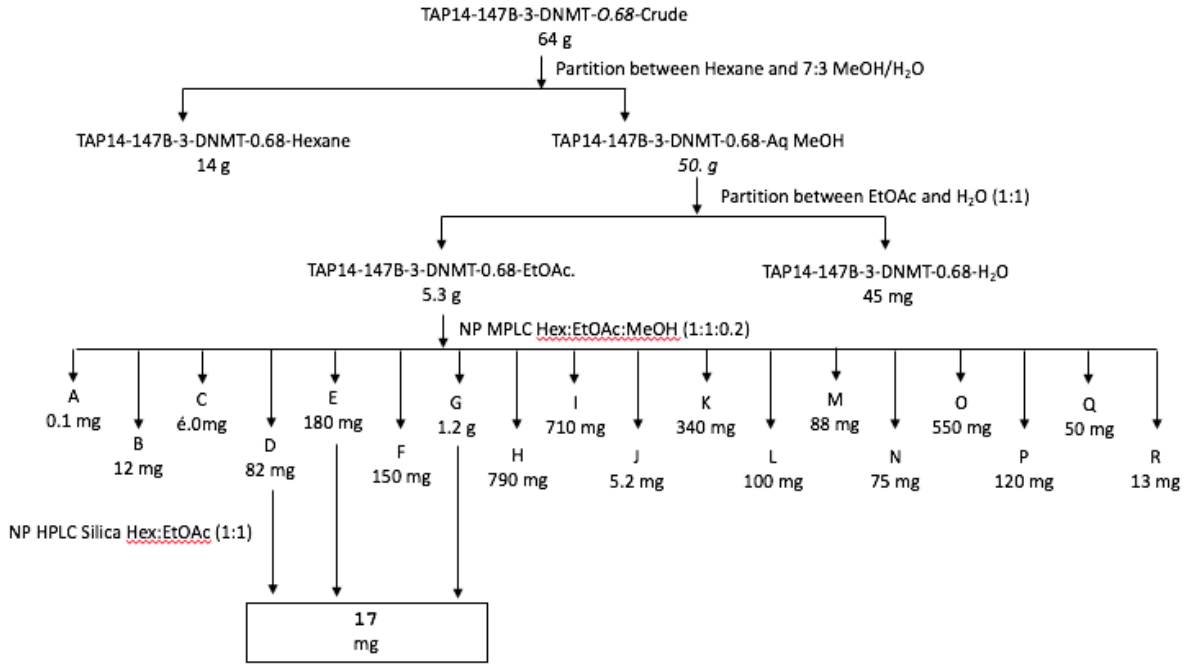

Scheme V.4.3.1. Fractionation Scheme of crude extract obtained from *Penicillium guanacastense* DNMT epigenetically modified culture on 6.8% saline rice medium.

www.manaraa.com

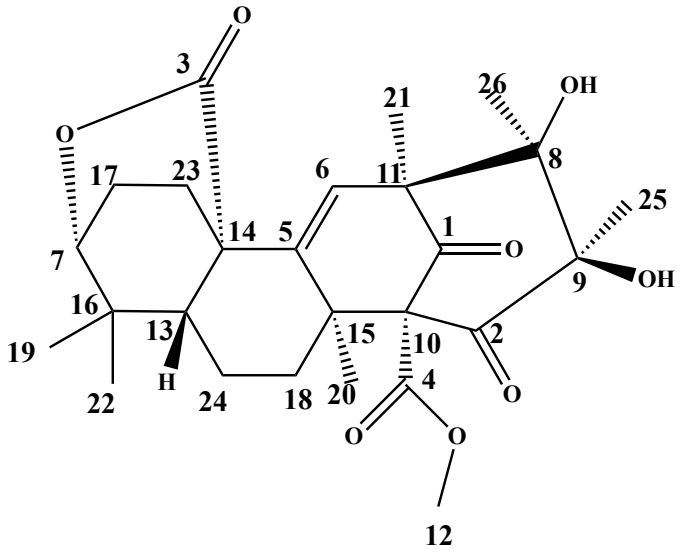

17

The HRESIMS value $[M + H]^+$: m/z 475.2338, calcd. for $C_{26}H_{34}O_8H$, m/z 475.2326, provided the molecular formula $C_{26}H_{34}O_8$ for **17**, implying the presence of 10 degrees of unsaturation.

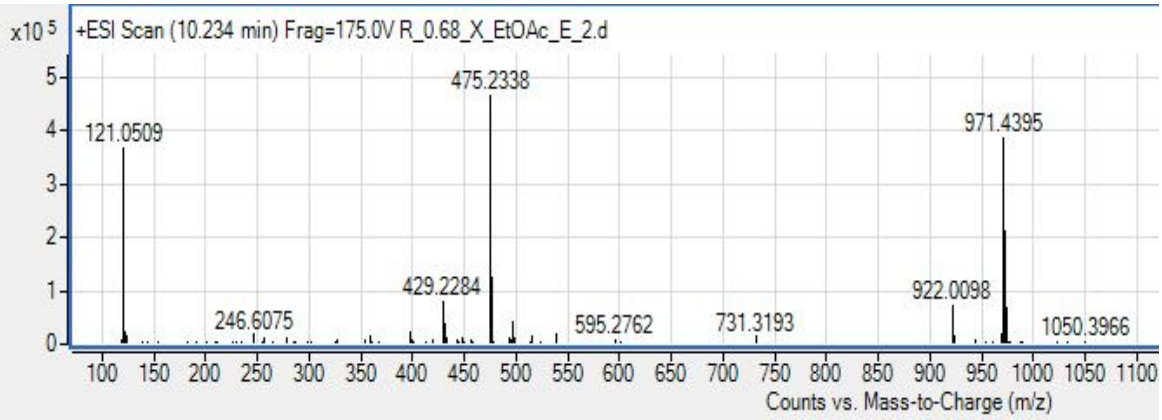

Figure V.4.3.3. MS for compound **17**.

Depicting eight distinct singlets and six multiplets, the proton NMR spectra patterns hinted scaffold similarities with Tapachulanone A (**13**).

www.manaraa.com

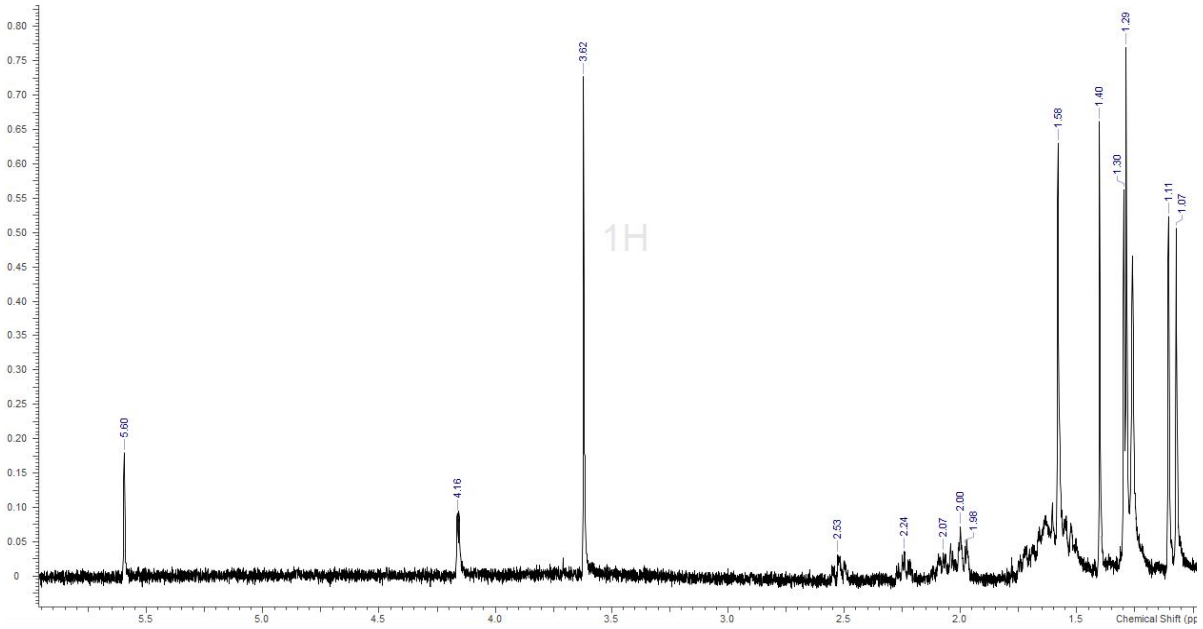

Figure V.4.3.4. ^{1}H NMR spectrum of compound **17** in $CDCl_3$ (500 MHz)**.**

The carbon spectrum presented twenty-six chemical shift signals, of which, five quaternary ones were found above 100 ppm: two ketones C-1 (δ_C 202.7) and C-2 (δ_C 202.5), two ester-like carbonyl carbons C-3 (δ_C 175.8) and C-4 (δ_C 167.5) and an olefinic carbon C-5 (δ_C 143.1).

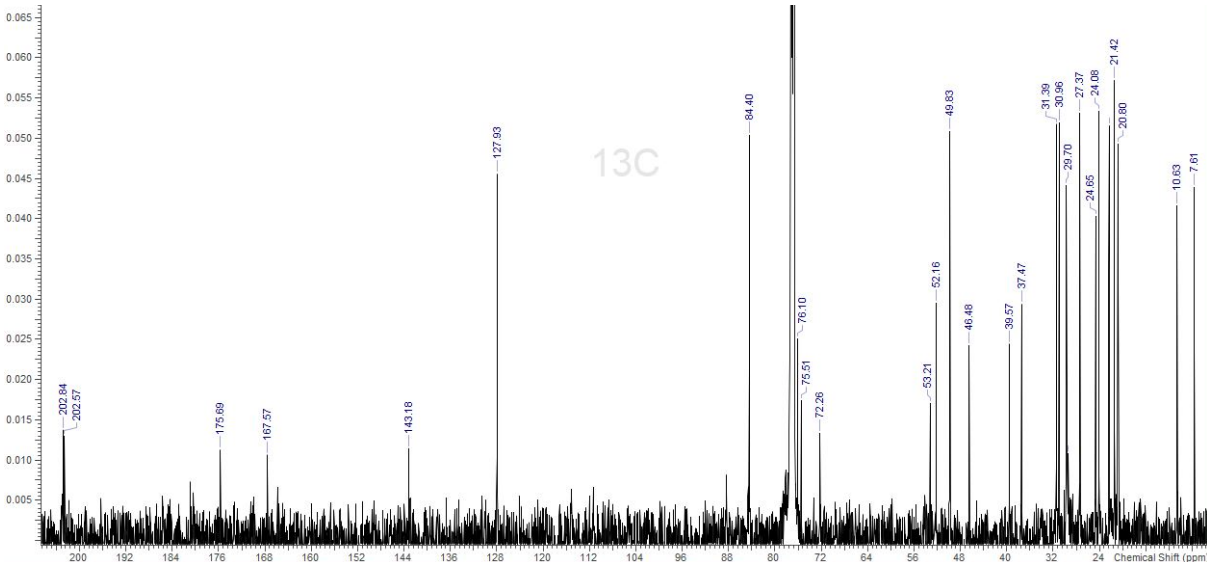

Figure V.4.3.5. ^{13}C NMR spectrum for compound **17** in $CDCl_3$ (125 MHz).

Three tertiary ones with C-6 (δ_C 127.9), C-7 (δ_C 84.4), and C-13 (δ_C 49.8) appearing on HSQC to be connected to the respective protons at 5.57, 4.14, and 1.57 ppm. The HMBC confirmed

www.manaraa.com

correlation of the olefinic proton on C-6 with C-5, as well as four additional correlations to three other quaternary carbons: C-11 (δ_C 53.1), C-14 (δ_C 46.4), and C-15 (δ_C 39.5). A final correlation was recorded with methyl substituent C-21 (δ_C 24.0) also establishing two-bond correlation with C-11 versus three bond correlation with C-1, C-6, C-8 (δ_C 76.0). The proton on C-7 correlated to C-3, C-13 (δ_C 49.8), C-17 (δ_C 84.4), and C-22 (δ_C 84.4) uncovering a connectivity pattern with an oxygen to form a δ-lactone, previously encountered in tapachulanone A (**13**). Reciprocally, two methyl groups linked to C-19 (δ_C 27.3) and C-22 (δ_C 22.3) exhibit three bond correlations with C-7 along with C-13 and each other, hinting a gem dimethyl pattern confirmed by the two-bond correlation with quaternary C-16 (δ_C 37.4). The methylene on C-17 confirmed two-bond correlation with C-7 but also, longer range ones with C-16 and C-5 through a "W" coupling effect.

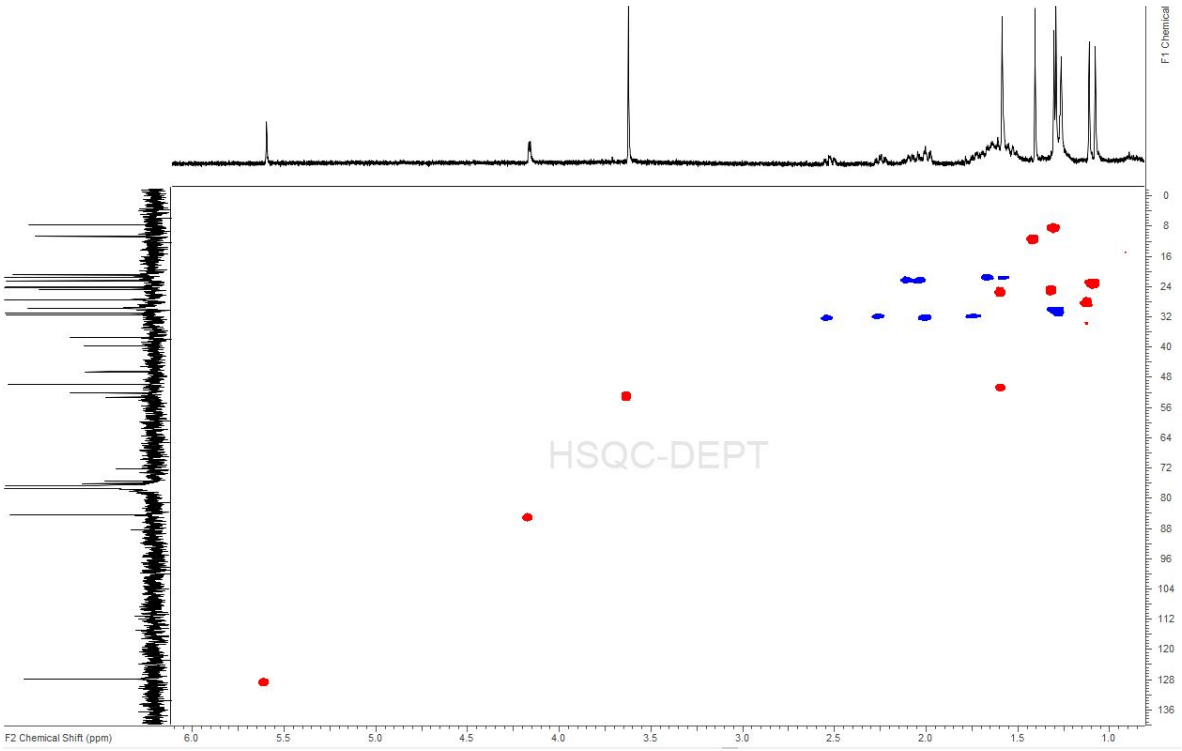

Figure V.4.3.6. HSQC NMR spectrum of compound **17** in $CDCl_3$ (500 MHz).

www.manaraa.com

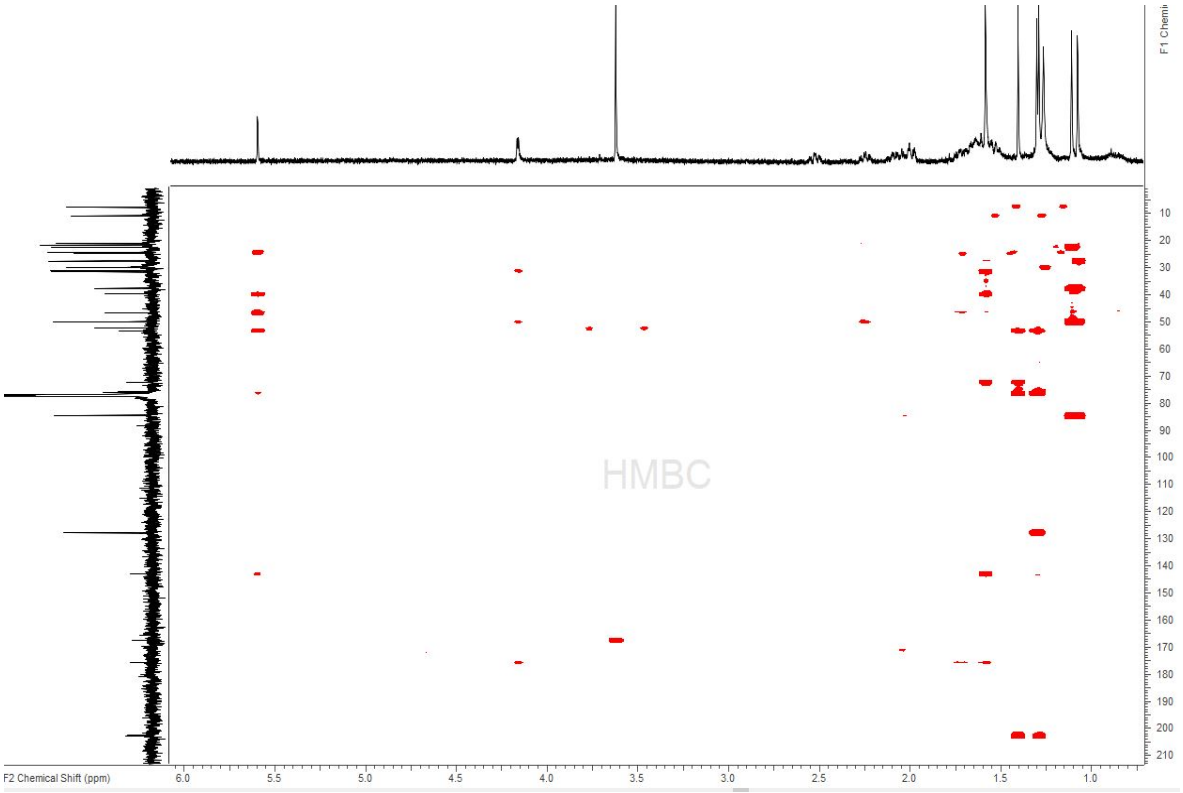

Figure V.4.3.7. HMBC NMR spectrum of compound **17** in $CDCl_3$ (500 MHz).

Also correlating with C-7 is methylene on C-23 (δ_C 21.4); longer-range correlation is observed with C-6 while two-bond correlation is seen with C-17 and supported by COSY correlation to establish the adjacency of both C-17 and C-23. The methine on C-13 confirmed correlation with quaternary C-3 and C-4, which allows completion of the bicyclic system formed by the δ-lactone bridging over a cyclohexane.

NOESY correlation between the hydrogens on C-7 and C-13 helped settle the forward out of plane stereochemistry of both methine. Two other methylene groups at C-24 (δ_C 20.7) and C-18 (δ_C 30.9) displayed COSY correlation making them direct neighbors. Additional HMBC three-bond correlations were seen with C-3 and C-14 for the C-24 methylene, with C-13 and C-14 for the C-18 methylene. However, C-20 methyl also correlated with C-18, as well as C-5, C-10, and C-15. A correlation between C-20 and C-24, was not recorded on HMBC but was definitely seen on NOESY two-dimensional spectrum.

www.manaraa.com

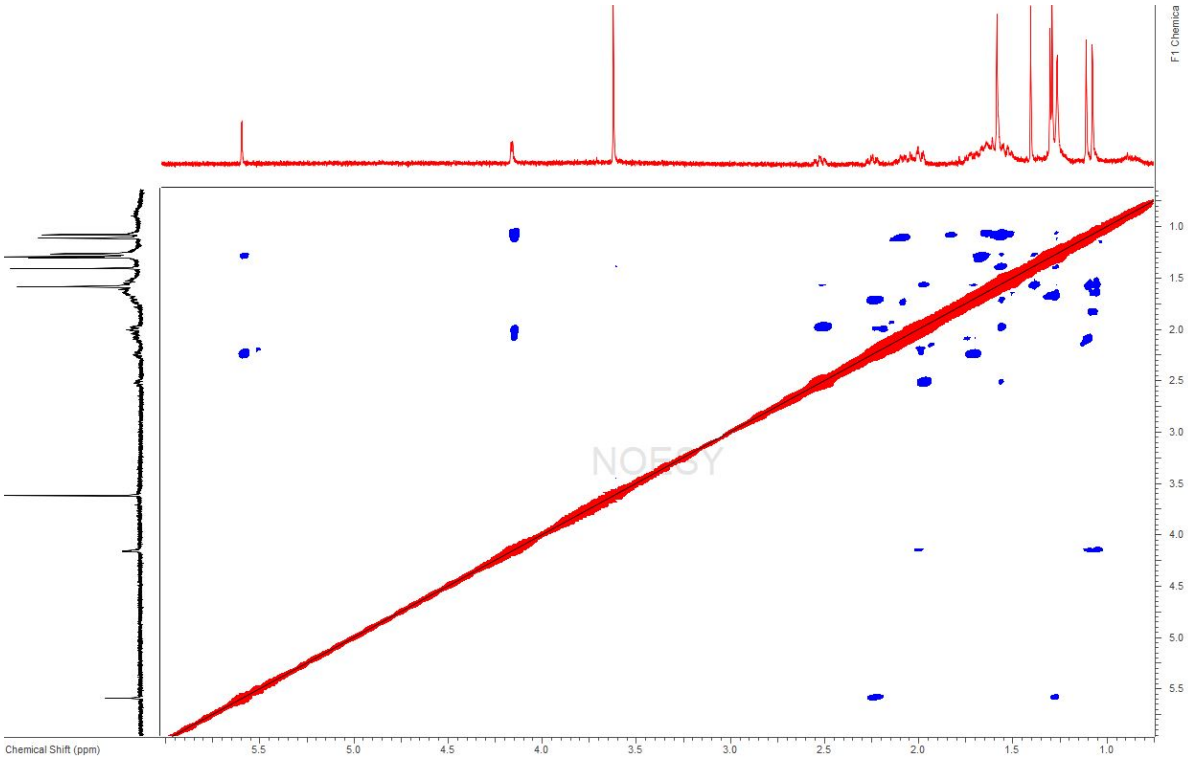

Figure V.4.3.8 NOESY NMR spectrum of compound **17** in $CDCl_3$ (500 MHz).

These connections complete the third cyclohexane ring constituting the molecule. With three rings, a lactone, an olefin and three rings described, five more degrees of unsaturation remain. The striking methyl proton signal at 3.61 ppm related to C-12 (δ_C 27.3) is indicative of a methoxy group. Indeed, HMBC revealed it to be connected to C-4 only which supports the presence of an ester function. Three degrees of unsaturation remain with two accounting for two ketones. Methyl groups on C-25 (δ_C 10.6) and C-26 (δ_C 7.5) respectively correlate to ketone on C-2 and C-1. Additionally, C-25 methyl protons establish long range HMBC correlation with C-8, C-10, C-11, and C-26, while C-26 methyl protons correlate with C-6, C-9, C-11, and C-25. Compared to C-9, C-8 displays a higher chemical shift. This may be resulting from the ß position it occupies away from both ketone functional groups, hence the stronger deshielding effect, also experienced by the olefinic proton, in ß position of the C-1 ketone. Furthermore, each methyl substituent communicates with a specific ketone, but do interact with each other through long-range correlation. Finally, the chemical shifts of carbon atoms placed at ring junctions tend range from

www.manaraa.com

30 up to 60 ppm. In the case of C-10, the higher chemical shift observed can be explained by the triple carbonyl surrounding the atom, caging him into a greater deshielding effect. NOESY correlations, confirmed the relative stereochemistry for the methyl groups on C-7, C-13, C-20, C-21, C-25, and C-26.

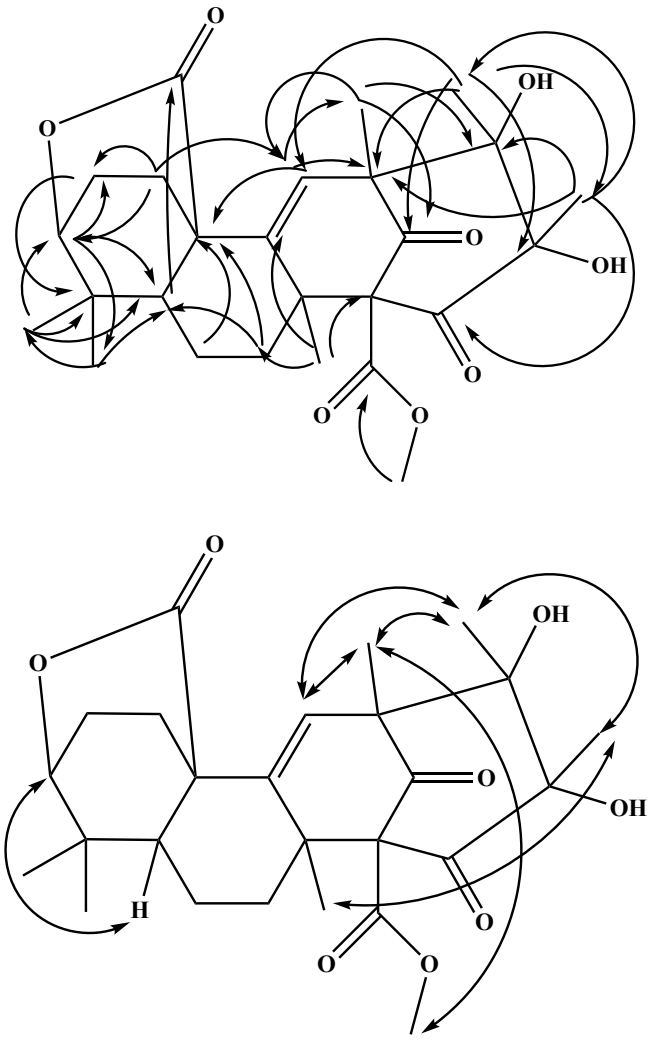

Figure V.4.3.9. Key HMBC (⌒) and NOESY (⌒) correlations establishing the structure of compound **17**.

www.manaraa.com

Table V.4.3. ^{13}C and ^{1}H NMR Data for novel sesterterpene **(17).**

Position	δC[a]	δH[b], int.(J in Hz)
1	202.7	
2	202.5	
3	175.8	
4	167.5	
5	143.1	
6	127.9	5.57, 1H
7	84.4	4.14, 1H
8	76.0	
9	75.5	
10	72.2	
11	53.1	
12	52.1	3.61, 3H
13	49.8	1.57, 1H
14	46.4	
15	39.5	
16	37.4	
17	31.3	2.50 and 1.98, 2H
18	30.9	2.22 and 1.72, 2H
19	27.3	1.09, 3H
20	24.6	1.55, 3H
21	24.0	1.28, 3H
22	22.3	1.05, 3H
23	21.4	2.12 and 2.01, 2H
24	20.7	1.65 and 1.55, 2H
25	10.6	1.38, 3H
26	7.5	1.26, 3H

[a] ^{13}C shift values recorded in $CDCl_3$ at 125 MHz, reported in ppm. [b] ^{1}H NMR spectrum shift and integration recorded in $CDCl_3$ at 500 MHz, reported in ppm.

The bioactivity of compound **17** against the *Leishmania donovani* parasite remains to be tested.

V.5. Moving Forward...

After nine attempts, failure to optimize rice cultures for the production of tapachulanone A **(13)** indicates that alternative strategies are required.

www.manaraa.com

The experimental laboratory bench procedures may certainly require some updates and modifications. One of them would be to monitor the crude extract composition over 21 days to track the optimal time for the formation of the compound. A small scaled experiment growing the endophyte on rice in regular control condition, would generate 21 crude extracts to be further screened with LC-MS/MS method. These results should assess whether to move further with scaled up conditions.

Additionally, the pool of information provided by the OSMAC study offers other media options worth exploring. In a similar small scaled fashion, the optimal culture can be spotted, and guide further scale up development. Also, for time efficiency, accuracy, and reliability, the assistance of the analytical LC-MS/MS instrumentation, software programs, and databases ought to be included.

Compound **17** shows many resemblances to tapachulanone A (**13**). However, shared edges within the molecular network were not found. Therefore, deeper understanding of the biosynthetic pathway is more than necessary. The goal to attain more production of tapachulanone A (**13**) was not achieved, but the results do not refute the production in the co-culture conditions and require optimization. A collaborative approach must be outlined in the quest to harness the production of tapachulanone A (**13**) using synthetic chemistry, biology along with the metabolomics studies. Being aware of epigenetic phenomena constantly happening and evolving, the potential for gene mutation cannot be omitted. That is why the future acquisition of genetic profile for both endophytic species involved, will provide tangible biosynthetic gene clusters to rely on and perhaps a deeper understanding of the production of tapachulanone A (**13**). Afterall, the compound has not been found again yet, but a novel compound, potentially related, was serendipitously found in the process, and there is always room for even more bioactive chemistry to be isolated. Epigenetically modified endophytic cultures have proven once

www.manaraa.com

more successful in providing chemical novelty, and that is why they will continue to drive drug discovery. Also, biological activities assessments against the *Leishmania donovani* parasite remain to be conducted.

V.6. Experimental

V.6.1. General Procedures

Normal phase Medium Pressure Liquid Chromatography (MPLC) separations were conducted using a Teledyne CombiFlash Rf200i fitted with UV and ELS detection. A RediSepRf silica column was used for each extract separation and was chosen so the loaded sample mass did not exceed half of the maximum theoretical mass allowed on the column. For HPLC separation, all solvents were obtained from Fisher Scientific and were HPLC grade (>99% purity) unless otherwise stated. All HPLC analysis were performed on a Shimadzu LC20-AT system equipped with either an evaporative light scattering detector (ELSD) ELSD II and/or a SPD-M20A UV-Vis detector. For normal phase separation, analytical [Phenomenex Luna Silica (250 x 4.6 mm, 5 µm)], semi-preparative [Phenomenex Luna Silica (250 x 10 mm, 5 µm)], or preparative [Phenomenex Luna Silica (250 x 21.2 mm, 5 µm)] were used, while reverse phase separation employed analytical [YMC packed C-18, A-304-10, S-10 ,120Å ODS], or preparative [YMC packed CN SH-543-10P, S-10P, µm, 12 nm, 250 x 20 mm, 120Å ODS] columns. All NMR spectra were acquired in $CDCl_3$ with residual solvent referenced as an internal standard (7.26 ppm). All ^{1}H NMR spectra were recorded on a Varian 500 MHz Direct Drive instrument and ^{13}C NMR spectra were recorded at 125 MHz. Analytical LC/MS was performed on a Phenomenex Kinetex C18 column (50 x 2.1 mm, 2.6 µm) on an Agilent 6230 LC/TOF-MS with electrospray ionization detection. Optical rotations were measured on a Rudolph Research Analytical AUTOPOL IV digital polarimeter.

www.manaraa.com

V.6.2. OSMAC analysis

The influence of various parameters on the production of tapachulanone A (**13**) was assessed testing different culture conditions. Large stock of 1 L of media were prepared of which 5 mL of media were dispensed in 20 mL scintillation vials then autoclaved at liquid 15/121. Media were prepared according to the following proportions:

- Medium A: 2.2 g of actino agar + 0.4 mL of glycerol in 100 mL of deionized water, or acidic buffer, or alkaline buffer, or 3.4% saline or 6.8% saline.
- Medium B: 1.2 g of potato dextrose broth + 1.5 g of agar in 100 mL of deionized water, or acidic buffer, or alkaline buffer, or 3.4% saline or 6.8% saline.
- Medium C: 3.0 g of Sabouraud dextrose broth + 1.5 g of agar in 100 mL of deionized water, or acidic buffer, or alkaline buffer, or 3.4% saline or 6.8% saline.
- Medium D: 1.5 g of malt broth + 1.5 g of agar in 100 mL of deionized water, or acidic buffer, or alkaline buffer, or 3.4% saline or 6.8% saline.
- Medium R: 3g of brown rice in agar in 100 mL of deionized water, or acidic buffer, or alkaline buffer, or 3.4% saline or 6.8% saline.

Each set of culture was duplicated and repeated for each environmental conditions of growth.

Two buffers acidic MES (pH= 6.2) and alkaline Tris (pH= 8.4) were prepared at 5 µM concentration to infuse the culture media. When stated as provided neutral control conditions, deionized water was used to prepare the medium.

Saline solution mimicking the average 3.4% salinity of the ocean found in the tropical mangrove regions, was accurately prepared using a one-liter volumetric flask. One liter of deionized water was used to dissolve 34g of sodium chloride salt (NaCl). Another solution with double level of salinity (6.8%) was prepared in a similar fashion using 68g of NaCl salt. Miniature

www.manaraa.com

size in 20mL scintillation vials were used to prepare each culture condition medium and autoclaved.

To evaluate the influence of time factor on culture production, two moments of extraction were set. The first extraction (E1) happened seven days after the inoculation process, while the second one (E2) happened fourteen days after inoculation.

Two temperature conditions were experimented: 23°C corresponding to the laboratory room temperature and 30°C created with incubator. To isolate and protect the cultures from outside contamination and environmental fluctuations, the cultures were kept at 23°C in a biological hood with a constant running air flow.

The light exposure was simulated using artificial light conditions being turned on or off in the biological hood, or the darkness of the incubator at 30°C. The dark conditions at 23°C were simulated covering the biohood sash with opaque paper to shield the light, while heated water baths helped the incubation of the cultures in biohood with light.

A DNMTi modified Sabouraud Dextrose Broth (0.024 mg/mL) was prepared and dispensed (1 mL) in Eppendorf tubes. The pieces of diced fungus (2, 4, or 8 as shown on **Figure V.2.1.**) were added to the solution, and then poured over the medium. After seven days of cultures, a set of 13 vials for each medium was extracted overnight with ethyl acetate. The second set of remaining 13 vials stayed untouched and grew for an additional 7-day period and were extracted after. The whole experiment provided for each medium two sets of extracts at two time periods: E1 at 7 days and E2 at 14 days. Cultures where Tapachulanone A (**13**) was found, are listed according to decreasing abundance. (See Appendix C **Table C.V.1.**).

V.6.3. LC-MS/MS chromatography

The crude extracts were dried and then reconstituted in LC-MS grade acetonitrile and filtered through a Phenomenex PTFE membrane filter (0.25 µm), to prepare samples at a

www.manaraa.com

concentration of 1 mg/mL in the same solvent system for analysis. A standard sample of the compound of interest tapachulanone A **(13)** was also prepared at 0.2 mg/mL. Each sample was run on Agilent LC-MS/MS QToF using electrospray (ESI). Standard reverse phase liquid chromatography was performed using an elution gradient H_2O:ACN using a Phenomenex® Kinetex® C-18 column (150 x 3 mm, 2.6 µm, 100Å). All samples were analyzed with injection volumes of 10 µL. The instrument parameters are reported in Appendix C **Figure C.V.3., Figure C.V.4., Figure C.V.5.,** and **Figure C.V.6.**

V.6.4. Scaled up cultures

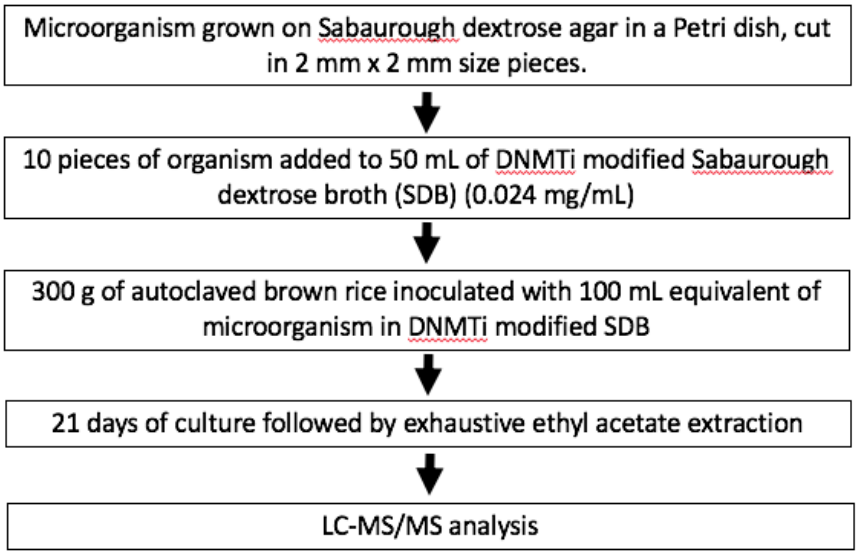

Scheme V.6.4. Scheme for scaled up cultures process.

Three bags of culture containing 300 g of autoclaved rice were prepared for each culture. Depending on the experimental environment (neutral or saline), 500 mL of the adequate water solution was used for the autoclaving process. Then, 20 pieces (2 mm x 2 mm) of fungus in 100 mL of DNMTi modified SDA (0.024 mg/mL) were inoculated per pure fungal strain culture bag, while 10 pieces of the *Penicillium* sp. and 10 pieces (2 mm x 2 mm) of the *Streptomyces* sp. in 100 mL of DNMTi modified Sabouraud dextrose agar (SDA) were prepared for the co-culture. An

www.manaraa.com

exhaustive ethyl acetate extraction allowed the fungal culture to seat overnight and filtered to obtain a crude extract. The procedure was repeated two subsequent times. The crude extracts obtained from each filtration was dried down and reconstitutes using a 70% aqueous methanol solution. A partition with hexanes was then applied. Both parts were dried down. The dried material from the aqueous part was reconstitutes in water and partitioned using ethyl acetate. Upon solvent evaporation, the ethyl acetate extract was separated on normal phase MPLC using a Teledyne CombiFlash fitted with UV and ELS detection. RediSep silica columns were used according to the mass of crude extracts to be separated. The choice of the column size was determined to allow half of the capacity of the column to be used for optimal separation and peak resolution purposes.

V.6.5. Spectral data

Tapachulanone B (17): translucent solid; $[\alpha]^{20}_{D}$ +19.99° (c = 0.5, CH_3Cl); UV (CH_3Cl) λ_{max} (log ε) (2.52) 205; (2.50) 215 nm; (2.82) 230; (2.54) 240 nm; IR υ (thin film): 3200, 2900, 1700 cm^{-1}; ^{1}H and ^{13}C NMR data see **Table V.4.3.**; HRESIMS $[M + H]^+$: m/z 475.2338, calcd. for $C_{26}H_{34}O_8H$, m/z 475.2326.

References

(1) Aksenov, A. A.; Da Silva, R.; Knight, R.; Lopes, N. P.; Dorrestein, P. C. Global chemical analysis of biology by mass spectrometry. *Nat. Rev. Chem.* **2017**, *1*.

(2) Gauglitz, J. M.; Aceves, C. M.; Aksenov, A. A.; Aleti, G.; Almaliti, J.; Bouslimani, A.; Brown, E. A.; Campeau, A.; Caraballo-Rodríguez, A. M.; Chaar, R.; et al. Untargeted mass spectrometry-based metabolomics approach unveils molecular changes in raw and processed foods and beverages.

www.manaraa.com

2019, *https://doi.org/10.1016/j.foodchem.2019.125290.*

(3) Martinsen, D. P. Survey of computer aided methods for mass spectral interpretation. *Appl. Spectrosc.* **1981**, *35*, 255–266.

(4) Grim, C. M.; Luu, G. T.; Sanchez, L. M. Staring into the void: demystifying microbial metabolomics. *FEMS Microbiol. Lett.* **2019**, *366*.

(5) Caesar, L. K.; Kellogg, J. J.; Kvalheim, O. M.; Cech, N. B. Opportunities and limitations for untargeted mass spectrometry metabolomics to identify biologically active constituents in complex natural product mixtures. *J. Nat. Prod.* **2019**, *82*.

(6) Conde-Martínez, N.; Bauermeister, A.; Pilon, A. C.; Lopes, N. P.; Tello, E. Integrating molecular network and culture media variation to explore the production of bioactive metabolites by *Vibrio diabolicus* a1sm3. *Mar. Drugs* **2019**, *17*, 1–18.

(7) Bouslimani, A.; Sanchez, L. M.; Garg, N.; Dorrestein, P. C. Mass spectrometry of natural products: current, emerging and future technologies. *Nat. Prod. Rep.* **2014**, *31*, 718–729.

(8) Ziemert, N.; Alanjary, M.; Weber, T. The evolution of genome mining in microbes-a review. *Natural Product Reports*. Royal Society of Chemistry, **2016**, 988–1005.

(9) Wolfender, J. L.; Marti, G.; Thomas, A.; Bertrand, S. Current approaches and challenges for the metabolite profiling of complex natural extracts. *Journal of Chromatography A*. Elsevier, **2015**, 136–164.

(10) Bucar, F.; Wube, A.; Schmid, M. Natural product isolation-how to get from biological material to pure compounds. *Nat. Prod. Rep.* **2013**, *30*, 525–545.

(11) Wolfender, J. L.; Marti, G.; Thomas, A.; Bertrand, S. Current approaches and challenges for the metabolite profiling of complex natural extracts. *J. Chromatogr. A* **2015**, *1382*, 136–164.

(12) Sithersingh, M.J. Determination of polar solvents by static headspace extraction-gas

www.manaraa.com

chromatography (SHE-GC). Thesis. **2018.** Seton Hall University Dissertations and Theses (ETDs). 2573.

(13) Kwan, M. W. C.; Weisenseel, J. P.; Giel, N.; Bosak, A.; Batich, C. D.; Willenberg, B. J. Detection and quantification of trace airborne transfluthrin concentrations via air sampling and thermal desorption gas chromatography-mass spectrometry. *J. Chromatogr. A.* **2018**, *1573*, 156–160.

(14) Guo, Z.; Shao, C.; She, Z.; Cai, X.; Liu, F.; Vrijimoed, L. L. P.; Lin, Y.; Kong, H. Spectral assignments and reference data and 13 c NMR assignments for two oxaphenalenones bacillosporin c and d from the mangrove endophytic fungus sbe-14. *Magn. Reson. Chem.* **2007**, *45*, 439–441.

(15) Cech, N. B.; Enke, C. G. Practical implications of some recent studies in electrospray ionization fundamentals. *Mass Spectrom. Rev.* **2001**, *20*, 362–387.

(16) Daly, N. R. Scintillation Type Mass Spectrometer Ion Detector. *Rev. Sci. Instrum.* **1960**, *31* (3), 264–267.

(17) Huang, E. C.; Wachs, T.; Conboy, J. J.; Jack, D. Atmospheric Pressure Ionization Mass Spectrometry. *Anal. Chem.* **1990**, *62*, 713–725.

(18) Bode, H. B.; Bethe, B.; Höfs, R.; Zeeck, A. Big effects from small changes: possible ways to explore nature's chemical diversity. *ChemBioChem* **2002**, *3*, 619–627.

(19) Pan, R.; Bai, X.; Chen, J.; Zhang, H.; Wang, H. Exploring structural diversity of microbe secondary metabolites using osmac strategy: a literature review. *Front. Microbiol.* eCollection **2019**, *10*.

(20) McAlpine, J. B.; Chen, S. N.; Kutateladze, A.; Macmillan, J. B.; Appendino, G.; Barison, A.; Beniddir, M. A.; Biavatti, M. W.; Bluml, S.; Boufridi, A.; et al. The value of universally available raw nmr data for transparency, reproducibility, and integrity in natural product

www.manaraa.com

research. *Nat. Prod. Rep.* **2019**, *36*, 35–107.

(21) Romano, S.; Jackson, S. A.; Patry, S.; Dobson, A. D. W. Extending the one strain many compounds (OSMAC) principle to marine microorganisms. *Mar. Drugs* **2018**, *16*, 244.

(22) Djukovic, G. A. N. G. and D. Overview of mass spectrometry-based metabolomics: opportunities and challenges. **2014**, *1198*, 15–27.

(23) Nakano, Y.; Taniguchi, M.; Fukusaki, E. High-sensitive liquid chromatography-tandem mass spectrometry-based chiral metabolic profiling focusing on amino acids and related metabolites. *J. Biosci. Bioeng.* **2019**, *127*, 520–527.

(24) Wang, M. Spectral library construction and matching of ms/ms spectra at repository scales. **2007**.

(25) Wang, M.; Bandeira, N. Spectral library generating function for assessing spectrum-spectrum match significance. *J. Proteome Res.* **2013**, *12*, 3944–3951.

(26) Allard, P. M.; Péresse, T.; Bisson, J.; Gindro, K.; Marcourt, L.; Pham, V. C.; Roussi, F.; Litaudon, M.; Wolfender, J. L. Integration of molecular networking and in-silico ms/ms fragmentation for natural products dereplication. *Anal. Chem.* **2016**, *88*, 3317–3323.

www.manaraa.com

CLOSING REMARKS

"Ever tried. Ever failed. No matter. Try again.

Fail again. Fail better." —Samuel Beckett

The scientific community tends to focus on positive results as a general pattern to follow, but lest not forget that progress is made through failure, and the so-called failed project must be valued as much as the more successful ones.[1-3] Even though reproducibility has yet to be proven for some scientific models, inexactitude still remains unexplained. They allow development of other models but remain in the pipeline of studies and contribute to scientific advancements.

Mainly due to political agenda, energy, time and money seem to remain the challenges of research development. Pharmaceutical companies lobbying joined with nation leaders focus more on lucrative activities rather than the meaning of health and respect of life. Even if natural and holistic practices such as homeopathy and phytochemistry specialties, find painfully their seat at the drug discovery table, the egos of powerful executives tend to prevail and lead to depreciation, segregation, dismissal, and forgetfulness of Nature's chemical treasure.

This was the case for tropical plant pharmacopoeia from the French oversea lands.

During the 1791 Haitian revolution which started in 1791, the knowledge of pharmacognosy from François Makandal was valued and became a privileged weapon to poison colon adversaries. The usage of natural products was essential to the island of Haiti in earning its independence in 1804. The practice became known as *Makandalism*. Feeling threatened by the

www.manaraa.com

development of plant poisoning, the colons of the French Caribbean colonies updated and extended the 1764 article 293. On the 8th of March 1799, a judgement (n°892) of the sovereign council of France prohibited people of color from performing activities involving medicine and pharmacognosy.[4]

> *« La raison de cette prohibition est la crainte, trop justifiée d'ailleurs, des empoisonnements auxquels les nègres se livraient fréquemment pour assouvir leurs vengeances. Une ordonnance royale du 30 avril 1764, renouvelant et précisant une déclaration royale du 30 décembre 1746, défend, dans son article 16, très expressément aux nègres et à tous gens de couleur libres ou esclaves d'exercer la médecine ou la chirurgie, ni de faire aucun traitement de malade sous quelque prétexte que ce soit, à peine de 500 livres d'amende pour chaque contravention et de punition corporelle, suivant l'exigence des cas. Une ordonnance des administrateurs de la Guadeloupe, article 9, s'était, la même année le 3 mars, exprimée dans des termes exactement semblables. »*

American English translation:

> ***"The reason for this prohibition is the fear, too much justified, of the poisonings to which the Negroes frequently gave themselves up to satisfy their vengeance. A royal decree of April 30, 1764, renewing and specifying a royal declaration of December 30, 1746, defends, in its article 16, very expressly to negroes and all colored people free or slaves to practice the medicine or the surgery, nor of no treatment of a patient under any pretext, a fine of not more than 500 pounds for each contravention and corporal punishment, depending on the requirement of the case. An order of the administrators of Guadeloupe, article 9, was the same year March 3, expressed in terms exactly similar."***

Auguste Lebeau. De la condition des gens de couleur libres sous l'ancien régime. D'après des documents des Archives coloniales. 1903

www.manaraa.com

Despite the 1794 first abolition, slavery was re-established three years later and was not abolished again until 1848.

Beyond the awful human rights violations stated, this prohibition also created a prejudice against science and nature that persisted over 200 years before being recently acknowledged. In spite of the wealth of natural therapeutics offered by the 3,800 species of tropical plants present on the islands of Guadeloupe, Martinique, Guyane, and Reunion, even with the generational transmission of knowledge through the traditional customs, the French tropical biodiversity and pharmacopoeia was not valued until recently. In 2005, the Guadeloupean natives, former pharmacist Henry Joseph associated to his natural products chemist mentor Paul Bourgeois, created *Phytobokaz* a laboratory developing therapeutics valuing the traditional medicinal plants.[5-7] Their mission expands beyond scientific levels. After a 12-year of legal fights, the public health code article L 5112-1, finally recognizes and stipulates:

"The pharmacopoeia includes the European and French pharmacopoeia, including the French overseas one."[8]

The apothecary was the original pharmacist, and prepared remedies from natural resources. A shift was operated with the development of synthetic method and petroleum industry. The loss of apothecaries also led men to devalue and forget Nature. However, natural product therapeutics have been around for thousands of years, and various communities continue to advocate for these. Natural products resources continue to serve the humankind by providing treatments and prove that proximity to Nature and its resources are vital to humanity. Without life, discomfort and most likely death emerges. Dismissing the power of natural chemodiversity, does not only prevents from healthy development promoting survival, it also closes the scope of drug options. As the most significant pharmaceutical progress revolves around natural products chemistry, the field of drug discovery must re-evaluate its goals and ethos.

www.manaraa.com

References

(1) Redish, A. D.; Kummerfeld, E.; Morris, R. L.; Love, A. C. Reproducibility failures are essential to scientific inquiry. *Proc. Natl. Acad. Sci. U. S. A.* **2018**, *115*, 5042–5046.

(2) Parkes, E. Scientific progress is built on failure. *Nature* **2019**, No. January, 1–5.

(3) Issues, L.; In, S. How to turn failure into success. **2019**, *23*, 1–9.

(4) Lebeau, A. De la condition des gens de couleur libres sous l'ancien régime d'après des documents des archives coloniales. **1903**, 1 vol. (VI-133 p.).

(5) Le-Bail, A.; Godard, A.; Loisel, C.; Prost, C.; Ranou, C.; Salles, C.; Guichard, E.; Thomas-Danguin, T.; Neiers, F.; Briand, L. Miraculine as a natural sweetener; the n3s qualiment project: potential interest in baking. *31 EFFoST Int. Conf.* **2017**, *16*, 9–10.

(6) Biabiany, M. Recherche et développement d'extraits antifongiques issus de la flore guadeloupéenne: caractérisations phytochimiques, pharmacologiques et formulation. **2011**, 1–3.

(7) Bugaud C.1, Fahrasmane L.2, Daribo M.O.1, Aurore G.3, Chillet M.4, Fils-Lycaon B.2, R. D. Innovations agronomiques. **2011**, *16*, 75–87.

(8) Iii, L. Article L300-2. **2013**, *2* (V), 2009–2010.

www.manaraa.com

APPENDIX A:

EXPERIMENTAL AND SUPPORTING DATA FOR CHAPTER III

MPLC Chromatograms
Fractionation Schemes
Compound Data
Additional NMR Spectra for (S)-3-(hydroxymethyl)-4,7,7-trimethyl-3,6,7,8-tetrahydro-1H-indeno[4,5-c]furan-1-one,4,12 Bis(acetyl)alcyopterosin O, and alcyopterosin compounds C, E, G, and L, compounds **10**, **11**, *and* **12**.

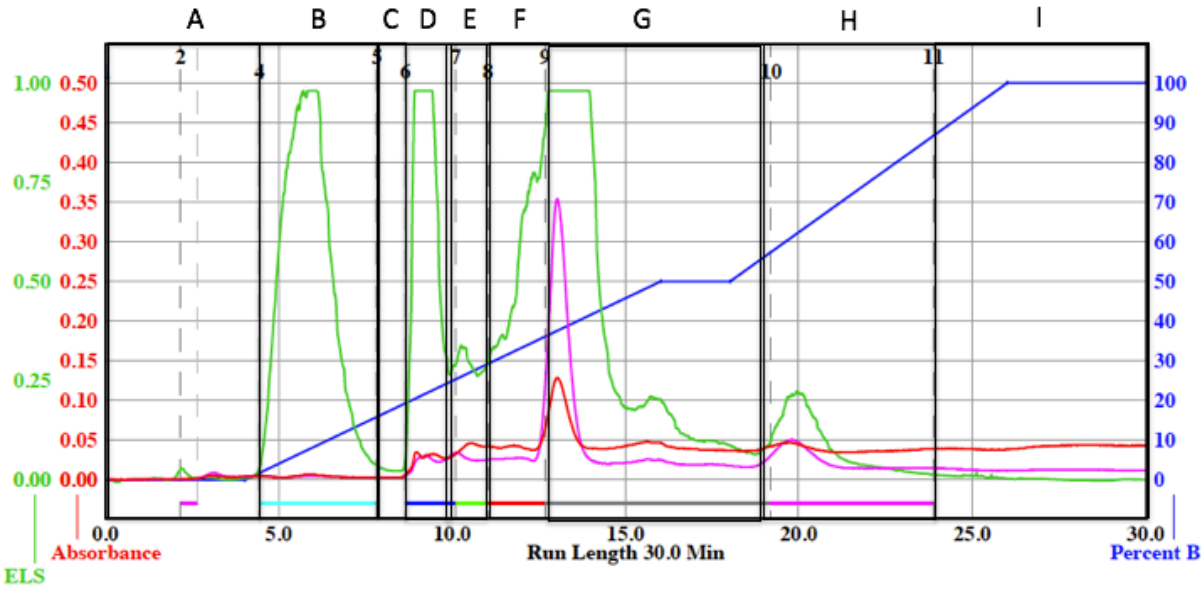

Figure A.III.1. NP MPLC Chromatogram of Antarctic deep sea octocoral extracted in DCM:MeOH (1:1).

www.manaraa.com

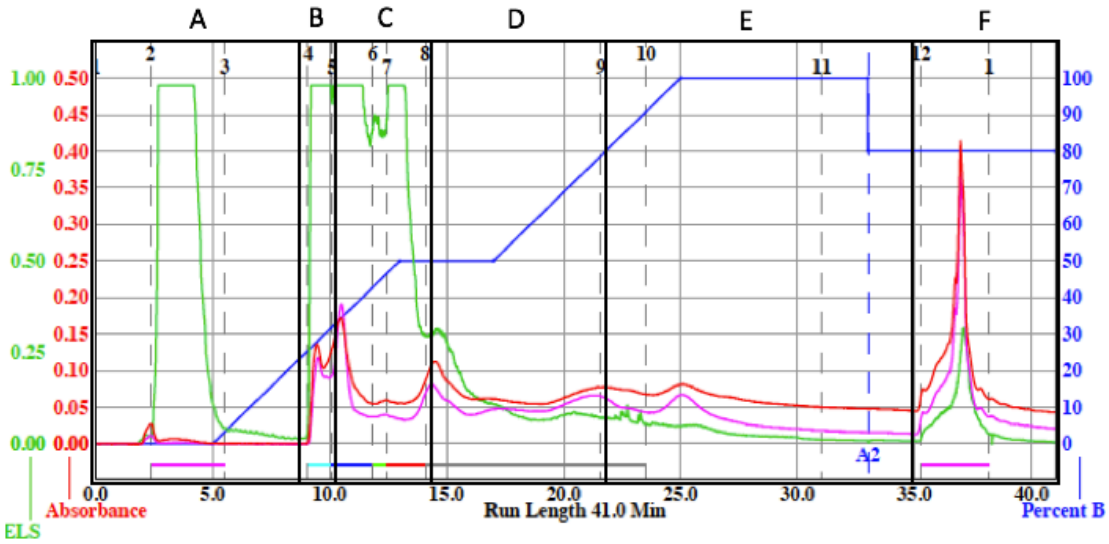

Figure A.III.2. NP MPLC Chromatogram of Antarctic deep sea octocoral sample I extracted in 100% DCM with Soxhlet apparatus.

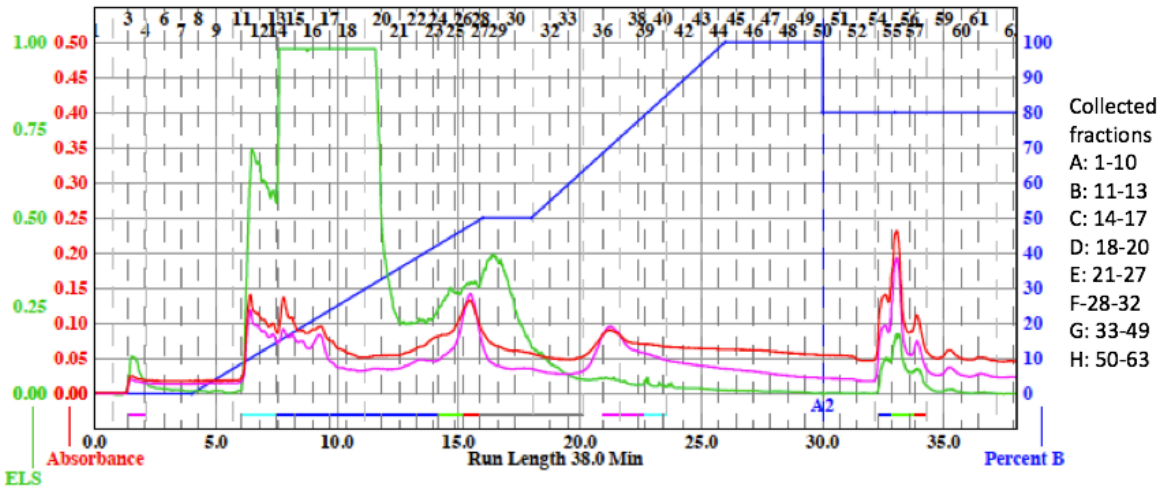

Figure A.III.3. NP MPLC Chromatogram of Antarctic deep sea octocoral sample II extracted in 100% DCM with Soxhlet apparatus.

www.manaraa.com

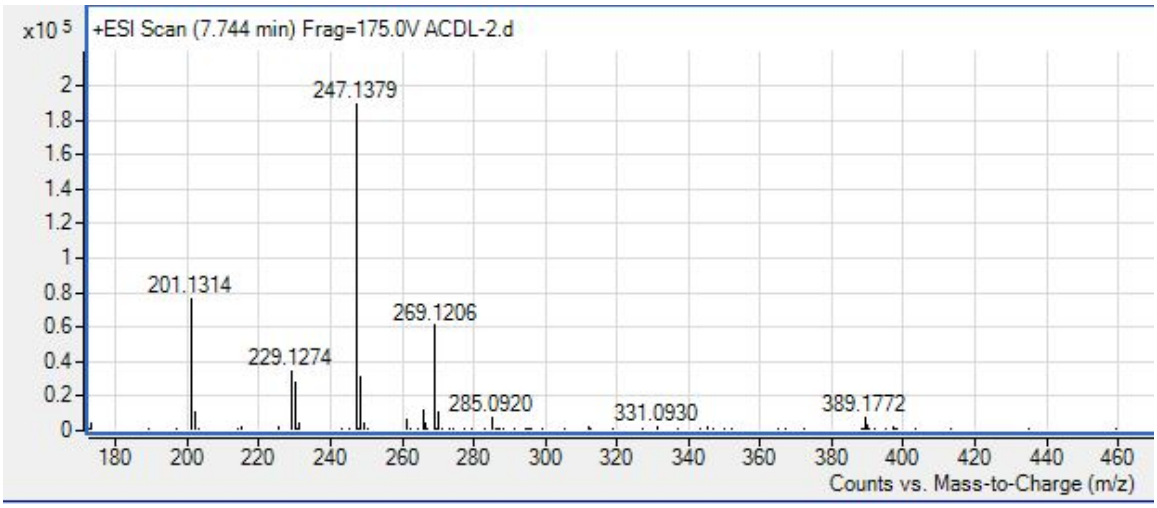

Figure A.III.4. MS of (*S*)-3-(hydroxymethyl)-4,7,7-trimethyl-3,6,7,8-tetrahydro-1*H*-indeno[4,5-*c*]furan-1-one.

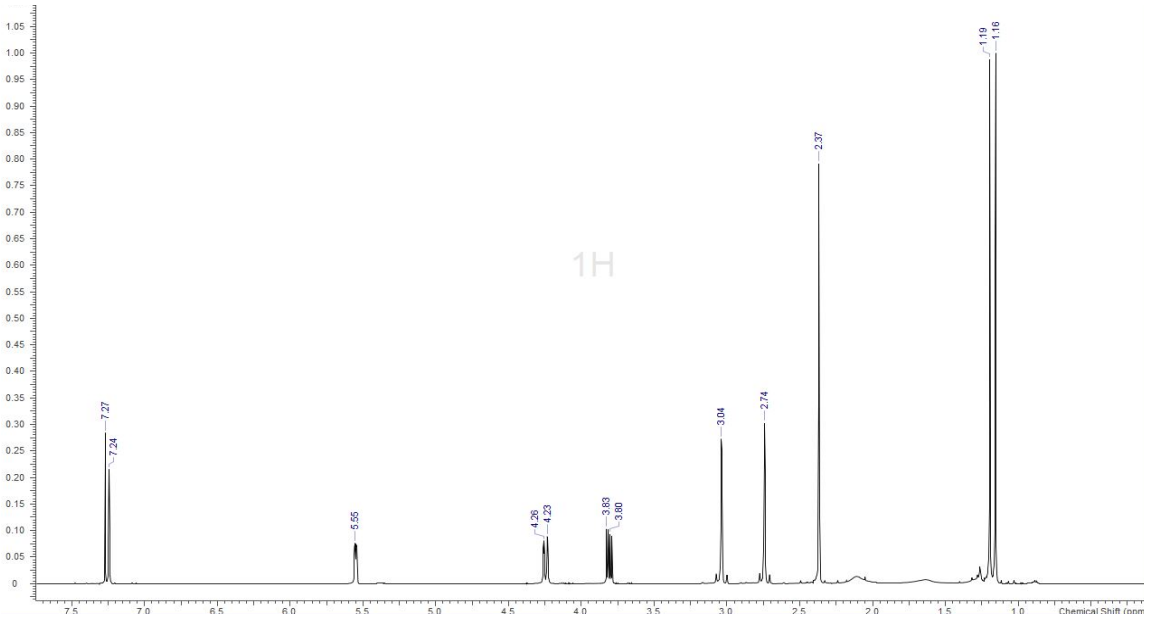

Figure A.III.5. ^{1}H NMR Spectrum ($CDCl_3$, 500 MHz) of known (*S*)-3-(hydroxymethyl)-4,7,7-trimethyl-3,6,7,8-tetrahydro-1*H*-indeno[4,5-*c*]furan-1-one.

www.manaraa.com

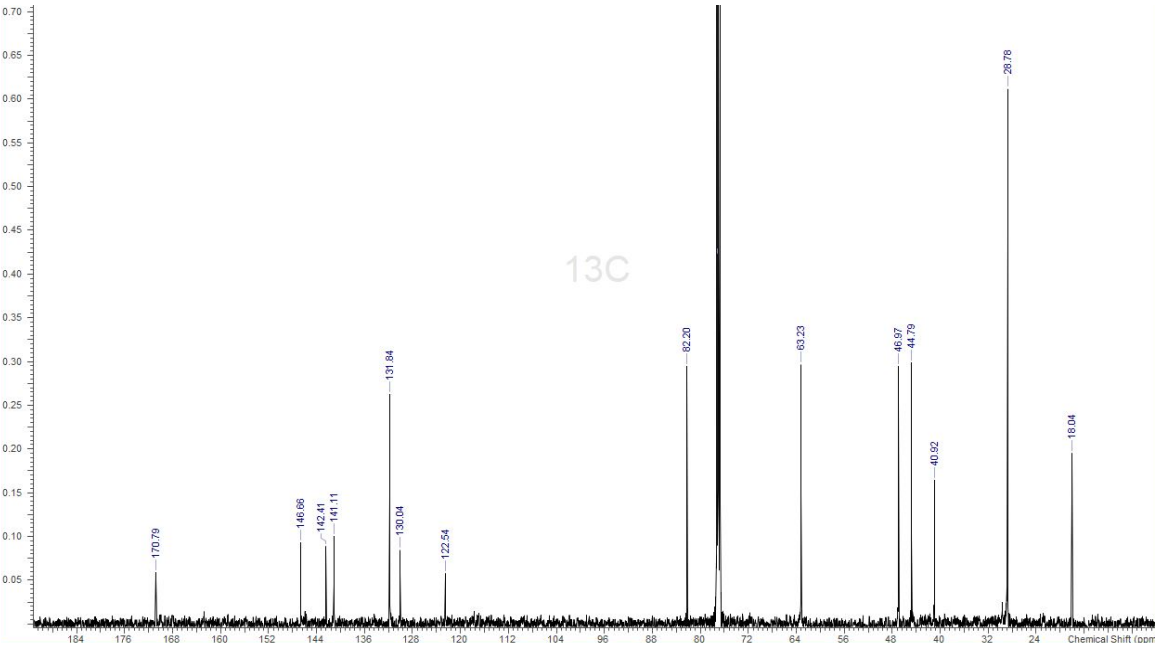

Figure A.III.6. ^{13}C NMR Spectrum ($CDCl_3$, 125 MHz) of known (***S*)-3-(hydroxymethyl)-4,7,7-trimethyl-3,6,7,8-tetrahydro-1*H*-indeno[4,5-*c*]furan-1-one.**

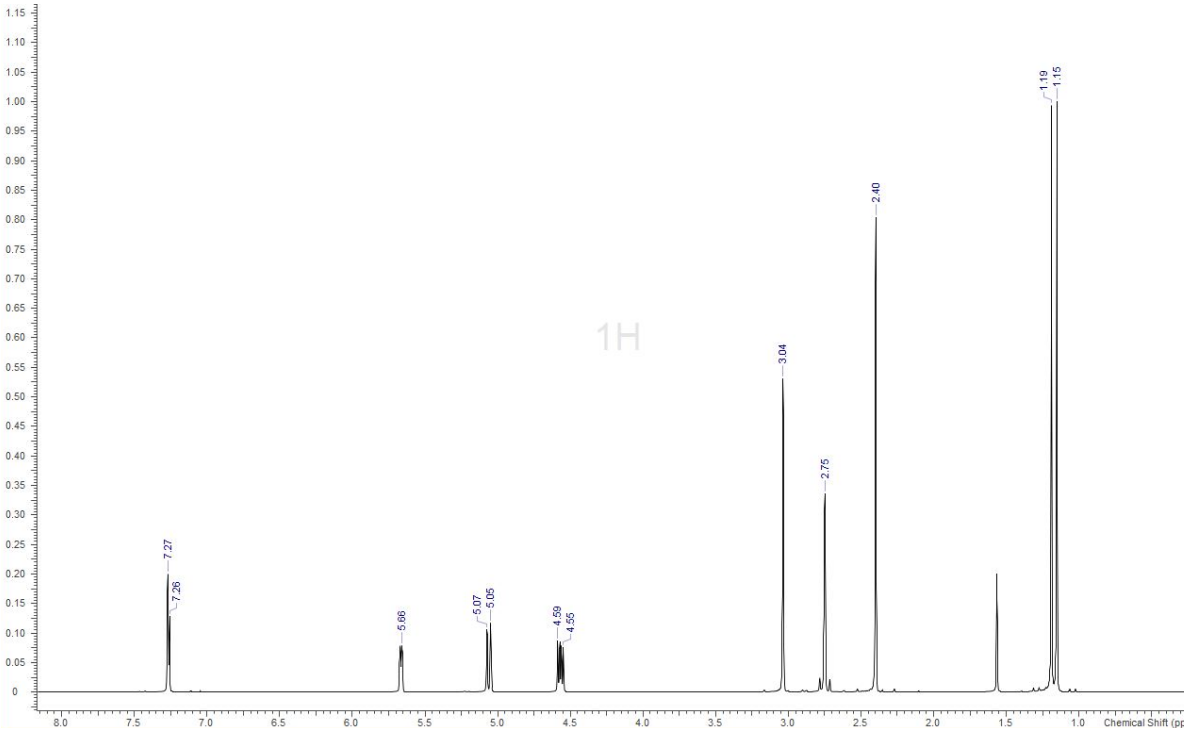

Figure A.III.7. ^{1}H NMR Spectrum ($CDCl_3$, 500 MHz) of known **alcyopterosin E.**

www.manaraa.com

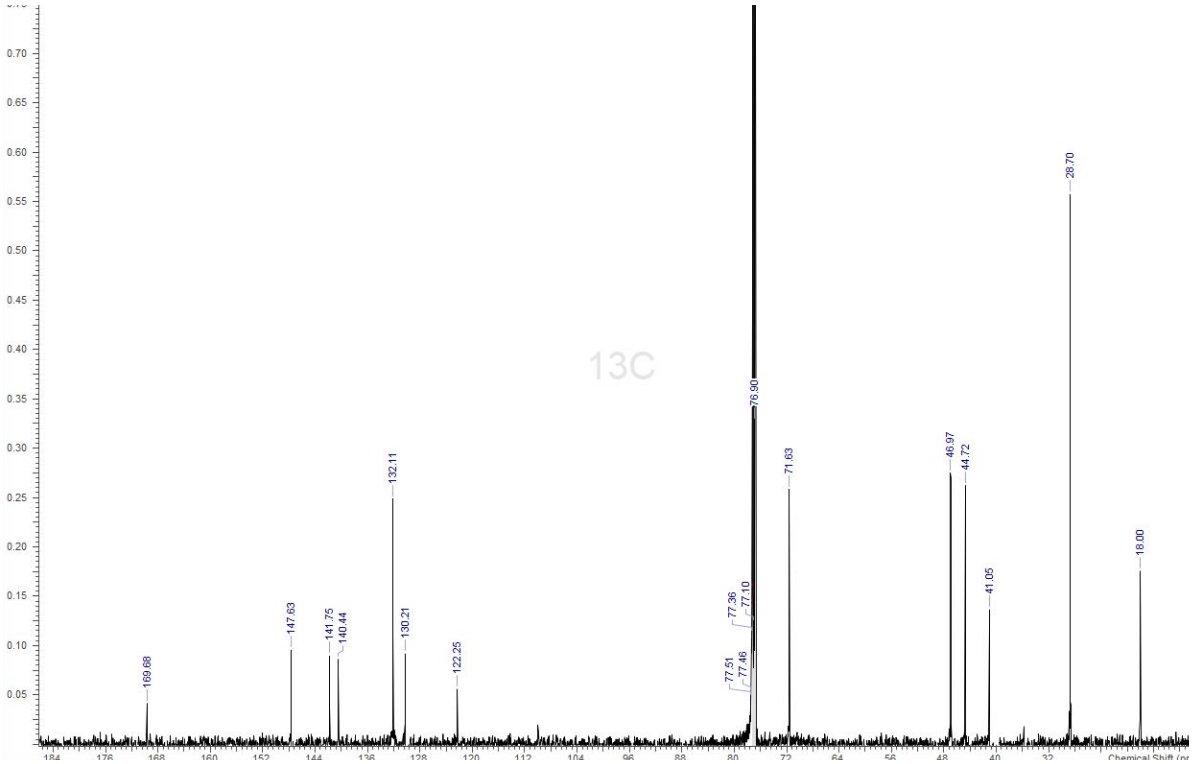

Figure A.III.8. ^{13}C NMR Spectrum ($CDCl_3$, 125 MHz) of known **alcyopterosin E.**

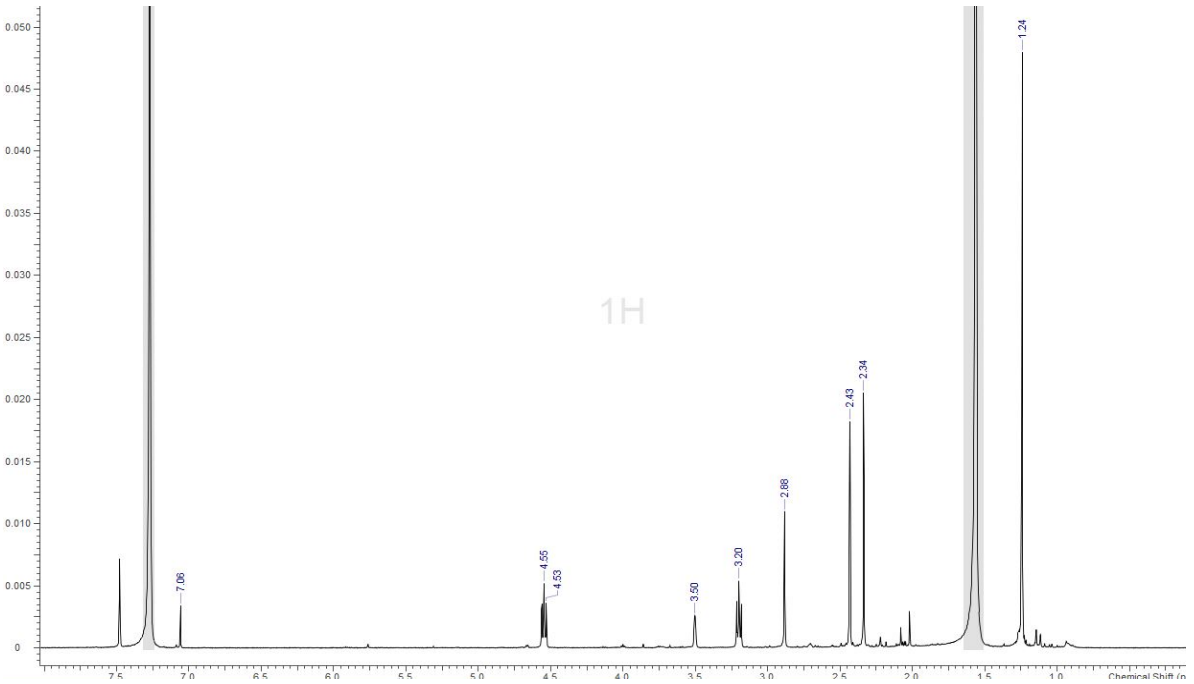

Figure A.III.9. ^{1}H NMR Spectrum ($CDCl_3$, 500 MHz) of known **alcyopterosin C.**

www.manaraa.com

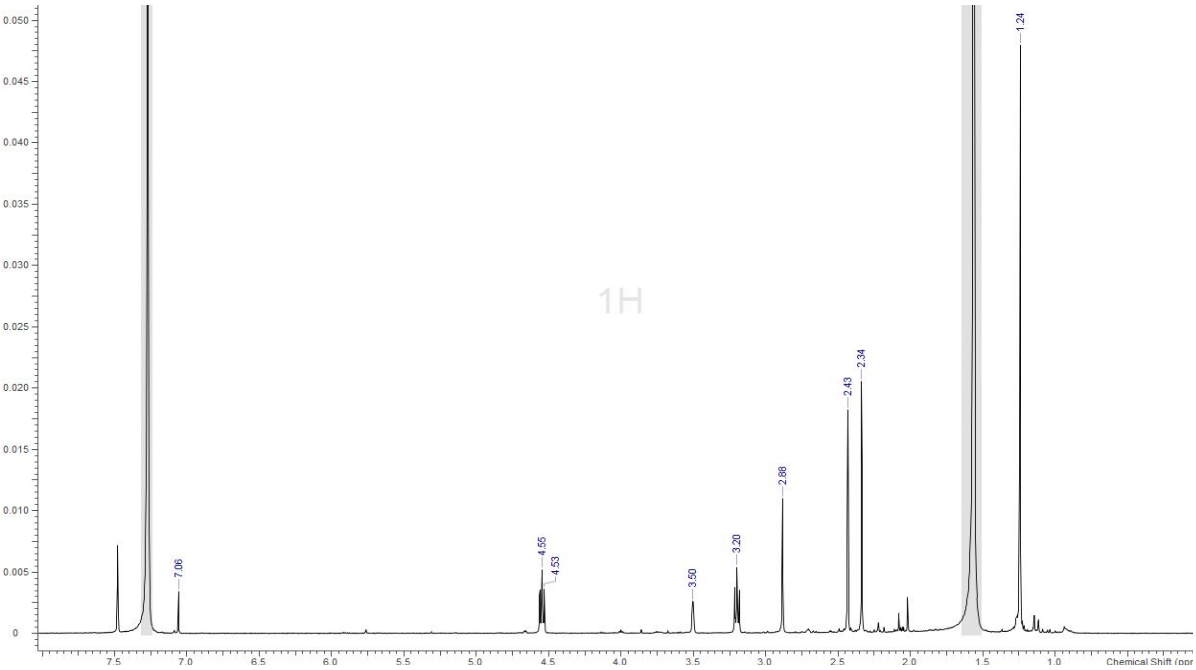

Figure A.III.10. ^{1}H NMR Spectrum ($CDCl_3$, 500 MHz) of knonwn **alcyopterosin G.**

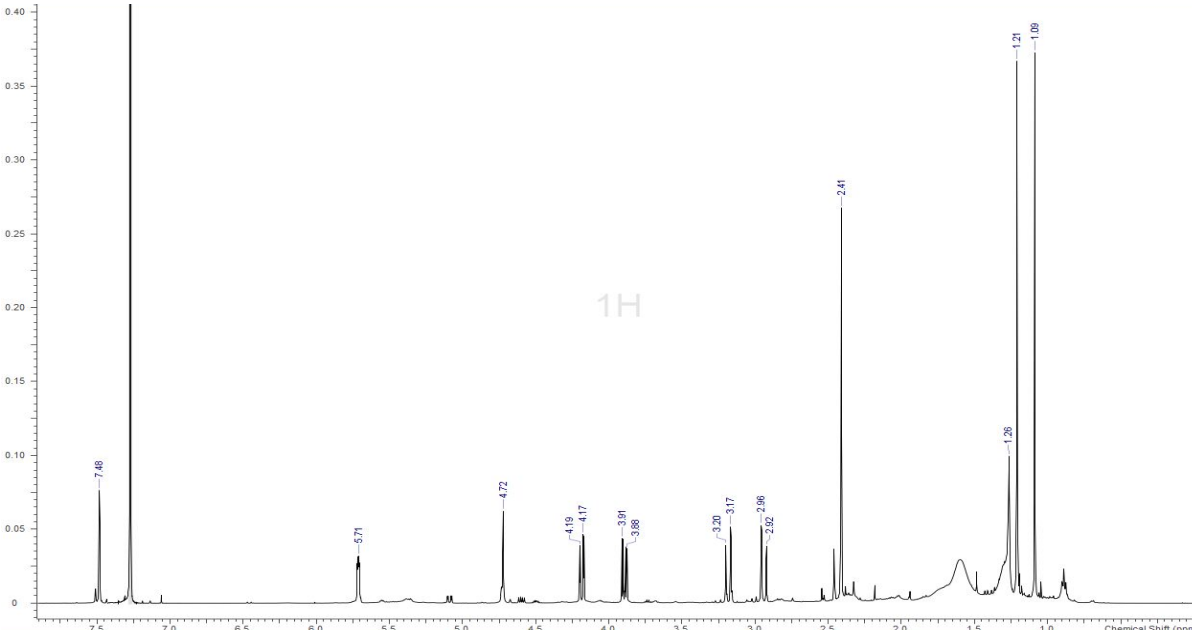

Figure A.III.11. ^{1}H NMR Spectrum ($CDCl_3$, 500 MHz) of known **alcyopterosin L.**

www.manaraa.com

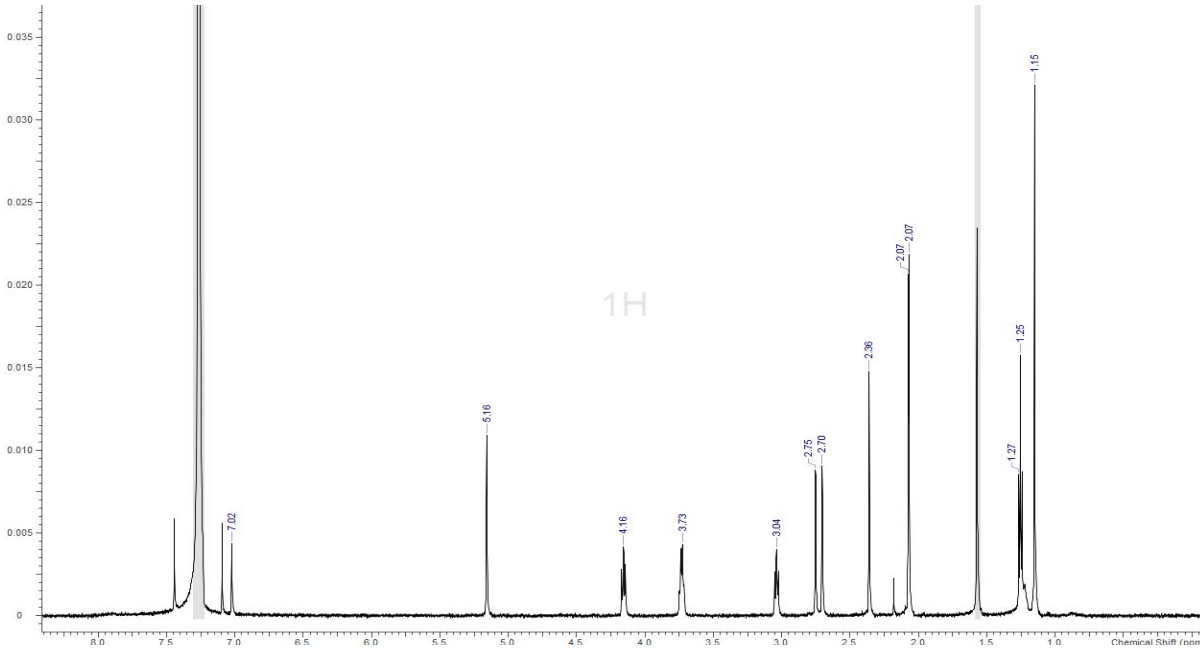

Figure A.III.12. ^{1}H NMR Spectrum ($CDCl_3$, 500 MHz) of known **4,12-Bis(acetyl)alcyopterosin O.**

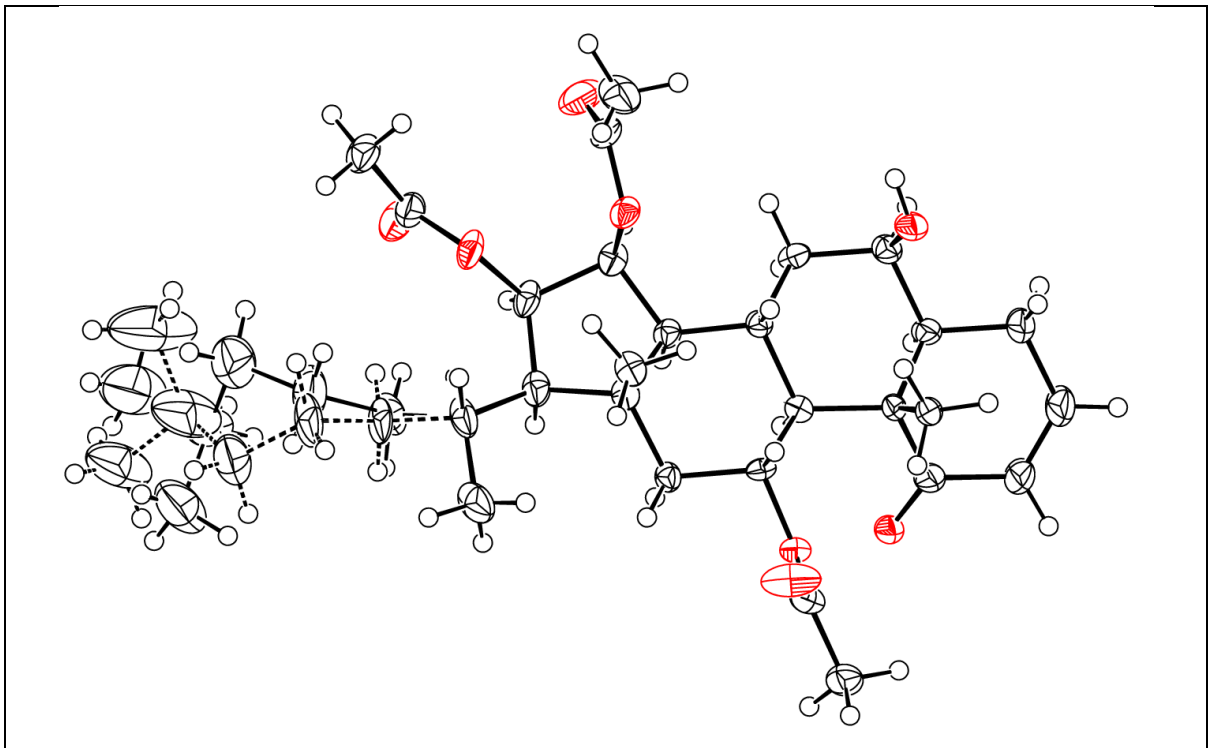

Fig.1. Asymmetric unit of **ACDL_21**. Anisotropic displacement parameters were drawn at 50% probability level.

Figure A.III.13. Asymmetric unit of compound **9.**

www.manaraa.com

Table A.III.1. Crystal structure information for compound **9**.

Table 1 Crystal data and structure refinement for ACDL-21.	
Identification code	ACDL_21
Empirical formula	$C_{33}H_{50}O_8$
Formula weight	574.73
Temperature/K	100.0
Crystal system	orthorhombic
Space group	$P2_12_12_1$
a/Å	6.9203(5)
b/Å	14.3360(10)
c/Å	32.173(2)
α/°	90
β/°	90
γ/°	90
Volume/Å^3	3191.8(4)
Z	4
ρ_{calc}g/cm^3	1.196
μ/mm^{-1}	0.681
F(000)	1248.0
Crystal size/mm^3	0.042 × 0.036 × 0.018
Radiation	CuKα (λ = 1.54178)
2Θ range for data collection/°	5.494 to 137.154
Index ranges	-7 ≤ h ≤ 8, -16 ≤ k ≤ 17, -38 ≤ l ≤ 38
Reflections collected	32338
Independent reflections	5867 [R_{int} = 0.1453, R_{sigma} = 0.0776]
Data/restraints/parameters	5867/258/437
Goodness-of-fit on F^2	1.026
Final R indexes [I>=2σ (I)]	R_1 = 0.0659, wR_2 = 0.1389
Final R indexes [all data]	R_1 = 0.1009, wR_2 = 0.1577
Largest diff. peak/hole / e Å^{-3}	0.40/-0.26
Flack parameter	-0.10(19)

www.manaraa.com

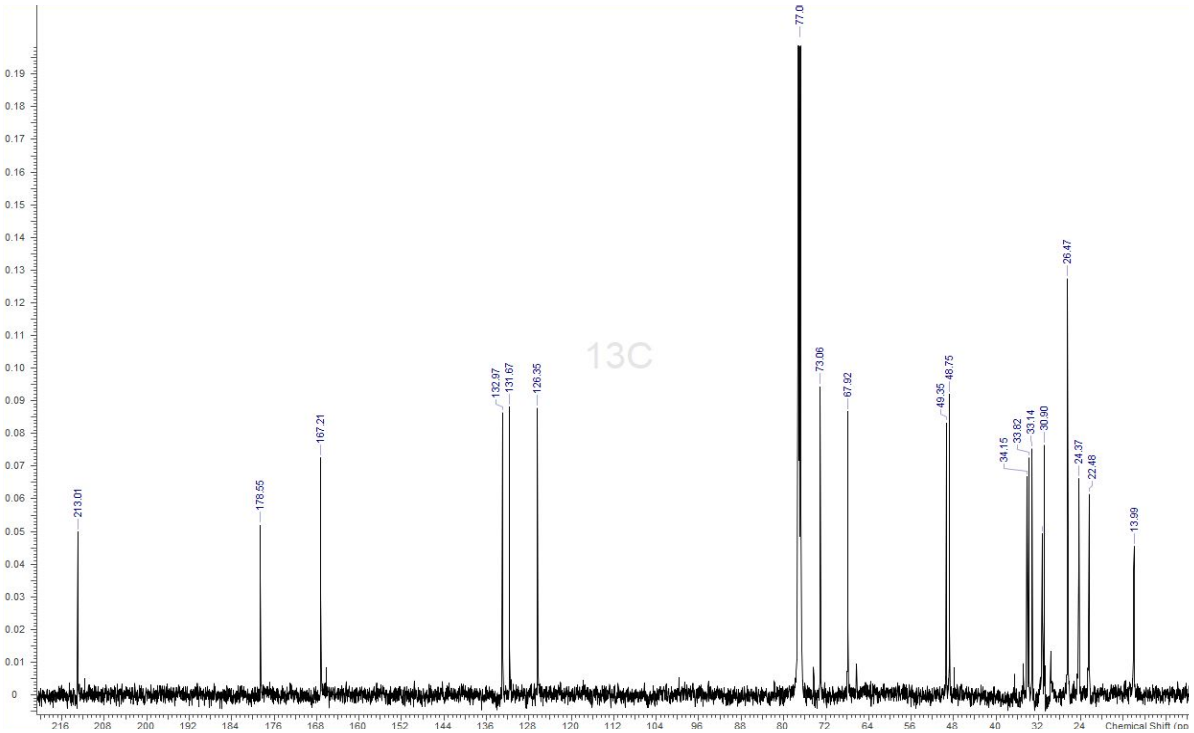

Figure A.III.14. ^{13}C NMR Spectrum ($CDCl_3$, 125 MHz) of **10.**

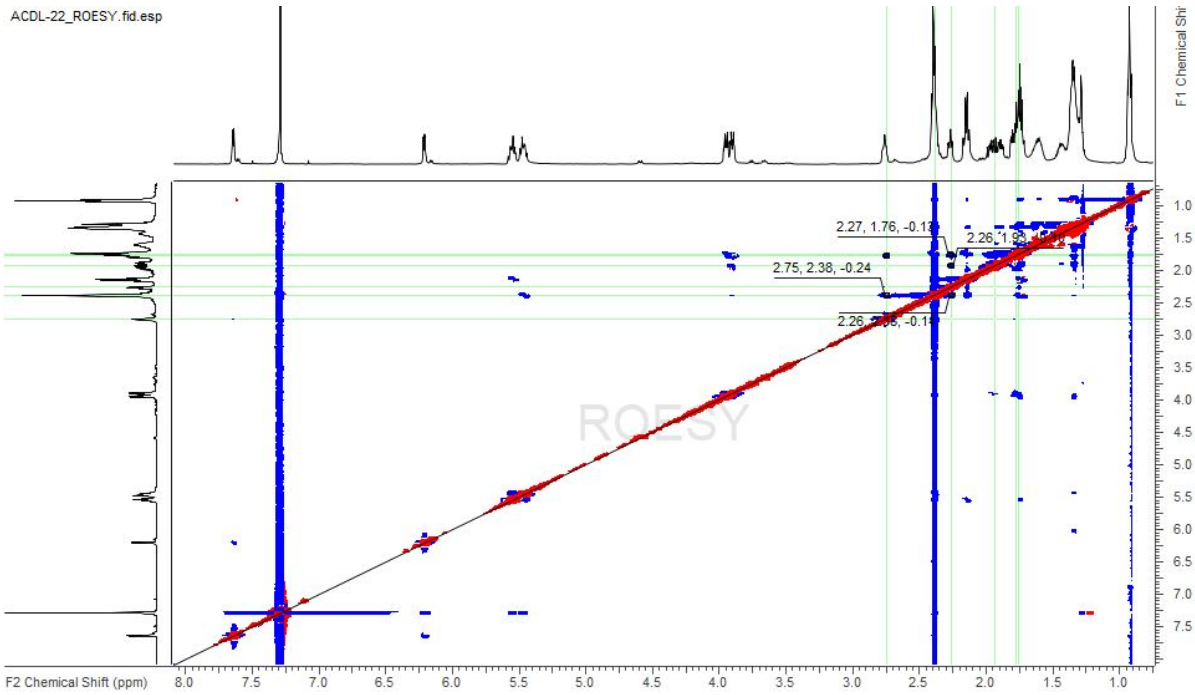

Figure A.III.15a. ROESY Spectrum ($CDCl_3$, 500 MHz) of **10.**

www.manaraa.com

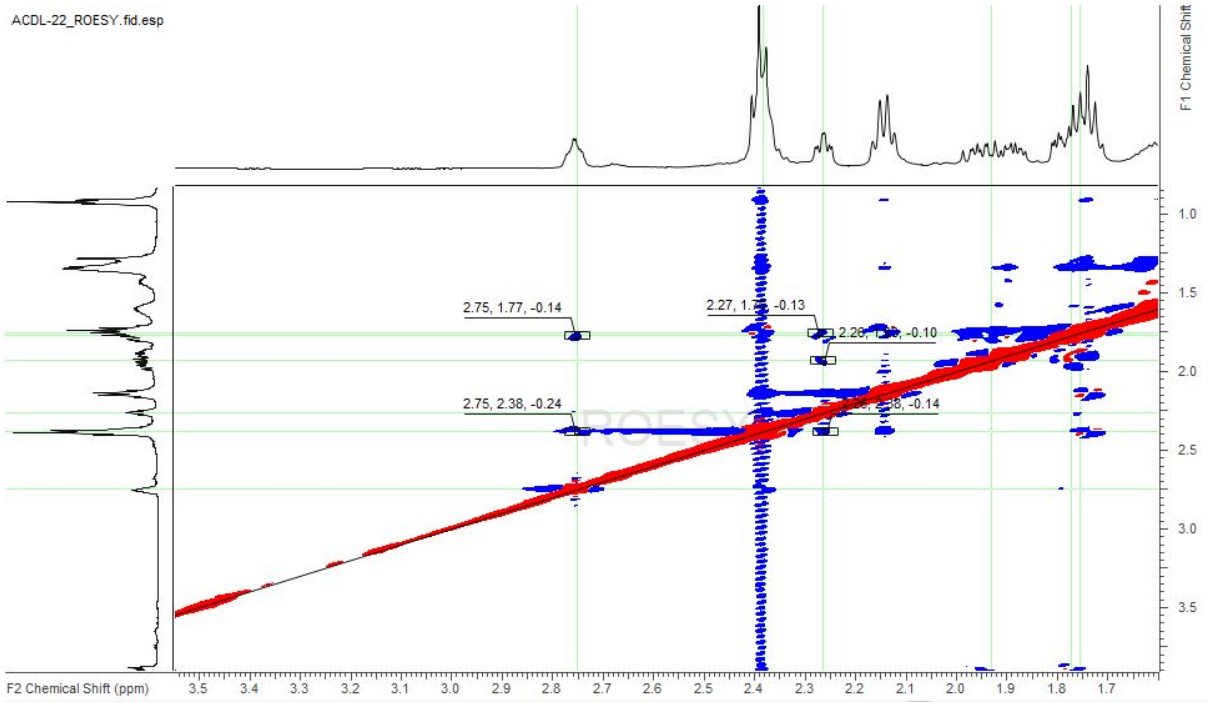

Figure A.III.15b. Zoomed in ROESY Spectrum ($CDCl_3$, 500 MHz) of **10.**

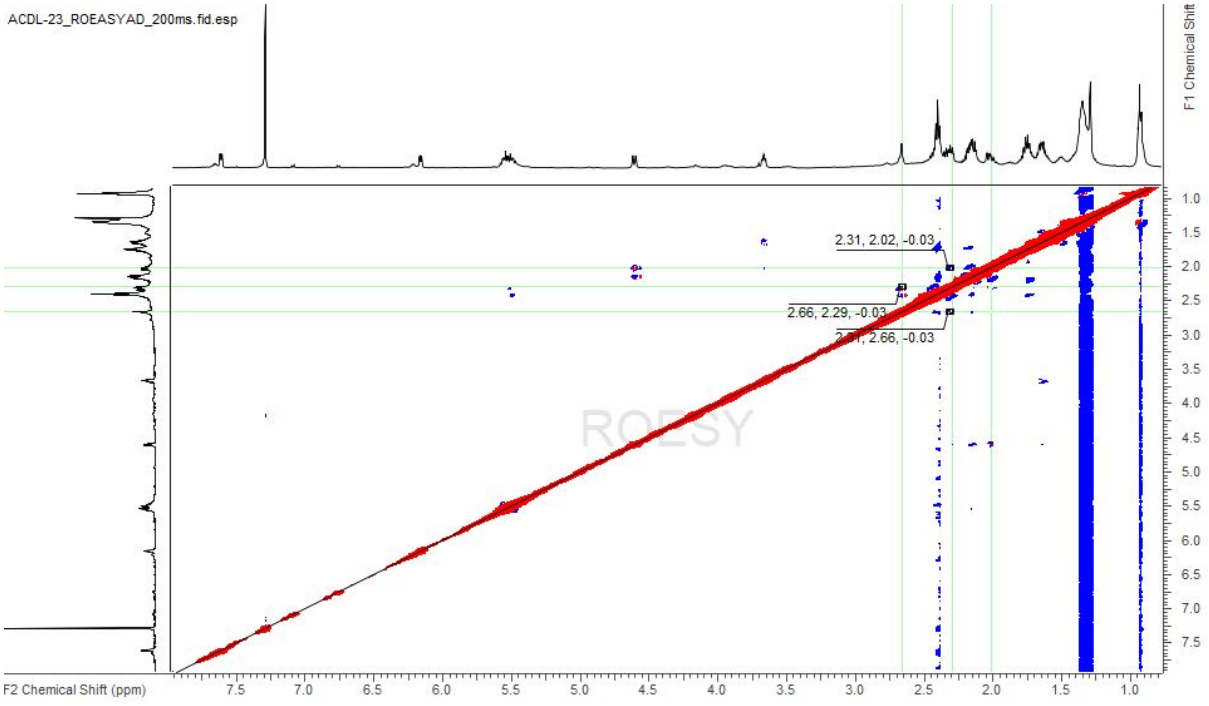

Figure A.III.16a. Full ROESY Spectrum ($CDCl_3$, 500 MHz) of **11.**

www.manaraa.com

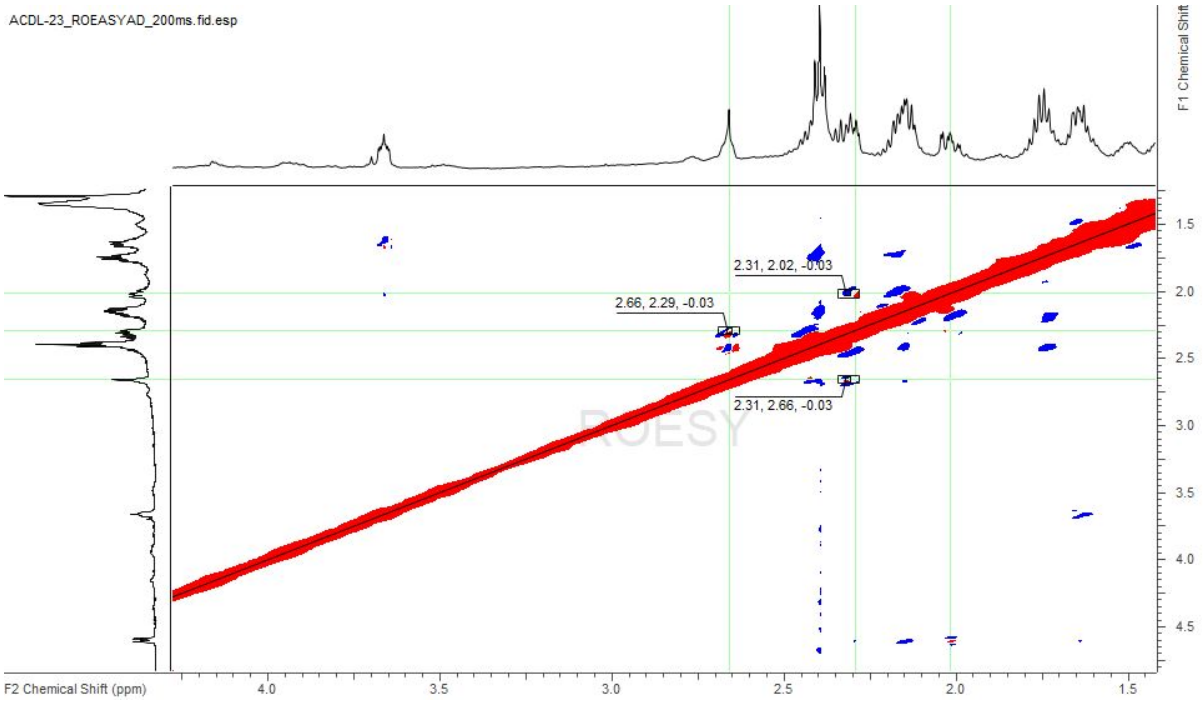

Figure A.III.16b. Zoomed in ROESY Spectrum ($CDCl_3$, 500 MHz) of **11.**

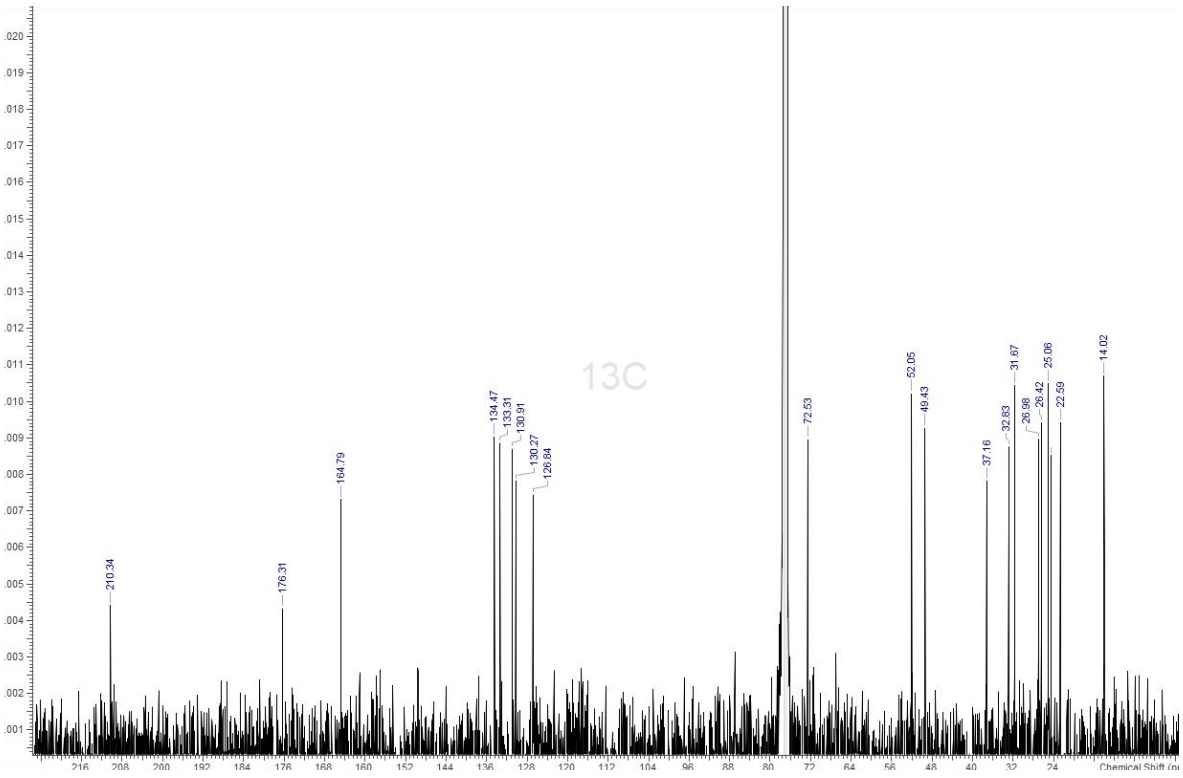

Figure A.III.17. ^{13}C NMR Spectrum ($CDCl_3$,125 MHz) of **12.**

www.manaraa.com

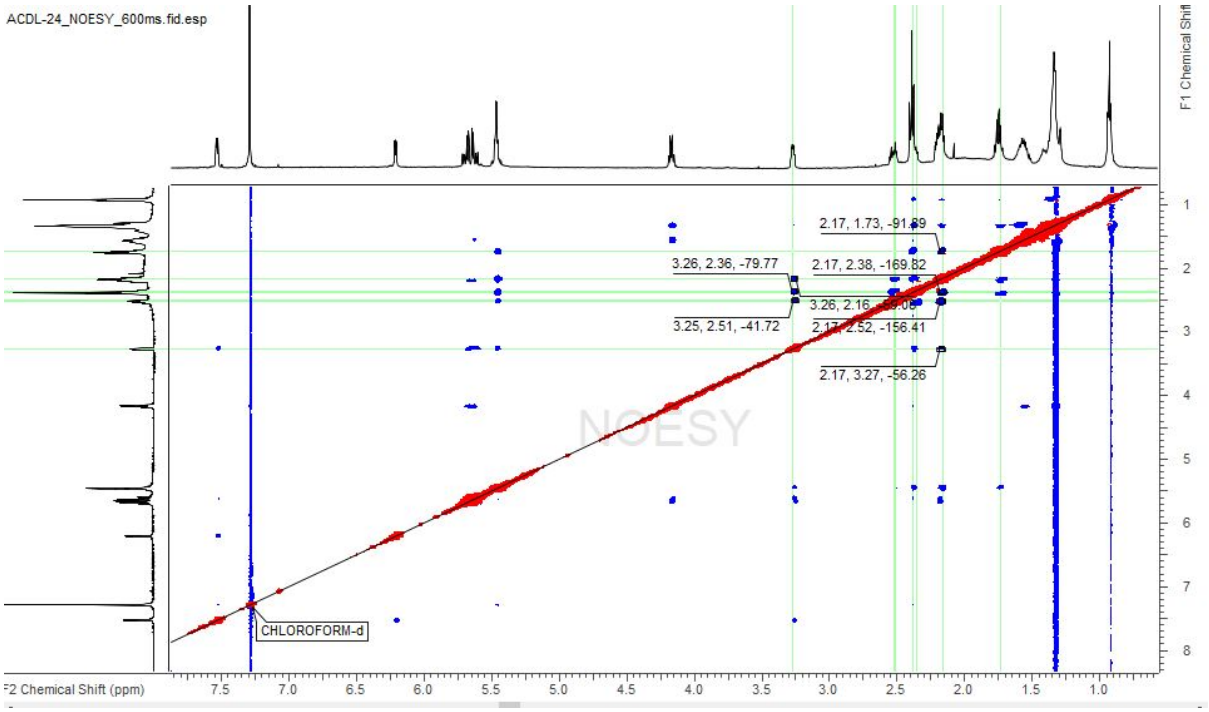

Figure A.III.18a. NOESY Spectrum ($CDCl_3$, 500 MHz) of **12.**

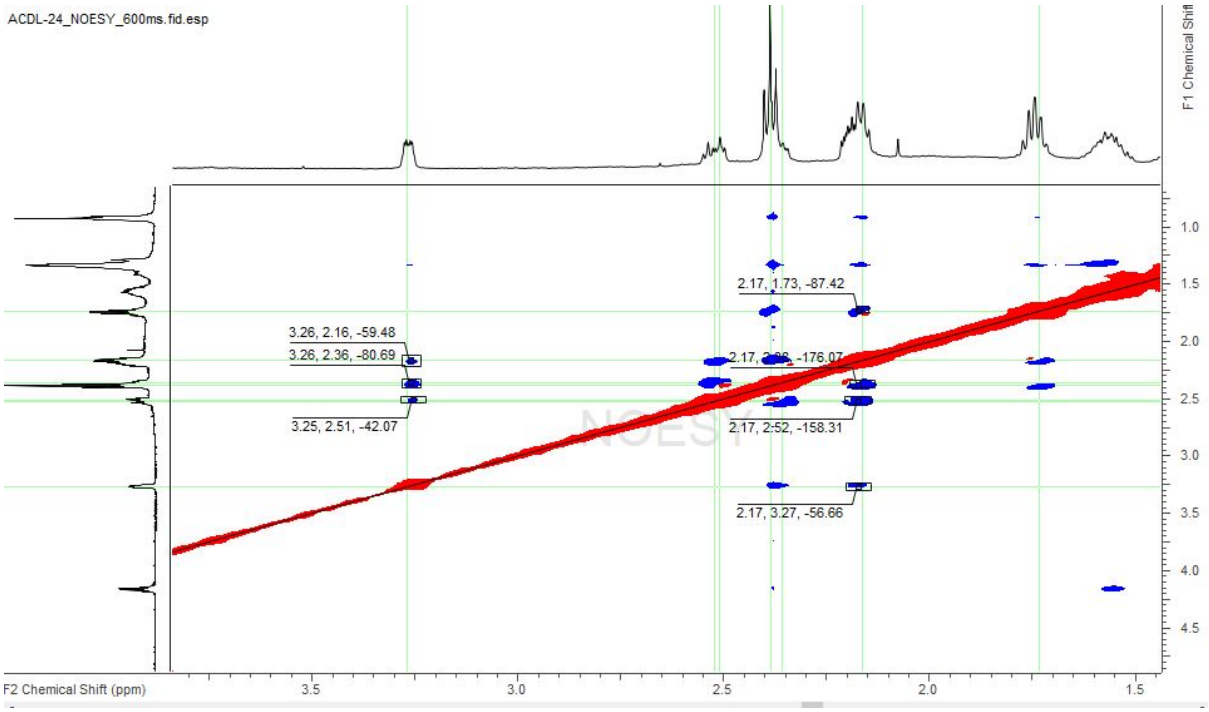

Figure A.III.18b. Zoomed in NOESY Spectrum ($CDCl_3$, 500 MHz) of **12.**

www.manaraa.com

APPENDIX B:

EXPERIMENTAL AND SUPPORTING DATA FOR CHAPTER IV

Biological assay results for Penicillium guanacastense extracts results
MPLC Chromatogram
Fractionation Scheme
Compound Data for tapachulanone A
Report of genetic identification of fungal endophyte *Penicillium guanacastense*

Table B.IV.1. Biological activities against *L. donovani* of screened *Penicillium guanacastense* HDACi, DNMTi, and Control extracts.

Sample name	Axenic Amastigote IC50(µg/ml)	Cytotox (J774) LC_{50}(µg/ml)	Infected Macrophage IC_{50}(µg/ml)	Therapeutic Index TI = LC_{50} / IC_{50}
TAP14-147B-3-Control	14.3	50.0	1.77	28.2
TAP14-147B-3-HDAC	20.0	50.0	1.77	28.2
TAP14-147B-3-DNMT	2.69	50.0	0.076	658

Table B.IV.2. Biological activities against *L. donovani* of extracts generated from scaled up DNMTi modified culture of *Penicillium guanacastense*.

Sample name	Axenic Amastigote IC50(µg/ml)	Cytotox (J774) LC_{50}(µg/ml)	Infected Macrophage IC_{50}(µg/ml)	Therapeutic Index TI = LC_{50} / IC_{50}
TAP14-147B-3-DNMT-crude	-	50.0	3.21	15.6
TAP14-147B-3-DNMT-EtOAc	-	50.0	0.297	168
TAP14-147B-3-DNMT-H2O	-	50.0	>10	5.0
TAP14-147B-3-DNMT-hex	-	50.0	0.205	244

www.manaraa.com

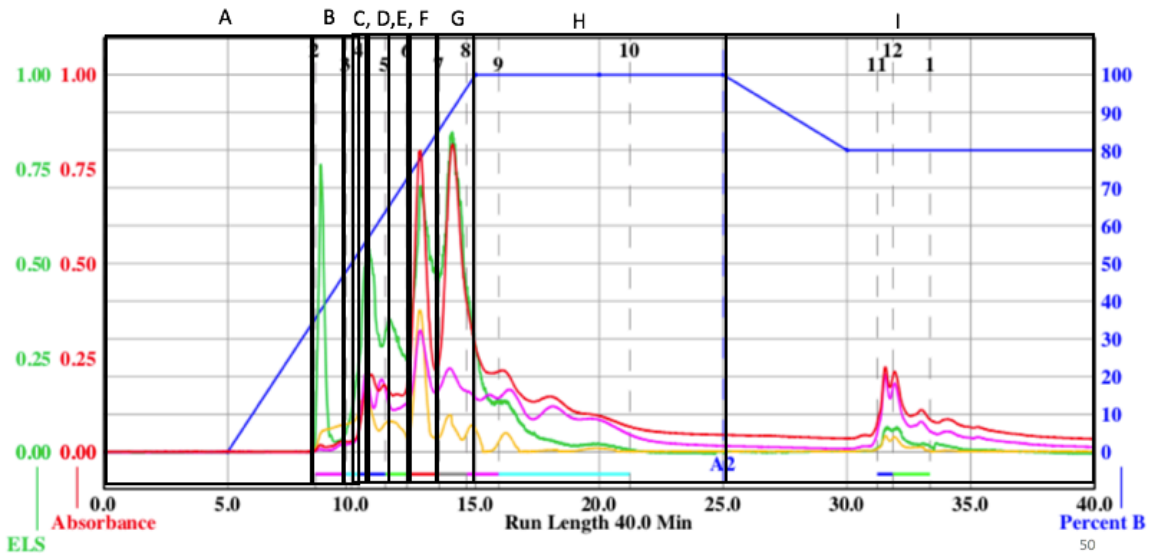

Figure B.IV.1. NP MPLC Chromatogram of ethyl acetate extract obtained from a DNMTi modified culture of *Penicillium guanacastense* grown on rice medium.

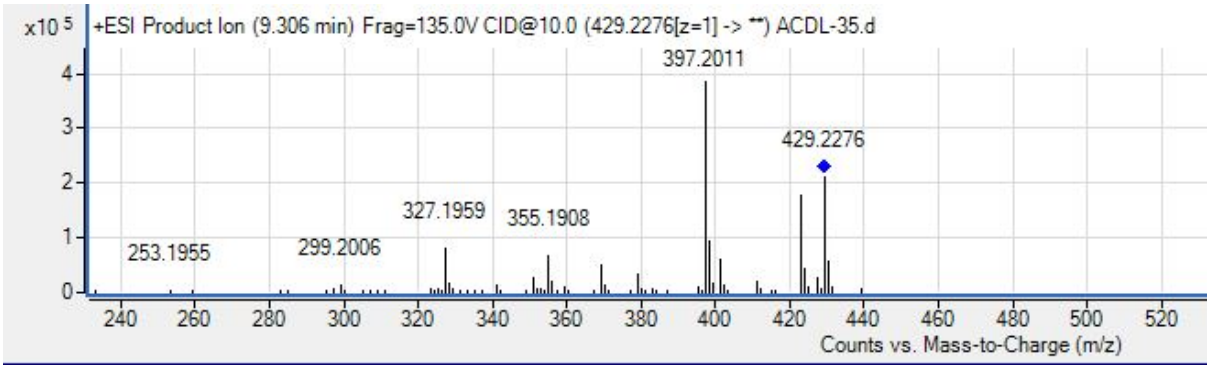

Figure B.IV.2. MS of tapachulanone A **(13)**.

www.manaraa.com

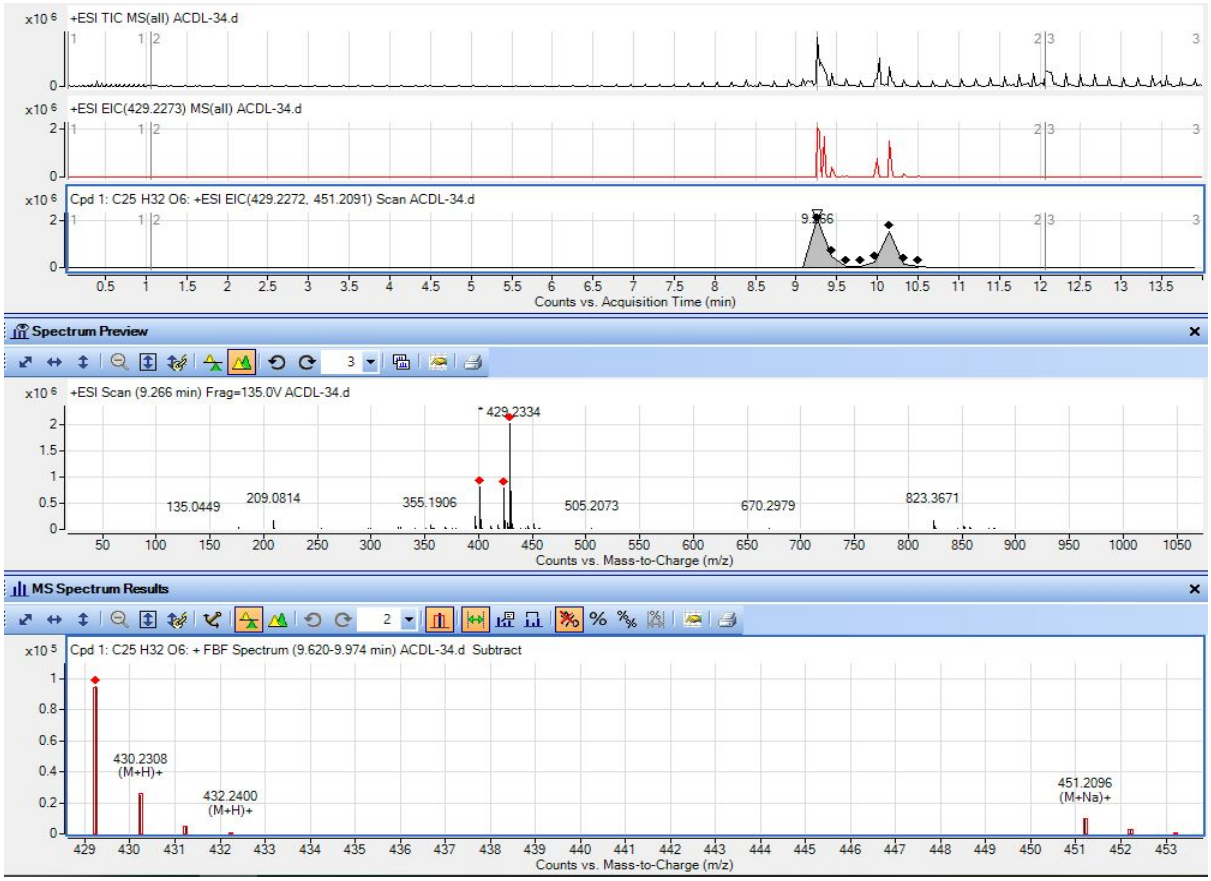

Figure B.IV.3. LC-MS/MS-QToF Chromatogram and Mass Spectrum of tapachulanone A.

Description	Max Score	Total Score	Query Cover	E value	Per. Ident	Accession
Penicillium guanacastense strain SFC102452 small subunit ribosomal RNA gene, partial sequence; internal transcribed spacer 1 and 5.8S ribosomal RNA gene, complete sequence; and internal transcri	609	609	65%	5e-170	96.12%	MH374548.1
Ascomycota sp. isolate LTS567 internal transcribed spacer 1, partial sequence; 5.8S ribosomal RNA gene and internal transcribed spacer 2, complete sequence; and large subunit ribosomal RNA gene,	609	694	75%	5e-170	96.12%	MH430766.1
Penicillium multicolor strain XQ24 18S ribosomal RNA gene, partial sequence; internal transcribed spacer 1, 5.8S ribosomal RNA gene, and internal transcribed spacer 2, complete sequence; and 28S ri	609	750	75%	5e-170	96.12%	KU216726.1
Penicillium guanacastense strain XQ22 18S ribosomal RNA gene, partial sequence; internal transcribed spacer 1 and 5.8S ribosomal RNA gene, complete sequence; and internal transcribed spacer 2, p	609	609	65%	5e-170	96.12%	KU216724.1
Penicillium sclerotiorum strain FRR 1202 18S ribosomal RNA gene, partial sequence; internal transcribed spacer 1, 5.8S ribosomal RNA gene, and internal transcribed spacer 2, complete sequence; anc	609	680	75%	5e-170	96.12%	AY373931.1
Penicillium guanacastense strain JP-NJ2 18S ribosomal RNA gene, partial sequence; internal transcribed spacer 1, 5.8S ribosomal RNA gene, and internal transcribed spacer 2, complete sequence; anc	609	694	75%	5e-170	96.12%	KF991208.1
Penicillium guanacastense strain AS3.15350 18S ribosomal RNA gene, partial sequence; internal transcribed spacer 1, 5.8S ribosomal RNA gene, and internal transcribed spacer 2, complete sequence;	609	694	75%	5e-170	96.12%	KF302657.1
Penicillium guanacastense DAOM 239912 ITS region: from TYPE material	609	680	75%	5e-170	96.12%	NR_111673.1
Penicillium sclerotiorum strain TRXY-33-2 internal transcribed spacer 1, partial sequence; 5.8S ribosomal RNA gene, complete sequence; and internal transcribed spacer 2, partial sequence	601	601	65%	1e-167	95.84%	KP204359.1
Penicillium sclerotiorum isolate F26-05 18S ribosomal RNA gene, partial sequence; internal transcribed spacer 1, 5.8S ribosomal RNA gene, and internal transcribed spacer 2, complete sequence; and 2	595	680	77%	8e-166	95.16%	KX664361.1
Penicillium sp. strain SC13d small subunit ribosomal RNA gene, partial sequence; internal transcribed spacer 1 and 5.8S ribosomal RNA gene, complete sequence; and internal transcribed spacer 2, par	593	593	65%	3e-165	95.84%	MG461662.1
Penicillium sclerotiorum strain SC13c small subunit ribosomal RNA gene, partial sequence; internal transcribed spacer 1 and 5.8S ribosomal RNA gene, complete sequence; and internal transcribed spa	593	593	65%	3e-165	95.84%	MG461661.1
Penicillium vanoranjei CBS 134406 ITS region: from TYPE material	593	669	75%	3e-165	95.84%	NR_120267.1
Penicillium vanoranjei strain DTO119G8 18S ribosomal RNA gene, partial sequence; internal transcribed spacer 1, 5.8S ribosomal RNA gene, and internal transcribed spacer 2, complete sequence; and	593	669	75%	3e-165	95.84%	KC695692.1
Penicillium johnkrugii strain DAOM 239946 internal transcribed spacer 1, partial sequence; 5.8S ribosomal RNA gene and internal transcribed spacer 2, complete sequence; and 28S ribosomal RNA gen	593	678	75%	3e-165	95.84%	JN686450.1
Penicillium sp. strain PC22C small subunit ribosomal RNA gene, partial sequence; internal transcribed spacer 1 and 5.8S ribosomal RNA gene, complete sequence; and internal transcribed spacer 2, pa	585	585	65%	8e-163	95.57%	MH933698.1
Penicillium sp. strain SN22 internal transcribed spacer 1, partial sequence; 5.8S ribosomal RNA gene, complete sequence; and internal transcribed spacer 2, partial sequence	585	585	65%	8e-163	95.29%	MH782634.1
Penicillium sp. strain JC24 small subunit ribosomal RNA gene, partial sequence; internal transcribed spacer 1, 5.8S ribosomal RNA gene, and internal transcribed spacer 2, complete sequence; and larg	585	657	75%	8e-163	95.57%	MG437230.1
Penicillium sp. isolate SI_2 small subunit ribosomal RNA gene, partial sequence; internal transcribed spacer 1, 5.8S ribosomal RNA gene, and internal transcribed spacer 2, complete sequence; and larg	585	857	75%	8e-163	95.57%	MH398044.1
Penicillium sp. isolate SFC102200 small subunit ribosomal RNA gene, partial sequence; internal transcribed spacer 1 and 5.8S ribosomal RNA gene, complete sequence; and internal transcribed spacer	585	627	70%	8e-163	95.57%	MF186132.1
Penicillium sclerotiorum strain SCZ20-2 small subunit ribosomal RNA gene, partial sequence; internal transcribed spacer 1 and 5.8S ribosomal RNA gene, complete sequence; and internal transcribed sp	585	585	65%	8e-163	95.57%	KY445830.1
Penicillium sclerotiorum strain SCZ16-1 internal transcribed spacer 1, partial sequence; 5.8S ribosomal RNA gene, complete sequence; and internal transcribed spacer 2, partial sequence	585	585	65%	8e-163	95.57%	KY445813.1

Figure B.IV.4. Genetic identification report of the fungal endophyte used in all rice cultures.

www.manaraa.com

Table B.IV.3. Crystal structure information for compound tapachulanone A **(13)**

TITL acl_e_3_c_0m_a.res in P2(1)2(1)2(1)

acl_e_3_c_0m.res

created by SHELXL-2017/1 at 13:26:07 on 06-Apr-2018

REM Old TITL ACL_E_3_C_0m in P2(1)2(1)2(1)

REM SHELXT solution in P2(1)2(1)2(1)

REM R1 0.137, Rweak 0.046, Alpha 0.002, Orientation as input

REM Flack x = 0.196 (0.211) from Parsons' quotients

REM Formula found by SHELXT: C25 O6

CELL 1.54178 8.002 12.9619 20.8449 90 90 90

ZERR 4 0.0002 0.0003 0.0006 0 0 0

LATT -1

SYMM 0.5-X,-Y,0.5+Z

SYMM -X,0.5+Y,0.5-Z

SYMM 0.5+X,0.5-Y,-Z

SFAC C H O

UNIT 100 128 24

L.S. 10

PLAN 20

SIZE 0.026 0.05 0.27

TEMP -173.16

BOND $H

list 4

fmap 2

www.manaraa.com

Table B.IV.2. Crystal structure information for compound tapachulanone A **(13)** (cont.)

REM <olex2.extras>

REM <HklSrc "%.\\ACL_E_3_C_0m.hkl">

REM </olex2.extras>

WGHT 0.040600 0.532500

FVAR 0.20813

C1 1 0.262785 0.634966 0.592789 11.00000 0.02916 0.03001 =

0.04109 0.00595 -0.00307 0.00601

AFIX 137

H1A 2 0.290623 0.652803 0.637208 11.00000 -1.50000

H1B 2 0.184732 0.576707 0.592456 11.00000 -1.50000

H1C 2 0.210854 0.694500 0.571755 11.00000 -1.50000

AFIX 0

C2 1 0.371954 0.581201 0.487369 11.00000 0.04669 0.02975 =

0.03327 -0.00029 -0.01433 0.00564

AFIX 137

H2A 2 0.328074 0.643796 0.467082 11.00000 -1.50000

H2B 2 0.285749 0.527499 0.487093 11.00000 -1.50000

H2C 2 0.470017 0.557005 0.463561 11.00000 -1.50000

AFIX 0

C3 1 0.422086 0.605162 0.556837 11.00000 0.02371 0.02408 =

0.02719 0.00112 -0.00246 0.00391

C4 1 0.547385 0.694556 0.555805 11.00000 0.02921 0.02209 =

0.03120 0.00715 0.00206 0.00287

www.manaraa.com

Table B.IV.2. Crystal structure information for compound tapachulanone A **(13)** (cont.)

AFIX 13

H4 2 0.494419 0.756092 0.535218 11.00000 -1.20000

AFIX 0

C5 1 0.610509 0.723708 0.621479 11.00000 0.03223 0.02174 =

0.03358 -0.00101 -0.00083 -0.00211

AFIX 23

H5A 2 0.515403 0.741176 0.649847 11.00000 -1.20000

H5B 2 0.684466 0.784739 0.618423 11.00000 -1.20000

AFIX 0

C6 1 0.707688 0.631639 0.649174 11.00000 0.03010 0.02527 =

0.02773 0.00015 -0.00379 -0.00347

AFIX 23

H6A 2 0.659974 0.612508 0.691348 11.00000 -1.20000

H6B 2 0.825853 0.651590 0.655811 11.00000 -1.20000

AFIX 0

C7 1 0.699290 0.537428 0.603335 11.00000 0.01957 0.02164 =

0.02523 0.00157 -0.00116 -0.00183

C8 1 0.510453 0.513186 0.591816 11.00000 0.02097 0.02085 =

0.02452 0.00127 -0.00309 0.00059

AFIX 13

H8 2 0.458007 0.508406 0.635259 11.00000 -1.20000

AFIX 0

O9 3 0.691856 0.661379 0.517282 11.00000 0.03455 0.02824 =

www.manaraa.com

Table B.IV.2. Crystal structure information for compound tapachulanone A **(13)** (cont.)

0.03192 0.00887 0.00720 0.00262

C10 1 0.771423 0.576425 0.540198 11.00000 0.02353 0.02940 =

0.02812 0.00402 0.00162 -0.00189

O11 3 0.889141 0.542078 0.510865 11.00000 0.03379 0.04212 =

0.03691 0.00836 0.01346 0.00333

C12 1 0.794962 0.444423 0.630631 11.00000 0.01685 0.02331 =

0.02470 0.00213 0.00442 -0.00032

C13 1 0.748081 0.334695 0.609567 11.00000 0.02523 0.02604 =

0.02304 -0.00064 -0.00242 0.00460

C14 1 0.836892 0.306898 0.546303 11.00000 0.05119 0.03432 =

0.02675 -0.00463 0.00454 0.00814

AFIX 137

H14A 2 0.955042 0.326268 0.549145 11.00000 -1.50000

H14B 2 0.784303 0.344264 0.510766 11.00000 -1.50000

H14C 2 0.827818 0.232482 0.538759 11.00000 -1.50000

AFIX 0

C15 1 0.557343 0.322761 0.599956 11.00000 0.02634 0.02198 =

0.03759 -0.00153 -0.00998 -0.00093

AFIX 23

H15A 2 0.534674 0.255964 0.578634 11.00000 -1.20000

H15B 2 0.502089 0.321546 0.642444 11.00000 -1.20000

AFIX 0

C16 1 0.482407 0.409269 0.559938 11.00000 0.03240 0.02192 =

www.manaraa.com

Table B.IV.2. Crystal structure information for compound tapachulanone A **(13)** (cont.)

0.03556 -0.00199 -0.01332 -0.00050

AFIX 23

H16A 2 0.534391 0.409405 0.516841 11.00000 -1.20000

H16B 2 0.361018 0.397305 0.554569 11.00000 -1.20000

AFIX 0

C17 1 0.918877 0.458648 0.672676 11.00000 0.01772 0.02495 =

0.03121 0.00018 0.00153 -0.00284

AFIX 43

H17 2 0.951458 0.527663 0.681558 11.00000 -1.20000

AFIX 0

C18 1 1.010204 0.374336 0.706819 11.00000 0.02009 0.03199 =

0.03656 0.00249 -0.00539 0.00180

C19 1 1.187860 0.405109 0.725169 11.00000 0.02520 0.03892 =

0.05227 0.00633 -0.00794 -0.00214

AFIX 137

H19A 2 1.253100 0.418027 0.686200 11.00000 -1.50000

H19B 2 1.239848 0.349204 0.749736 11.00000 -1.50000

H19C 2 1.184779 0.467866 0.751360 11.00000 -1.50000

AFIX 0

C20 1 0.910201 0.325315 0.764015 11.00000 0.02988 0.02569 =

0.03293 0.00393 -0.00276 -0.00032

C21 1 0.916721 0.364830 0.831170 11.00000 0.05104 0.03986 =

0.03195 0.00484 -0.00742 -0.00868

www.manaraa.com

Table B.IV.2. Crystal structure information for compound tapachulanone A **(13)** (cont.)

AFIX 137

H21A 2 0.850484 0.319762 0.859069 11.00000 -1.50000

H21B 2 0.871032 0.434942 0.832569 11.00000 -1.50000

H21C 2 1.032933 0.365750 0.845995 11.00000 -1.50000

AFIX 0

O22 3 0.987428 0.224620 0.749913 11.00000 0.03296 0.03150 =

0.04202 0.00724 -0.00891 0.00457

C23 1 0.990810 0.261954 0.682675 11.00000 0.02264 0.03062 =

0.03370 0.00543 -0.00347 0.00345

C24 1 1.123447 0.208335 0.643879 11.00000 0.02867 0.04397 =

0.06277 -0.00312 0.00360 0.01153

AFIX 137

H24A 2 1.229514 0.209828 0.667364 11.00000 -1.50000

H24B 2 1.136960 0.243680 0.602644 11.00000 -1.50000

H24C 2 1.090263 0.136569 0.636357 11.00000 -1.50000

AFIX 0

C25 1 0.799903 0.259924 0.665655 11.00000 0.02101 0.02321 =

0.02519 -0.00103 -0.00120 0.00299

C26 1 0.737204 0.150618 0.653325 11.00000 0.03244 0.02484 =

0.03465 -0.00248 -0.00681 0.00676

O27 3 0.808545 0.089799 0.619656 11.00000 0.04706 0.03208 =

0.06068 -0.01546 0.00252 0.00581

O28 3 0.592574 0.131149 0.682192 11.00000 0.03073 0.02164 =

www.manaraa.com

Table B.IV.2. Crystal structure information for compound tapachulanone A **(13)** (cont.)

```
      0.05045    0.00086   -0.00407   -0.00457
C29   1    0.513447    0.034257    0.664378    11.00000    0.04148    0.02265 =
      0.07206    0.00342   -0.01542   -0.00622
AFIX 137
H29A  2    0.490715    0.034107    0.618181    11.00000   -1.50000
H29B  2    0.408236    0.026597    0.687966    11.00000   -1.50000
H29C  2    0.588083   -0.023208    0.674986    11.00000   -1.50000
AFIX   0
C30   1    0.742056    0.306344    0.731144    11.00000    0.02539    0.01818 =
      0.02846    0.00640    0.00161   -0.00231
O31   3    0.605695    0.323296    0.751092    11.00000    0.02608    0.03510 =
      0.03294   -0.00020    0.00564   -0.00186
HKLF 4
REM  acl_e_3_c_0m_a.res in P2(1)2(1)2(1)
REM R1 =  0.0457 for    3595 Fo > 4sig(Fo)  and  0.0617 for all    4369 data
REM    287 parameters refined using      0 restraints
END

WGHT      0.0406      0.5324
REM Highest difference peak  0.194,  deepest hole -0.223,  1-sigma level  0.044
Q1    1   0.6528  0.4170  0.6983  11.00000  0.05    0.19
Q2    1   0.8745  0.1919  0.7708  11.00000  0.05    0.18
Q3    1   0.8095  0.4408  0.6676  11.00000  0.05    0.18
```


www.manaraa.com

Table B.IV.2. Crystal structure information for compound tapachulanone A **(13)** (cont.)

Q4 1 0.8976 0.2493 0.6621 11.00000 0.05 0.17

Q5 1 0.4628 0.5554 0.5694 11.00000 0.05 0.17

Q6 1 0.4917 0.6397 0.5477 11.00000 0.05 0.17

Q7 1 0.9601 0.4189 0.6923 11.00000 0.05 0.16

Q8 1 0.7700 0.2966 0.6310 11.00000 0.05 0.16

Q9 1 0.9969 0.5635 0.4889 11.00000 0.05 0.16

Q10 1 0.7552 0.2403 0.5371 11.00000 0.05 0.16

Q11 1 0.6583 0.3188 0.5980 11.00000 0.05 0.16

Q12 1 0.7374 0.4909 0.6137 11.00000 0.05 0.15

Q13 1 0.1857 0.6982 0.5855 11.00000 0.05 0.15

Q14 1 1.0943 0.3978 0.6959 11.00000 0.05 0.15

Q15 1 0.6241 -0.0182 0.6444 11.00000 0.05 0.15

Q16 1 0.7717 0.2803 0.6988 11.00000 0.05 0.14

Q17 1 1.0010 0.4588 0.6074 11.00000 0.05 0.14

Q18 1 0.6650 0.2793 0.7538 11.00000 0.05 0.14

Q19 1 0.3763 0.0397 0.6793 11.00000 0.05 0.14

Q20 1 1.0628 0.0546 0.7057 11.00000 0.05 0.14

REM The information below was added by Olex2.

REM

REM R1 = 0.0457 for 3595 Fo > 4sig(Fo) and 0.0617 for all 16442 data

REM n/a parameters refined using n/a restraints

REM Highest difference peak 0.19, deepest hole -0.22

REM Mean Shift 0, Max Shift 0.000.

www.manaraa.com

Table B.IV.2. Crystal structure information for compound tapachulanone A **(13)** (cont.)

REM +++ Tabular Listing of Refinement Information +++

REM R1_all = 0.0617

REM R1_gt = 0.0457

REM wR_ref = 0.1043

REM GOOF = 1.046

REM Shift_max = 0.000

REM Shift_mean = 0

REM Reflections_all = 16442

REM Reflections_gt = 3595

REM Parameters = n/a

REM Hole = -0.22

REM Peak = 0.19

REM Flack = 0.26(13)

www.manaraa.com

APPENDIX C:

EXPERIMENTAL AND SUPPORTING DATA FOR CHAPTER 5

Genetic report
Data sets spreadsheet
MPLC Chromatogram
Fractionation Scheme
LC-MS/MS QToF Tuning reports

Description	Max Score	Total Score	Query Cover	E value	Per. Ident	Accession
Streptomyces azureus strain CDMUM60.1 16S ribosomal RNA gene, partial sequence	821	942	66%	0.0	97.78%	MN004836.1
Streptomyces thermocarboxydus strain VIEV_MKB_Cattle_245-VIEV 16S ribosomal RNA gene, partial sequence	821	821	58%	0.0	97.78%	MK968097.1
Streptomyces thermocarboxydus partial 16S rRNA gene, isolate YPD_B3_IIIB	821	821	58%	0.0	97.78%	LR215106.1
Streptomyces thermocarboxydus strain VIEV_MKB_Cattle_236-VIEV 16S ribosomal RNA gene, partial sequence	821	821	58%	0.0	97.78%	MK967807.1
Streptomyces sp. strain A22 16S ribosomal RNA gene, partial sequence	821	861	60%	0.0	97.78%	MK949152.1
Streptomyces thermocarboxydus gene for 16S ribosomal RNA, partial sequence, strain: AH AF1	821	821	58%	0.0	97.78%	LC152202.1
Streptomyces sp. strain PU MM29 16S ribosomal RNA gene, partial sequence	821	821	58%	0.0	97.78%	MH179306.1
Streptomyces werraensis strain BPSCV128 16S ribosomal RNA gene, partial sequence	821	821	58%	0.0	97.78%	MK855316.1
Streptomyces cellulosae strain BPSCV123 16S ribosomal RNA gene, partial sequence	821	821	58%	0.0	97.78%	MK855311.1
Streptomyces steffisburgensis strain BPSCV117 16S ribosomal RNA gene, partial sequence	821	887	63%	0.0	97.78%	MK855305.1
Streptomyces sp. strain BPSCV111 16S ribosomal RNA gene, partial sequence	821	821	58%	0.0	97.78%	MK855299.1
Streptomyces cellulosae strain BPSCV103 16S ribosomal RNA gene, partial sequence	821	821	58%	0.0	97.78%	MK855291.1
Streptomyces cellulosae strain BPSCV101 16S ribosomal RNA gene, partial sequence	821	821	58%	0.0	97.78%	MK855289.1
Streptomyces atrovirens strain BPSCV90 16S ribosomal RNA gene, partial sequence	821	821	58%	0.0	97.78%	MK855278.1
Streptomyces cellulosae strain BPSCV79 16S ribosomal RNA gene, partial sequence	821	821	58%	0.0	97.78%	MK855267.1
Streptomyces cellulosae strain BPSCV53 16S ribosomal RNA gene, partial sequence	821	821	58%	0.0	97.78%	MK855241.1
Streptomyces cellulosae strain BPSCV45 16S ribosomal RNA gene, partial sequence	821	821	58%	0.0	97.78%	MK855233.1
Streptomyces thermocarboxydus strain KAS-1 16S ribosomal RNA gene, partial sequence	821	821	58%	0.0	97.78%	MK788355.1
Streptomyces werraensis strain TB21 16S ribosomal RNA gene, partial sequence	821	928	66%	0.0	97.78%	MH656775.1
Streptomyces sp. strain PU-MM23 16S ribosomal RNA gene, partial sequence	821	821	58%	0.0	97.78%	MH173267.1
Streptomyces sp. strain IR-SGS-Y1 16S ribosomal RNA gene, partial sequence	821	821	58%	0.0	97.78%	MK719896.1
Streptomyces thermocarboxydus strain A15 16S ribosomal RNA gene, partial sequence	821	865	60%	0.0	97.78%	MK680818.1

Figure C.V.1. Genetic identification report of the *Streptomyces azureus* contaminant found.

www.manaraa.com

Ranking of culture conditions

The Mass Hunter software evaluated the amount of tapachulanone A produced in each OSMAC cultures designed. The name of samples reflects the conditions in which the cultures were grown according to the following scheme:

M – T – X – Y – Z – E

M= medium (A, B, C, D, or R), T= Temperature (23 or 30), X= Light conditions (L or D), Y= pH (6.2 or 8.4) or salinity (3.4 or 6.8), Z = amount of fungus inoculated (2, 4 or 8), E= extraction stage (E1 or E2).

When detected, the intensity of the molecular ion (m/z 429.2273 $[M+H]^+$) provided ranking of the 526 culture conditions listed in the table below.

Table C.V.1. OSMAC cultures variations.

			Temperature (°C)				pH		Salinity		Pieces of fungus added			
#	Sample Name	Mass crude (mg)	23	30	Light	Dark	acid	base	3.4%	6.8%	2	4	8	429.2273 peak intensity detected in LCMS (x10^5)
1	B30-D-2-ac-E2	7.1	0	1	0	1	1	0	0	0	1	0	0	0.75
2	A23-L-8-ac-E2	3.3	1	0	1	0	1	0	0	0	0	0	1	0.6
3	A23-L-4-ba-E1	5.4	1	0	1	0	0	1	0	0	0	1	0	0.45
4	R23-L-8-6.8-E1	35	1	0	1	0	0	0	0	1	0	0	1	0.45
5	R23-L-2-6.8-E1	7.5	1	0	1	0	0	0	0	1	1	0	0	0.4
6	R23-L-4-6.8-E2	12	1	0	1	0	0	0	0	1	0	1	0	0.4
7	R23-L-4-ba-E2	14	1	0	1	0	0	1	0	0	0	1	0	0.4
8	R23-L-4-ba-E1	9.6	1	0	1	0	0	1	0	0	0	1	0	0.35
9	R23-L-8-ba-E1	36	1	0	1	0	0	1	0	0	0	0	1	0.35
10	A23-L-2-E2	3.5	1	0	1	0	0	0	0	0	1	0	0	0.3
11	A23-L-4-ac-E1	11	1	0	1	0	1	0	0	0	0	1	0	0.3
12	C23-L-8-ba-E1	26	1	0	1	0	0	1	0	0	0	0	1	0.3
13	D23-L-4-ba-E1	16	1	0	1	0	0	1	0	0	0	1	0	0.3
14	R23-L-2-3.4-E1	16	1	0	1	0	0	0	1	0	1	0	0	0.3

www.manaraa.com

Table C.V.1.cont.

15	R23-L-2-3,4-E2	13	1	0	1	0	0	0	1	0	1	0	0	0.3
16	R23-L-8-3,4-E1	17	1	0	1	0	0	0	1	0	0	0	1	0.3
17	B23-L-2-E1	1.6	1	0	1	0	0	0	0	0	1	0	0	0.27
18	B23-L-2-ba-E2	1.9	1	0	1	0	0	1	0	0	1	0	0	0.26
19	A23-L-2-E1	3.1	1	0	1	0	0	0	0	0	1	0	0	0.25
20	R23-L-4-ac-E1	7.1	1	0	1	0	1	0	0	0	0	1	0	0.25
21	R23-L-8-3,4-E2	13	1	0	1	0	0	0	1	0	0	0	1	0.25
22	D23-L-2-ba-E2	2.2	1	0	1	0	0	1	0	0	1	0	0	0.24
23	B23-L-8-ba-E2	1.3	1	0	1	0	0	1	0	0	0	0	1	0.23
24	D23-L-2-ac-E1	44	1	0	1	0	1	0	0	0	1	0	0	0.22
25	A23-L-2-3,4-E1	3.4	1	0	1	0	0	0	1	0	1	0	0	0.2
26	A23-L-2-3,4-E2	0.71	1	0	1	0	0	0	1	0	1	0	0	0.2
27	A23-L-4-ba-E2	0.76	1	0	1	0	0	1	0	0	0	1	0	0.2
28	B23-L-2-ba-E1	6.1	1	0	1	0	0	1	0	0	1	0	0	0.2
29	C23-L-8-ac-E2	21	1	0	1	0	1	0	0	0	0	0	1	0.2
30	D23-L-4-3,4-E1	5.7	1	0	1	0	0	0	1	0	0	1	0	0.2
31	R30-D-4-ac-E1	7.8	0	1	0	1	1	0	0	0	0	1	0	0.2
32	D23-L-4-ac-E2	49	1	0	1	0	1	0	0	0	0	1	0	0.18
33	D23-L-8-ba-E2	1.7	1	0	1	0	0	1	0	0	0	0	1	0.16
34	B23-L-4-3,4-E2	2.2	1	0	1	0	0	0	1	0	0	1	0	0.15
35	B23-L-8-ba-E1	9.5	1	0	1	0	0	1	0	0	0	0	1	0.15
36	C23-L-2-ac-E2	4.9	1	0	1	0	1	0	0	0	1	0	0	0.15
37	C23-L-4-ac-E2	5.5	1	0	1	0	1	0	0	0	0	1	0	0.15
38	D23-L-2-ba-E1	4.8	1	0	1	0	0	1	0	0	1	0	0	0.15
39	R30-L-8-3,4-E1	21	0	1	1	0	0	0	1	0	0	0	1	0.15
40	C23-L-8-ba-E2	1.7	1	0	1	0	0	1	0	0	0	0	1	0.14
41	D23-L-8-ac-E2	6	1	0	1	0	1	0	0	0	0	0	1	0.14
42	A30-L-2-E1	20	0	1	1	0	0	0	0	0	1	0	0	0.14
43	B30-L-2-ac-E1	1.1	0	1	1	0	1	0	0	0	1	0	0	0.14
44	B30-L-8-ac-E1	1.1	0	1	1	0	1	0	0	0	0	0	1	0.14
45	B30-L-8-ba-E1	0.5	0	1	1	0	0	1	0	0	0	0	1	0.14
46	B30-L-8-ba-E2	2.3	0	1	1	0	0	1	0	0	0	0	1	0.14
47	D30-L-4-ac-E1	1.1	0	1	1	0	1	0	0	0	0	1	0	0.14
48	R30-L-2-3,4-E2	34	0	1	1	0	0	0	1	0	1	0	0	0.14
49	A30-L-2-ac-E1	1.4	0	1	1	0	1	0	0	0	1	0	0	0.13
50	C30-L-8-ba-E2	6.2	0	1	1	0	0	1	0	0	0	0	1	0.13
51	R30-L-4-3,4-E1	8.9	0	1	1	0	0	0	1	0	0	1	0	0.13
52	R30-L-4-ac-E1	11	0	1	1	0	1	0	0	0	0	1	0	0.13
53	R30-L-8-ac-E1	64	0	1	1	0	1	0	0	0	0	0	1	0.13
54	D23-L-2-ac-E2	3.9	1	0	1	0	1	0	0	0	1	0	0	0.12
55	B30-L-2-E2	3.5	0	1	1	0	0	0	0	0	1	0	0	0.12
56	C30-L-2-E2	4.1	0	1	1	0	0	0	0	0	1	0	0	0.12

www.manaraa.com

Table C.V.1.cont.

57	D30-L-8-ac-E2	8.3	0	1	1	0	1	0	0	0	0	0	1	0.12
58	R30-L-4-3.4-E2	13	0	1	1	0	0	0	1	0	0	1	0	0.12
59	A30-L-4-ac-E2	5.5	0	1	1	0	1	0	0	0	0	1	0	0.11
60	R30-D-8-ac-E1	12	0	1	0	1	1	0	0	0	0	0	1	0.11
61	C23-L-2-ba-E2	4.6	1	0	1	0	0	1	0	0	1	0	0	0.1
62	D23-L-4-3.4-E2	2.6	1	0	1	0	0	0	1	0	0	1	0	0.1
63	R23-L-2-6.8-E2	12	1	0	1	0	0	0	0	1	1	0	0	0.1
64	R23-L-2-ac-E1	8.5	1	0	1	0	1	0	0	0	1	0	0	0.1
65	A30-L-8-ac-E1	1.5	0	1	1	0	1	0	0	0	0	0	1	0.1
66	C30-L-4-ac-E1	23	0	1	1	0	1	0	0	0	0	1	0	0.1
67	R30-L-2-E2	18	0	1	1	0	0	0	0	0	1	0	0	0.1
68	R30-L-8-ac-E2	7	0	1	1	0	1	0	0	0	0	0	1	0.1
69	R30-D-4-3.4-E2	17	0	1	0	1	0	0	1	0	0	1	0	0.1
70	R30-L-4-0.68-E1	100	0	1	1	0	0	0	0	1	0	1	0	0.09
71	R30-L-4-ac-E2	13	0	1	1	0	1	0	0	0	0	1	0	0.09
72	A30-D-8-3.4-E1	0.46	0	1	0	1	0	0	1	0	0	0	1	0.09
73	B23-L-8-3.4-E2	71	1	0	1	0	0	0	1	0	0	0	1	0.08
74	D23-L-4-ac-E1	28	1	0	1	0	1	0	0	0	0	1	0	0.08
75	A30-L-2-E2	0.81	0	1	1	0	0	0	0	0	1	0	0	0.08
76	A30-L-8-ac-E2	10	0	1	1	0	1	0	0	0	0	0	1	0.08
77	D30-L-2-E2	2.9	0	1	1	0	0	0	0	0	1	0	0	0.08
78	R30-D-2-3.4-E2	15	0	1	0	1	0	0	1	0	1	0	0	0.08
79	A23-L-8-ba-E2	3.6	1	0	1	0	0	1	0	0	0	0	1	0.075
81	D23-L-8-3.4-E1	8.7	1	0	1	0	0	0	1	0	0	0	1	0.07
82	C30-L-4-ac-E2	8.2	0	1	1	0	1	0	0	0	0	1	0	0.07
83	C30-L-8-ac-E2	5.4	0	1	1	0	1	0	0	0	0	0	1	0.07
84	R30-D-8-ba-E2	25	0	1	0	1	0	1	0	0	0	0	1	0.07
85	B23-L-8-3.4-E1	11	1	0	1	0	0	0	1	0	0	0	1	0.06
86	D23-L-2-E2	3.9	1	0	1	0	0	0	0	0	1	0	0	0.06
87	R23-L-4-6.8-E1	71	1	0	1	0	0	0	0	1	0	1	0	0.06
88	A23-D-8-3.4-E1	4.4	1	0	0	1	0	0	1	0	0	0	1	0.06
89	B23-D-4-ba-E2	0.61	1	0	0	1	0	1	0	0	0	1	0	0.06
90	A30-L-2-ac-E2	9.5	0	1	1	0	1	0	0	0	1	0	0	0.06
91	C30-L-2-E1	1.7	0	1	1	0	0	0	0	0	1	0	0	0.06
92	R30-L-2-3.4-E1	9.1	0	1	1	0	0	0	1	0	1	0	0	0.06
93	R30-L-4-0.68-E2	66	0	1	1	0	0	0	0	1	0	1	0	0.06
94	C30-D-4-ac-E1	3.5	0	1	0	1	1	0	0	0	0	1	0	0.06
95	R30-D-2-ac-E1	12	0	1	0	1	1	0	0	0	1	0	0	0.06
96	R30-D-8-3.4-E1	43	0	1	0	1	0	0	1	0	0	0	1	0.06
97	R30-D-8-6.8-E1	61	0	1	0	1	0	0	0	1	0	0	1	0.06

www.manaraa.com

Table C.V.1.cont.

98	C30-L-2-ac-E2	6.9	0	1	1	0	1	0	0	0	1	0	0	0.055
99	B30-D-2-E2	1.6	0	1	0	1	0	0	0	0	1	0	0	0.055
100	C23-L-4-3.4-E2	2.4	1	0	1	0	0	0	1	0	0	1	0	0.05
101	R23-L-2-ba-E1	7.6	1	0	1	0	0	1	0	0	1	0	0	0.05
102	A23-D-8-ba-E1	0.41	1	0	0	1	0	1	0	0	0	0	1	0.05
103	B30-L-2-3.4-E1	1.3	0	1	1	0	0	0	1	0	1	0	0	0.05
104	B30-L-2-ac-E2	17	0	1	1	0	1	0	0	0	1	0	0	0.05
105	C30-L-2-ac-E1	3.4	0	1	1	0	1	0	0	0	1	0	0	0.05
106	R30-L-2-E1	39	0	1	1	0	0	0	0	0	1	0	0	0.05
107	B30-D-4-6.8-E1	0.48	0	1	0	1	0	0	0	1	0	1	0	0.05
108	C30-D-2-E2	3.9	0	1	0	1	0	0	0	0	1	0	0	0.05
109	B23-D-2-6.8-E2	2.1	1	0	0	1	0	0	0	1	1	0	0	0.04
110	R23-D-8-3.4-E1	8.2	1	0	0	1	0	0	1	0	0	0	1	0.04
111	A30-L-2-6.8-E1	0.46	0	1	1	0	0	0	0	1	1	0	0	0.04
112	B30-D-8-ac-E1	2.5	0	1	0	1	1	0	0	0	0	0	1	0.04
113	B30-D-8-ba-E1	26	0	1	0	1	0	1	0	0	0	0	1	0.04
114	D23-L-2-E1	105	1	0	1	0	0	0	0	0	1	0	0	0.035
115	A30-L-8-ba-E1	4.6	0	1	1	0	0	1	0	0	0	0	1	0.035
116	D30-L-8-ac-E1	1.9	0	1	1	0	1	0	0	0	0	0	1	0.035
117	D23-L-8-ba-E1	25	1	0	1	0	0	1	0	0	0	0	1	0.03
118	R23-D-8-6.8-E1	6.7	1	0	0	1	0	0	0	1	0	0	1	0.03
119	C30-L-8-ba-E1	4.7	0	1	1	0	0	1	0	0	0	0	1	0.03
120	C30-D-2-ac-E2	3.3	0	1	0	1	1	0	0	0	1	0	0	0.03
121	R30-D-2-3.4-E1	27	0	1	0	1	0	0	1	0	1	0	0	0.03
122	A30-L-4-ac-E1	1.7	0	1	1	0	1	0	0	0	0	1	0	0.025
123	D30-L-2-E1	1.4	0	1	1	0	0	0	0	0	1	0	0	0.025
124	R30-D-8-ba-E1	17	0	1	0	1	0	1	0	0	0	0	1	0.025
125	A30-L-4-3.4-E1	2.1	0	1	1	0	0	0	1	0	0	1	0	0.022
126	D23-L-8-3.4-E2	4.2	1	0	1	0	0	0	1	0	0	0	1	0.02
127	B23-D-2-ba-E1	7.8	1	0	0	1	0	1	0	0	1	0	0	0.02
128	A30-L-8-ba-E2	0.12	0	1	1	0	0	1	0	0	0	0	1	0.02
129	A30-D-2-E1	28	0	1	0	1	0	0	0	0	1	0	0	0.02
130	A30-D-4-ac-E1	68	0	1	0	1	1	0	0	0	0	1	0	0.02
131	R30-D-4-ac-E2	10	0	1	0	1	1	0	0	0	0	1	0	0.02
132	D23-L-4-ba-E2	0.8	1	0	1	0	0	1	0	0	0	1	0	0.01
133	B30-D-4-3.4-E1	2.9	0	1	0	1	0	0	1	0	0	1	0	0.008
134	B30-D-4-3.4-E2	7.3	0	1	0	1	0	0	1	0	0	1	0	0.008
135	B30-D-8-ac-E2	50	0	1	0	1	1	0	0	0	0	0	1	0.006
136	C30-D-2-ba-E1	31	0	1	0	1	0	1	0	0	1	0	0	0.006

www.manaraa.com

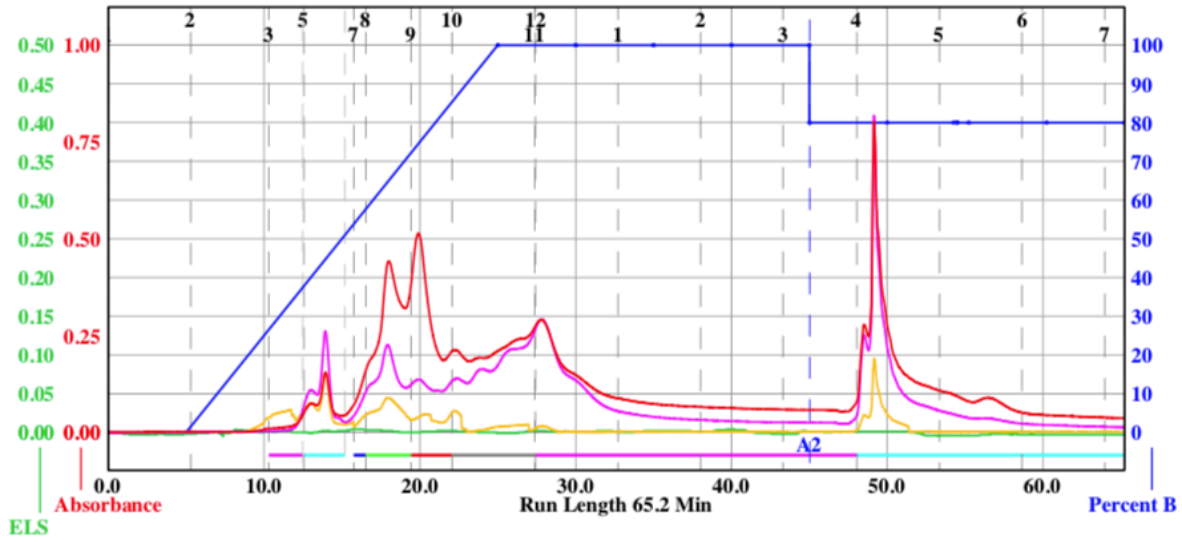

Figure C.V.2. NP MPLC Chromatogram of ethyl acetate extract obtained from a DNMT modified culture of *Penicillium guanacastense* grown on 6.8% saline rice medium.

HiP Sampler	
Injection Volume	10.0 µL
Injection with needle wash	Yes
Needle Wash Mode	Flush Port
Needle Wash Time	3.0 sec
Draw Speed	100.0 µL/min
Eject Speed	100.0 µL/min
Draw Position	0.0 min
Equilibration Time	0.0 sec
Sample Flush-out Factor	5.0x Inj. Volume

Pump	
Flow	0.40 mL/min
Solvent A	H2O+0.1% Formic acid
Solvent B	ACN+0.1% Formic acid
Pressure Limit Min	0.00bar
Pressure Limit Max	600.00 bar
Stop Time	14.00 min
Posttime	1.00 min

Time Table

Time [min]	A [%]	B [%]	Flow [mL/min]
0.00	90.00	10.00	0.40
0.01	98.00	2.00	0.40
2.00	98.00	2.00	0.40
10.00	2.00	98.00	0.40
12.00	2.00	98.00	0.40
12.01	98.00	2.00	0.40
14.00	98.00	2.00	0.40

Figure C.V.3. Acquisition parameters for LC-MS/MS experiments.

www.manaraa.com

TOF Results

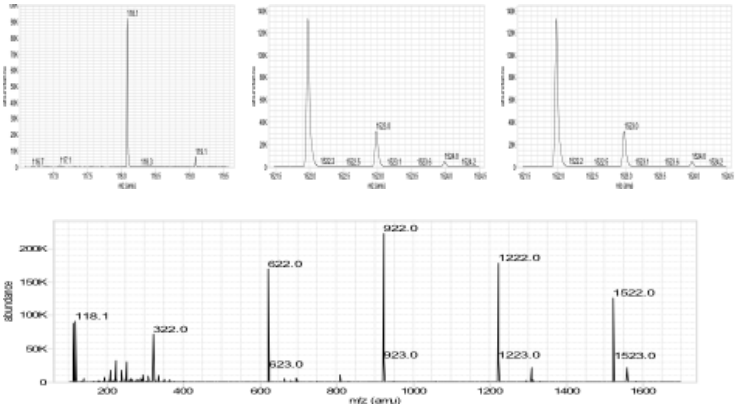

Calibration Data Table

m/z	Actual	Time	Abund	Res	FWHM	Delta (m/z)	Delta (PPM)
118,086255	118,086255	32,241674	89835	10725	0,0114	0	0
322,048121	322,048128	52,585452	76244	15436	0,0213	0,000007	0,02
622,02896	622,028908	72,687426	175655	25557	0,0247	-0,000052	-0,08
922,009798	922,009924	88,275525	232808	33721	0,0277	0,000126	0,14
1221,990637	1221,990515	101,473346	189185	35591	0,0347	-0,000122	-0,1
1521,971475	1521,971517	113,128184	133404	34617	0,0444	0,000042	0,03

Setpoints

Parameter	Setting	Actual
Source		
Gas Temp	325	330
Drying Gas	5	5
Nebulizer Pressure	20	20
Capillary	4000	-4000
Sheath Gas Temperature	295	
Sheath Gas Flow	12	
Nozzle Voltage	2000	
Optics 1		
Fragmentor	176	
Skimmer	44,5	
Oct 1 RF Vpp	750	
Oct DC 1	25	
Lens 1	22,6	
Lens 2	10,5	
Lens 2 RF Enabled	Yes	
Lens 2 RF Voltage	0	
Lens 2 RF Phase	0	
Quad		
TTI Quad AMU	148	
Quad DC	21,5	
Post Filter DC	21,5	
Cell		
Col Cell Gas Flow	22	
Hex RF	550	
Hex DC	19,5	
Hex Delta	-7	
Cell Entrance	20,5	
Hex 2 RF	600	
Hex 2 DC	12,5	
Hex 2 DV	-0,4	
Hex 3 DC	11,2	
Optics 2		
Ion Focus	-40	
Slicer	-4,5	
Extractor DC	13,5	
Top Slit	-0,8	
Bottom Slit	-0,65	

Parameter	Setting	Actual
TOF		
Pusher	1200	
Puller	-700	
Puller Offset	34	
Acc Focus	-1930	
Front Mirror	-7000	
Mid Mirror	-1676,1	
Back Mirror	1250	
Minimum Mass	100	
Maximum Mass	1700	
Acquisition Rate	1	
Acquisition Time	1000	
Length of Transients	423216	
#Transients / Spectrum	8148	
Low Gain PreAmpOffset	33108	
Gain Abund Ratio	12.0	
Gain T0 Offset	-0.088	
Acq Hold Off Delay (ns)	13704	
Detector		
MCP	815	
PreAmpOffset	30006	

Other Actuals:

Parameter	Actual
Quad Temp	100
Rough Vac	1,96
Quad Vac	2,32E-05
TOF Vac	4,67E-07
Capillary Current	5,468
Chamber Current	6,59
Turbo 1 Speed	100
Turbo 1 Power	165
Turbo 2 Speed	100
Turbo 2 Power	42

Calibration Coefficients (in µs) *alWeighting:*

a	0,3479649	**a2**	1,72493E-06	**c2**	2,2033E-11	**e2**	0
t0	1,012121	**b2**	-1,48257E-09	**d2**	-8,924E-14	**f2**	0

Term Flags: 0x0074 **Trad:** 0 **Poly:** 6

Figure C.V.4. LC-MS/MS QToF tuning report for experiment with deionized water rice culture.

www.manaraa.com

TOF Results

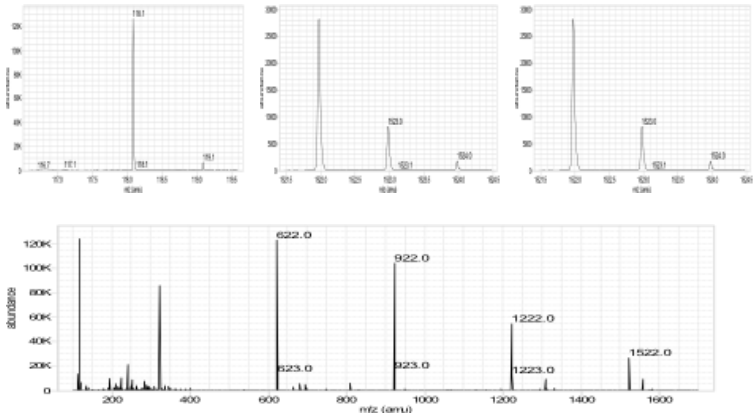

Calibration Data Table

m/z	Actual	Time	Abund	Res	FWHM	Delta (m/z)	Delta (PPM)
118,086255	118,086254	32,242595	122283	11162	0,0109	-0,000001	0
322,048121	322,048123	52,587064	83366	15955	0,0206	0,000002	0,01
622,02896	622,028959	72,689705	119691	27060	0,0233	-0,000001	0
922,009798	922,00979	88,278281	91071	36355	0,0257	-0,000008	-0,01
1221,990637	1221,990648	101,476514	49729	39614	0,0312	0,000011	0,01
1521,971475	1521,971471	113,131692	24424	39521	0,0389	-0,000004	0

Setpoints

Parameter	Setting	Actual
Source		
Gas Temp	325	326
Drying Gas	5	5
Nebulizer Pressure	20	20
Capillary	4000	-4000
Sheath Gas Temperature	295	
Sheath Gas Flow	12	
Nozzle Voltage	2000	
Optics 1		
Fragmentor	176	
Skimmer	44,5	
Oct 1 RF Vpp	750	
Oct DC 1	25	
Lens 1	22,6	
Lens 2	10,5	
Lens 2 RF Enabled	Yes	
Lens 2 RF Voltage	0	
Lens 2 RF Phase	0	
Quad		
TTI Quad AMU	148	
Quad DC	21,5	
Post Filter DC	21,5	
Cell		
Col Cell Gas Flow	22	
Hex RF	550	
Hex DC	19,5	
Hex Delta	-7	
Cell Entrance	20,5	
Hex 2 RF	600	
Hex 2 DC	12,5	
Hex 2 DV	-0,4	
Hex 3 DC	11,2	
Optics 2		
Ion Focus	-40	
Slicer	-4,5	
Extractor DC	13,5	
Top Slit	-0,8	
Bottom Slit	-0,55	

Parameter	Setting	Actual
TOF		
Pusher	1200	
Puller	-700	
Puller Offset	31	
Acc Focus	-1930	
Front Mirror	-7000	
Mid Mirror	-1674,6	
Back Mirror	1250	
Minimum Mass	100	
Maximum Mass	1700	
Acquisition Rate	1	
Acquisition Time	1000	
Length of Transients	423216	
#Transients / Spectrum	8148	
Low Gain PreAmpOffset	33108	
Gain Abund Ratio	12.0	
Gain T0 Offset	-0.088	
Acq Hold Off Delay (ns)	13704	
Detector		
MCP	815	
PreAmpOffset	30006	

Other Actuals: Parameter	Actual
Quad Temp	100
Rough Vac	2,1
Quad Vac	2,18E-05
TOF Vac	3,00E-07
Capillary Current	4,828
Chamber Current	6,27
Turbo 1 Speed	100
Turbo 1 Power	171
Turbo 2 Speed	100
Turbo 2 Power	42

Calibration Coefficients (in µs) *alWeighting:*

a	0,347954	**a2**	3,71771E-08	**c2**	8,7529E-12	**e2**	0
t0	1,012134	**b2**	-1,12936E-09	**d2**	-1,155E-18	**f2**	0

Term Flags: 0x0138 **Trad:** 0 **Poly:** 6

Figure C.V.5. LC-MS/MS QToF tuning report for experiment with deionized water rice co-culture.

www.manaraa.com

TOF Results

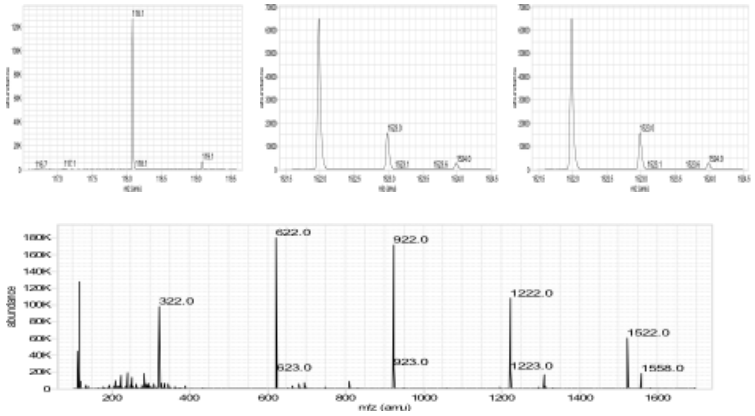

Calibration Data Table

m/z	Actual	Time	Abund	Res	FWHM	Delta (m/z)	Delta (PPM)
118,086255	118,086253	32,247048	140235	10891	0,0112	-0,000002	-0,02
322,048121	322,048141	52,591936	95571	15440	0,0213	0,00002	0,06
622,02896	622,028897	72,694992	176935	25867	0,0244	-0,000063	-0,1
922,009798	922,009879	88,283915	166138	33956	0,0275	0,000081	0,09
1221,990637	1221,990592	101,48244	100262	35440	0,0348	-0,000045	-0,04
1521,971475	1521,971484	113,137898	54569	35570	0,0432	0,000009	0,01

Setpoints

Parameter	Setting	Actual
Source		
Gas Temp	325	325
Drying Gas	5	5
Nebulizer Pressure	20	20
Capillary	4000	-4000
Sheath Gas Temperature	295	
Sheath Gas Flow	12	
Nozzle Voltage	2000	
Optics 1		
Fragmentor	176	
Skimmer	44,5	
Oct 1 RF Vpp	750	
Oct DC 1	25	
Lens 1	22,6	
Lens 2	10,5	
Lens 2 RF Enabled	Yes	
Lens 2 RF Voltage	0	
Lens 2 RF Phase	0	
Quad		
TTI Quad AMU	148	
Quad DC	21,5	
Post Filter DC	21,5	
Cell		
Col Cell Gas Flow	22	
Hex RF	550	
Hex DC	19,5	
Hex Delta	-7	
Cell Entrance	20,5	
Hex 2 RF	600	
Hex 2 DC	12,5	
Hex 2 DV	-0,4	
Hex 3 DC	11,2	
Optics 2		
Ion Focus	-110	
Slicer	-4,5	
Extractor DC	13,5	
Top Slit	-0,8	
Bottom Slit	-0,7	

Parameter	Setting	Actual
TOF		
Pusher	1200	
Puller	-700	
Puller Offset	36	
Acc Focus	-1930	
Front Mirror	-7000	
Mid Mirror	-1675,1	
Back Mirror	1250	
Minimum Mass	100	
Maximum Mass	1700	
Acquisition Rate	1	
Acquisition Time	1000	
Length of Transients	423248	
#Transients / Spectrum	8148	
Low Gain PreAmpOffset	33108	
Gain Abund Ratio	12.0	
Gain T0 Offset	-0.088	
Acq Hold Off Delay (ns)	13704	
Detector		
MCP	815	
PreAmpOffset	30006	

Other Actuals:

Parameter	Actual
Quad Temp	100
Rough Vac	2,05
Quad Vac	2,42E-05
TOF Vac	3,33E-07
Capillary Current	5,114
Chamber Current	6,27
Turbo 1 Speed	100
Turbo 1 Power	171
Turbo 2 Speed	100
Turbo 2 Power	42

Calibration Coefficients (in µs) *alWeighting*

a	0,3479464	**a2**	1,24667E-06	**c2**	9,8368E-12	**e2**	0
t0	1,015853	**b2**	-8,85835E-10	**d2**	-2,224E-16	**f2**	0

Term Flags: 0x00B4 **Trad:** 0 **Poly:** 6

Figure C.V.6. LC-MS/MS QToF tuning report for experiment with 6.8% saline in rice culture.

www.manaraa.com

ABOUT THE AUTHOR

Born and raised on the island of Guadeloupe in the French West Indies, Anne-Claire is the youngest of her family. Her passion for nature and natural products chemistry started as she would take strolls around the home garden with her parents and learn about botany. From junior high school to university, she pursued scientific studies in physics, chemistry, and biology, while still being a fervent member of the school track running team and finding time to play the piano. Upon graduating with a Masters of Valorisation de la Biodiversité Tropicale, she took the leap and moved to the United States where she taught bioorganic chemistry for almost 10 years.

Deep down, Anne-Claire always knew she was going to pursue a PhD, but waited for the right fit. In 2015, she seized the opportunity to join Bill Baker's research lab. Thanks to her parents' professional assignments, she developed her taste for traveling. By the age of 27, she had already visited more than thirty countries, which only strengthened her desire to see more of the world. The various immersion in foreign cultures and wisdom, has given her strength, courage, and resilience to face the vicissitudes of life. Moving forward, Anne-Claire hopes to unite her passions for Natural Products Chemistry, teaching science, traveling, and spending time with her loved ones.

www.manaraa.com